University of Southampton

North Atlantic octocorals: Distribution, Ecology and Phylogenetics.

By

Kirsty Janet Morris

A thesis submitted in partial fulfilment for the degree of Doctor of Philosophy

in the

Faculty of Natural and Environmental Science School of Ocean and Earth Sciences.

October 2011

Declaration of Authorship

I, Kirsty Janet Morris, declare that this thesis titled, “North Atlantic octocorals: Distribution, Ecology and Phylogenetics” and the work presented in it are my own. I confirm that:

- This work was done wholly or mainly while in candidature for a research degree at this University.
- Where any part of this thesis has previously been submitted for a degree or any other qualification at this University or any other institution, this has been clearly stated.
- Where I have consulted the published work of others, this is always clearly attributed.
- Where I have quoted from the work of others, the source is always given. With the exception of such quotations, this thesis is entirely my own work.
- I have acknowledged all main sources of help.
- Where the thesis is based on work done by myself jointly with others, I have made clear exactly what was done by others and what I have contributed myself.

Signed:

Date:

“Nothing in this world can take the place of persistence.
Talent will not; nothing is more common than unsuccessful men with talent.
Genius will not; unrewarded genius is almost a proverb.
Education will not; the world is full of educated derelicts.
Persistence and determination alone are omnipotent.

The slogan Press On! has solved and always will solve the problems of the human race”

Calvin Coolidge

UNIVERSITY OF SOUTHAMPTON

Abstract

Faculty of Natural and Environmental Sciences
School of Ocean and Earth Science
Doctor of Philosophy

North Atlantic octocorals: Distribution, Ecology and Phylogenetics

by Kirsty Janet Morris

Most studies of deep-sea benthic fauna have concentrated on soft sediments with little sampling in rocky areas and even less on non-vent mid-ocean ridges and within submarine canyons, mainly as a result of difficulty accessing them. To assess the distribution and abundance of cold-water corals along an Axial Volcanic Ridges along the Mid-Atlantic ridge at 45^{o}N 27^{o}W, and within the Whittard Canyon along the Irish Margin video footage from the ROV *Isis* taken during a three scientific cruises was analysed. Samples were also taken to allow taxonomic and phylogentic work to be completed. Abundance of octocorals per 100 m transect were calculated and mapped using Arc GIS, with a maximum of 59 in the AVR compared to 855 within the Whittard Canyon. Thirty-one putative species were identified within the Whittard Canyon including some scleractinians, Eleven more than were found in along the AVR. Both locations indicated differences in coral assemblages dependent on substratum type with sedimented areas having increased occurrence of Pennatulidae and Chrysogorgiidae within the AVR and an increased abundance of *Acanella* and *Radicipes* upon sediment in comparison to rock within the Whittard Canyon. It is suggested that these differences in abundance and assemblage structure, both within and between the AVR and Whittard Canyon sites, reflects higher food availability as well as differences in substratum type on which coral larvae settle.

Taxononomic investigations identified 4 new species from samples taken along the AVR, and are described within the thesis. Phylogenetic analysis of novel sequences obtained throughout this study, as well as published sequences, showed the presence of 3 clades A) Calcaxonia and some Alcyoniidae B) Holoaxonia and Pennatulacea C) some Alcyoniidae, *Corallium* and *Paragorgia*. When individual *MSH1* and *ND2* genes were combined the Pennatulacea separated out as a fourth clade. This was attributed to an increase in resolution when two or more genes are used for analysis. Results indicate that morphological taxonomy and molecular analysis are not in agreement and there is a requirement for some taxonomic revisions using molecular data to confirm species boundaries and help guide taxonomic decisions.

Acknowledgements

I would like to thank my supervisors Paul Tyler and Alex Rogers without whom I would not be where I am today. I would particularly like to thank Paul for his support and listening ear, his quick feedback and for not giving up on me. Thank you also to my panel chair for your unwavering support and guidance. I would also like to thank my funding body NERC for my studentship NE/F009097/1. Thanks also go to Les Watling, Scott France, Catherine McFadden and Phil Alderslade for stimulating chats, thought provoking emails, helpful guidance and data provisions.

I would like to give some special thank you for people at NOC who have gone above and beyond their duty to help me with this project; Chrysoula Gubili without who I would still be in a state of phylogenetic confusion, Chris Hauton for help and advice, Tim Le bas and Simon Dodds for technical assistance. Bramley Murton for allowing me to go on JC24 without which my data would be severely depleted.

I would like to thank my friends. Joanne for long phone calls and always being there to help, officemates especially Sarah Taws and Verity Nye for helpful distractions, and my friends at NOC for much needed social interactions and fun times especially, Ellen, Sally, John P, Mary, Jo and Rose. A special thank you to Gerard for your support and putting up with me.

Finally I would like to thank my family who have also given me unwavering support and belief. You have given me strength when I needed it and have always been on the other end of the phone. Although you were never really sure what my project was about you have always made me feel like you were proud of me for pursuing my goal. Thank you.

Contents

Table of figures

Chapter 1: General Introduction

Chapter 2. Lower Bathyal and abyssal distribution of coral in the Axial Volcanic Ridge of the Mid-Atlantic Ridge at 45°N

Chapter 3; The distribution of deep-sea Octocorals within the Whittard submarine Canyon.

Chapter 4: The Phylogenetic analysis of cold-water Octcorals using *MSH1* and *ND2* genes.

Chapter 5: New deep-sea coral species from the Mid-Atlantic Ridge 45°N

Table of Tables

Chapter 1: General Introduction

Chapter 2. Lower Bathyal and abyssal distribution of coral in the Axial Volcanic Ridge of the Mid-Atlantic Ridge at 45 ^{o}N

Chapter 3; The distribution of deep-sea Octocorals within the Whittard submarine Canyon.

Chapter 4: The Phylogenetic analysis of cold-water Octcorals using *MSH1* and *ND2* genes

Chapter 5: New deep-sea coral species from the Mid-Atlantic Ridge 45^{o}N

Chapter 1: General Introduction

1.1General Introduction

The oceans occupy ~70% of the Earth's surface, and with an average depth of ~3,800 m the deep-sea is the largest habitat in the world (Tyler, 2003). Despite this, the remoteness and difficulties in accessing the deep-sea renders it one of the least studied habitats on Earth. Studies of the deep-sea environment only began in the 19th century, encouraged by the dispute on whether life existed within the ocean's depths (Tyler, 2003; Ramirez-Llodra *et al.*, 2011). Sir John Ross was one of the first to discover life at depth when he collected a single *Gorgonocephalus*, a type of ophiuroid, using a small bottom grab in the Arctic in 1818 (Mills, 1983). Edwars Forbes was the first to specifically investigate the deep-sea in 1844, sampling to a depth of 600 m in the Aegean Sea. He discovered very little life and concluded the deep-sea was an azoic environment (Mills, 1983; Tyler, 2003). In 1861 a Swedish expedition discovered life in samples from 1,400 fathoms (2,560 m), and by 1868 more than 400 species had been discovered below 300 fathoms (550 m) in the Norwegian fjords by a series of dredges (Mills, 1983).

Investigations in the North East Atlantic included the pioneering voyages of the H.M.S. *Lightning* and H.M.S. *Porcupine* led by Charles Wyville-Thomson and the world famous cruise of the H.M.S. *Challenger* (1872–1876). Despite a high level of controversy and a wide-spread reluctance to admit the existence of life in the deep sea, these voyages sampled organisms at all depths leading to a rejection of the azoic theory. Studies within North-American waters agreed with the discovery of life in the deep sea. Pourtales discovered coral skeletons, along with forminiferans and shells in sediments from a depth of 1,920 m during a study of the Gulf Stream in 1853 (Mills, 1983). However, it was still believed that the deep-sea had low biodiversity, little food, and an unvarying habitat (Tyler, 2003; Roberts *et al.*, 2009; Ramirez-Llodra *et al.*, 2011). This belief was compounded when the researcher Agassiz, based in the USA, compared samples from the

American collection to that of the Challenger expedition and found most samples from these collections were very similar to one another. This resulted in his conclusion " I think it can be fairly stated that the great outlines of deep sea fauna are now known, and that although many interesting forms will undoubtedly be dredged in the shallower water, between 100 and 300 fathoms, we can hardly expect to add materially to the types discovered by the dredging expeditions of the last ten years" (Mills, 1983).

In the decades following these cornerstone expeditions, new expeditions were fairly common, including an expedition to the Faeroe-Shetland Channel by H.M.S. *Triton* in 1882, from which many zoological samples were taken (Mills, 1983). However, as a result of the death of Whyville-Thomson, British deep-sea exploration was halted for over 40 years, although explorations did continue in America and throughout Europe (Mills, 1983). It was not until the 1960s and 1970s, with an increase in technology and further investigations that the deep-sea was found to be much more diverse than previously thought (Tyler, 2003; Ramirez-Llodra *et al.,* 2011). More recent studies have also proven the presence of seasonality, a wide variety of ecosystems within the deep sea, diurnal tidal variation, the existence of chemosynthetic ecosystems and turbidity currents. It is apparent from the frequency of new discoveries that yet much more remains to be discovered (Billett *et al.*,1983; Gage and Tyler, 1991).

Advances in deep-sea research were furthered by the first use of underwater photography in 1939 mainly using drop-camera systems (Ewing & Worzel, 1967; Hersey, 1967). There are many advantages to using photographic data, not only does it allow the presence of fauna which are often poorly represented by sampling to be observed and identified (Rice *et al.,* 1982), it also allows local environmental data, such as relation the substratum and local food availability to be observed (Svoboda, 1985; Bett *et al*., 1995). It is a natural progression that leads from underwater photography to underwater video cameras. These are now present on many submersibles and remotely operated vehicles and will be used

during this study. Underwater videos have allowed for the investigation of many organisms and habitat types from bioluminescent profiles to deep-sea vents and cold-water corals (Copley *et al.*,2007; Heger *et al.*, 2008**).** Video surveys allow a large area to be investigated with little impact on the habitat. Collection of corals and other epibenthic fauna via dredging or trawling leads not only to damage of the collected specimens but also damages biogeneic habitats including reefs and coral gardens on the benthos. It was via photographic and video footage corals were observed *in-situ* at depths in excess of 1,000 m. However, despite the exceptional technological development in the past decade leading to the creation of high definition footage, it is not possible to identify corals taxonomically from photography. Thus it is still important that token samples are taken to allow an accurate identification to be achieved.

Forty years ago the deep-sea was considered a series of sedimentary basins, however in has now become clear that it is formed from a series of discreet ecosystems including; Seamounts (Pitcher *et al.,* 2007), hydrothermal vents (Van Dover, 2000), cold-seeps (Tunicliffe *et al*, 2003**)**, steep slopes and canyons (de Stigter *et al.*, 2007; de Leo *et al.*, 2010), abyssal plains (Thistle, 2003) and oceanic trenches (Jamieson, in prep). The least explored systems within the deep-sea are non-vent mid-ocean ridges and canyon systems, which will be considered within this thesis.

1.1.1 Cold-water corals

When people think of corals they imagine pristine shores in the tropics with coral reefs filling the shallow crystal-clear water with life and colour. However, corals are not a shallow water phenomena, two thirds of all known coral species are cold-water species occurring in depths from 50 m to over 4,000 m (Koslow, 2007; Roberts *et al.*, 2009). Corals belong to the phylum Cnidaria which also includes, hydroids, jellyfish and sea anemones and are defined by Cairns, (2007) as "Animals in the cnidarian classes Anthozoa

and Hydrozoa that produce either calcium carbonate (aragonitic or calcitic) secretions resulting in a continuous skeleton or as numerous microscopic, individualised sclerites, or that have a black, horn like, proteinaceous axis". In 1860 the cold-water coral species *Caryophyllia borealis* was one of the first deep-sea organisms to be discovered. It found on a piece of submarine cable at a depth of 1,200 fathoms (2,194 m), contributing to the rejection of the azoic theory (Menzies *et al.*, 1973).

Cold-water corals are azooxanthellate so, unlike their shallow water counterparts, they do not require direct sunlight for photosynthesis. They are suspension filter feeders depending on particulate organic matter (POM) falling from the surface waters (Risk *et al.*, 2002). There are five cold-water coral taxa Scleractinia, Zoanthidae, Antipatharia, Stylasteridae and the Octocorallia on which this project focuses (Roberts *et al.*, 2009).

1.1.2 Coral structure

Corals are fairly simple organisms. Each polyp is composed of two layers, the epidermis to the outside and a gastrodermis facing the internal gastrovascular cavity. These layers are separated by a gelatinous substance called the mesoglea (Roberts *et al.*, 2009). The polyps consist of a central mouth surrounded by a ring of tentacles, and a pharynx running down from the oral cavity into the internal or gastric cavity (Figure 1.1). The gastric cavity is then subdivided into longitudinal compartments by the presence of mesenteries (with the exception of stylasterids which belong to the class Hydrozoa) (Bayer *et al.*, 1983; Roberts *et al*., 2009). It is these mesenteries which are the essence of the polyp, carrying oocytes and spermacysts for expulsion as well as carrying digestive cells within the polyp (Roberts *et al*., 2009).

The polyps do not contain defined sexual organs. The gametes develop in the mesoglea in hexacorals or along the mesentery edge in octocorals and are then passed into the gastric cavity before being released into the water column (Roberts *et al.*, 2009). Individual polyps are connected by a tissue called coenenchyme, which often surrounds a central skeletal axis which itself is covered by an axis sheath (Bayer *et al.*, 1983). Each polyp also contains nematocyst stinging cells which can be used to defend both the organism and aid in the capture of prey, a defining feature of Cnidarians.

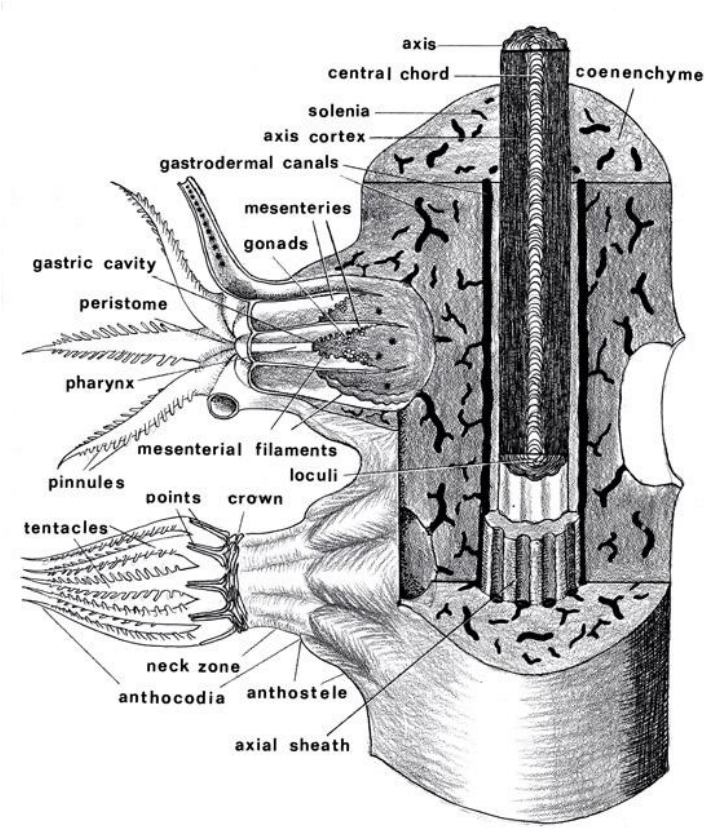

Figure 1.1. General diagram of octocoral Anatomy. Images shows placement of mesenteries within the polyp and tentacle structure along with axial morphology. Figure taken from Bayer et al., 1983.

1.1.3 Subclass Octocorallia

More than 40 families of Octocorallia have been identified (Table 1.1) containing ~ 2,325 cold-water species, often found associated with reefs and other hard-bottomed communities (Wirshing *et al*., 2005; Daly *et al*., 2007; Roberts *et al*., 2009). Octocorallia is a subclass of Anthozoa which as the name would suggest has eight fold symmetry. Each individual polyp has eight tentacles, which have a feather like shape as a result of multiple pinnules (Figure 1.2). The eight fold symmetry is continued with the presence of eight mesenteries surrounding the pharynx, which is tubular in shape and originates from the mouth slit, dividing the upper part of the gastrovasular cavity (Figure 1.1 and 2) (Wirshing *et al.*, 2005; Daly *et al.*, 2007).

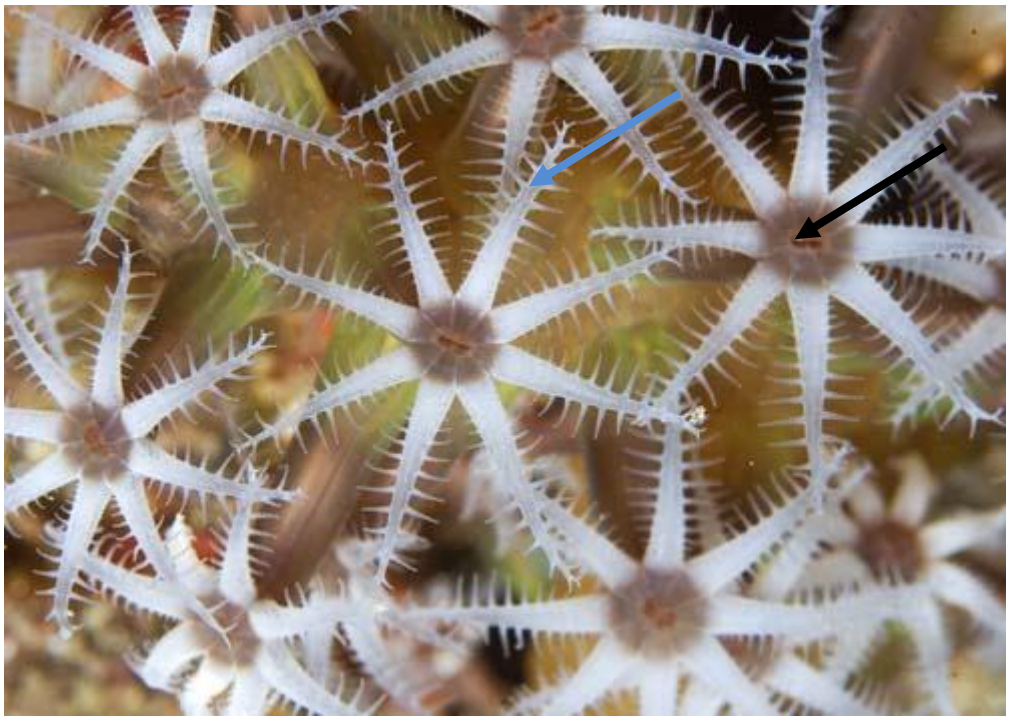

Figure 1.2. Octocoral tentacles. Octocorals have an eight fold symmetry seen here with the presence of eight pinnate tentacles per polyp (pinnules highlighted by a blue arrow). The centre of the polyp contains the slit like mouth connected (highlighted by the black arrow) by a pharynx to the gastric cavity. Picture taken from www.eco-divers.com (4/9/11).

Table 1. 1.List of all families which are included in the Octocorallia subclass modified from Daly et al., (2007):

Order Alcyonacea

Group Alcyoniina

Alcyoniidae Lamouroux, (1812) comprises 34 genera
Nephtheidae Gray, (1862) comprises 20 genera
Nidaliidae Gray, (1869) comprises 7 genera
Paralcyoniidae Bayer, (1981) comprises 4 genera
Xeniidae Wright & Studer, (1889) comprises 14 genera

Suborder Calcaxonia

Chrysogorgiidae Verrill, (1883) comprises 12 genera
Dendrobrachiidae Brook, (1889) monogeneic family
Ellisellidae Gray, (1859) comprises 10 genera
Ifalukellidae Bayer, (1955) comprises 2 genera
Isididae Lamouroux, (1812) comprises 38 genera
Primnoidae Gray, (1857) comprises 32 genera

Suborder Holaxonia

Acanthogorgiidae Gray, (1859) comprises 6 genera
Gorgoniidae Lamouroux, (1812) comprises 17 genera
Keroeididae Kinoshita, (1910) comprises 5 genera
Plexauridae Gray, (1859) comprises approximately 38 genera

Group Protoalcyonaria: (solitary polyps)

HaimeidaeWright, (1865) comprises four monospecific genera
Taiaroidae Bayer & Muzik, (1976) is a monospecific family

Group Scleraxonia:

Anthothelidae Broch, (1916) comprises approximately 13 genera
Briareidae Gray, (1859) comprises 2/3 genera
Coralliidae Lamouroux, (1812) comprises 3 genera,
Melithaeidae Gray, (1870) comprises approximately 6 genera
Paragorgiidae Kükenthal, (1916) comprises 2 genera
Parisididae Aurivillius, (1931) is a monogeneric family
Subergorgiidae Gray, (1859) comprises three genera

Group Stolonifera:

Acrossotidae Bourne, (1914) is a monogeneric family
Clavulariidae Hickson, (1894) comprises approximately 24 genera
Coelogorgiidae Bourne, (1900) is a monospecific family
Cornulariidae Dana, (1846) is a monogeneric family
Pseudogorgiidae Utinomi & Harada, (1973) is a monospecific family
Tubiporidae Ehrenberg, (1828) is a monogeneric family

Order Helioporacea

Helioporidae Moseley, (1876) is a monospecific family
Lithotelestidae Bayer & Muzik, (1977) monogeneic family

Order Pennatulacea

Anthoptilidae Kölliker, (1880) is a monogeneric
Chunellidae Kükenthal, (1902) comprises 3 genera
Echinoptilidae Hubrecht, (1885) comprises 2 genera
Funiculinidae Gray, (1870) is a monogeneric family
Halipteridae Williams, (1995) is a monogeneric family
Kophobelemnidae Gray, (1860) comprises 3 genera

Pennatulidae Ehrenberg, (1834) comprises 6 genera
Protoptilidae Kölliker, (1872) comprises 2 genera
Renillidae Gray, (1870) is a monogeneric family
Scleroptilidae Jungersen, (1904) is a monogeneric family
Stachyptilidae Kölliker, (1880) comprises 2 genera
Umbellulidae Kölliker, (1880) is a monogeneric family
Veretillidae Herklots, (1858) comprises 5 genera
Virgulariidae Verrill, (1868) comprises 5 genera

Each polyp is embedded within the coenenchyme of the colony. The coenenchyme is the colonial tissue which joins all polyps within a colony and allows the flow of water and nutrients between all polyps in the colony (Bayer *et al*, 1983). This coenenchyme covers the entire central axis of the colony and contains the jelly-like substance mesogloea which separates the two epithelial layers (Bayer *et al*, 1983). The internal axis can be composed of proteinaceous gorgonin or solid calcium carbonate (Roberts *et al.,* 2009). All octocorals contain sclerites, small structures composed of calcitic calcium carbonate. It is these sclerites that maintain the structural integrity of the octocoral colonies (West, 1997). Sclerites act like reinforcements on the skeleton to prevent deformities from currents (West, 1998).

The current taxonomic divisions of Octcorallia contains three orders; Alcyonacea (Figure 1.3) with ~30 families, Pennatulacea (Figure 1.4) with 14 families and Helioporacea (Figure 1.5) with 2 families. Alcyonacea is subdivided into sub-ordinal groups which are defined by skeletal axis and colony architecture (McFadden *et al., 2006).* These divisions reflect a previous classification scheme where the Octocorallia was divided into seven orders Helioporacea, Pennatulacea, Alcyonacea, Gorgonacea, Stolonifera, Telestacea and Protoalcyonaria. Helioporacea and Pennatulacea are the only two orders which have distinct morphologies (McFadden et al., 2006).

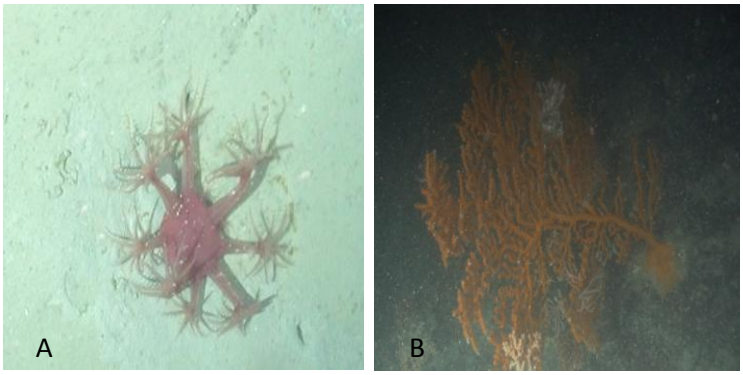

Figure 1.3. Example of species belonging to Alcyonacea A) Anthomastus *sp B) Orange Paragorgia. These individuals clearly illustrate the scope of morphologies within the order Alcyonacea. Photos obtained during RRS James Cook cruise JC26*

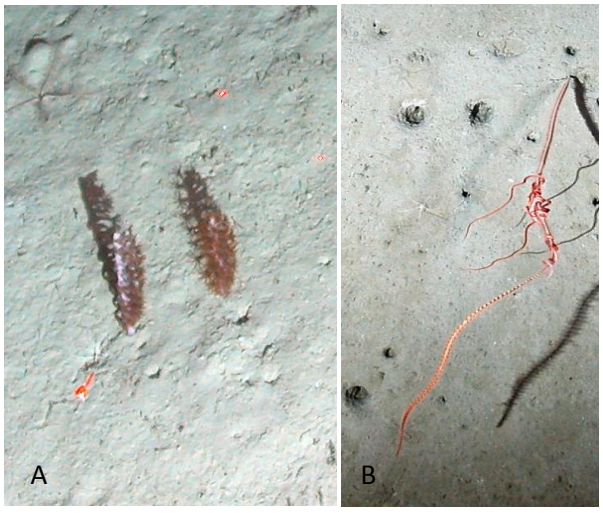

Figure 1.4 Examples of species belonging to Pennatulacea (A) Kophobelemnon *sp (B)* Distichoptilum gracile. *Photos obatained during RRS James Cook cruise JC26*

Figure 1.5. Heliopora coerulea *coral from the order* Helioporacea. *Photo Courtesy John Rice and taken from* http://animal-world.com/Aquarium-Coral-Reefs/Blue-Coral *(7/10/11)*

The remaining orders were previously classified by colony growth morphology which is now known be a continuous process- meaning that this cannot be successfully implemented as a diagnostic feature (McFadden et al., 2006). Subsequently these five original orders have now been placed into the single order Alcyonacea by Bayer (1981).

The physical make up of the order Helioporacea is different from all other octocorals. Helioporacea produce calcified skeletons of crystalline aragonite as opposed a supporting axis composed of scleroproteinous gorgonin and /or calcite or no supporting axis at all as with all other octocorals (Daly *et al.,* 2007). The Pennatulacea are possibly the most distinct group of octocorals. Each colony is supported by a bulbous peduncle which is used to anchor the rod-like calcite axis into soft sediment substratum (Daly *et al.,* 2007). The Alcyonacea contains the majority of cold-water octocoral species, distinguished from one another by the overall growth form, presence or absence of a skeletal axis and the shape and distribution of sclerites (Daly *et al.*, 2007). Alcyonacea contains two morphologically distinct groups of gorgonian: Calcaxonia those with a solid core and Holaxonia those with

a hollow core (Sánchez et *al.,* 2003). However, many of the features used to classify individuals traditionally are not informative, e.g. branching vs. non-branching in Isididae (France *et al.,* 2007), suggesting many families within the Alcyonacea require taxonomic revisions (McFadden *et al.,* 2006, Daly *et al.,* 2007).

1.1.4 Octocorallia Taxonomy and Systematics

The first report on the order Octocorallia from the deep-sea was based on data collected from the HMS *Challenger* expedition (Thomson and Murray, 1889). Within this report multiple genera and species were described mainly by Verrill. A subsequent follow up supplementary report was printed by Professor Studer, to allow the inclusion of further new species which were not included in the original report. This report was highly influential within the world of octocoral biology and is used to this day for taxonomic identifications. Grasshoff was also highly influential within octocoral taxonomy, producing many species descriptions including ten species from the family Plexauridae (Watling and Auster, 2005). A further 186 species incorporating 48 genera and 4 families were described by Bayer over his career, making a large contribution to knowledge on deep-sea octocorals (Cairns, 2009). Bayer was also highly influential in the development of taxonomic methodology, being the first to use scanning electron microscope (SEM) pictures for species description, creating a key for most genera (Cairns, 2009) and publishing a trilingual glossary for morphological terms (Bayer *et al,* 1983). His work will impact taxonomic research for many years. Despite these classical works octocorals, have a poorly defined taxonomy at generic levels (Aguilar and Sánchez , 2007).

Sclerite morphology is the most effective way to differentiate between species, within the 40 families of the Octcorallia (Janes and Mei Wah, 2005). However, the classification of Octocorallia has lead to many problems. The main issues responsible for this difficulty are widespread plasticity occurring among and within species, morphological paucity, intra species variation and poor fossil records (Giammon and Stanton, 1980; Williams and Alderslade, 1999; McFadden *et al*., 2006; Roberts *et al*., 2009). Many older species

descriptions contained poor illustrations, or none at all, and many of the older specimens have been badly preserved which can lead to a disparity in identifications between taxonomists and a general confusion as to the correct identification (Sánchez , 2007).

Previous taxonomic work on octocorals has focused on characteristics such as calyx and sclerite morphology, growth form, axis composition and arrangement of sclerites (Wirshing *et al.*, 2005; McFadden *et al.*, 2011). This has often resulted in the misclassification of octocorals into families or genera upon the presence or absence of a morphological feature, such as polyp spine development, which have since been found to be non-definitive (Cairns and Baco, 2007). These problems have lead to octocoral taxonomy being some of the most difficult in the invertebrate phyla, with modern taxonomists calling for an overhaul to the octocoral systematic system (Powers, 1970; Bayers *et al.*, 1983; Berntson *et al.*, 2001; Janes and Mei Wah, 2005; McFadden *et al.*, 2006, 2011). It has also become clear that for a fuller and deeper understanding of octocoral systematics and evolutionary history molecular techniques must be implemented and paired with taxonomy.

Despite being an important and relatively abundant group there has been very little molecular work carried out on cold-water corals with even less focusing on octocorals (Smith *et al.*, 2004; McFadden *et al.*, 2006, France, 2007). In theory molecular techniques allow the separation of sister taxa, which can be difficult using traditional systematic techniques. They also allow for the creation of taxonomic trees, giving an insight into Octocorallia evolutionary history, which due to a lack of fossil record is difficult to achieve using morphological data alone.

The molecular markers originally used for octocoral phylogenetics (16s and 18s) only allowed individuals to be resolved to genus or family level (Berntson *et al.*, 2001; France, 2007). However, recently new markers *MSH1*, a mitochondrial mismatch repair gene found in no other metazoans (Culligan *et al.*, 2000), and *ND2* a mitochondrial protein-coding gene, have been implemented and were found to have a higher resolution than the original markers within the Octocorallia (McFadden *et al.*, 2006; 2011).

The improved phylogenies resulting from *MSH1* and *ND2* indicated that Octocorallia is made up of two large distinct clades, one with the Pennatulacea, Heliopora and Calaxonia and the other containing Holaxonia, Scleraxonia and Stolonifera, with a third smaller and less defined clade which included the Alcyoniidae and Corallium (France *et al.*, 1996; Berntson *et al.*, 2001; McFadden *et al.*, 2006). Although these studies all agree with the previous findings using16s and 18s genes, none agree with the traditional taxonomic divisions placed within the Octocorallia (McFadden *et al.*, 2006). To date no phylogeny has included all octocorallian families, limiting the information gleaned from these studies (McFadden *et al.*, 2006). To allow for a better understanding of the sub-class Octocorallia further taxonomic, genetic and overall ecological investigations must occur.

1.1.5 Cold-water octocoral reproduction

Comprehension of reproductive processes is vital to the understanding of a species, how it survives within its environment, or how it will react to the effects of increasing anthropogenic impacts (Waller, 2005). In shallow water Octocorallia reproductive biology varies among and within species. However, very little is known about the reproductive biology of deep-sea cold-water corals, with the majority of knowledge on cold-water Ocotorallia reproduction relying on a few studies from the Order Pennatulacea (Rice *et al.*, 1992; Tyler *et al.*, 1995) and some Antarctic species (Orejas *et al.*, 2002, 2007) . This is compounded by a lack of observations and little sampling for histological investigations,

with most studies which have occurred on cold-water corals focusing on scleractinians (Burgess and Babcock, 2005; Waller, 2005; Waller and Tyler, 2005). Shallow water octocorals have been observed to reproduce both sexually and asexually (Lasker *et al.*, 1996; Simpson, 2009).

A variety of different asexual reproductive patterns have been observed within shallow water octocorals, mainly from the soft corals and some gorgonians. These techniques include fission, reattachment and survival of broken fragments as well as parthenogenesis (development of a planula without the presence of sperm) (Simpson, 2009). However, it is believed that the majority of octocorals, and thus most deep-sea octocorals reproduce sexually.

Generally sexually-reproducing octocorals are gonochoristic, (meaning the individuals will have separate sexes), with others showing hermaphroditic reproduction (Simpson 2009; Roberts *et al.,* 2009). Both brooding and broadcasting sexual patterns have been observed in octocorals. Broadcast spawners release sperm and eggs into the water column. Such behaviour means the degree of fertilisation success is dependent on the timing of the release of the gametes, the water currents and the availability of complementary gametes. Lasker *et al*., (1996) found that in the Caribbean octocorals *Plexaura kuna* and *Pseudoplexaura porosa* reproductive success was limited by the availability of sperm, with a low percentage of eggs being fertilised. However, environmental factors such as currents can lead to the dilution of the gamete density within the water column which can lead to a variation between years on fertilization rates and success (Lasker *et al.,* 1996). As an attempt to increase the chance of successful fertilisation shallow water broadcast breeders have often been observed to participate in mass spawning events (Lasker *et al*., 1996; Simpson, 2009). It is expected such events occurring in the deep sea adhere to seasonality, often corresponding to the sinking of the surface phytoplankton bloom, this effect is lessened in the tropics where seasonality is reduced (Waller and Tyler, 2005; Sun *et al.,*

2010). Broadcast fertilisation is liable to be less successful within cold-water species than in shallow-water octocorals, as a result of reduced densities (with the exception of reef building species such as *Lophelia*) and the large distances gametes must cover in order to come into contact with one another. This would lead to what is known as the allee effect which suggests that in small populations reproduction and survival rate will increase with increased population density. This in turn implies some isolated coral colonies may continue to produce gametes, but will never contribute to the next generation.

Brooders retain their eggs either within the polyp or upon the colony until they are fertilised, when they will then release the larvae into the water column (Sun *et al.*, 2010). This technique increases the probability of a higher level of fertilisation success and would be highly beneficial if individuals do not partake in co-ordinated mass spawning. This reproductive technique has been suggested to compensate for a reduced fecundity in individuals by leading to an enhanced larval survival rate (Babcock, 1990). Orejas *et al.* (2007) indicated that reproductive adaptations observed in cold-water corals may not be substantially different from their shallow water counterparts, and suggested octocoral morphology may play a crucial role in determining reproductive output. Deep-sea alcyonaceans and some deep-sea scleractinians are known to brood, whilst pennatulids have been observed to spawn (Cordes *et al.*, 2001; Sun *et al.*, 2010).

It is vital to have a clear understanding of cold-water coral reproduction to allow there effective management and conservation. The variability of reproductive schemes used by cold-water corals may lead to the requirement of the implementation of a range of management schemes dependent upon the species present within a location. Such schemes could include the complete closure of fisheries throughout spawning times and the prevention of fishing in areas where the coral densities are falling below the threshold for successful reproduction, enabling future repopulation of the area. However, more information is required before management decisions can be made.

1.1.6 Cold-water octocoral growth

Difficulty in obtaining samples has resulted in very little knowledge of the growth rates of cold-water corals, with those studies which have occurred generally focusing on scleratinians (Orejas *et al*., 2011). From these studies a general consensus of slow growth rates (0.01 to 25 mm per year dependent on the species in comparison of up to 150 mm per year in shallow waters) in cold-water corals has emerged (Risk *et al.*, 2002; Freiwald *et al*., 2004; Roberts *et al.*, 2009; Sherwood and Edinger, 2009; Orejas *et al*., 2011). However, the considerable variance in growth rates among and within taxa (Thresher, 2009; Orejas *et al.*, 2011) is difficult to explain. It is expected food availability and oceanographic regimes play a role in this variance (Tracey *et al.*, 2007; Thresher, 2009; Orejas *et al.*, 2011).

Thresher *et al.* (2009) studied the growth rates in 23 cold-water Isididae or bamboo coral specimens (so called for the occurrence of dark nodes and lighter internodes on the skeleton), encompassing a variety of species. They found growth rates decrease with increased depth and temperature accounts for half of the overall difference in growth rates among specimens. It is likely that this temperature effect is because of some unknown physiological constraints that result in cold-water coral growth becoming optimal between 2^{o}C and 5^{o}C. Depth of the occurance of an individual within a population plays a role in the growth rate and form of the individual.

The morphology of a species can change depending upon the depth at which it is found. In the shallow water species *Briareum asbestinum* it has been found that the depth at which the colony grows affects the length and width of the colony, with those in shallow water having a more short-stout appearance than those which occur at deeper depths (West *et al.*, 1993). From this it might be expected that the general morphology of octocoral colonies in the deep-sea will be long and slender, as a result of reduced currents. However, there may be some exceptions to this where current speeds are higher, such as within

canyons, or on steep topography, such as mid-ocean ridges or seamounts. Shallow-water colonies were also found to have a higher number of polyps and shorter sclerites. West *et al.* (1993) suggested this difference was a result of higher currents which would increase the chance of the sclerites breaking, thus shallow-water colonies will adapt to prevent this. Sherwood and Edinger (2009) also found that individuals within high current areas would require a higher degree of axial thickening to withstand the current stress. These combined results indicate that growth rate and form variations between individuals could be partially caused by current regimes within the local area.

Increased currents may enhance growth in individuals as a result of improved food availability for the coral colonies. Seban *et al.* (1984, 2003) found, using a shallow water species of *Alcyonium,* that there was a correlation between the size of a colony and the flow rate in area. Octocorals are suspension feeders, capable of ingesting particulate organic matter (Ribes *et al.*, 1999), as well as being able to capture zooplankton using nematocysts on their tentacles (Coma *et al.*, 1994). The food capture rate is dependent on prey availability and water flow rate (Coma *et al.*, 1994). Therefore areas of enhanced water flow would lead to an increase in size of the colonies as a result of enhanced food supply by the currents.

1.1.7 Cold-water octocoral distribution.

Cold-water octocorals have a cosmopolitan distribution, occurring throughout all the world oceans at depths from 50 m to more than 4 km, mainly settling on hard substratum (Risk *et al.*, 2002). However, the fine-scale distribution of these individuals is largely unknown. Scleractinians tend to form large reef complexes or are solitary, whilst octocorals are ahermatypic often occurring alone or in patches. Scleractinians are also more depth limited than octocorals, occurring above the aragonite saturation zone, below which creating a skeleton becomes more difficult because of aragonite dissolution (Orr *et al.*, 2005;

Guinotte *et al.*, 2006; Turley *et al.*, 2007). These factors together make scleractinians a more highly studied group with investigations into distribution more wide spread (Taviani *et al.*, 2005; Alvarez-Perez *et al.*, 2005; Schroeder *et al.*, 2005).

The requirement for hard substratum for most species of octocoral (with the exception of pennatulids) (Gass and Willison, 2005) and the fact that areas of high topography lead to enhanced water flow (Genin *et al*., 1989; Tyler and Zibrowius, 1992; Sebens *et al*., 2003; Mortensen *et al.*, 2008; Orejas *et al.*, 2009; Woodby *et al.*, 2009), which in turn leads to enhanced food supply (Bryan and Metaxas, 2006; Mortensen *et al*., 2008; Orejas *et al*., 2009; Watanabe *et al.*, 2009) means octocorals are often observed in areas such as seamounts, mid-ocean ridges (see Chapter 2 for more information) and canyons (see Chapter 3 for more information). The small scale distribution of octocorals upon these features is generally unknown and will be investigated within this thesis.

1.1.8 Why study cold-water octocorals?

Octocorals create a higher level of three dimensional complexity, increasing the number of niches available for other organisms (Morgan *et al.*, 2005). Octocorals have a variety of associated organisms present upon or around them, ranging from hydroids and anemones to polychaetes and ophiuroids (Buhl-Mortensen and Mortensen, 2005). The number of octocorals within an area has been shown to have a positive correlation with the number of megafauna within that area (Mortensen and Buhl-Mortensen, 2005). All of these factors make octocorals important for deep-sea biodiversity, both in their own right and as biogenic engineers. The recent acknowledgment that octocorals make an important contribution to deep-sea biodiversity has arrived as anthropogenic impacts threaten to hamper the existence of these important organisms, (Rogers, 1999; Mortensen and Buhl-Mortensen, 2005).

Deep-sea fishing is a major anthropogenic threat within the deep sea (Ramirez-Llodra *et al.*, 2011). At least 40% of the worlds trawling grounds now occur in waters deeper than the continental shelf edge (Roberts, 2002). During the late nineteen eighties there was a marked increase in deep-sea fishing fuelled by an increase in demand for deep-sea species such as the orange roughy (*Hoplostethus atlanticus*) (Hall-Spencer *et al.* , 2002) and as a result of declining catches in traditional stocks (Roberts, 2002). Technology advances have allowed development of more successful trawls, fish-finding and navigation devices, stronger cables and powerful winches, allowing the fisheries to gain access to environments and depths never reached before (Roberts, 2002). These trawls have been shown to leave large scars on the substratum, reaching lengths up to 4 km (Hall-Spencer *et al.*, 2002), as well as directly impacting corals. Some fishing vessels have been known to deliberately crush corals, making way for trawling gear (Grehan *et al.*, 2004) perhaps sharing the opinion of the French biologist Joubin who said in a 1915 paper "deep-water corals, a nuisance for trawlers" (Freiwald *et al.* , 2004).

Auster (2005) observed that in a trawl mark though an octocoral (*Primnoa*) habitat in the Gulf of Alaska, 31 colonies remained in the area with 7 of these missing over 80 % of their branches, seven years after a haul of 1,000 kg of coral colonies. In 2005 The National Marine Fisheries Service in Alaska's Aleutian Island region estimated that 87 % of all coral bycatch occurred though trawling activities, removing 2 million kg of coral and sponge as bycatch during the years 1990-2002 (Shester and Ayers, 2005; Roberts *et al*., 2009). Those corals left behind are often damaged as a result of the fragility of the individuals (Hall-Spencer *et al.*, 2002; Auster, 2005) with many buried, wounded, infected or crushed (Fossa *et al.*, 2002). Life history traits such as, high longevity, slow growth and infrequent reproduction, mean that recovery from fishing events will be prolonged. In addition to this, increasing anthropogenic CO_2 emissions are changing the chemistry of the oceans, leading to ocean acidification. This increase is expected to cause a decline in habitat availability for cold-water corals (Tittensor *et al*., 2010), although it is likely to

have a larger effect on scleractinians, by shallowing the aragonite saturation zone (the depth at which the ocean becomes undersaturated with respect to aragonite).

To ensure the survival of octocorals and their associated species into the future it is vital that we understand their basic biology. At present there are many large holes in the knowledge surrounding cold-water octocorals. It is important to enhance the understanding of the small-scale distribution of octocorals (i.e. at local population levels including topographic features and individual ocean basins), as well as understanding the large global scale distribution. It is also essential to understand which species make up local assemblages within an area and to understand the genotypic make up of an assemblage to ensure rarer genotypes are preserved. It is not until we fully understand these organisms that protection measures such as marine protected areas (MPAs) be implemented effectively.

1.2 Aims of thesis

- Determine if depth, substratum or slope have an effect on cold-water coral assemblages along the AVR at 45^{o}N and within the Whittard Canyon.
- Compare cold-water coral assemblages along the AVR at 45^{o}N and within the Whittard Canyon.
- Create a comprehensive phylogenetic tree of the order Octocorallia including new samples obtained from various sites within the Atlantic using both the *MSH1* and *ND2* genes.
- Identify and describe new cold-water coral species found along the AVR at 45^{o}N upon the MAR.

Objectives

- Analysis of all video footage available will be completed for both the Whittard Canyon and the AVR, identifying Octocoral species noting: density, position

and substratum type, to allow statistical analysis of the coral assemblage structure and comparisons between sites to be made.

- Octocoral samples from the Atlantic will be collected and subjected to Molecular analysis for the MSH1 and ND2 genes. These will be added to samples already available on the NCBI database to create a full genetic alignment which will subsequently be subjected to phylogenetic model analysis to allow the creating on phylogenetic trees.
- Identify New Octocoral species which will then be described within using a new system implemented by Les Watling (Hawaii) and Scott France (Louisiana). Genetic sequencing based on the *MSH1* gene were used to support these descriptions.

Chapter 2: Lower Bathyal and abyssal distribution of coral in the Axial Volcanic Ridge of the Mid-Atlantic Ridge at 45 °N

2.1 Introduction

Corals are best known from shallow tropical seas, although >65 % of the world's estimated number of coral species occur in water greater than 50 m depth (Cairns, 2007; Lindner *et al*., 2008; Roberts *et al*., 2009). Deep-water or cold-water corals can be defined as a "paraphyletic assemblage of organisms belonging to phylum Cnidaria" (Morgan *et al*., 2005) belonging to the classes Anthozoa and Hydrozoa, producing either aragonitic or calcitic skeletons or sclerites, or which have a black, proteinaceous, horn-like structure (Cairns, 2007; Lindner *et al.*, 2008). Roberts *et al.* (2009) defined five cold-water coral taxa; Scleractinia, Zoanthidae, Antipatharia, Octocorallia and Stylasteridae. In contrast to their shallow-water counterparts cold-water corals do not require light or high temperatures to survive in deep-waters. This results in cold-water corals having a cosmopolitan distribution, occurring in most, if not all, of the world oceans.

The morphology of cold-water corals allows them to contribute structural complexity to deep-sea ecosystems (Watanabe *et al.*, 2009) and to provide a habitat for a wide variety of different species (Clark *et al.*, 2006). Buhl-Mortensen and Mortensen (2005) identified 114 associated species, mainly invertebrates, within just 25 coral samples from the North-West Atlantic off the coast of Canada. Previously >1,300 different species have been found associated with reefs of the scleractinian *Lophelia pertusa* in the North-East Atlantic, underlining their importance as sources of biogenic habitat (Roberts *et al.*, 2006). Recognition that these ecosystems make a potentially significant contribution to deep-sea biodiversity has come at a time when anthropogenic impacts, particularly bottom fishing, have been identified as a threat to cold-water coral assemblages (Clark *et al*., 2006, 2010;

Roberts *et al*., 2009). In addition, CO_2 emissions are leading to changes in ocean chemistry, through acidification, that are also predicted to cause a decline in habitat availability for cold-water corals (Tittensor *et al*., 2010). Such existing and future threats have led to a requirement for better understanding of the distribution of coral habitats in the deep ocean in order to improve the management of these ecosystems.

Despite its size, and the diversity of the animal assemblages within it, the deep sea remains one of the least studied environments on Earth. This is particularly true in areas of elevated topography, such as the mid-ocean ridges, systems that are often remote from land and present extremely rugged bottom topography. The increase in technology over recent decades has allowed scientists to move from using trawls for biological investigation to using devices such as AUVs (Autonomous Underwater Vehicles), ROVs (Remotely Operated Vehicles) and manned submersibles that allow visual data to be collected. The main advantage of video or photograpic data are that they provide a visual record of fauna that are poorly sampled by traditional methods (Rice *et al*., 1982), as well as allowing observations of behaviour and the presence of species associations (Bett *et al*., 1995; Eastman and Barry, 2002).

Mid-ocean ridges represent a significant habitat in the deep ocean and create a network running for more than 64,000 km around the Earth. To date, work on the benthic ecology of mid-ocean ridges has focused on hydrothermal vent ecosystems, although some studies have been undertaken on the assemblages living on non-hydrothermally active parts of the ridge system. These studies have included observations of coral distribution on mid-ocean ridges. For example, Copley *et al.* (1996) found that corals were more likely to be recovered during dredging from sites with little or no sediment than from highly sedimented areas. Coral distribution was strongly influenced by substrata with some species confined to soft sediments but most occurring on basalt outcrops (Mortensen *et al*., 2008). It is commonly accepted that coral colonies require hard substrata on which to settle

(Mortensen *et al.,* 2008). Mid-ocean ridges, especially active areas such as Axial Volcanic Ridges (AVR) provide a variety of settings in which hard substrata occur such as pillow ridges, hummocks and flat-topped seamount, all of which are generally uncommon in the global ocean (Young, 2009), making them potentially important habitats for coral distribution throughout the world. The variety of habitats present provides an ideal setting in which to investigate how different substrata and other expressions of topography, particularly slopes, influence coral distribution and assemblage structure on the Mid-Atlantic Ridge.

2.1.1 Mid-Atlantic Ridge

The Mid-Atlantic Ridge (MAR) is a slow spreading (<25mm yr^{-1}in comparison to the East Pacific Rise which has a fast spreading rate of >130 mm yr^{-1}) oceanic ridge system running along the length of the Atlantic Ocean, forming part of the longest mountain chain in the world (Smith and Cann, 1993). Mid-ocean ridges are believed to be free from continental erosion processes, such as fluvial action and thus are often interpreted in terms of primary geological action (Mitchell *et al.,* 2000). They occur on divergent plates, using tectonic and magmatic processes to form new oceanic crust (Smith and Cann, 1993). Crustal topography changes from ridge to ridge, influenced by spreading speed and underlying volcanic activity. Unlike some other ridges the MAR does not have a steady magma chamber but instead has a discrete magma chamber leading to the creation of many small volcanoes (Smith and Cann, 1993). These volcanoes become agglomerated and combine with hummocky and smooth flows creating a patchy topography leading to the creation of an Axial Volcanic Ridge (AVR). The MAR is dominated by these AVR structures, which range in size from several hundred metres to 5 km in width and from several to tens of kilometres long (Smith and Cann, 1993; Searle *et al.,* 2010). AVRs have been found in most spreading sections of the MAR and are considered to be the primary site of crustal accretion within the MAR (Smith and Cann, 1992, Searle *et al.,* 2010). It is not clear exactly how AVRs form (either episodically or in a steady state) because they

have all been formed within the past 780,000 years making magnetic dating difficult to achieve. However, new AVRs have been estimated to arise in a time frame of between 25,000 – 600,000 years (Searle *et al.,* 2010). Generally it the episodic creation theory which has been accepted with Parson *et al.,* (1993) speculating that AVRs are initiated at cooler sections of the Axial zone and that they are cyclic in nature, resulting from episodic magma fluxes being tectonically focused to the area.

2.1.2 Axial Volcanic ridge at 45 °N

The present study focuses on the distribution of deep-sea corals, between 2,600 m and 3,600 m along an Axial Volcanic Ridge (AVR) of the MAR at approx 45° 30' N. From the primary geological study, which took place from the video data obtained in this study, it is known that the AVR here is well defined with a highly typical "hour-glass" shape (Searle *et al.,* 2010). The AVR is shown to include a variety topographic features including; hummocky volcanoes, seamounts, linear ridges and lava terraces with a range of hard substrata (Smith and Cann, 1999; Searle *et al.,* 2010).

TOBI data collected through this study indicated that the AVR is situated between 45° 24'N to 45° 35'N covering a distance of 18 km and an estimated volume of 16 km^3 (assuming a flat base at a depth of 3,100m), with monotonically deepening flanks and a sharp linear crest (Searle *et al.,* 2010). The AVR is situated within an axial valley which at its widest covers a distance of 6 km. A spreading rate of 2.1 cm per year would suggest the AVR has a maximal age of 286,000 years (Saunder and Francis, 1985; Yeo *et al.,* 2011), with the northern area of the AVR expected to be older than the southern section (Searle *et al.,* 2010). Lines of volcanic cones creating narrow ridges and some spurs were observed within the AVR, however very few faults were seen (Searle *et al.,* 2010). The volcanic cones appear to be numerous and follow one of four distribution patterns 1) along the AVR 2) parallel to the crest but on the flank 3) normal to the AVR crest 4) in an arc curving from the mid-flank to the NE. Some cones were randomly distributed within or between

the defined patterns. A few fissures and some hummocky terrain as well as areas of high sedimentation in the region of 10 cm thick were also observed from the footage (Searle *et al.*, 2010; Yeo *et al.*, 2011; personal observation). Areas with differing degrees of sedimentation are expected to be related to local topography and flow rather than the age of the lava (Searle *et al*., 2010), with slower flowing areas having increased sedimentation rates.

More than 3,000 hummocky volcanoes built almost entirely of basalt lavas were observed using side-scan sonar throughout the AVR ranging in diametre of 5 – 450 m (Yeo *et al.*, 2011). Most of the small hummocky volcanoes recorded within this AVR are monogenetic, volcanic edifices (Yeo *et al.*, 2011). Yeo *et al.* (2011) found that around a third of the hummocks observed along the AVR had collapsed losing 40 % of their volume, converting the hummocks into talus slopes, and thus creating a new habitat type for organism colonisation.

2.1.2 Water masses at 45°N

At 45°N in the Western basin of the Atlantic the general hydrographic regime roughly consists of surface water down to 1000 m, Antarctic Intermediate water from 1,000-1,700 m followed by North Atlantic Deep Water, of which there are two distinct layers the top (1,700-2,800 m) originating from the Labrador Sea and the bottom layer (2,800-4,000 m) originating from the Greenland Sea. There is also a slight input of Eurafrican Mediterranean water into the basin at around 1,000 m. Below 4,000 m depth, as with all Atlantic deep basins, Antarctic Bottom Water dominates (Matthias and Godfrey, 2003).

Very little work has been completed on the water flows along AVRs. Thurnherr *et al.* (2002) investigated the flow and mixing in the rift valley of the Mid-Atlantic Ridge. They

found that tidal motion was present within the valley at 36 25°N creating an isopycnal deviation of 50-100 m, with the fastest velocities occurring in deep sites near the sill of the valley, where the water tumbles over into the AVR. These tidal velocities varied between 0.03 and 0.04 ms^{-1}, with a general slight decrease with depth. Rossby waves, waves which move along the thermocline, were also observed within the valley creating small oscillations in the water flow. Thurnherr *et al.* (2002) characterised the area around 36 °N as containing monotonically increasing salinities and temperature in a North-Eastwardly direction, this was in agreement with Saunders and Francis, (1985) previous work on temperature. The main inflow of water into the valley is from the Eastern flank of the ridge, creating a unidirectional flow (Thurnherr *et al*., 2002). However the area between 40°N and 50°N in the Atlantic has been described as an area with strong eddy flows, with valley flushing events occurring at regular intervals. These events are most likely to be a result of gravitational convection at the sills, with tidal motions modulating the spilling of cold-water into the axial valley. Once the cold-water has spilled into the valley, warmer water will become up-welled (Saunders and Francis,1985). Data collected by Saunders and Francis, (1985) suggest that, along the 45°N segment of the MAR, the sills rise to a depth of 2,650 m. However, Searle *et al.* (2010) found that the AVR is hourglass in shape with a sill at 2,850 m present at 45 29°N, 500 m above the median depth of the seafloor in this region. This ridge creates what is almost a basin-like shelf with a high lip at one end, which is suspected to be important for the water flow within the AVR.

Water flow into and out of an AVR at 29 °N along the MAR, containing the hydrothermal vent Broken Spur, was investigated by Murton *et al.* (1999). They used a "Bath-tub" experiment where the inflow and outflow of water along the AVR was monitored with the objective to determine the rate and volume of water flow though the AVR. They found that depths below the Axial Valley walls acted as a partially enclosed system trapping water in the AVR system for a longer time than if it was an open system (29 °N had a water residence time of approximately 262 days within the AVR, followed by a flushing event). Between flushing events the water will slowly warm and homogenise the old and new deep

water (Saunders and Francis, 1985; Murton *et al.,* 1999). Murton *et al.,* (1999) found that the rugged topography of the AVR meant that the hydrothermal products created by the Broken Spur vent site were accumulated in the water column enclosed in the AVR.

The MAR has had very little biological studies completed within it and in situ studies of coral distribution at depths >2,500m globally are scarce (Gebruk *et al*., 2010). Therefore it is important to obtain any information from this site, despite the footage not being ideal for biological investigation, as it was primarily collected for geology. The variety of habitats present on the AVR provides an ideal setting in which to investigate how different substrata and other expressions of topography, particularly slopes, influence coral distribution and assemblage structure..

2.1.3 Aims

Very little biological exploration has occurred at 45°N in the Northern Atlantic. An opportunity arose to use ROV *Isis* to collect video footage of the AVR at 45°N to analyse the coral assemblage present. This study will focus on the hydrozoan family Stylasteridae and the anthozoan taxa Antipatharia and all Octocorallia, including sea pens. No species of Scleractinia or Zoanthidae were observed. The aim of this chapter is to determine if depth, substratum or slope have an effect on cold-water coral assemblages along the AVR at 45°N. This will be achieved by addressing the following objectives:

1- Analysis of all video footage available for the AVR at 45°N identifying Octocoral species noting: density, position, depth and substratum type.
2- Use positional data to create a density map and slope map of the Octocoral observed within the AVR, to allow distribution patterns to be ascertained.
3- Use statistical methods (ANOSIM and SIMPER) to determine if depth or substratum type has an effect on the Octocoral assemblages observed.

2.2 Materials and methods

2.2.1 Data collection

Observations of the seabed were taken with video and still imagery using the ROV *Isis* (Figure 2.1) during RRS *James Cook* cruise 24 (JC24) in June/July 2008 to the Mid-Atlantic Ridge at approx 45° 30' N. A total of 14 dives were completed of which 10 (Table 2. 1) provided imagery of sufficient quality for analysis.

Isis is fitted with multiple cameras, which are used for piloting and scientific purposes. For JC24 the scientific cameras comprised of a fixed Atlas 3-chip camera with a 14x optical zoom, the Pegasus pan and tilt camera, which both record onto DVCAM tapes and DVD, and the Scorpio 3.34 mega-pixel digital still colour camera. In order to obtain video footage, the sea floor is illuminated by two 600 J strobe lamps, five 250 W incandescent lamps and three HMI 1,200 W lamps (http;//www.noc.soton.ac.uk/nmf/sea_sys_index.php?page=isis).

2.2.2 Image analysis

The video footage was analysed using computer package U-lead Video, version 10. Each video was watched in its entirety with the occurrence of any individual organisms being noted along with the time, depth and substratum type. Although laser scales are used in conjunction with video on *Isis*, it was not always possible to view where they mark the seabed, due to changes in ROV altitude (Table 2. 2), making the area of the field of view hard to determine. It was therefore decided to analyse the images in terms of time, as during transect mode *Isis* travelled at a speed of 0.1 knots (5 cm s^{-1}), rather than area.

Table 2. 1. Date, positions and depths recorded by ROV Isis during JC24 video dives

Dive no	Date	Start Longitude (W)	Start Latitude (N)	End Longitude (W)	End Latitude (N)	Dive Duration (Hours)	Max depth (m)
80	1/6/08	27.8768	45.4028	27.8727	45.4803	31	3000
81	2/6/08	27.7854	45.7158	27.7981	45.6422	38	3600
82	4/6/08	27.7984	45.6423	27.8422	45.6040	23	3576
83	5/6/08	27.8982	45.5563	27.8855	45.5463	14	3341
84	7/6/08	27.8859	45.5465	27.8571	45.5303	18	3176
88	14/6/08	27.910	45.4383	27.41	45.41	31	3271
89	16/6/08	27.8027	45.575	27.8077	45.5961	31	3523
90	17/6/08	27.8066	45.5964	27.8394	45.6025	14	3304
92	19/6/08	27.9086	45.4866	27.8658	45.4811	43	3118
93	21/6/08	27.8433	45.4877	27.9	45.49	31	3109

Each dive took place along the MAR at 45°N with video footage being recorded by the ROV Isis during 2008. Degrees are in decimal degrees. Coral assemblages were recorded between 2,600 m and 3,600 m.

Figure 2.1. ROV Isis being deployed from the side of the RRS James Cook during JC24. It is possible to observe the pilot cameras at the front of the vehicle and rock collecting compartments.

Table 2. 2. ROV Isis altitude data from JC24 dives.

Dive no	Mean altimetre height (M)	Maximum altimetre height (M)	Minimum altimetre height (M)
80	3.7	13.4	0.75
81	3.1	9.8	0.75
82	2.9	8.7	0.75
83	3.1	8.4	0.75
84	3.4	10.9	0.75
88	2.7	7.7	0.75
89	2.2	11.1	0.75
90	3.2	10.2	0.75
92	3.5	9.8	0.75
93	3.3	9.6	0.75

It must be noted that these values may not be 100% accurate as the altimetre appeared to be faulty with the raw data containing jumps. To negate these jumps zeros and unreasonably high values were deleted.

2.2.3 Data analysis

2.2.3.1 Map creation

2.2.3.1.1 Density Map

All data were collated and formatted for compatibility with ESRI ArcGIS. A single bathymetric map was created from TOBI (Towed Ocean Bottom Instrument) data collected during the cruise. Once video analysis was complete, latitudes and longitudes were assigned to each observation by identifying the time of observation in the *Isis* data string. Depth was also obtained in this manner. A density map was subsequently created by calculating the distances between observations using the following formula to convert degrees to metres;

$$\text{Distance} = 1.8520 * 60 * \sqrt{((\cos(\text{dlat}/2) * \text{dlon})^2 + (\text{dlat}^2))}$$

Where 1.8520 is the conversion of nautical miles to KM and 60 is the conversion for degrees to nautical miles

This gave the result that each 0.01 degrees of latitude travelled corresponds to 99 m and each 0.01 degrees in longitude corresponds to 111 m. From this information the distance between coral sightings was calculated using the following formula where x = latitude and y = longitude;

Distance= $\sqrt{((x1-x2)*111)^2+((y1-y2)*99)^2}$.

Data were then grouped into 100 m transect bands, creating a density per 100 m transect.

The data were transferred to a comma-delimited MS Excel file and transferred into Arc GIS using ET GeoWizzard. Once in ArcGIS, a graduated colour scheme was applied to allow the difference in coral density to be visualised (Figure 2.3).

2.2.3.1.2 Slope map

A slope map was created using the computer programme Erdas imagine v9.3. This was achieved by performing a topographical analysis on the area bathymetry. Black was used to represent flat ground, with white representing the steepest slopes. The resulting raster file was then imported to Arc GIS. Substratum type was divided into "sediment", "mixed sediment and rock" and" rock" (including both flat rock and rock slope) and overlaid onto the slope map. The occurrence of Whip corals, Spiral corals and *Isididae n. sp*. 1, as well as complete coral density was overlaid on the map.

2.2.3.2 Random sampling

Data were sorted into depth bands (200 m) for each dive. As a result of *Isis* moving along the AVR the time spent in each depth band was not continuous. Therefore five minute continuous segments were taken from each dive, at each depth band and combined to make one 50 minute segment which was used for analysis. This results in one 50 minute segment per dive, per depth. This procedure was repeated for substratum types, resulting in one 50

minute segment from each dive for each substratum present (flat rock, sloped rock, sediment and mixed sediment and rock).

2.2.3.3 Multivariate analysis

Multivariate analysis was carried out with PRIMER v6. A fourth- root transformation was used to reduce the effect of the dominant species on the faunal abundance data analyses (Clarke and Warwick, 1994) allowing SIMPER (Similarity Percentages- species contributions) to be employed to investigate which species are responsible for the changes in assemblage structure between variables. A Bray-Curtis resemblance was applied allowing ANOSIM (Analysis of Similarity) to analyse for both depth and substratum type. Multi-dimensional scaling (MDS) was also used to provide a visual representation of the data. MDS ordinates were plotted against substratum type. Kruskal-Wallis test was carried out on the measn number of individuals observed per substratum type.

ANOSIM and MDS plots were also carried out for both non-transformed data and square-root transformed data, as well as for rare taxa only (less than 30 occurrences throughout the sampling) and common taxa. The conclusions from these different approaches were in agreement, indicating that they are robust and driven by the common taxa, thus do not need to be included in the results section.

2.2.3.4 Cumulative frequencies

Cumulative frequencies of substratum types as well as the number of corals from the top 3 species responsible for the assemblage structure differences, as identified by SIMPER, were plotted against depth.

2.3 Results

2.3.1 Environmental setting

The AVR is situated to the South-West of the UK at 45°N 27°W along the MAR, (Figure 2.2). The sea-floor along the AVR included areas of sediment as well as exposed rock, including basalt pillows, lava sheets, rubble and sheer walls, with varying levels of sedimentation. Throughout the dives rock piles, rock walls and a flat-topped seamount provided sloped rocky areas. The dominant sediment type observed was sand with some pteropod shells whilst the dominant hard substratum was pillow basalts.

Fauna observed in the videos, other than corals, included; echinoids, ophiuroids, holothurians, crinoids and fishes. It was evident purely from observation that the sandy areas upon the AVR held the majority of the holothurians, with echinoids and ophiuroids tending to increase in areas with exposed rock. No reef systems or coral gardens were observed during this study, but some areas of increased coral abundance were seen.

Ten usable dives (a usable dive being where it was possible to clearly view the substratum without a high sediment load in the water), were completed, resulting in 258 hours of usable footage (Figure 2.3, Table 2. 1). These dives spanned a depth range of 2,600 to 3,600 m within the AVR. Throughout the dives five different substrata classifications were identified; flat rock, rock slope, mixed substratum, sediment and sedimented slope.

There was insufficient footage of sedimented slope throughout the survey to allow reliable analysis and therefore it was removed from further analysis. There was no evidence of any hydrothermal deposits in the study area, although slight plumes were detected using Mapper tow-yos.

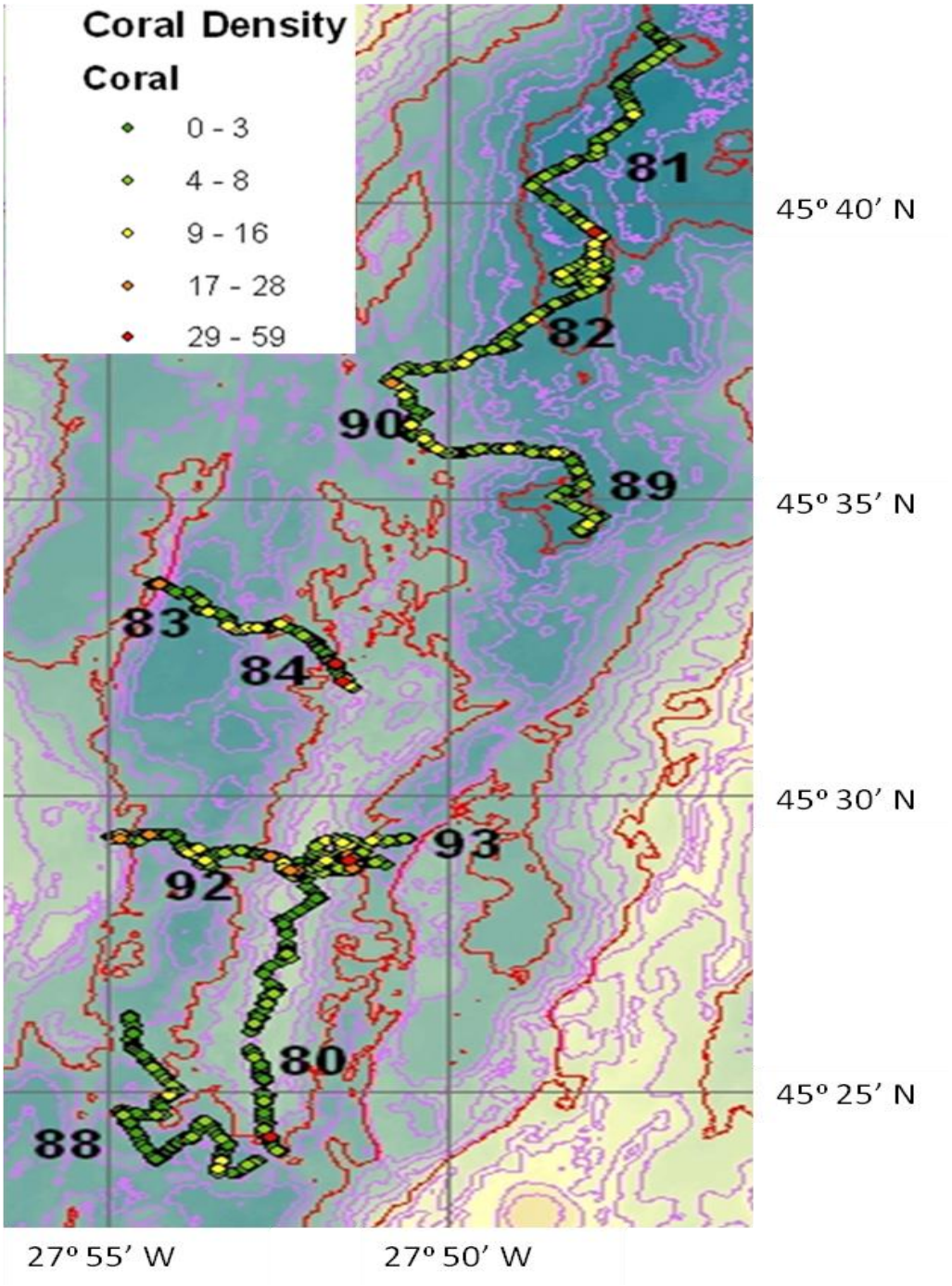

Figure 2.2. Location of AVR within the Atlantic and Density per 100m ^{2} and Distribution of Corals identified during JC24. The AVR is situated to the South-West of the UK and Ireland along the Mid-Atlantic Ridge. Numbers on the map representing ISIS dive numbers. Each dot represent a 100 m transect along the AVR with colour gradation indicating density of corals found along the transect.

2.3.2 Distribution and abundances of coral

Throughout the dives 20 putative species of coral (Table 2. 3, Figure 2, Appendix 1) were identified from the video data totalling 3,188 individuals. Where the camera was too high above the sediment, it was not always possible to distinguish between *Radicipes* and Spiral black coral, so these were grouped together under the heading Spiral coral, which is included in the family Chrysogorgiidae. Of the 20 assigned species the most common, occurring in all dives, was the whip coral (Figure 2.3a), which accounted for 2,244 individual observations. The second most abundant was *Isididae n. sp. 1*. (Figure 2.3b) and the least abundant being *Paragorgia* (2.3c) found only once. Dive 92 yielded the highest number, with 695 corals being observed. The lowest number of individuals (151) was observed during dive 83. The highest density of individuals per 100 m^2 (29-59) occurred on five points throughout the study each corresponding with a topographic peak (Figure 2.2 and Figure 2.9). The lowest density of individuals occurred along the central valley or spine of the AVR, were there is little or no slope (Figure 2.2). Intermediate densities were observed on the flanks (Figure 2.2).

2.3.3 Depth and distribution

Of the 21 coral species identified 8 occur in all 200 m depth bands. Individual depth bands contained similar numbers of species with 16 species being found in the 3001-3200 m band, 15 species in both the 2601-2800 m and 3401-3600 m bands, 14 in the 2801-3000 m and the least number of species (11) being found in 3201-3400 m depth band (Table 2. 3). Multivariate analysis of assemblage differences with depth revealed no obvious depth segregation (Figure 2.4). No significant difference was observed in the overall coral assemblage composition in different 200 m depth intervals (ANOSIM, N=25, R=0.102, P=0.13) (Table 2. 4. As a result, depth was not considered as a co-variant in subsequent analysis.

Table 2. 3. Coral species observed and their presence and absence within given depth range .

Taxa	**2601-2800m**	**2801-3000m**	**3001-3200m**	**3201-3400m**	**3401-3600m**
Subclass Hexacorallia					
Order Antipatharia					
Family Schizopathidae					
Bathypathes sp. 1	+		+	+	+
Subclass Octocorallia					
Order Gorgonacea					
Family Unknown					
White gorgonian	+	+	+	+	+
Gorgonian fan 1			+		
Whip Coral	+		+	+	+
Fluffy Whip Coral	+	+	+		+
Order Alcyoniina					
Family Alcyoniidae					
Anthomastus sp.	+	+			
Order Scleraxonia					
FamilyParagorgiidae					
Paragorgia sp.	+	+	+	+	+
Order Calcaxonia					
Family Chrysogorgiidae					
Chrysogoria sp. 1	+	+	+	+	+

Iridogorgia sp.	+	+			
Spiral coral	+	+	+	+	+
Family Isididae					
Isididae n. sp.1	+	+	+	+	+
Bamboo coral 1	+	+	+	+	+
Bamboo coral 2		+	+	+	
Family Primnoidae					
Narella sp. 1	+	+	+	+	+
Order Pennatulacea					
Family Pennatulidae					
Yellow Pennatulid					+
White Pennatulid			+		+
Pink Pennatulid			+	+	+
Brown Pennatulid	+	+			+
Umbellula sp.	+		+		+
Subclass Hydroidolina					
Order Anthoathecata					
Family Stylasteridae					
Stylasterid sp. 1	+	+	+		

+ indicates the presence of a species within the given depth band.

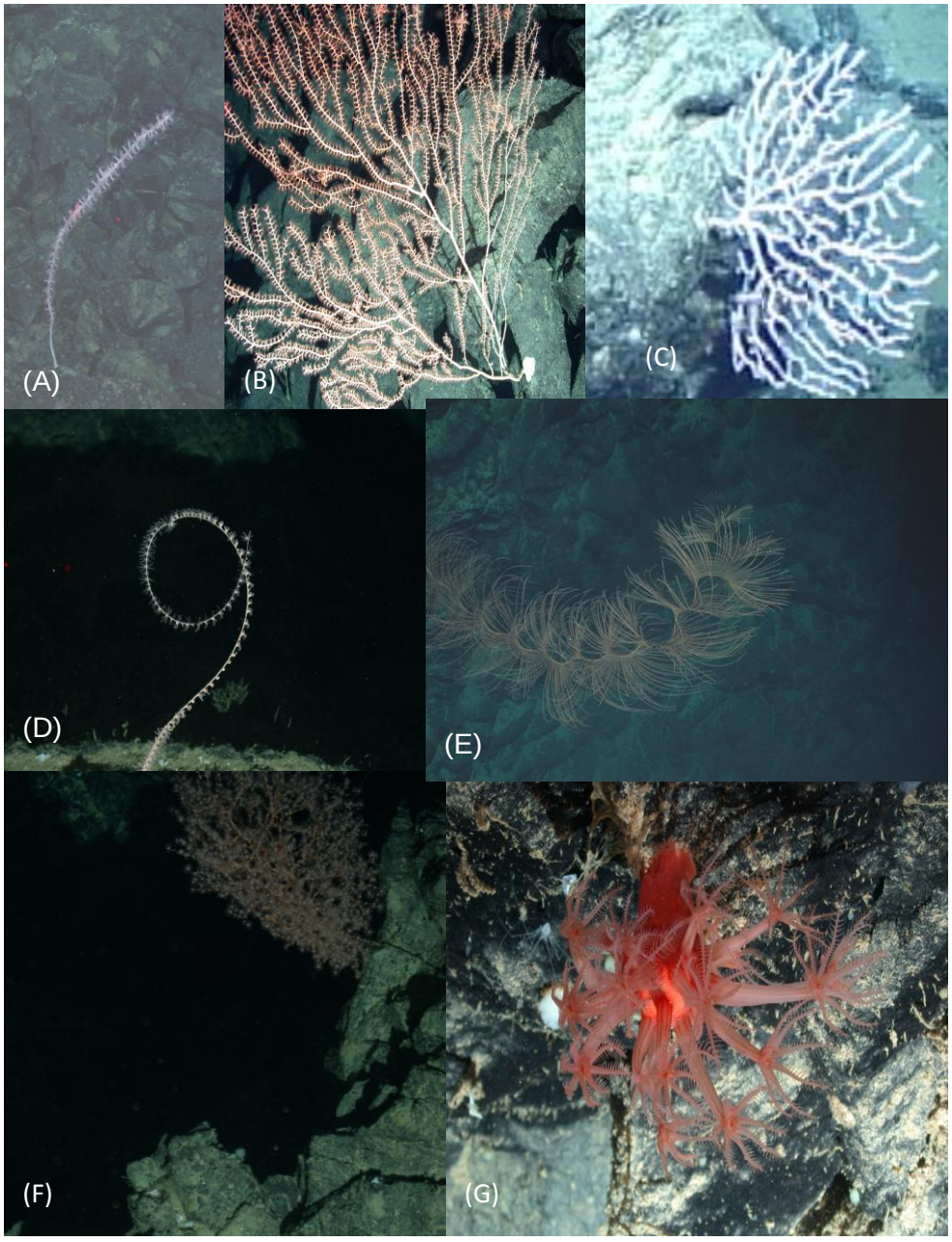

Figure 2.3. Subsample of Coral species found throughout the JC24 cruise (A) Whip corals (~70 cm) (B*) Isididae n. sp. 1 (190 cm) (C)* Paragorgia *sp.(~45 cm) (D) Spiral Coral,(~55cm) (E)* Iridogorgia *sp (~175cm).* (F) Chrysogorgia *sp (~40cm).* (G) Anthomastus sp. (~10cm). *It is not possible to include scale bars due to the lack of laser point visualisation throughout the dives therefore reough estimations of size have been given. Further examples can be found in electronic Appendix 1 Figure Ap1.1*

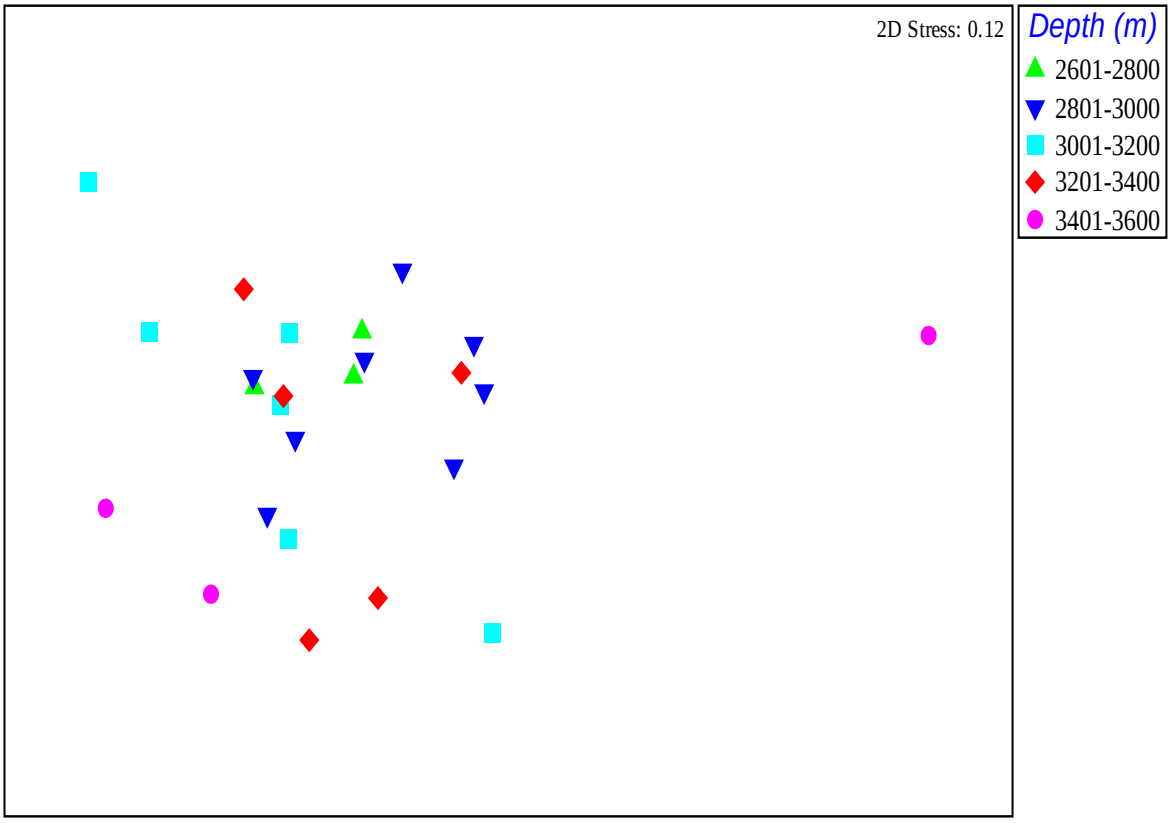

Figure 2.4. MDS ordination of coral assemblage structure at different depth bands. Each symbol represents 50 minutes of video footage (comprised of ten 5 minute continuous segments) from a single dive in the corresponding depth band. Further information can be obtained in Appendix 1 Table ap1.1 N=25

Table 2. 4 Results of ANOSIM tests comparing coral assemblage composition from 200 m depth strata across JC24 dives N =25

Global R=0.102 **P=0.13**	**2601-2800m**	**2801-3000m**	**3001-3200m**	**3201-3400m**
2801-3000m	R=-0.374 P=1.0			
3001-3200m	R=-0.16 P=0.75	R=0.168 P=0.07		
3201-3400m	R=-0.231 P=0.92	R=0.007 P=0.45	R=-0.101 P=0.81	
3401-3600m	R=0.296 P=0.10	R=0.669 P=0.006	R=0.247 P=0.17	R=0.303 P=0.14

R levels below 0.4 considered to have no difference

R levels >0.4 and <0.7 considered to be the same as they are different

R levels >0.7 considered different

P values <0.05 considered significant

2.3.4 Coral Distribution and Substratum type

Time normalised data showed that within each 50 minute observation period, the highest mean number of individuals occurs on rock slope (46.4 ± 8.3), with more than ten times the number observed than on sediment (4.4 ± 0.67). Coral densities are higher on flat rock (29.2 ± 4.4) than on mixed substratum (23.8 ± 2.96) (Figure 2.5). This was shown to be a significant difference at the 10 % level (Kruskal-wallis, N=27, DF=3, P=0.08)

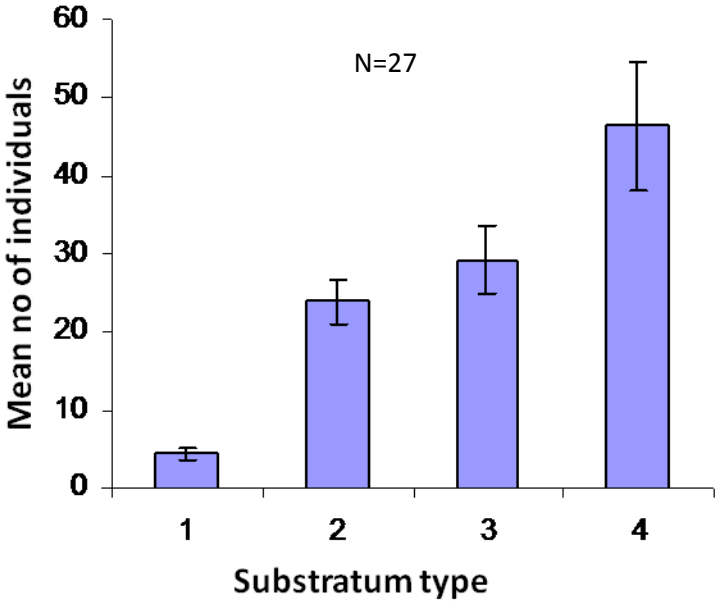

Figure 2.5. Mean number of individual corals observed over 50 minute time period on different substrata types from the JC24 dives.1= Sediment, 2= Mixed sediment and rock, 3= Flat rock, 4= Rock slope. Error bars indicate standard deviation from the mean and n= 27

Mixed rock and sediment has the highest overall percentage of Alcyoniidae, Gorgonacea sp, Primnoidae, Pennatulidae and Whip coral in comparison to the other substratum types (Table 2. 5). Sediment shows the second highest percentage of Pennatulidae. Neither flat rock nor Rock slope show any dominance of the families despite being shown to have a higher number of individuals per 50 minute segment (Figure 2.5, Table 2. 5). However, it must be noted that different amounts of time were spent in each substratum type over the entirety of the survey, thus this type of analysis can lead to a false impression of the dominance unless normalised. Considering the percentage of individual species within the assemblage per single substratum type is more effective (Table 2. 6).

Table 2. 5. Percentage Coral assemblage composition based on coral type

	Mixed substratum	Flat Rock	Sediment	Rock Slope
Schizopathidae	92.30	0	0	7.69
Stylasteridiae	20	0	0	80
Gorgonacea spp.	61.86	18.93	0	19.17
Whip coral	57.41	15.76	2.98	23.83
Alcyoniidae	66.66	0	0	33.33
Chrysogorgiidae	47.74	7.09	14.19	30.96
Isididae	49.52	21.09	1.65	27.72
Primnoidae	55.81	13.95	2.32	27.90
Pennatulidae	62.06	1.72	31.03	5.17

Coral species have been placed into families except for the Gorgonian species for which the family is unknown; these were grouped together as Gorgonacea apart from the whip coral which was separated due to high abundance.

Table 2. 6. Percentage Coral assemblage composition based on Substratum type

	Mixed substratum	Flat rock	Sediment	Rock slope
Schizopathidae	0.69	0.00	0.00	0.12
Stylasteridiae	0.06	0.21	0.00	0.36
Gorgonacea spp.	2.06	2.28	0.00	0.61
Whip coral	73.23	70.60	57.76	69.01
Alcyoniidae	0.38	0.00	0.00	0.36
Chrysogorgiidae	3.88	2.28	18.10	6.30
Isididae	16.57	23.19	7.76	20.70
Primnoidae	1.19	1.24	0.86	2.06
Pennatulidae	1.94	0.21	15.52	0.48

Coral species have been placed into families except for the Gorgonian species for which the family is unknown; these were grouped together as Gorgonacea apart from the whip coral which was separated due to high abundance.

When the whole coral assemblage composition is considered, clear differences can be seen in the percentage contribution at the higher taxon level between the different substratum types (Table 2. 6). Throughout all four substratum types, whip corals are the most abundant. The next most abundant family is the Isididae, followed by the Chrysogorgiidae, except in the sediment assemblage where both Chrysogorgiidae and the Pennatulidae are more abundant than the Isididae. The Pennatulidae has a low percentage contribution in all other substratum types. The sediment substratum supported the fewest families, among which the Alcyoniidae, Schizopathidae, Gorgonacea, and Stylasterida were absent. Only the Alcyoniidae and Schizopathidae were unrepresented on the flat rock substratum with all other families present. These differences indicate that the sediment assemblage structure is distinct from the others.

Multi-dimensional scaling (Figure 2.6) shows the sediment assemblages separated from the other substratum type assemblages, with the exception of one mixed substrata sample, (which had a relatively high sediment content). There was no significant difference in the overall assemblage composition among substratum types (ANOSIM, N=27, Global R=0.295, P=0.002) (Table 2. 7).

Despite this when pairs of substrata are considered, a clear significant difference (ANOSIM, N=27, R=0.761, P=0.001) is observed between rock slope and sediment. SIMPER analysis indicated that 75 % of the dissimilarities between these substratum types can be accounted for by the whip coral, Isididae n. sp. 1, bamboo coral A, *Chrysogorgia* sp. and Spiral coral. Assemblage differences were also observed between between flat rock and sediment (ANOSIM, N=27, R=0.621, P=0.002). Isididae n. sp. 1. whip coral, Spiral corals, *Narella* sp. and fluffy whip, together account for 73 % of the difference between the two assemblages (SIMPER). This suggests that the presence or absence of whip corals, Isididae n. sp. 1 and Spiral corals is important in determining the assemblage structure along the AVR.

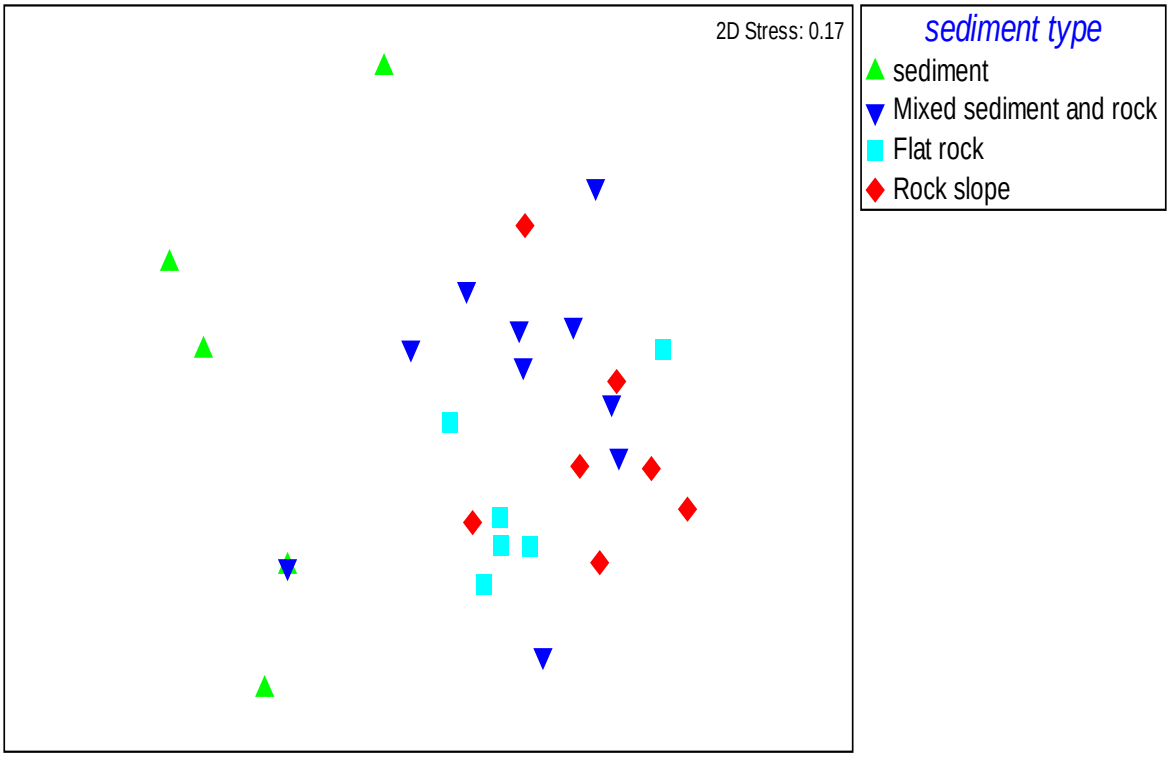

Figure 2 6. MDS ordination of coral assemblage structure from different substrata types across JC24 dives. *Each dot represents 50 minutes of video footage (comprised of ten 5 minute continuous segments) from a single dive in the corresponding substratum type. Further information can be obtained in Appendix 1 Table ap1.2 N=27*

When the MSD x co-ordinates were plotted against substratum type (Figure 2.7) it can be seen that there is a general shift from negative co-ordinate to positive co-ordinates with an increase in the habitat complexity, indicating habitat complexity has a marked effect on the assemblages present. However a few outliers are evident with flat rock having one largely positive co-ordinate and mixed substratum contains a negative outlier. These may be explained by a slight change in the exact substratum type i.e. an increase in boulders or an increase in sediment within the area.

Table 2. 7. Results of ANOSIM tests comparing coral assemblage composition upon different substrata across JC24 dives. N = 27

Global R= 0.295 P=0.002	**Sediment**	**Rock**	**Rock slope**
Rock	**R=0.621 P=0.002**		
Rock Slope	**R=0.761 P=0.001**	R=0.136 P=0.11	
Mixture substratum	R=0.541 P=0.002	R=0.103 P=0.17	R=0.136 P=0.11

Significant difference are highlighted in bold

R levels below 0.4 considered to have no difference

R levels >0.4 and <0.7 considered to be the same as they are different

R levels >0.7 considered different

P values <0.05 considered significant.

A cumulative frequency graph for the three species identified as most important in the determination of assemblage composition by SIMPER, (whip corals, Isididae *n. sp. 1* and Spiral corals) and substratum type (Sediment, mixed sediment and rock and rock), with depth shows an increase in sediment below 3,500 m indicating an increase in sediment at depth along the AVR (Figure 2.8). The largest increase in flat rock occurs between 2,900 m and 3,200 m, with Rock slope having a sharp increase between c 3,050 and 3,150 m. Mixed rock and sediment increases reasonably uniformly from 2,600-3,200 m, however 3,200-3,500 shows a decline in the occurrence with a sharp incline from 3,500.

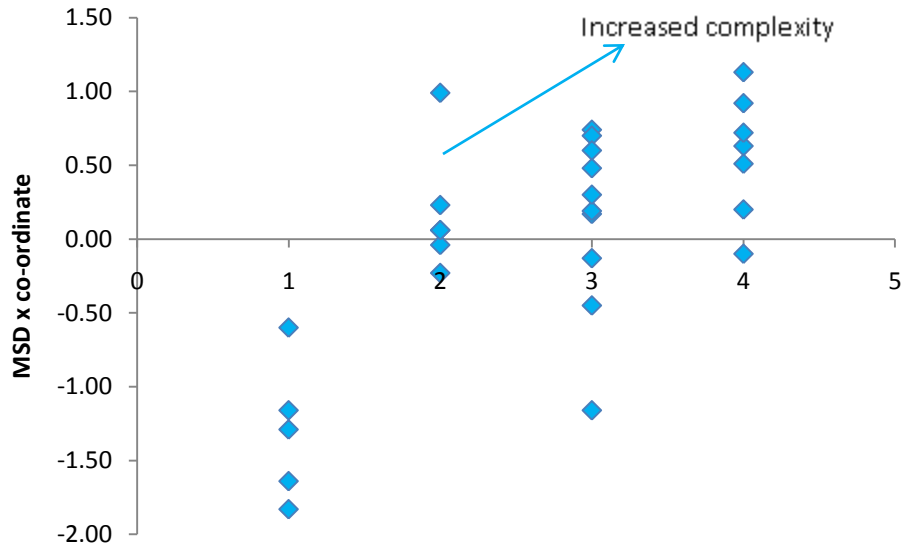

Figure 2.7. MDS x ordinate against substrata type. Each point represents a dive within that substratum type 1= sediment 2= flat rock 3= mixed substratum 4 = sloped rock

Whip coral occurrence closely follows that of mixed rock and sediment with Isididae n. sp. 1. following sloped rock closely in the shallower depths and then increases with flat rock at deeper depths. Spiral coral is absent between 2,700- 2,850 and 3,200-3,450 mirroring the absence of sediment substratum. There is a sharp increase in the Spiral coral at 3,500m where sediment increases (Figure 2.8). These results support those from the changes in the assemblage structure dependent on substratum type.

2.3.4 Assemblage structure and slope

The AVR contains many steep walls were the inclination reaches over 80 % in some areas, creating sheer faced walls (Figure 2.9). The steepest walls tend to occur South East of the AVR. Three circular patches with dark centres indicate small flat-topped hummocks. It can be seen that the AVR walls into the valley show a high level of rugosity, with the presence of darker areas.

Slope maps were generated for the three species identified as most important in the determination of assemblage composition, (whip corals, Isididae n. sp. 1 and Spiral corals) and substratum type (Sediment, mixed sediment and rock and rock) (Figure 2.9). Figure 2.9a shows a higher level of sediment in the Southern AVR, with rock cover increasing to the North. Mixed sediment and rock is found throughout the AVR and is the dominant substratum type. Whip corals are observed throughout all the dive transects and across all substratum types. The highest number of whips (9-13) observed occurred in three areas, two of which were mixed substratum areas and the third on rock substratum, with two occurring on slope and the other near a drop off (Figure 2.9b). Sediment contained the least amount of whips. Isididae n. sp. 1 (Figure 2.9c) did not occur in patches higher than two individuals throughout the whole AVR, mainly occurring as individuals. The highest density of Isididae n. sp. 1 occurred on rock and mixed substratum, associated with slopes down the Western flanks of the AVR. Spiral corals were observed less frequently than both whip and Isididae n. sp. 1 throughout the AVR (Figure 2.9d). Spiral coral occurrence generally coincides with sediment and mixed substratum, meaning that they are more prevalent within the Southern AVR. Reduced slope also appears to be more favourable for the Spiral coral, occurring on small dark patches within the slope map.

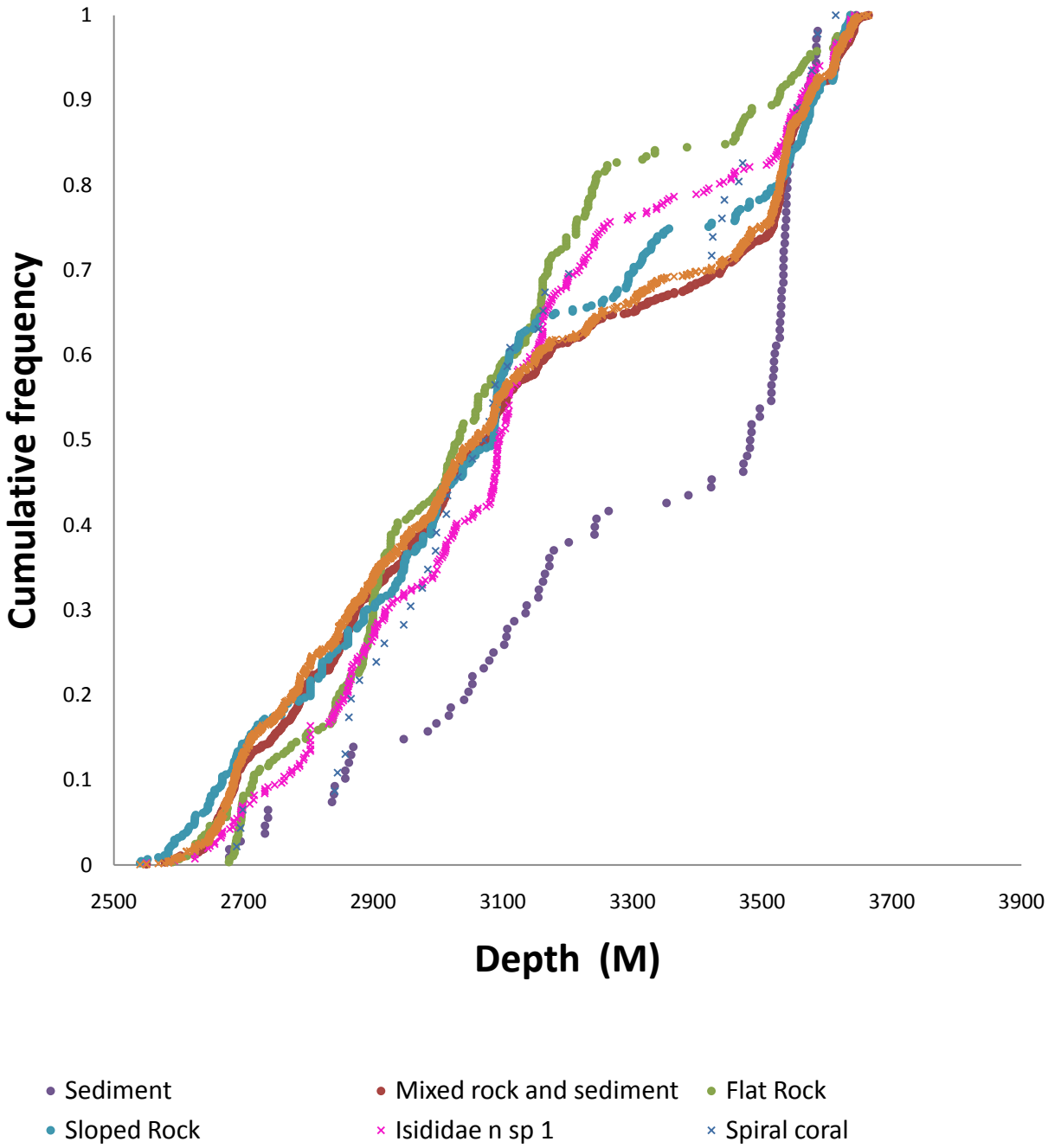

Figure 2.8. Cumulative Frequencies of substratum type and Whip coral, Spiral coral and Isididae n.sp 1 with depth from JC24.The three coral species were chosen as a result of their occurrence in SIMPER tests as species which caused dissimilarity between substratum types.

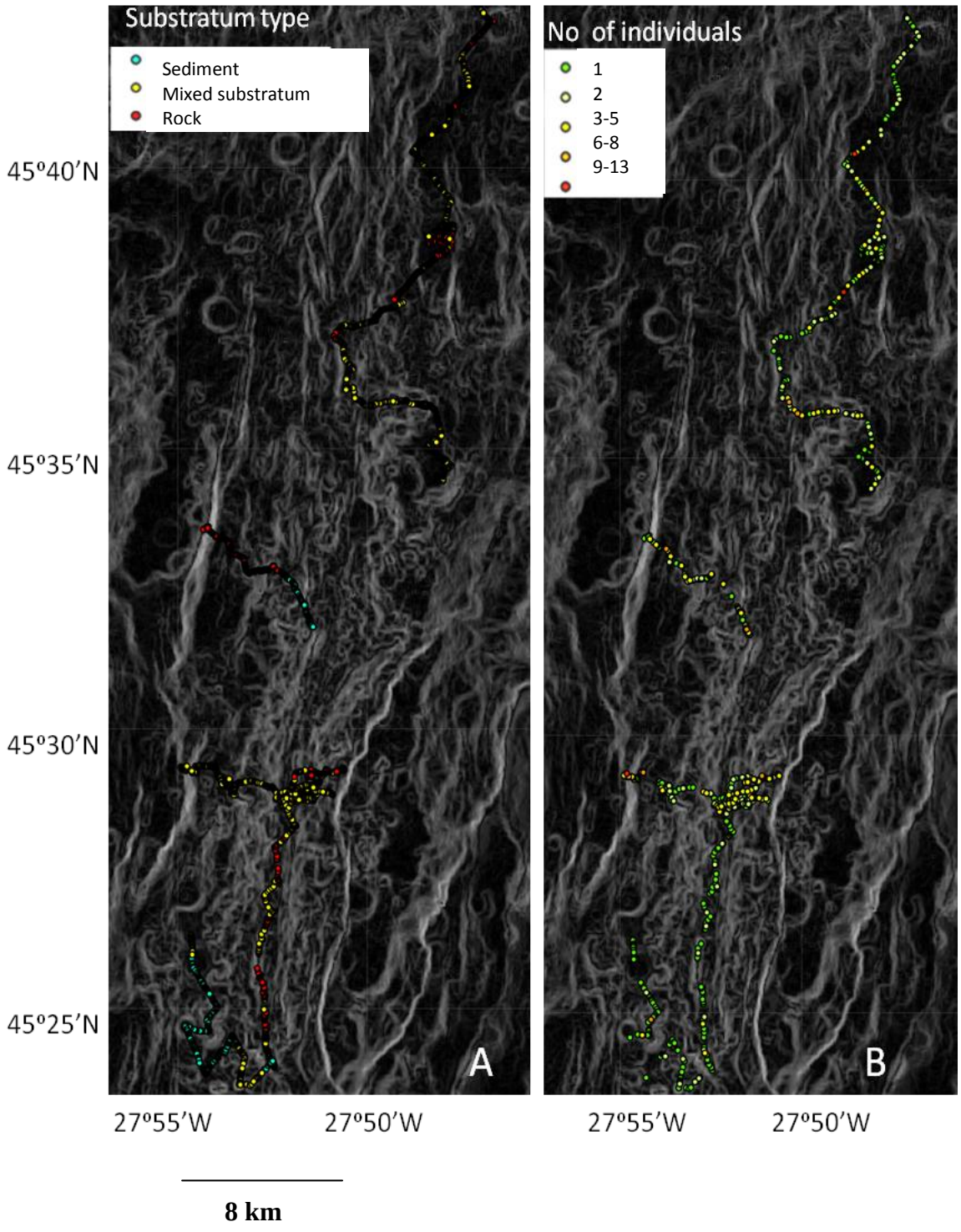

Figure 2.9. Slope, substratum type and distribution of Whip, Isididae n. sp. 1 and Spiral corals along 45°N. A, shows substratum type, B shows distribution of whip corals,

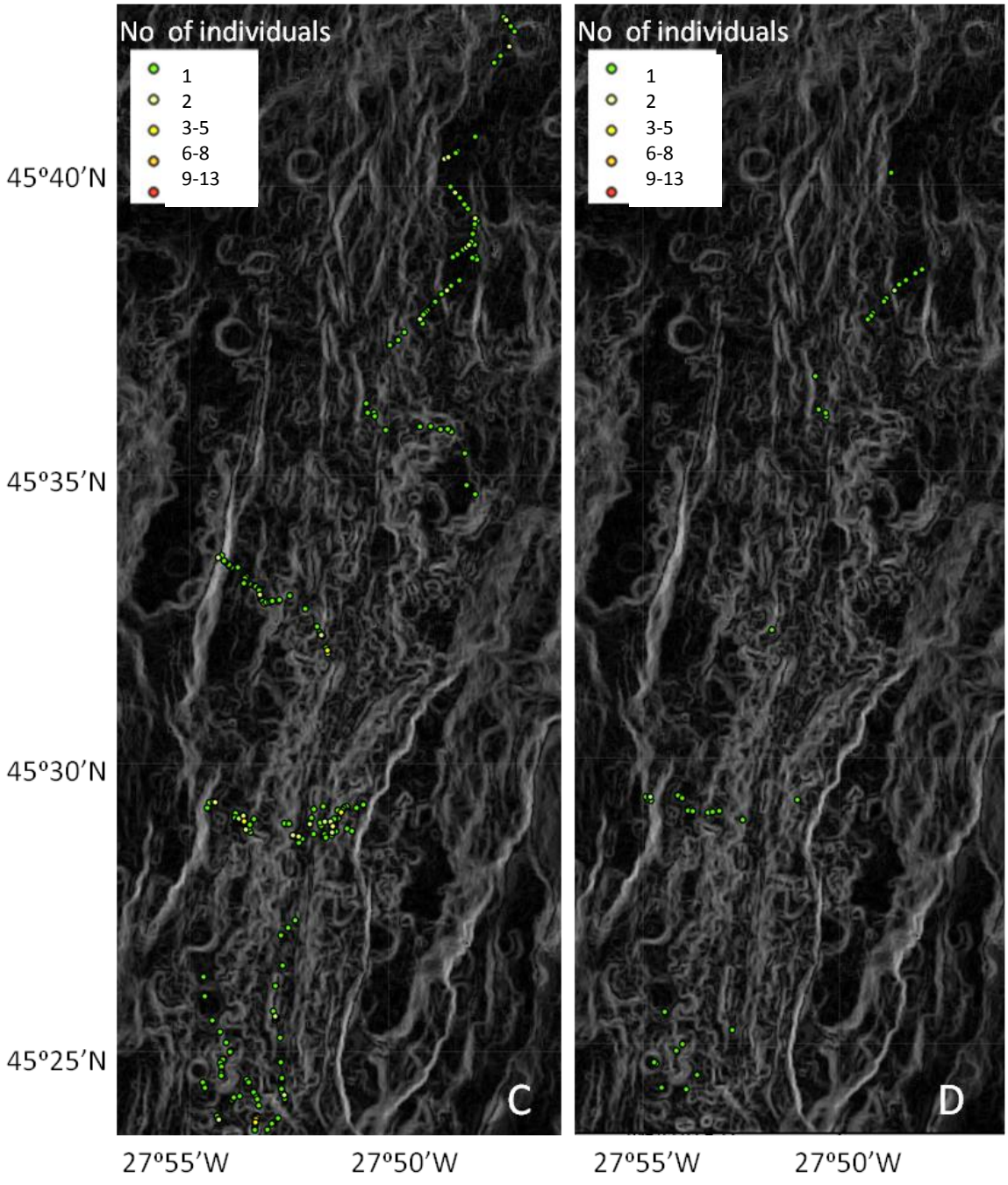

C, distribution of Isididae *n. sp. 1 corals and D distribution of Spiral corals. Where the map is lighter in colour indicates a larger degree of slope associated with the substratum and dark colours indicate a flatter surface.*

2.4.Discussion

2.4.1 Depth

Depth has often been seen asa key parameter determining marine organism assemblage structure, with increasing pressure expected to cause a change in the organisms that are able to thrive (Bianchellie *et al.*, 2010). Within this study it was found that there was no difference in the coral assemblage structure dependent on depth, over the range examined (Figure 2.4). It is possible that this may be attributed to the unequal sample sizes across the depth ranges. However, the cumulative data indicate that substratum type varied with depth, with increased sediment occurring at deeper depths. Corals were shown to follow substratum types closely with Spiral corals following sediment. The more dominant substratum effect could mask any weaker depth effects.

Gebruk *et al*. (2010), found 24 different coral species in a series of trawls ranging in depth from 1,237- 3,527 m across the MAR from the Azores to Reykjanes Ridge. Of the species identified by Gebruk *et al*. (2010), 8 were scleractinians, of which none were observed during the present study. The highest diversity of scleractinians occurs in the upper 1,500m of the oceans (Rogers *et al.*, 2007; Fautin *et al*., 2009; Roberts *et al.*, 2009) and it is likely that their occurrence at the depths of the present study is limited by food supply and low saturation or undersaturation of aragonite. The aragonite saturation horizon at 45°N in the Northern Atlantic is located between 2,000 m and 3,000 m depth (Orr *et al*., 2005; Guinotte *et al*., 2006). The larger area trawled by Gebruk *et al.* (2010) will also have increased the chances of encountering a higher number of habitat types and thus species than the present study. Gebruk *et al*. (2010) were not able to determine the substratum type during their study, making it difficult to compare results. The difficulties involved in identifying corals from images may have lead to an underestimation to the number of species identified during the present study, especially with the whip corals. The video footage collected during this study was primarially collected for geological study, meaning it was not ideal for biological studies with very few close ups occurring. This

makes identification difficult, the whips were likely to include Isididae but it is possible other species were also present. Samples of corals were taken when possible throughout the study but many of these were destroyed on the transit to the surface meaning very few samples were able to be identified from token specimens. However, from those which were sampled at least 4 new species of coral have been discovered and will be described in Chapter 5.

2.4.2 Assemblage structure on substratum types.

The deep-sea floor below 3,000 m occupies 50 % of earth's surface (Gage and Tyler, 1991). Much of this seafloor is comprised of fine sediments. Most earlier studies of faunal composition have concentrated on soft sediments with little known about rocky areas and even less about non-vent Mid-ocean ridges (Gebruk *et al.*, 2010). Previous studies indicate that coral density and diversity increase where there is exposed rock (Carey *et al.*, 1990; Chave *et al.*, 1991; Tyler and Zibrowius, 1992; Copley *et al.*, 1996; Mortensen and Buhl-Mortensen, 2004; Mortensen and Buhl-Mortensen., 2005; Mortensen *et al.*, 2008). Chave *et al*. (1991) identified 30 different species of coral, with only one occurring on sandy areas, the others confined to rocky substrata.

Percentage of species per substratum type gives a more accurate representation of the assemblage structure than the overall percentage of that coral species within this study. This is because there was more time spent in the mixed substratum type than any other, resulting in an increase in the number of corals observed overall. This increase in individuals observed create a false dominance over other substratum types in which less time was spent. By calculating the percentage per substratum type it is possible to account for this and illuminate patterns which would otherwise be missed.

In this study the species observed on sediment consisted predominantly of Pennatulidae and Chrysogorgiidae (largely Spiral corals). The cumulative curve demonstrates this well

with Spiral corals closely following the occurrence of sediment, showing absence where there is no sediment. The Pennatulacea is the only octocoral order adapted for living in soft sediment by virtue of the presence of a root-like peduncle (Woodby *et al.*, 2009); some Chrysogorgiidae are also known to have root like systems (Mortensen and Buhl-Mortensen., 2005; Woodby *et al*., 2009) allowing them to colonise areas of sediment.

The fact that Spiral corals were mainly observed in flat sedimented areas would indicate that they require deep areas of sedimentation for "rooting". Flat topography will often lead to slow flow rates in comparison to sloped areas (Genin *et al.*, 1989; Koslow, 2007). The reductions in flow rates will consequently allow higher levels of sediment deposition upon the flat topography in comparison to sloped areas. The increase in Spiral coral observations in the South of the AVR where flow rates are believed to be slowest (Thurnherr *et al.*, 2002), would support this.

Sediment deposition upon cold-water coral reefs (primarily *Lophelia*) has previously been shown to cause mortality (Larsson and Purser, 2011). With the reduction in flow rates in flat areas of high sedimentation, there is less chance that the sediment will be disturbed and thus a reduced likelihood that it will be deposited on the corals surface. The physical structure and flexibility of Pennatulidea and Spiral corals will reduce the ability of sediment to settle on them in comparison to more solid coral structures, making them more suitable for settlement in sediment.

Mortensen *et al*. (2008) noted that *Acanella* (belonging to Isididae) dominated some soft sedimented areas (to depths of 2,100 m) on the Mid Atlantic Ridge. In the present study we found Isididae n. sp. 1. living on the sedimented substrata, indicating that species within the Isididae are also capable of colonising sedimented areas. However, most of these corals

require a solid substratum for settlement, illustrated by the whip coral closely following the occurrence of mixed substratum. Isididae n. sp. 1 also increased with an increase of hard substratum. It is therefore possible that they are attached to small rocks that cannot be seen in the videos because they are covered in a thin layer of sediment (Watanabe *et al*., 2009; Woodby *et al.*, 2009).

It was demonstrated that flat rock and sloped rock have the highest density of corals in comparison to sediment and mixed substrata. Overall, the density of corals observed on the mixed substratum is closer (in average numbers per 50 minute time period) to rock substrata than sediment and contains both rock and sediment-dwelling species. This was corroborated by the MDS ordinates which showed that there was a change in the assemblage structure with a change in the substratum type. Sediment was the only substratum type in which all of the x ordinates are negative, indicating a less structurally complex habitat. Both flat rock and mixed substratum have a slight outlier. With the mixed substratum this outlier is more negative than the other points which could be an indication that the dive represented by this point has higher sediment content than other dives. The outlier observed in the flat rock has a higher positive x ordinate is much higher than all of the other points. This may be explained by an increase in pillow tubes or rubble in comparison to sheet rock, increasing the complexity of the habitat. The increased complexity will lead to a higher number of surfaces on which the corals are able to grow, i.e. the side of a basalt pillow, and thus is likely to lead to a change in the coral assemblage composition.

The results in this study agree with Mortensen *et al*. (2008) who found the number of coral taxa was strongly correlated with hard rocky substrata, the majority being found on the steep sides of basaltic outcrops. This study is also in agreement with Watanabe *et al*. (2009) who reported an increase in abundance of gorgonians on hard substrata. These studies indicate that the presence of rock is a major contributing factor to settlement in

deep-sea corals. However, suitable substrata are often not fully colonised (Smith *et al*., 2009), suggesting that its availability is not the only limiting factor for deep-sea corals.

The deep-sea is a food-limited environment (Smith *et al.,* 2009) where the food available to organisms is often scarce and its distribution patchy (Gage and Tyler, 1991). AVRs have been shown to accumulate hydrothermal chemicals within and above them as a result of the rugged topography and the subsequent increased flow rate over obstacles (Genin *et al.,* 1989; Murton *et al.,* 1999; Koslow, 2007). Should this ability to accumulate particles hold true for AVRs in general this has connotations in that the AVR topography can lead to the accumulation of surface derived nutrients above and within the AVR at 45°N, leading to sufficient nutrients for the corals survivals within the AVR even in areas of reduced flow and relatively reduced food availability.

The main food source in the deep-sea for corals is particulate organic carbon (POC), derived from surface production, which is transported from the surface layers down through the water column as a rain of detrital particles. The sinking rate is estimated to be in the range of 100 m per day (Deuser, 1986; Tyler, 2003). Much of the POC is eaten, recycled or dissolved during transport and the percentage of surface production reaching the seafloor therefore decreases exponentially with depth (Johnson *et al*., 2007) with <5% sinking to abyssal depths (Deuser and Ross, 1980; Lampitt and Antia, 1997; Smith *et al*., 2009). POC flux is directly related to surface production. In temperate regions it often has a strong seasonal component which is probably linked to seasonality reported in the deep-sea. Thus the food supply may control coral reproductive cycles and growth (Gage, 2003; Waller and Tyler 2005).

Reduced and patchy food supply in the deep-sea may partly explain why the density of corals found in this study is relatively low in comparison to previous studies. Mortensen *et al*. (2008) investigated waters between 800 and 2,400 m depth and found that most corals

occurred shallower than 1,400 m. According to Freiwald (2002) and Bryan and Metaxas (2006) the maximal abundance of coral occurs between 200 and 1,000 m. The present study examined a small patch of about 10 km^2 at depths between 2,600 m and 3,600 m, which probably explains the lower density compared to shallower habitats. A larger area would also have shown latitudinal and longitudinal variation (Willig *et al*., 2003) as well as variance in other biotic and abiotic variations such as oxygen availability, temperature and current regime (Levin *et al.*, 2001), which will not have as large an impact, if any, in this study. Johnson *et al*. (2007) found that between 60-70 % of variation in the standing stock of the deep-sea benthic assemblages can be accounted for by the POC flux. This leaves 30-40 % which must be accounted for by other biotic or abiotic factors, such as substratum type (previously discussed) and substratum elevation.

2.4.3 Elevation and assemblage structure

Within the study area the observed increase in density of corals on rocky slopes in comparison to flat rock is in agreement with previous studies (Copley *et al.*, 1996; Bryan and Metaxas, 2006; Mortensen *et al.*, 2008; Orejas *et al.*, 2009). This could be attributed to enhanced water flow, and hence food supply in these areas. Areas of raised topography have a profound effect on the surrounding currents, tides and internal waves, as well as providing hard substratum for the attachment of sessile organisms (Genin *et al*., 1986; Genin *et al.*, 1989; Rogers, 1994; Dower and Mackas, 1996; Koslow, 2007). Deep-sea currents are relatively weak, typically only a few centimetres per second (Thistle, 2003; Koslow, 2007). Ledwell *et al*. (2000) found an increase in the degree of mixing associated with ocean ridge abyssal hills, believed to be associated with the breaking of internal waves. It is possible that the small hills and rock walls encountered during this study behave as obstacles, which are known to lead to the creation of an accelerated and more turbulent flow on their lee side (Genin *et al.*, 1989; Dower and Mackas, 1996; Koslow, 2007).

The increased water flow over sloped (often hard) substrata (Genin *et al*., 1989; Tyler and Zibrowius, 1992; Sebens *et al*., 2003; Mortensen *et al.*, 2008; Orejas *et al.*, 2009; Woodby *et al.*, 2009) will in turn lead to an increase in local food availability (Bryan and Metaxas,

2006; Mortensen *et al*., 2008; Orejas *et al*., 2009; Watanabe *et al.*, 2009). Turbulence could also lead to a local retention of food. When the shape of the seabed, depth, impinging current and stratification meet certain conditions this can lead to the creation of Taylor columns, which can enhance vertical mixing (White and Mohn, 2004) maintaining or concentrating the supply of particulate food on which deep-sea corals feed (Frederiksen *et al.*, 1992; Boehlert and Mundy, 1993; Mullineaux and Mills, 1996; White *et al.*, 2005; Samadi *et al.*, 2006; Mienis *et al.*, 2007; White *et al.*, 2007). The resulting increase in the food supply to the corals (Genin *et al*., 1986), together with the provision of a hard substratum for attachment will tend to enhance the density of corals in a particular area.

2.4.4 Conclusion

This study has shown that within the depth range studied, depth itself had no effect on the coral assemblage composition. Coral densities and taxa numbers were higher on hard rock substratum than on sediment only substratum, with a further increase on sloped rock substratum. There was also a change in the assemblage composition dependent upon the substratum type, with mixed sediment and rock containing elements of both sediment only and rock only substrata assemblages. The increase in coral colony density on the sloped rock in comparison to flat rock probably reflects increased current flow and hence food supply on inclined surfaces.

Chapter 3: The distribution of deep-sea octocorals within the Whittard submarine Canyon.

3.1.1 Introduction

Submarine canyons are steep-sided valleys that cut across the continental margin and are common on many continental shelf edges and slopes (de Stigter *et al.,* 2007; de Leo *et al.,* 2010). They exhibit a range of morphologies from relatively shallow systems with many gullies to deeply incised sinuous valleys (de Stigter *et al.,* 2007). Canyons have been known about since the late 1800s (Dana, 1863) with cable laying projects providing impetus to determining the presence of canyons. Very little in-depth exploration of canyons occurred until the 1960s, with early explorations being limited to traditional line sounding with later works using echo-sounding techniques (Rowe, 1971). Lack of previous exploration is a direct result of technological limitations for investigations and difficulties accessing submarine canyons safely. Shepard *et al.* (1964) were able to investigate a submarine canyon below scuba diving range, using the diving saucer two man submarine. They were able to dive in the Scripps and the La Jolla canyons using a pinger and directional receiver to record location within the canyon (Shepard *et al.,* 1964). This allowed Shepard and his colleagues to observe directly the currents, tributaries and canyon walls for the first time. Such investigations proved that submarine canyons are topographically complex habitats, with a variety of bottom types (Schlachter *et al., 2*007; Davies *et al., 2*008; Tyler *et al., 2*009) ranging from exposed rocky slopes to a flat sedimented seafloor; sediments can range from coarse sand to fine soft mud.

Submarine canyon genesis is, as yet, not fully understood (Ridente *et al.,* 2007). Original theories ranged from fresh water springs to tsunamis and subareal erosion by rivers during the Pleistocene (Rowe, 1971). However, the similarity of these structures to onshore canyons and glacial valleys would indicate that submarine canyons are formed by long-

lasting erosion events under the influence of prolonged sediment down-slope transport (Rowe, 1971; de Stigter *et al.,* 2007). The shape of most submarine canyons is more "landslide" in nature than "glacial valley", with very few intermediate stages being observed (Rowe, 1971). This would indicate that glacial-like sediment slumps moving downstream, along an existing fault or topographic low, can turn into turbidity currents (discussed later) creating the canyon valley (Morganstern, 1967; Rowe, 1971; Canals *et al., 2*006). The cascade of dense shelf water (a seasonal event resulting from the formation of dense water by cooling or evaporation. This results in the generation of a density gradient within the water column and subsequently downward cascading) may also be responsible for mass migration of sediment, including large-grain sediment, deeper into the canyon as well as the creation of deep furrows in the canyons (Canals *et al.,* 2006; Lastras *et al.,* 2007). The use of side scan sonar and swath bathymetry in recent years has meant that more canyons, and at greater resolution, are being discovered and mapped. By analysing the images produced from these instruments it is possible to begin to understand how each individual canyon has redeveloped (Lastras *et al.,* 2007).

The flow of water in canyons is governed by the surrounding topography and the physical environment, which differ from the continental slope (Davies *et al., 2*008). Water in the deep sea tends to flow at a slow rate, which increases when it comes into contact with steep topography, with an increase on the lee side of any obstacle (Genin *et al.,* 1986; Genin *et al.,* 1989). In a canyon this is coupled with the creation of higher intensity internal waves than the surrounding slopes (Quaresma *et al., 2*007) and increased turbulence as a result of the meeting of water masses. This water mass meeting also leads to the creation of nepheloid layers (a layer of water which sits above the sea floor containing a significant amount of suspended material) at different levels within the canyon (Pattenden, 2008). The combination of these phenomenon makes canyons significant for shelf-slope particulate exchange (Oliveria *et al., 2*002; de Stigter *et al., 2*007; Quaresma *et al., 2*007; Arzola *et al., 2*008; Garcia *et al., 2*008).

Submarine canyons are often cited as conduits of sediment from the continental slope to the abyssal plain (de Stigter *et al., 2*007; Arzola *et al., 2*008; Garcia *et al., 2*008). Hydrographical conditions are responsible for the degree and speed of sediment transportation and settlement with a canyon system; however this varies from canyon to canyon and as yet is still poorly resolved (McCave and Hollister, 1985; Tyler, 1995; Okey 1997; de Stigter *et al., 2*007). Sediment collects at the canyon head as a result of fluvial or along shelf coastal transport (Arzola *et al., 2*008). Infrequent storm surges lead to the flushing of sediment and suspended load down the canyon preventing the upper reaches of the canyon becoming filled with sediment. Normal transportation of sediment though the canyon occurs in a variety of ways such as tidal currents, internal waves, turbidity flows and mass wasting events.

3.1.1.1-Tidal currents

Linearly reversing tidal currents are partly responsible for the downward flux of sediment within the Iberian margin. At a depth of around 250-300 m the reversals are related to the semidiurnal tide, with more infrequent reversals occurring at greater depths (Drake and Gorsline 1963; Shepard, 1975). These tidal events lead to sediment resuspension often resulting in the creation of nepheloid layers. Down-canyon flows were generally stronger and longer lasting than up-canyon flows. This consequently results in a net movement of water and sediment load down-canyon (Drake and Gorsline, 1963). However, there is not a consistent relationship between the depth, water velocity and the predominance of down-canyon sediment displacement (Drake and Gorsline, 1963). This would indicate that other factors have an effect on the sediment transportation throughout canyon systems.

3.1.1.2- Internal waves

Internal waves are ubiquitous dynamic features that occur within the water column rather than at the water surface. They may be created by Ekman Transport, where in the summer

deep-water upwelling replaces exported surface water. In winter the opposite will occur, often leading to the creation of internal waves.

Theory suggests these waves have a general focus of energy on to the shallowest section of the water column (Hotchkiss and Wunsch, 1982; Quaresma *et al.,* 2007).They are common over irregular features, with a variety of frequencies (Quaresma *et al.,* 2007). Experiments have shown that the energy of internal waves grows the further from the canyon mouth the water moves (Hotchkiss and Wunsch, 1982). Internal waves were found to propagate in from the sea, with a higher incidence occurring within the canyons than along the continental shelf (Tyler, 1995). Up-canyon internal wave propagation is common, increasing the number of internal waves at the head of the canyon**.** These internal waves will lead to the resuspension of sediment in the water column creating a nepheloid layer (Quaresma *et al.,* 2007). The nepheloid layer will carry sediment further into the canyon (Arzola *et al.,* 2008). Canyons dominated by internal wave transport show sedimentation concentrated on the canyon walls, whilst those dominated by down-canyon tidal circulation mainly transport organic matter to depth (Garcia *et al.,* 2008). The resuspenion of sediments in the upper reaches of the canyon can also lead to further erosion of the rock faces making the walls steeper (Hotchkiss and Wunsch, 1982).

Internal waves are also responsible for size sorting of sediment particles within a canyon. Particulate size deposited at the head of the Nazaré canyon was found to be coarser and less sorted than at the same depth on the shelf (Oliveira *et al.,* 2007). The finer particles are suspended in the nepheloid layer and carried to depth in the canyon where they become trapped (Drake and Gorsline, 1973; Tyler 1995; Quaresma *et al.,* 2007). Larger particles may also be found at depth in the canyon, composed of boulders as well as falling biogenic debris such as ostracods and forams (Oliveira *et al., 2*007).

Organic carbon content in the benthos at depth is generally lower than in the shallow water (de Strigter *et al., 2*007). Larger particles and biogenic debris are often concentrated in narrow steep-walled portions of canyons (Drake and Gorsline, 1973) leading to areas of carbon enrichment and making canyons a highly heterogeneous environment. It must be noted that the overall quality and quantity of the sediment settling anywhere within the canyon system is directly related to its origin and the biogenic transformation it undergoes on the way to the sea floor (Garcia *et al., 2*008).

3.1.1.3- Turbidity flows

Turbidity flows are water masses that are heavily saturated with suspended sediment moving downslope at the base of the water column (Hotchkiss and Wunsch, 1982). These are good examples of gravity flows, as it is the added density of the sediment that causes the water to move down-stream. The occurrence of turbidity flows decreases away from the canyon head (de Strigter *et al.,* 2007). This is because lower canyon regions are believed to be less active than the middle or upper canyon, with lower current rates, thus a general reduction in sediment resuspension, as well as a gentler slope in the middle and lower portions of the canyon.

Turbidity flows may also be important in the succession of canyon community assemblages. As flows move down-canyon they will disturb organisms present at the site of origin. These flows could also be responsible for carrying larvae deeper than they would normally be transported, possibly resulting in deeper colonisation by some species. The flows allow the transport of carbon-rich sediment deeper into the canyon leading to the provision of a food source which would otherwise not be present (Rowe, 1971).

3.1.1.4- Mass wasting

Okey (1997) found that mass wasting events tended to occur more frequently in canyons than along the continental margin, using Monterey Canyon, off California as a model. These major disturbances can be a result of dynamic events such as earthquakes and storms or from geological weakness such as under-consolidation or slope failure from undercutting or over steepening of the canyon walls as a consequence of hydrodynamic processes (Arzola *et al.,* 2008). Such mass events lead to a great deal of sediment flushing though the system and can ultimately lead to a destruction of the habitat and organisms present upon that site (Okey, 1997). This disturbance is generally recognised as important for the structure of the faunal assemblage and can lead to large changes. However, these large scale events are not believed to happen frequently.

3.1.2 Submarine Canyon Systems

Each Canyon is a unique environment where the sediment transportation from the shallows to the depths is achieved by a mixture of the above mechanisms owing to its hydrodynamic regime (Trincardi *et al.,* 2007). The Cap de Creus canyon was shown to be fairly inactive with a low level of mixing and deposition occurring in contrast to Nazaré and Sebutal canyons which have been found to be highly active canyons, with sporadic high sedimentation events (Arzola *et al., 2*008; Garcia *et al., 2*008). Despite individual differences in hydrodynamic regimes, canyons have always been shown to transport organic matter to greater depths in the ocean than surrounding areas. Pollutants and nutrients will also be transported to depth in this way (Cacchione *et al.,* 1978). Canyons are often sites of increased biomass which can be explained by the changes in hydrodynamic regime and its influence of food supply (Rowe *et al.,* 1982; Vetter and Dayton, 1998; Duineveld *et al.,* 2001).

Such a heterogenous environment leads to the creation of a large variety of niches available for biological colonisation. Also once detritus or particulate matter is within the

canyon it is transported further into the deep sea than would occur on the slopes by the mechanisms previously discussed. Diel migrating plankton are also often found to become trapped within the canyon (de Leo *et al., 2*010), increasing the food availability at depth in comparison to the surrounding slope. The combination of all of these factors as well as the heterogeneity of the substratum available for settlement leads to canyons becoming areas of enhanced biodiversity, often referred to as biodiversity 'hotspots'. Despite this very little work on the biological assemblage structure within canyons has occurred, with even less focusing on the cold- water coral assemblages.

Those biological studies which have been conducted are dependent on the technology available, including box cores, trawls, photography, grabs and submersibles to collect data (Rowe, 1971; Rowe, 1974; Haedrich *et al., 1*975; Rowe *et al., 1*982; Schlachter *et al., 2*007; Pattenden, 2008). Even with the recent exploration very few canyons have been investigated thoroughly, mainly as a result of the cost and the difficulties sampling. The heterogeneous terrain found within canyons makes sampling of megafauna difficult to achieve, without damaging or losing equipment. This has resulted in the majority of studies which have occurred in canyons to be concerned with the physical aspects of canyons such as distribution, morphology, hydrodynamics and genesis (Arzola *et al.,* 2008; Garcia *et al.,* 2008; De Leo *et al.,* 2010). However, with the assemblage structure remaining poorly understood (Davies, 2008), it is possible to use this information to allow for better planning when focusing on biologically-oriented studies.

The use of side-scan sonar and swath bathymetry through large multi-disciplinary projects such as HERMES and HERMIONE has allowed detailed maps to be produced of some canyons including the Nazaré Canyon, Lisbon Canyon and recently the Whittard Canyon. From these maps it is possible to plan and carry out more extensive ROV and submersible

dives which can be more clearly directed at biological sampling and recording, without damaging the equipment.

Although some investigations into faunal abundance have occurred in canyons there has been a high degree of contradiction within the reported results. Some reports have suggested that submarine canyons are biodiversity hotspots whilst others suggest that there is no marked different in abundance between the shelf and the canyons (Pattenden, 2008; Bianchellie et al., 2010). Tyler *et al.* (2009) found that within the Nazaré Canyon suspension and deposit feeders were dominant with a reduction in density in the middle and lower parts of the canyon, although no comparison was made with the shelf or slopes. Pattenden (2008) also found that suspension feeders tended to dominate the Nazaré, Lisbon, Setubal and Cascais Canyons, with the relative abundance of suspension feeders increasing within the more active canyons. All canyons showed higher abundances of suspension feeders than the continental shelf, with active canyons showing a larger increase. This could be attributed to the increase in suspended organic matter available for consumption, within the canyons (Bianchellie *et al*, 2010).

Vetter and Dayton (1998) found a general increase in infaunal density at canyon sites in comparison to open slope sites, with cluster analysis separating the assemblage samples into canyon and non canyon sites. However, they found that megafauna density increased on-slope in comparison to in-canyon sites (Vetter and Dayton, 1999). This was attributed to a high density of urchins on the slope; once urchins were removed from the analysis there was an increase in non-urchin densities within the canyon. There was also higher megafaunal species richness within the canyon than on the surrounding slopes. Vetter and Dayton (1999) also noted that sedentary sessile organisms show lower abundance and/or diversity in some of the canyons they investigated in comparison to the shelf. This may be

attributed to periodic disturbances such as turbidity flows reducing the community which is present and thus preventing them from reaching a high density.

Higher fishery productivity has also been reported in canyons in comparison to the surrounding slope (De Leo, *et al.,* 2010; Vetter *et al.,* 2010). This is likely a direct result of increased food availability. Vetter *et al.* (2010) found highly mobile organisms generally increased within canyons at the same depth as on the slope, indicating that canyons may be important sources of larvae for surrounding areas. As food-rich patches are often considered important for recruitment success for many species canyons may be important nursery areas for some organisms (Vetter *et al.,* 2010).

From the above it is clear that submarine canyons are important habitats for sediment flow from the shelf to the deep sea, species movement into deeper waters and possible increased species diversity and density in comparison to the surrounding shelf. With an estimated 660 canyons in the world's oceans (De Leo *et al., 2*010) (Figure 3.1) further investigation into the biological communities is imperative. This is particularly important for areas affected by fishing.

Canyons have been shown to lead to an increase in the abundance and biomass of fish in comparison to continental slopes (Stefanescu *et al.,* 1994). This has lead to an increase in fishing practices over recent years as a result of increased technology allowing fishing to occur in this hazardous environmental with minimal chance of damaging gear. An example of such a fishery is the Hoki fishery in New Zealand (De Leo *et al.,* 2010). These fishing practices are often very destructive and have previously been likened to forest clearcutting (Watling and Norse, 1998). The use of fishing gear often leads to the burial or crushing of individuals including corals as well as the destruction of their habitat (Watling and Norse,

1998). Recovery from fishing events is hampered in corals by slow growth and patchy recruitment making corals very sensitive to fishing.

3.1.3 Whittard Canyon

The Whittard Canyon occurs to the south east of Goban Spur, along the Irish Margin in the northern Bay of Biscay around 300 km south of Ireland (Figure 3.2). Within this region the general hydrographic regime consists of surface water down to 500 m Antarctic Intermediate water from 1,000-1,500 m depth followed by North Atlantic, Deep Water, of which there are two distinct layers the top (1,500-2,500 m depth) originating from the Labrador Sea and the bottom layer (2,500-4,000 m depth) originating from the Greenland Sea. There is also a slight input of Eurafrican Mediterranean water into the basin at around 1,000 m. Below 4,000 m Antarctic bottom water dominates (Matthias and Godfrey, 2003).

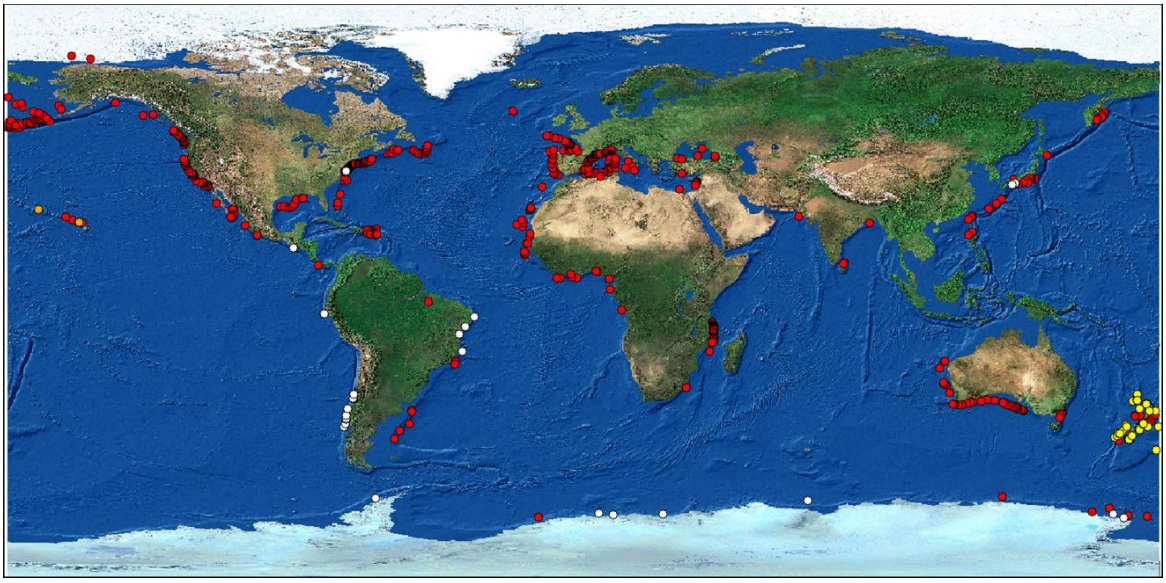

Figure 3.1. Submarine canyon global distribution. Red circles represent named canyons identified from Google Earth, white circles are unnamed canyons from Google-Earth, yellow circles from unpublished data on New Zealand canyons and orange circles from canyons identified in Vetter et al.(2010). Figure taken from De Leo et al. (2010)

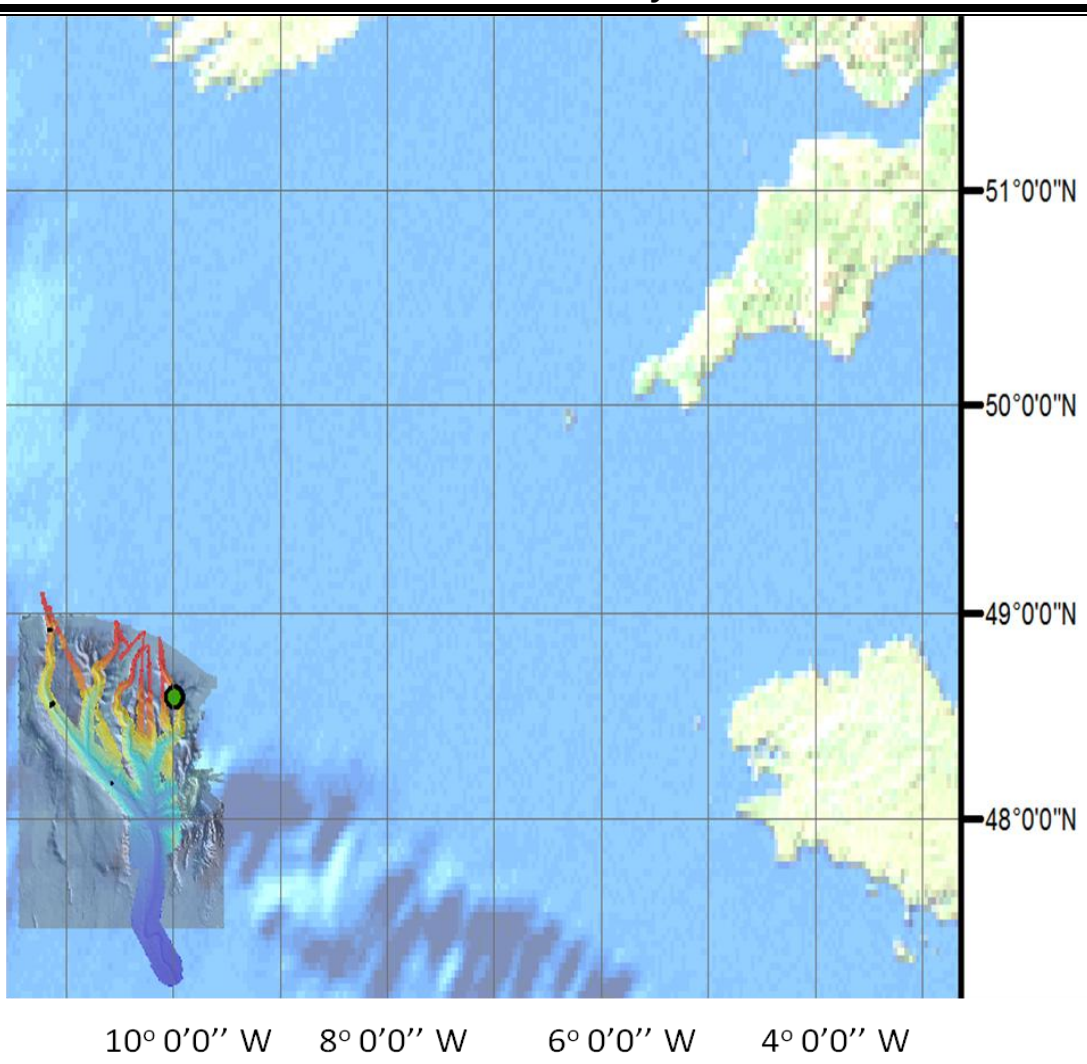

Figure 3.2. Location of Whittard Canyon. The Whittard Canyon is located on the Celtic margin, north of the Bay of Biscay, on the edge of the Irish Exclusive Economic Zone.

The canyon extends from the upper slope to abyssal depths, varying in depth between 200 and 4,000 m (Duineveld *et al., 2*001). The overall canyon structure contains two main branches, one to the east and one to the west. The eastern branch consists of four main tributaries which merge to form one branch, with the western branch made up of two merging tributaries (Figure 3.3). These run from the shelf edge down into the canyon and at approximately 3,700 m depth the two main branches merge to create one large channel

which eventually opens up into the Abyssal Plain. The overall distance covered by the canyon is believed to be in the region of 100 km.

The Whittard Canyon is suspected to be an active canyon system funnelling sediment from the Celtic margin down into the depths of the Atlantic. The Whittard Canyon has endured many mass wasting events during the last glacial period as the British-Irish ice sheet retreated and changes in flow of the 'Fleuve Manche' paleaeoriver occurred (Zaragosi *et al., 2*006; Toucanne *et al., 2*008). The annual melt water cycle induced by the ice sheet lead to an increase in 'Fleuve Manche' paleaeoriver discharge. This increased discharge resulted in a large turbidite event with an amplified sedimentation rate within the Whittard Canyon. Once the ice sheet had completely melted (and the sea level rose) a reduction in sedimentation rate within the Whittard Canyon along with the cessation of terrigeneous supply (suspected to coincide with reforestation of Western Europe) occurred leading to the creation of the modern hydrologic conditions (Zaragosi *et al., 2*006; Toucanne *et al., 2*008). Such events along with the presence of strong levees and low avulsion rates (where one channel is abandoned and a secondary channel created) (Zaragosi *et al., 2*008) within Whittard Canyon have sculpted it into its present form, where periodic mass gravity flows are now responsible for the deepening and widening of the canyon (Cunningham *et al., 2*005).

Currents within the Whittard Canyon have been found to run across and alongside the fan rather than up the gullies, with an increased velocity down canyon (Reid and Hamilton, 1990). The majority of the sea floor within the Whittard Canyon is covered in sediment, ranging from sand to foraminiferal ooze, with grain size decreasing down fan, there is very little exposed rock, other than on the extreme walls (Reid and Hamilton, 1990). Carbonate concentration also increases down canyon, indicating a change in the importance of pelagic processes away from the canyon mouth (Reid and Hamilton 1990). Duineveld *et al.* (2001) also found that the POC concentration was higher in the canyon than in the surrounding

area, indicating organic enrichment. The surface waters of the upper reaches of the canyon have a relatively high biological productivity as a result of nutrient upwelling on the Celtic shelf edge (Wall *et al., 2*010), this would result in increased nutrient transport through the canyon via mechanisms such as internal waves and turbidity flows previously discussed. Dunieveld *et al.* (2001) reported a strong indication of local carbon enrichment within the canyon resulting in a change in the assemblage structure, with increased suspension feeders in the canyon compared to the surrounding open slope area.

3.1.4 Aims

To date very little biological exploration has occurred within Whittard Canyon. he aim of this chapter is to determine if depth, substratum or slope have an effect on cold-water coral assemblages within the Whittard Canyon and to compare the coral assemblages present within the Whittard Canyon and along the AVR at 45^{o}N. This will be achieved by addressing the following objectives:

1- Analysis of all video footage available for the Whittard Canyon identifying Octocoral species noting: density, position, depth and substratum type.
2- Use positional data to create a density map and slope map of the Octocoral observed within the Canyon, to allow distribution patterns to be ascertained.
3- Use statistical methods (ANOSIM and SIMPER) to determine if depth or substratum type has an effect on the Octocoral assemblages observed.
4- Describe the similarities and the differences between the coral assemblages present within the Whittard Canyon with those found along the AVR at 45^{o}N.

3.2. Materials and methods

3.2.1 Data collection

Observations of the seabed were taken with video and still imagery using the ROV *Isis* during two cruises aboard the RRS *James Cook* cruise to the Whittard Canyon in 2007 (JC10) and June 2009 (JC36). From these two cruises a total of 13 video recording Dives were completed ranging in depth from c 700-4,000 m in depth (Table 3. 1), resulting in over 80 hours of video.

Isis is 2.7 m x 1.5 m x 2.0 m, weights 300 kg in air and can operate down to 6,500 m. She is fitted with 6 cameras, used for both piloting and scientific purposes. The scientific cameras used during JC10 and JC36 consisted of the fixed Atlas 3-chip camera with a 14x optical zoom and the Pegasus pan and tilt camera, which record onto DVCAM tapes and DVD, as well as the Scorpio 3.34 mega pixel digital still colour camera. For clear video footage to be obtained the sea floor is illuminated by two 600 J strobe lamps, five 250W incandescent lamps and three HMI 1200W lamps.

For successful navigation *Isis* was fitted with an Octans fibre-optic gyrocompass, a Kongsberg Simrad MS900 series; 675 kHz, 100m range-profiling sonar and a Kongsberg Simrad SM2000 series; 200 kHz, 400 m range forward- looking sonar, plus a crossbow three- component magnetometre and Paroscientific Digiquartz gauge. These instruments allow heading, and pressure (depth) to be recorded. Two Kraft TeleRobotic manipulator arms, one on either side of the main body, allow a variety of functions to be carried out including sampling.

3.2.2. Image analysis

The video footage was analysed using computer package I-movies. Each video was watched in entirety with the occurrence of each individual coral noted along with the time, depth and substratum type.

As with JC24 discussed in Chapter 2 it was not possible to work out an exact area of view from the videos as the altitude of the ROV in respect to the sea floor as well as the angle of tilt on the camera were not recorded. Although lasers are present on *Isis* with a fixed distance of 10 cm apart it was not always possible to see where these marked the substrata in the video recordings and thus could not be used to determine area during these dives. It was therefore decided that time would be used as a controlling factor in analysis and data were binned into 5 minute sections within a given substratum type, this would also allow the comparison to results from JC24.

3.2.3.1 Map creation

All data were collated and formatted for compatibility with ESRI ArcGIS version 9.2. A single bathymetric map was created from TOBI (Towed Ocean Bottom Instrument) data collected during the previous JC35 cruise. Once video analysis was complete, latitudes and longitudes were assigned to each observation by identifying the time of observation in the *Isis* track record. This also allowed depth to be obtained. The observations were then grouped according to position. Distances between observations were calculated using the following formula

Table 3. 1. Dates, positions and depths recorded by ROV Isis during Whittard Canyon video Dives.

***Isis* Dive no**	**Date**	**Start Longitude (W)**	**Start Latitude (N)**	**End Longitude (W)**	**End Latitude (N)**	**Max depth (m)**
63	03/07/07	10° 12’09	48°55.748	10° 13.307	47°55.45	4073
64	04/07/07	10° 9’195	48° 19.94	10° 11.48	48° 21.042	3455
65	04/07/07	10° 11’49	48° 21.042	9° 51.62	48° 26.387	2641
102	25/6/10	10° 54’48	48° 21.869	10° 55.638	48° 21.179	3163
105	28/6/10	11° 08.441	48° 33.257	11° 07.395	48° 33.67	3085
106	29/6/10	11° 09.48	48° 44.008	11° 11.042	48° 44.771	2300
107	30/6/10	11° 11.36	48° 59.38	11° 12.14	48° 59.802	1062
109	1/7/10	11° 08.16	48° 52.216	11° 08.218	48° 52.305	1727
113	13/7/10	10° 02.369	48° 22.292	10° 01.952	48° 21.468	3202
114	18/7/10	09° 58.004	48° 36.192	09° 57.28	48° 36.746	1640
115	19/7/10	09° 58.065	48° 36.278	09° 59.084	48° 35.849	1677
116	19/7/10	10° 01.854	48° 39.286	10° 03.047	48° 39.042	1370
117	20/7/10	09° 56.97	48° 27.65	09° 58.20	48° 27.60	2448

Each dive took place within the Whittard Cayon with video footage being recorded by the ROV Isis during both JC10 (dives 63-65) and JC36 (dives 102-117).

Distance = $1.8520 * 60 * \sqrt{((\cos(dlat/2) * dlon)^2 + (dlat^2))}$

Where 1.8520 is the conversion of nautical miles to KM and 60 is the conversion for degrees to nautical miles.

This gave the result that each 0.01 degrees of latitude travelled corresponds to 74 m and each 0.01 degrees in longitude corresponds to 111 m. From this information the distance between coral sightings was calculated using the following formula, where x = latitude and y = longitude

Distance= $\sqrt{((x1-x2)*111)^2+((y1-y2)*74)^2}$.

The results were then converted to metres and the data were segregated into 100 m transect bands in order to create a density map.

The data were transferred into a comma-delimited MS Excel file and transferred into Arc GIS using ET GeoWizzard. Once in ArcGIS, a graduated colour scheme was applied to allow the difference in coral density to be visualised (Figure 3.2).

Substratum type was also plotted as a layer on this map for dives 65, 106, 114 and 116 to allow an in-depth view of the relationship between substratum and the genera *Acanella, Anthomastus* and *Lophelia.*

A slope map was created using the computer programme Erdas imagine v9.3. This was achieved by performing a topographical analysis on the area bathymetry. Black was used

to represent flat ground, with white representing the steepest slopes. The resulting raster file was then imported to ArcGIS.

3.2.3.2 Random sampling.

Data were sorted into depth bands (200 m and 500 m) for each dive. As a result of *Isis* moving along the canyon the time spent in each depth band was not continuous. Therefore five minute continuous segments were taken from each dive, at each depth band and combined to make one 50 minute segment which was used for analysis. This results in one 50 minute segment per dive, per depth. This procedure was repeated for substratum types, resulting in one 50 minute segment from each dive for each substratum present (Sediment, Sediment slope, Mixed substratum, "*Lophelia* reef" and "*"Lophelia* and Rock").

3.2.3.3 Multivariate analysis

PRIMER v6 was used to carry out multivariate analysis. Where there were less than two species totalling ten individuals the data were disregarded as this would cause a large bias in the results. A log transformation was used allowing SIMPER (Similarity Percentages-species contributions) to be carried out. A Bray-Curtis resemblance was applied allowing ANOSIM (Analysis of Similarity) analysis for both depth and substratum type. Multi-dimensional scaling was used to show a visual representation of the data. MDS x-co-ordinates were then plotted against substratum type, this allowed for a visual representation of a change in the ordinates, indicating a change in the assemblage structure when there was an increase in the habitat complexity within the Whittard Canyon to be obtained. Kruskal-Wallis test was carried out on the mean number of individuals observed per substratum type.

3.2.3.4 Cumulative frequencies

Cumulative frequencies of substratum types as well as the number of corals from the top five species responsible for the assemblage structure differences, as identified by SIMPER, were plotted against depth.

3.3 Results

3.3.1 Environmental setting

Thirteen usable dives were completed within the Whittard Canyon during the two RRS *James Cook* cruises JC10 and JC36 in 2007 and 2009 respectively (Table 3.1). The seabed within the Whittard Canyon is dominated by sediment (sand) and highly sedimented rock. Where overhangs and steep sides occur, the degree of sedimentation was reduced exposing bare rock. Two Dives provided footage of *"Lophelia* reefs" on steep overhangs. In some cases, the *Lophelia* had been sedimented over and subsequently had perished. However, this led to a novel substratum type for the colonisation of octocorals on which this project primarily focuses and thus *"Lophelia reef*s" and "rock and *Lophelia*" where reefs were not created were considered substratum types.

Throughout the dives six different substrata types were identified; Sediment, Sediment slope, Mixed ubstratum, Sloped rock, "*Lophelia* reef" and *"Lophelia* and Rock". Insufficient footage of sloped rock occurred throughout the survey to allow reliable analysis; therefore it was removed from further analysis. The dominant sediment type was sand with the rock consisting of basalts and sedimentary rocks. Dives occurred to the North West, the North East and the Central valleys where the spurs joined within the canyon (Figure 3.3).

The Whittard Canyon is shown to have steeper slopes in the eastern branches in comparison to the west (Figure 3.4). There is a clear V-shaped valley running though all branches which widens to produce a U-shaped valley once all branches have joined to create the main Canyon Valley. The valley widens quickly where the two main eastern branches join and narrows after this. The western branches join into the main valley further south of than the eastern branches.

Fauna observed in the video, other than corals, included many ophiuroids, holothurians, cephalopods, and teleost fish. There were obvious patchy aggregations of ophiuroids in some areas. Areas of dead *Lophelia* were also observed in what looked like areas which may have previously been trawled, buy the presence of scars on the seabed. It is suspected that the presence of these trawl marks indicates that should this have been an undisturbed site higher abundance of *Lophelia* would have occurred. Increase fish abundance was observed in *Lophelia* habitats (personal observation).

3.3.2 Distribution and abundances of coral

Throughout the video footage a total of 10,353 individuals were counted and thirty-one potential cold-water coral species were identified (Table 3. 2, Figure 3.5-8). Of these only five "species" (*Lophelia, Madrepora, Dendrophyllum,* Stylasterid sp. and *Bathypathes*) are not octocorals. As always it was impossible to identify fully coral individuals to species level thus whip-like corals are clumped into two groups, whip coral and pink whip. Also where the species of pennatulid could not be discerned then these were added together under the general heading Pennatulacea.

Three species were responsible for 74.4% of all coral individuals counted; *Acanella, Anthomastus* and *Lophelia*. *Acanella* was found during all dives except JC36-107, *Anthomastus* was only absent from two dives (JC10-63, and JC36-107), with *Lophelia*

Table 3. 2. Presence/Absence data of Coral taxa observed within the Whittard Canyon during thirteen dives by the ROV ISIS.

	63	64	65	102	105	106	107	109	113	114	115	116	117
Subclass : Hexacorallia													
Order Antipatharia													
Family Schizopathidae													
Bathypathes sp.	+		+										
Order Scleractinia													
Family Caryophylliidae													
Lophelia sp.			+					+		+	+	+	+
Madrepora sp.			+							+			
Desmophyllum sp.								+		+		+	+
Subclass: Hydroidolina													
Order Anthoathecatae													
Family Stylasteridae													
Stylasterid sp			+										
Subclass : Octocorallia													
Order Gorgonacea													
Red gorgonian												+	
Whip coral													
Whip	+		+			+	+		+	+			
Pink whip		+							+	+			+

Sub-Order Alcyoniina														
Family Alcyoniidae														
Anthomastus sp.			+	+	+	+	+		+	+	+	+	+	+
Sub-Order Scleraxonia														
Family Paragorgiidae														
Orange Paragorgia										+				
Pink Paragorgia								+						
Sub-Order Calcaxonia														
Family Chrysogorgiidae														
Radicipes			+		+	+			+	+			+	
Family Isididae														
Acanella cf arbuscula	+	+	+	+	+	+	+	+	+	+	+	+	+	
Brush Isididae (Sp A)										+				
Bamboo fluffy bush coral (Sp B)			+											
Candelabra Isididae (Sp C)												+	+	
Pink Isididae (Sp D)	+		+									+		
Skeleton Isididae (Sp E)			+							+				
Whip Isididae (Sp F)		+	+	+										
Pink fan Isididae (Sp G)			+									+		
Frail Pink Isididae (Sp H)												+		
Family Acanthogorgiidae														
Acanthogorgia sp.			+			+		+	+	+	+	+	+	

Family Primnoidae												
Priminoa sp.						+						
Order Pennatulacea												
Sub-Order Sessiliflorae												
Family Kophoblemnidae												
Kophobelemnon sp.		+										
Family Umbellulidae												
Umbellula sp.	+	+	+	+	+		+	+	+	+		
Family Anthoptilidae												
Anthoptilum sp.		+		+	+	+		+	+		+	
Family Protoptillidae												
Distichoptilum gracile		+		+				+			+	
Family Pennatulidae												
Pennatula aculeata.		+			+			+	+	+	+	
Pennatulacea	+	+			+		+	+				
Unknown family												
Purple coral								+				
Peach single polyp									+	+		

Numbers correspond to ROV Isis dive numbers which took place during two cruises JC10 (63-65) and JC36 (102-117). Each + sign indicates the presence of that species within a given dive recorderd from video footage obtained by ROV Isis. All dives took place within the Whittard Canyon in the Northern Atlantic.

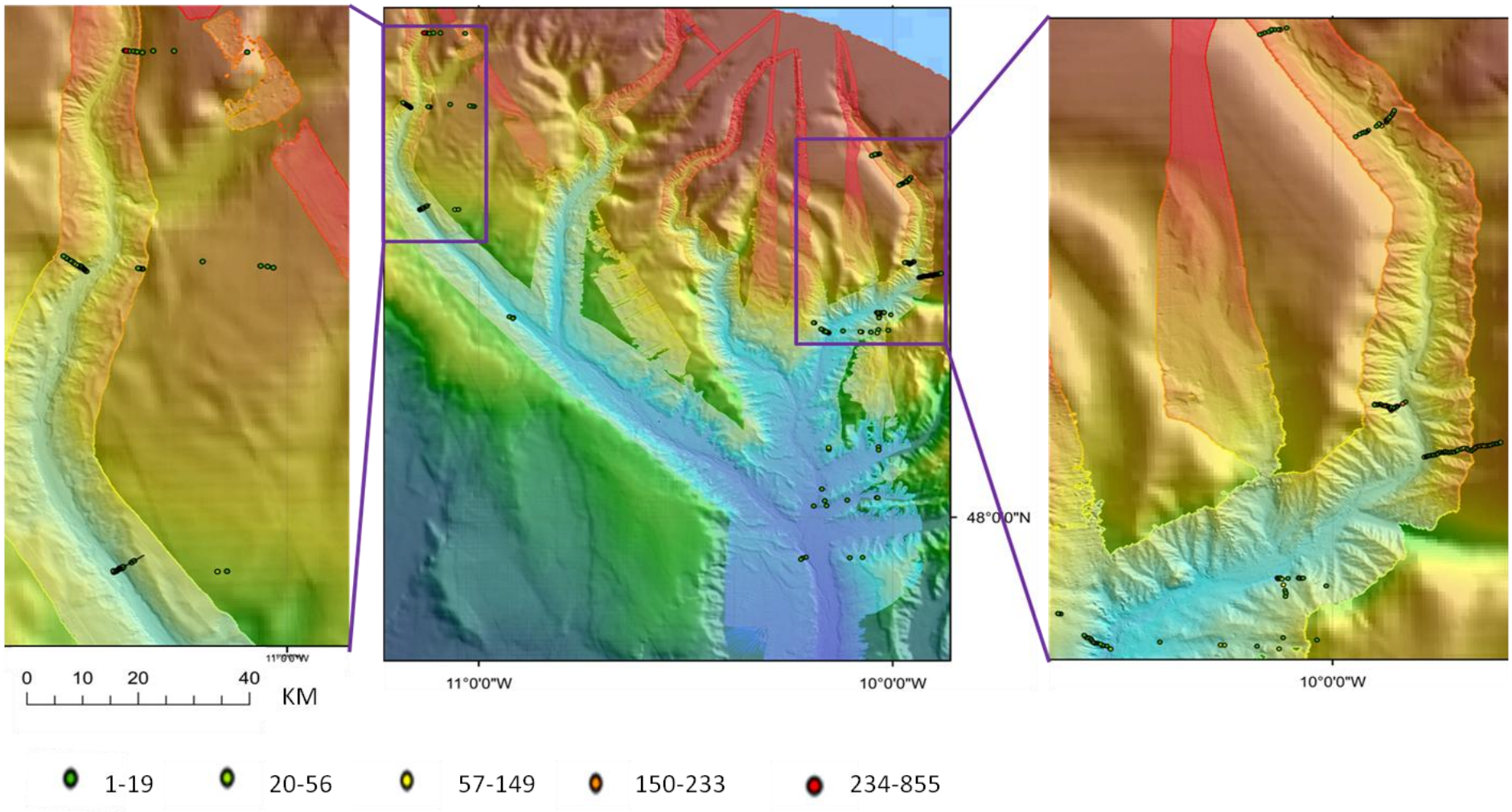

Figure 3.3. Density per 100m ^{2} and Distribution of Corals identified in the Whittard Canyon. Red dots indicate 234-855 individuals, orange 150-233 individuals yellow 57-149 and green 1-56 individuals of all coral species observed with a 100m transect. No contours were included as they are too close together and mask the coral occurrence.

Figure 3. 4. Slope map of Whittard Canyon system. Slope is depicted by the presence of a light area. The lighter the area the steeper the slope with dark patches showing flatter areas within the Canyon. It can be clearly seen from this Figure that steepest slopes occur up-canyon and a well defined valley runs throughout the canyon.

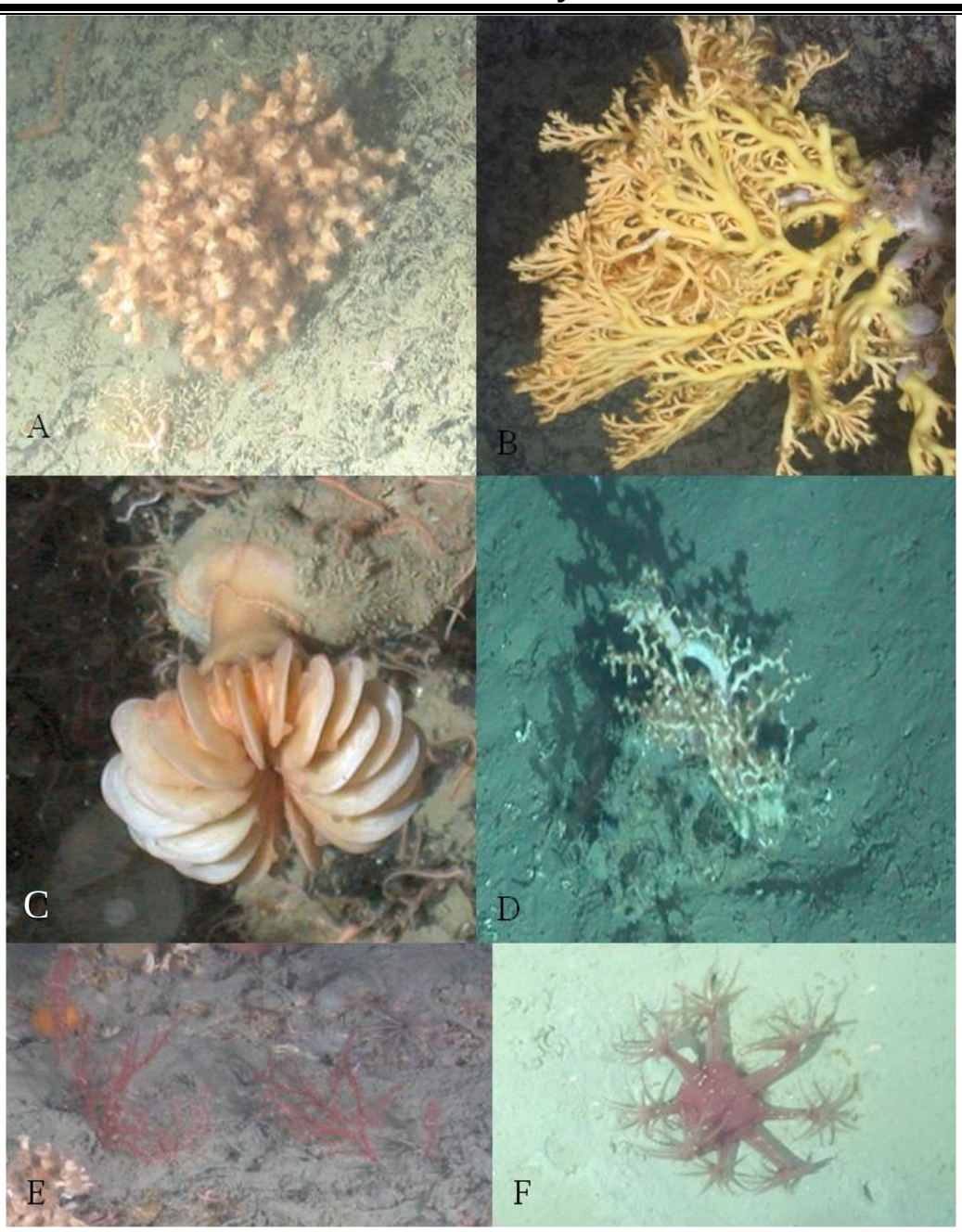

Figure 3. *5. Picture plate 1 of coral species observed during video footage of the Whittard Canyon (A)* Lophelia *(~30 c*m), *(B)* Stylasterid *sp*, (~50 cm) *(C)* Desmophyllum *sp.(~10cm) (D)* Madrepora *sp (~40cm).(E) Red Gorgonian (~20 cm) (F)* Anthomastus *sp.(~15cm) Scale could not be included as a result of a lack of Laser points within the pictures therefore rough estimations of size are given*

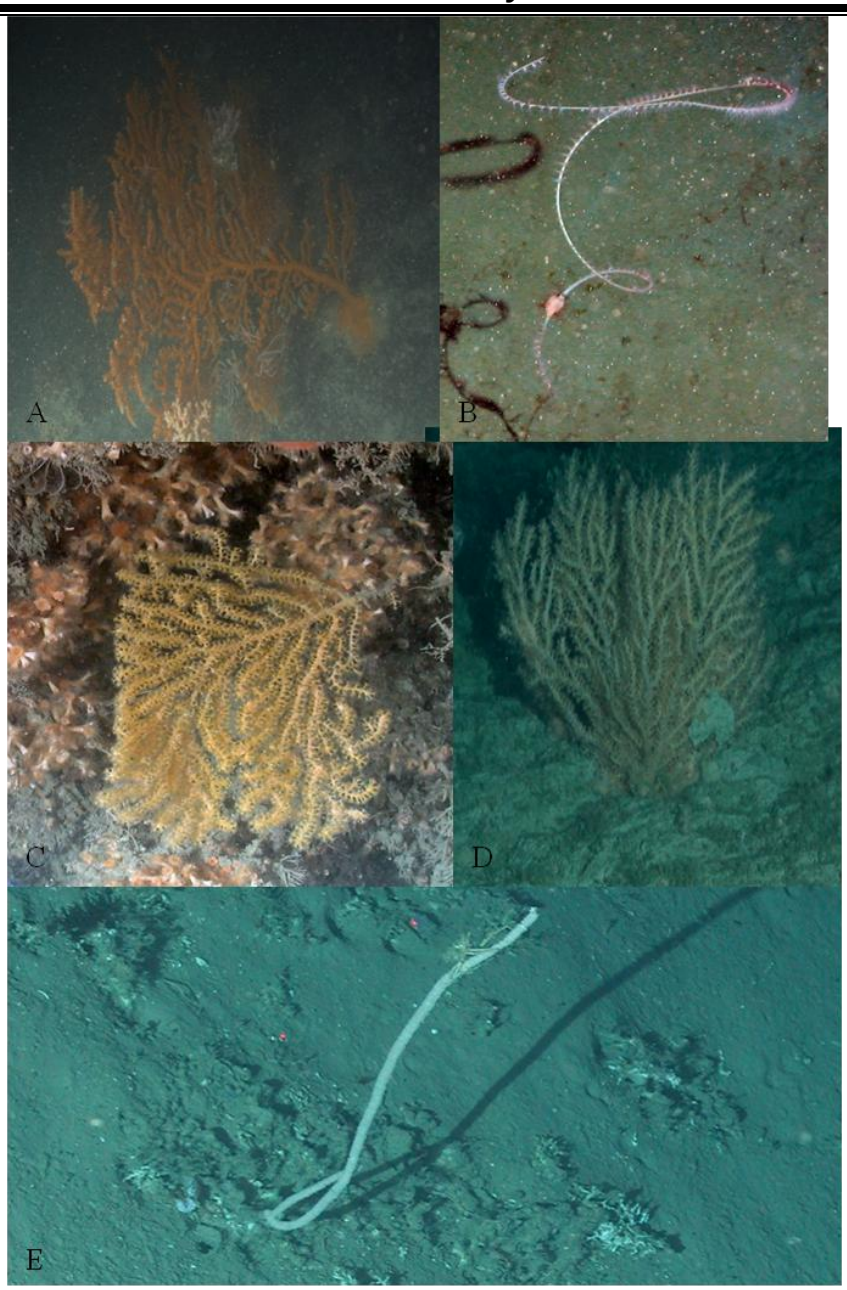

Figure 3. 6. Picture plate 2 of coral species observed during video footage of the Whittard Canyon (A)Orange Paragorgia (~ 70cm), (B) Radicipes sp. *(~90 cm) (C)* Acanthogorgia sp. *(~30 cm) (D)* Primnoa sp. (~60 cm) *(E) Whip Coral (~25cm). Scale could not be included as a result of a lack of Laser points within the picture therefore rough estimations of size are given*

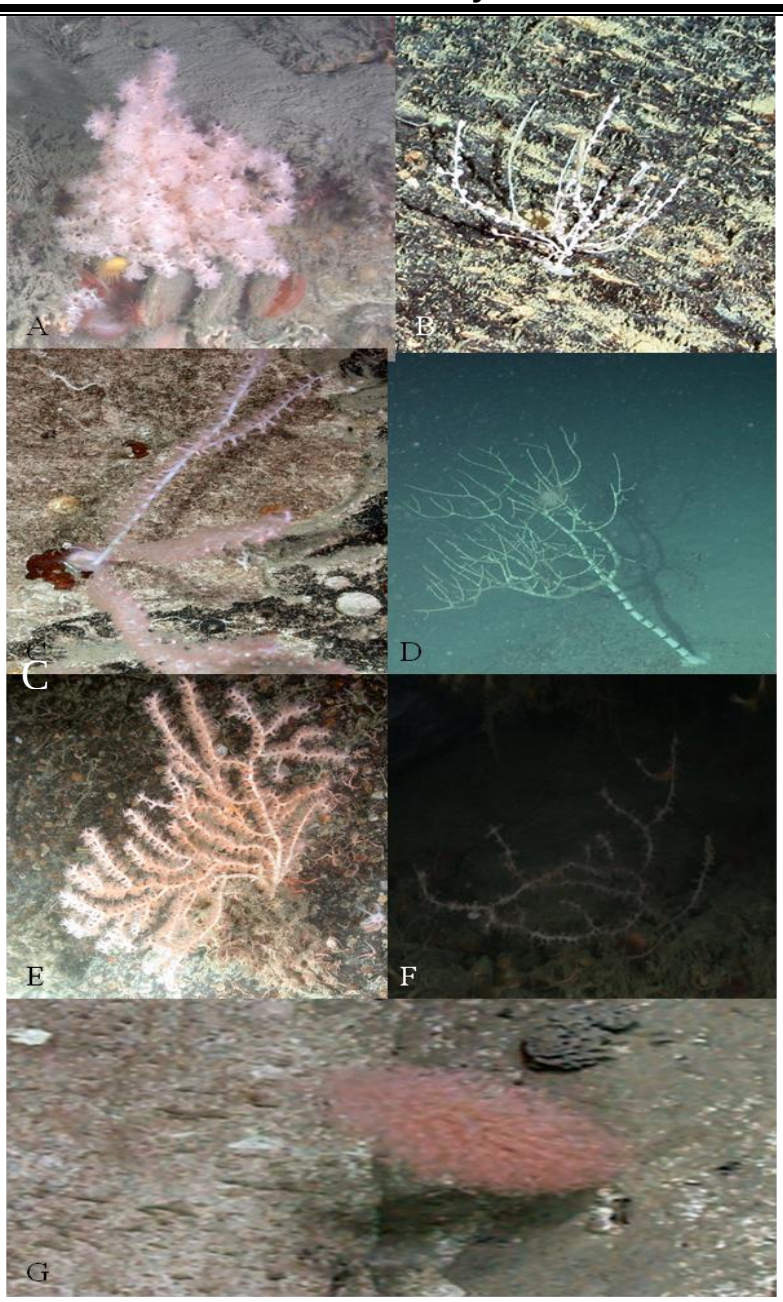

Figure 3. 7. Picture plate 3 of coral species observed during video footage of the Whittard Canyon (A) Bamboo fluffy bush coral, (~15cm) (B) Candleabra Isididae,(~10cm) (C) Pink Isididae (~25cm) ,(D) Skeleton Isididae,(~55cm) (E) Pink Fan Isididae (~40 cm), (F) Frail Pink Isididae (~15cm), (G) Acanella sp. *(~20cm) Scale could not be included as a result of a lack of Laser points within the picture therefore rough estimations of colony size are given.*

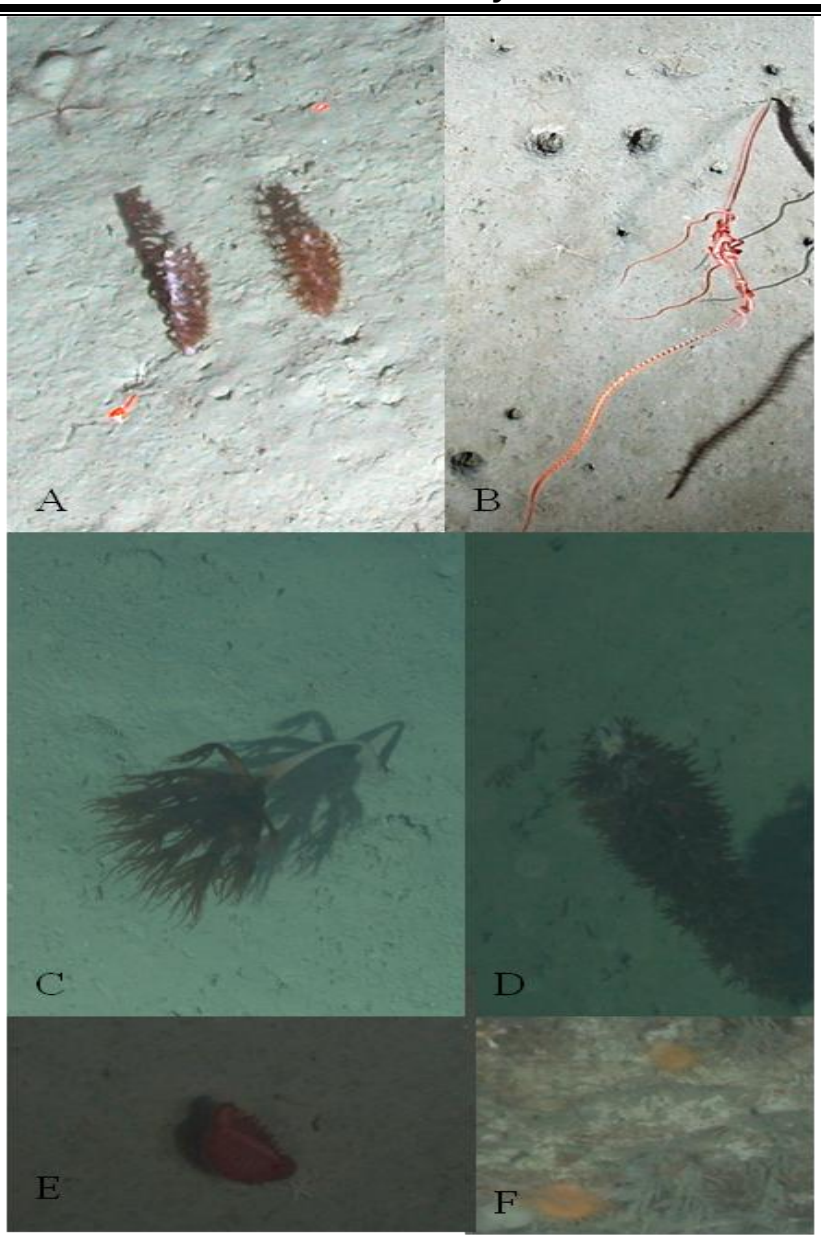

Figure 3. 8. Picture plate 4 of coral species observed during video footage of the Whittard Canyon (A) Kophobelemnon *sp. (~25 cm) (B)* Distichoptilum gracile (~45 cm) *(C)* Umbellula *sp. (~40 cm) (D)* Anthoptilum *sp.(~40 cm) (E)* Pennatula aculeata (~35 cm) *(F) Peach single polyp. Scale could not be included as a result of a lack of Laser points within the picture therefore rough estimations of colony size are given..*

only being present in half the dives yet had a large contribution to the overall count (Table 3. 2). Twelve species have less than 10 individuals throughout all the video footage. Dive JC36-102 and JC10-63 had the fewest number of individuals observed with JC36-117 containing the highest number.

The highest density of individuals per 100 m^2 (855) occurred during Dive JC36-116 along a *"Lophelia reef"* wall, where there is a steep overhang (Figure 3.3, 4). Although strictly from observation this is obviously the densest area of coral coverage, the absolute number could be inaccurate due to the video technique leading to the possibility of pseudoreplication. Other areas of high density occur during Dives JC36 117 and JC36-109. All of these areas correspond to areas of rock and *"Lophelia reef"*. The areas with the highest densities of individuals tended to occur up-canyon where the slope appears to be at its steepest (Figure 3.3, 3.4). Most areas contain either no coral or 1 to 56 coral per 100 m transect.

3.3.3 Depth and distribution

Multivariate analysis was used to examine assemblage differences with depth, taking 200 m intervals from 1,100-3,900 m. No apparent depth segregation was found (Figure 3.9). No significant difference was found in the coral assemblages composition at different 200 m depth intervals no difference (ANOSIM, N= 28, R=0.411, P=0.01) (Table 3. 3). However, at this degree of segregation it was possible that there were insufficient data in each category to show any differences, therefore a second MDS was carried out with 500 m segregations (Figure 3.10), but no obvious clusters could be discerned. |No significant difference between the coral assemblages was observed at the 500 m depth segregation (ANOSIM, N=17, R=0.033, P=0.36). As a result, depth was not considered as an important co-variant in subsequent analysis

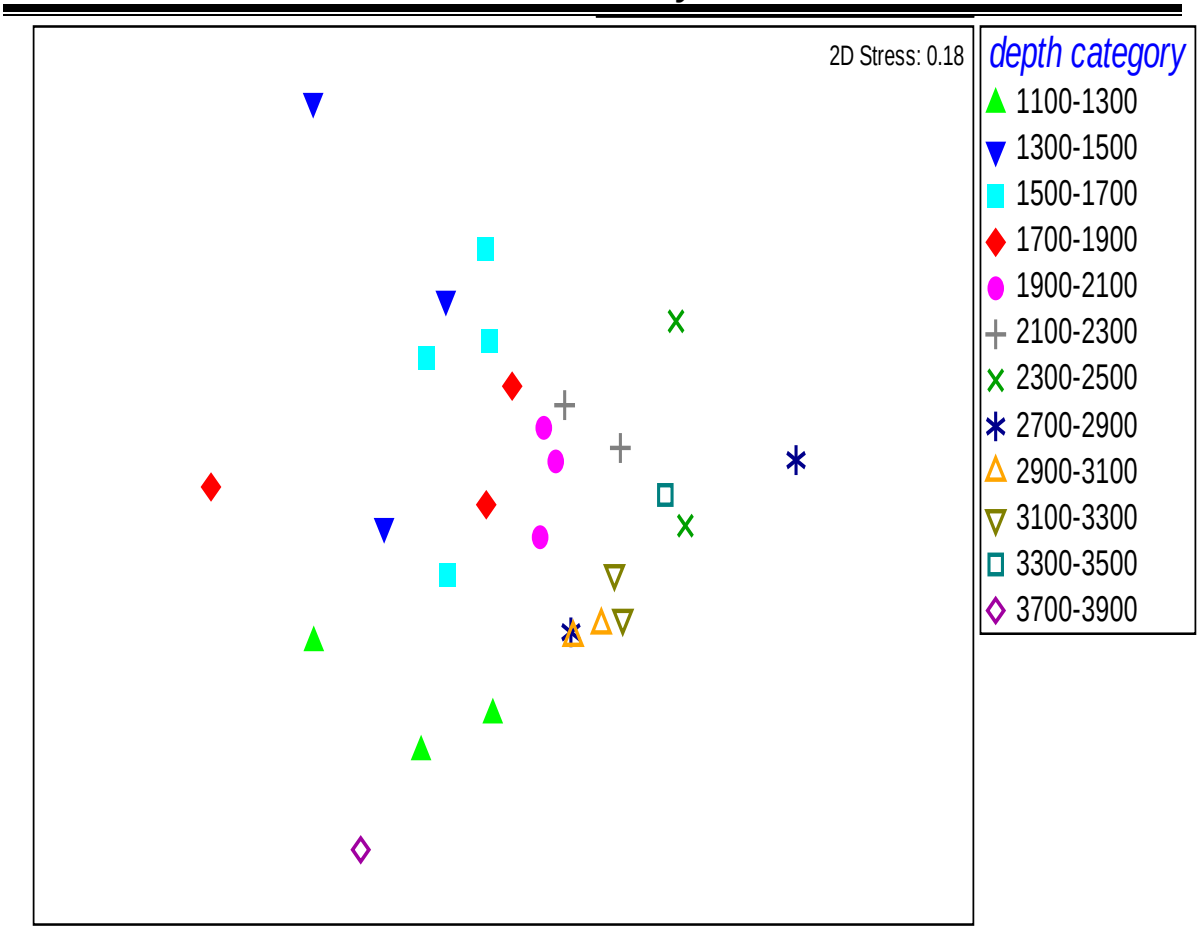

Figure 3.9. MDS ordination of coral assemblages structure at within 200 m depth bands within the Whittard Canyon. Each point represents a 50 minute time period within the given depth from an individual Isis dive. Further information can be obtained in Appendix 2 Table ap 2.1 N=28

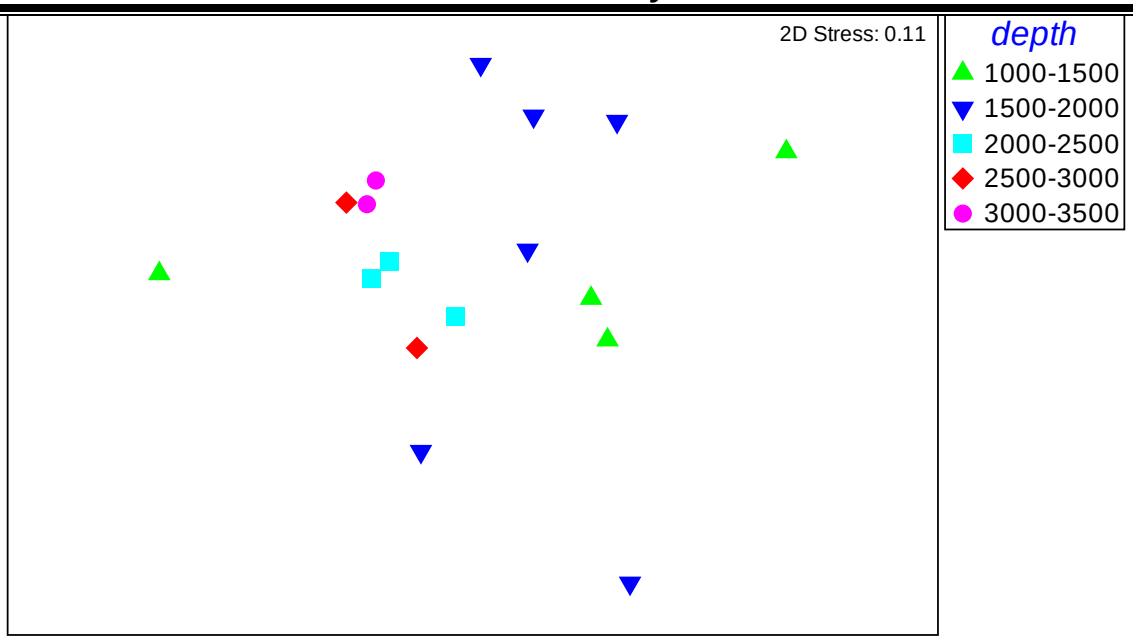

Figure 3.10. MSD ordination of coral assemblages structure at within 500 m depth bands within the Whittard Canyon. Each point represents a 50 minute time period within the given depth from an individual Isis dive. Further information can be obtained in Appendix 2 Table ap 2.2 N=17

3.3.4 Overall Distribution and Substratum type

Time-normalised data show that the mean number of individuals per 50 minute interval is highest on *"Lophelia* reef*"*, with the lowest occurring on Sediment (Figure 3.11). This difference is deemed significant at the 10% level (Kruskal-wallis, DF=4, N=17, P=0.054). Hoever large standard errors upon these results would indicate that there is a high degree of variation in the numbers observed within the substrata types, especially "*Lophelia* and Rock".

Sediment substratum contains the highest percentage of Isididae of all substratum types (Table 3. 3 and 3.4). This is mainly attributed to large *Acanella* aggregations. Both the "*Lophelia* and Rock" and "*Lophelia* reef" have a reduced number of families represented with *Lophelia* dominating (Table 3.3 and 3.4). Mixed substratum (Rock and Sediment) has a high occurrence of *Anthomastus* and 94 % of the *Bathypathes*. Pennatulidea are found within the sediment and rock and sediment substrata. 100 % of the Primnoidea occurred on the Rock and Sediment (Table 3. 3 and 3.4).

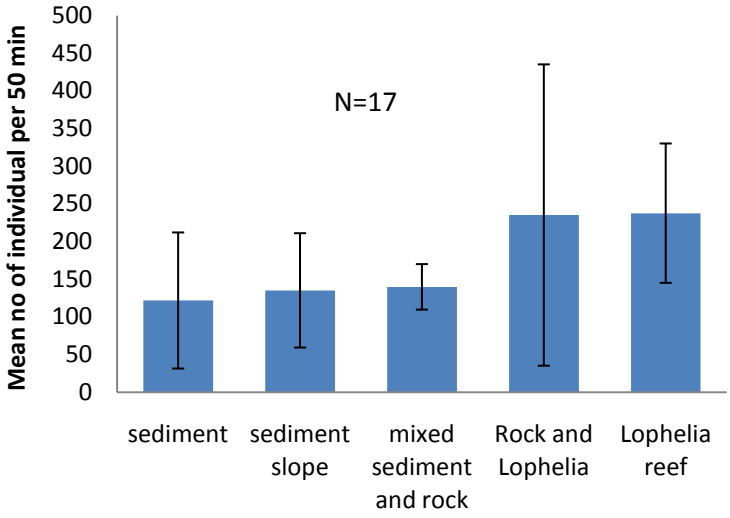

Figure 3.*11. Average number of individuals observed within a 50 minute period on different substrata types with the Whittard Canyon. Each 50 minute period is made up of ten 5 minute segments accumulated together. Error bars indicate standard deviation from the mean N= 17*

MDS shows a separation of the *"Lophelia* reef*"* and "*Lophelia* and Rock" to the left of the plot (Figure 3.12). Sediment and sediment slope are separated to the right of the plot with the mixed rock and sediment occurring in the centre. There is a higher degree of separation

of the *"Lophelia and rock"* and "*Lophelia Reef"* from the other substratum types. A change from negative to positive x co-ordinates in coral assemblages with an increase in habitat complexity and hard substrata is demonstrated using the MDS x co-ordinates and the substratum type (Figure 3.13).

Table 3. 3. Percentage of Coral assemblage composition determined by substratum

	Sediment	**Sediment slope**	**Rock and sediment**	**Rock with *Lophelia***	***"Lophelia reef"***
Schizopathidae	0	0.1	0.5	0	0
Carophyliidae	0	0	0.1	95.2	82.4
Gorgonacea sp.	0	0	0	0	3.5
Whip coral	0.4	0.4	2.4	0.5	0.3
Alcyoniidae	3.2	51.8	45.1	1.4	0
Paragorgiidae	0	0	0.02	0.2	0
Chrysogorgiidae	0.9	15.4	0.1	0	0
Isididae	85.7	31.1	28.5	2.1	13.8
Primnoidae	0	0	13.7	0.2	0
Pennatulacea	9.7	1	8.9	0	0
unknown	0.1	0.2	0.58	0.4	0

Each number represents the percentage from the total number of corals observed upon a given substratum type, of the named family. Each column totals 100 %

Table 3. 4. Percentage Coral assemblage composition determined from coral families

	Sediment	**Sediment slope**	**Rock and sediment**	**Rock with *Lophelia***	**"*Lophelia* reef"**
Schizopathidae	0	5.6	94.4	0	0
Carophyliidae	0	0	1.7	39.7	58.6
Gorgonacea sp.	0	0	0	0	100
Whip coral	8.6	5.8	80.8	2.9	1.9
Alcyoniidae	3.1	32.6	63.9	0.3	0
Paragorgiidae	0	0	50	50	0
Chrysogorgiidae	8.2	90.2	1.6	0	0
Isididae	55.9	13.1	27.2	0.3	3.4
Primnoidae	0	0	100	0	0
Pennatulacea	39.7	2.6	57.6	0	0
unknown	2.5	2.5	75	20	0

Each number represents the percentage from the total number of corals observed from a given family observed on different substratum types within the Whittard Canyon. Each row totals 100 %

No overall difference in octocoral assemblages among substratum types were observed (ANOSIM, N=17, R=0.501, P=0.001) (Table 3.5). Examination of individual pairings show a clear difference at the 5 % level between both "*Lophelia* reef" and "*Lophelia* and rock" with "Mixed sediment and rock" and "sediment" (Table 3.5). Further differences at the 10% level are observed between both Sediment and "*Lophelia* and Rock" and sediment and *"Lophelia* reef*"*, indicating that the *Lophelia* substratum types are mainly responsible for the differences observed between assemblages. The main genera responsible for the dissimilarity between the sediment types are *Lophelia*, *Acanella*, *Anthomastus*, *Primnoa* and *Pennatula aculeata* (SIMPER) (Table 3. 6).

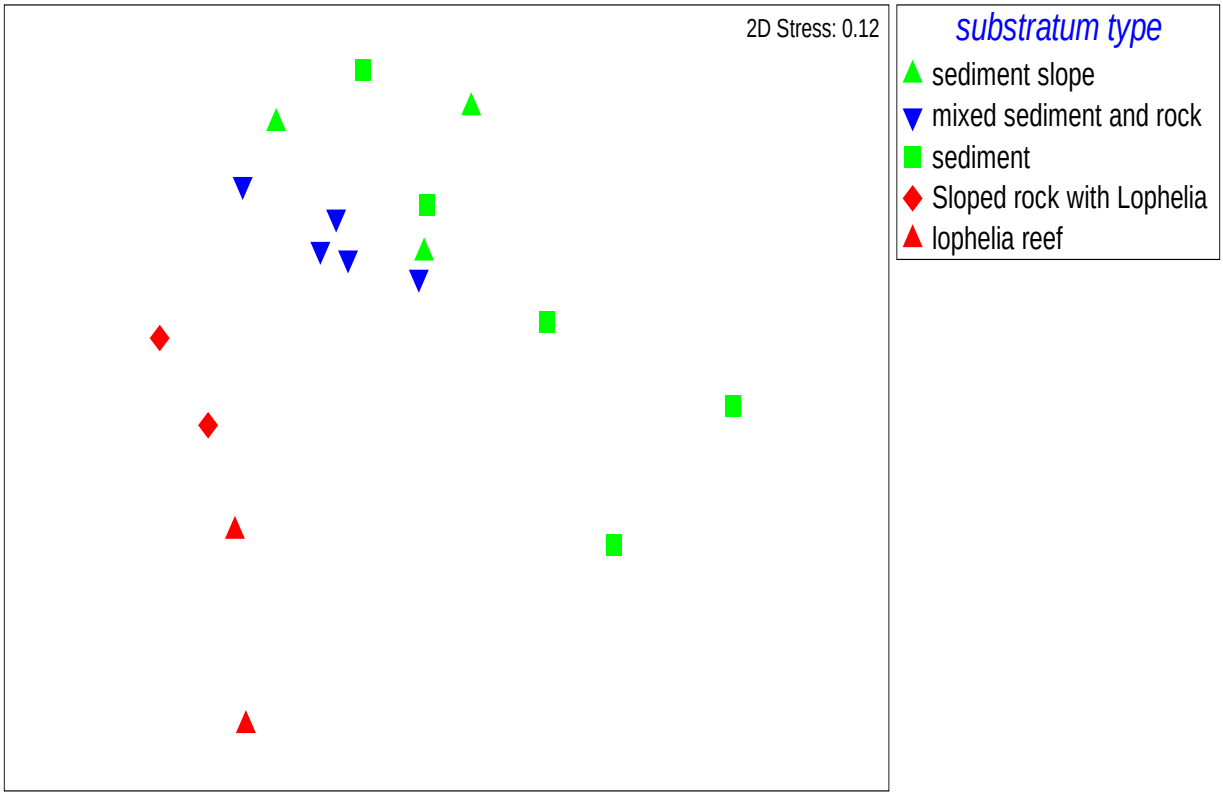

Figure 3.*12. MSD ordination of* coral assemblages *structure from different substrata types across the Whittard Canyon dives. Further information can be obtained in Appendix 2 Table ap 2.3*

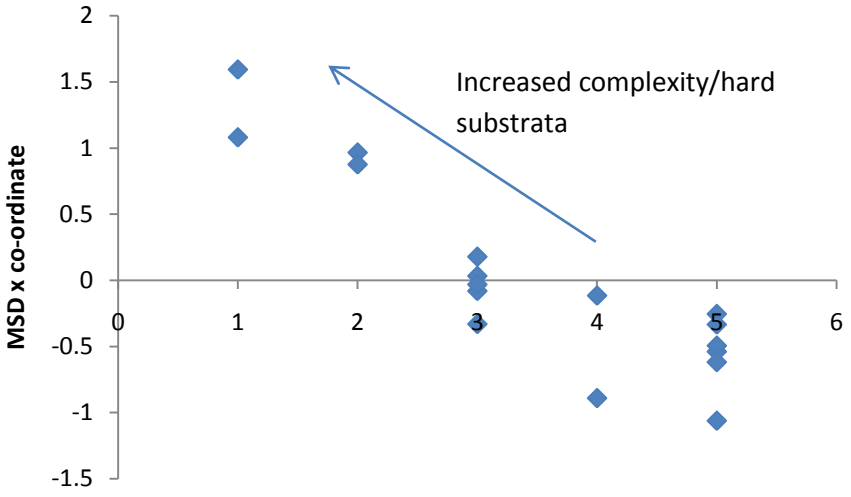

Figure 3.13. MDS x ordinate of coral assemblages against substrata type in the Wittard Canyon. 1= "Lophelia reef", 2= "Lophelia and rock", 3 = Mixed rock and sediment 4= Sloped sediment, 5 = Sediment

From the SIMPER test *Lophelia*, *Acanella* and *Anthomastus* were identified as important in the determination of the assemblage composition. Maps were created to allow the comparison of these taxa with the occurrence of substratum types along four different dive tracks (Dive 65, Dive 106, Dive 114 and Dive 116) encompassing all substratum types encountered throughout the study. It was not possible to do this fine scale investigation on the slope tracks as a result of loss in resolution in the maps.

Table 3. 5. Results of ANOSIM tests comparing coral assemblages composition upon different substrata across Whittard Canyon Dives. N= 17

Global R=0.102 **P=0.13**	**Sediment Slope**	**Mixed Rock and sediment**	***"Lophelia* reef"**	**"*Lophelia* and Rock"**
Sediment	R=0.138 P=0.26	R=0.468 P=0.02	**R=0.836** **P=0.04**	**R=0.709** **P=0.04**
Sediment Slope		R=0.231 P=0.16	**R=1** **P=0.1**	**R=0.833** **P=0.1**
Mixed sediment and rock			**R=0.945** **P=0.04**	**R=0.836** **P=0.04**
"Lophelia reef"				R=0.5 P=0.33

R levels below 0.4 considered to have no difference

R levels >0.4 and <0.7 considered to be the same as they are different

R levels >0.7 considered different

P values <0.05 considered significant at 5% level

P Values <0.1 considered significant at 10% level.

Those in bold are considered to be significantly different from one another.

Table 3. 6. Results of SIMPER tests comparing significantly different coral assemblages compositions upon different substrata across Whittard Canyon.

	***"Lophelia* reef"**	**"*Lophelia* and Rock"**
Sediment	92.0 %	88.98 %
	Lophelia	*Lophelia*
	Acanella	*Primnoa*
	Pennatula aculeata	*Anthomastus*
Sediment Slope	88.98 %	75.88 %
	Lophelia	*Acanella*
	Acanella	*Lophelia*
	Acanothogorgia	*Primnoa*
Mixed sediment and rock	86.12 %	67.19 %
	Lophelia	*Acanella*
	Anthomastus	*Lophelia*
	Acanella	*Primnoa*

Number represents the percentage of dissimilarity between the two substrata types with the top three contributes listed below.

Figure 3.14 shows that Dive 65 is mainly dominated by Mixed sediment and rock and sloped sediment, there is no occurrence of "*Lophelia* reef" or "*Lophelia* and rock" within this Dive. *Acanella* is found all along entire transect (3.14B), with the highest numbers coinciding with mixed rock and sediment slope. *Anthomastus* (Figure 3.14 C) was found mainly in the east of the transect, where the Canyon becomes deeper, associated with sloped sediment. A few observation of *Lophelia* occurred (Figure 3.14D) where there was mixed rock and sediment.

Lophelia was absent from Dive 106 (Figure 3.15D) where the dominant substratum type was mixed sediment and rock, with some sedimented areas also recorded (Figure 3.15A). Very few *Acanella* or *Anthomastus* (Figure 3.15B, 3.15C) were recorded during this dive; those which did occur were associated with mixed sediment and rock substratum.

Dive 114 shows the presence of sediment to the north-east of the transect line, mixed sediment and rock occurred in the central area, with a small area of "*Lophelia* and rock" and "*Lophelia* Reef" occurring in the central area (Figure 3.16A). Sloped sediment was also observed in the south-west of the transect line. *Acanella* (Figure 3.16B) was present in high abundance along the sediment line, with reduced occurrence where hard substratum was present. Very few *Anthomastus* (Figure 3.16C) were observed within this region with none in the sediment only area to the north-east. A few were associated with sediment slope. *Lophelia* (Figure 3.16D) was also observed during this Dive, coinciding with a small reef structures and some patches of "*Lophelia* and rock", which themselves were scattered throughout mixed sediment and rock substratum type.

Dive 116 consisted of a sediment track followed by the occurrence of a "*Lophelia* reef" to the East (Figure 3.17A). Few *Acanella* (Figure 3.17B) or *Anthomastus* (Figure 3.17C) were

observed during this Dive, and all occurred to the Eastern area. A high density of *Lophelia* (Figure 3.17D) was found along the Reef structure.

Species and substratum cumulative curves (Figure 3.18) show that *Lophelia*, unsurprisingly, follows the occurrence of "*Lophelia* and Rock" and *"Lophelia reef"* with all *Lophelia* sightings within the upper 1,800 m of the ocean. *Pennatula aculeata* only occurs within the upper 1,800 m. *Acanella* closely follows the combination of sediment and sediment slope and sediment with rock and is found at all depth ranges within this study. *Anthomastus* has a greater occurrence below 1,800 m depth and from 2,800m closely follows the trend set by sediment and rock. Below this depth the relationship is not as clear but does still exist. *Primnoa* was only found within one dive and occurs between 1,500 and 1,800 m depth. This upward trend can be related to an increase in the availability for the sediment and rock substratum at this depth.

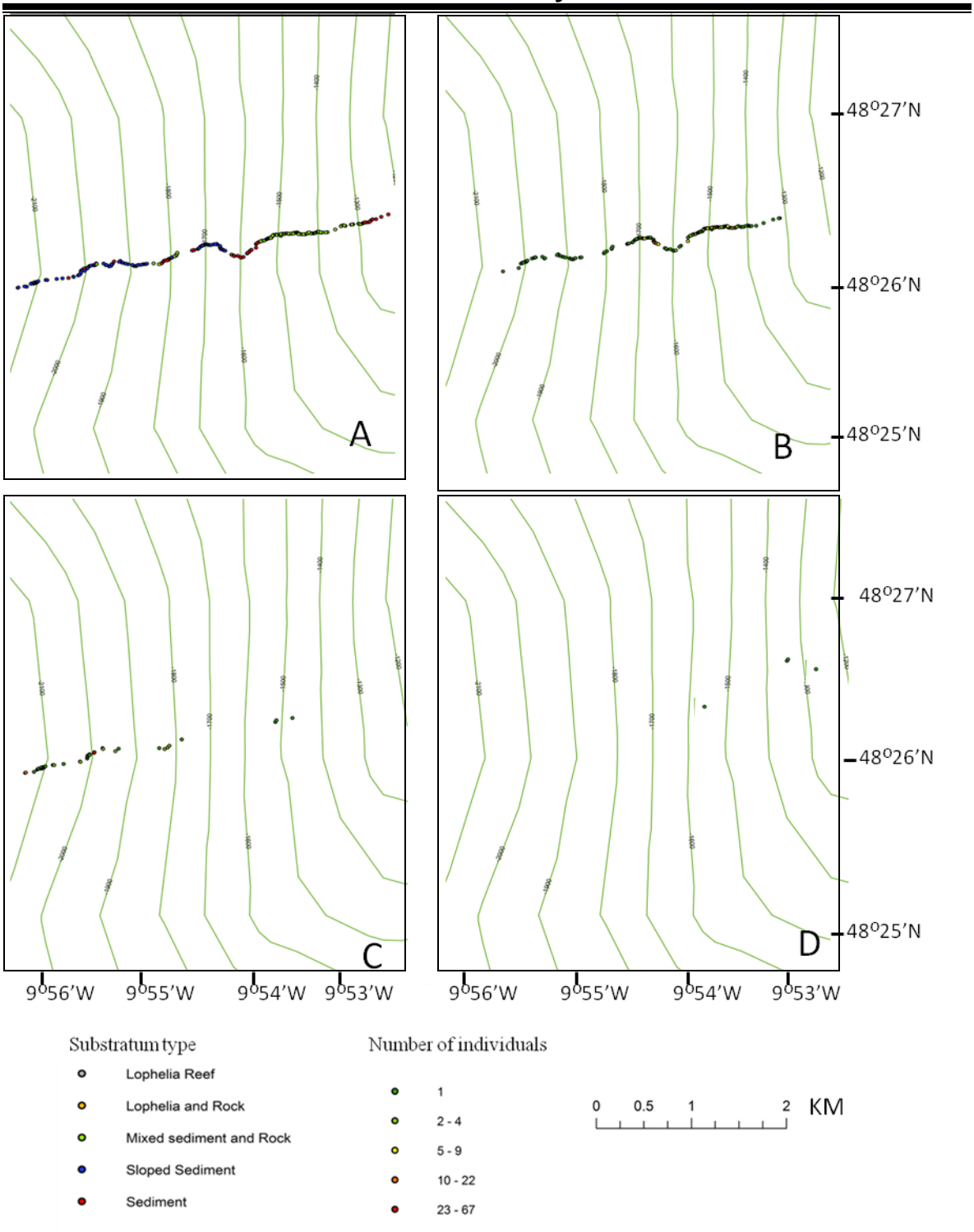

Figure 3.*14. Substratum type,* Acanella, Anthomastus *and* Lophelia *distribution within Isis Dive track 65. A= Substratum type, B-* Acanella *C=*Anthomastus *D=* Lophelia

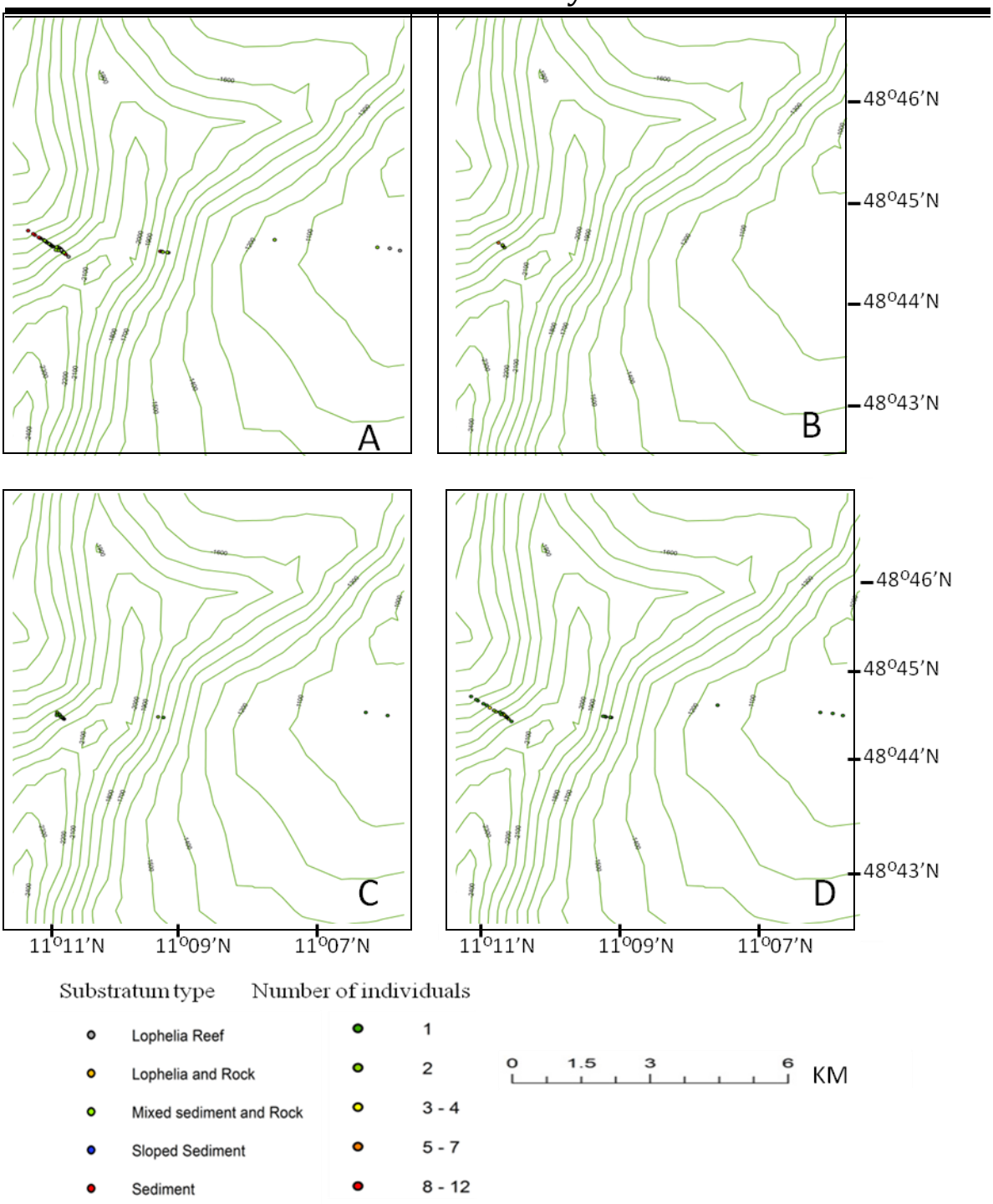

Figure 3.*15. Substratum type,* Acanella, Anthomastus *and* Lophelia *distribution within Isis Dive track 106. A= Substratum type, B-* Acanella *C=* Anthomastus *D=* Lophelia

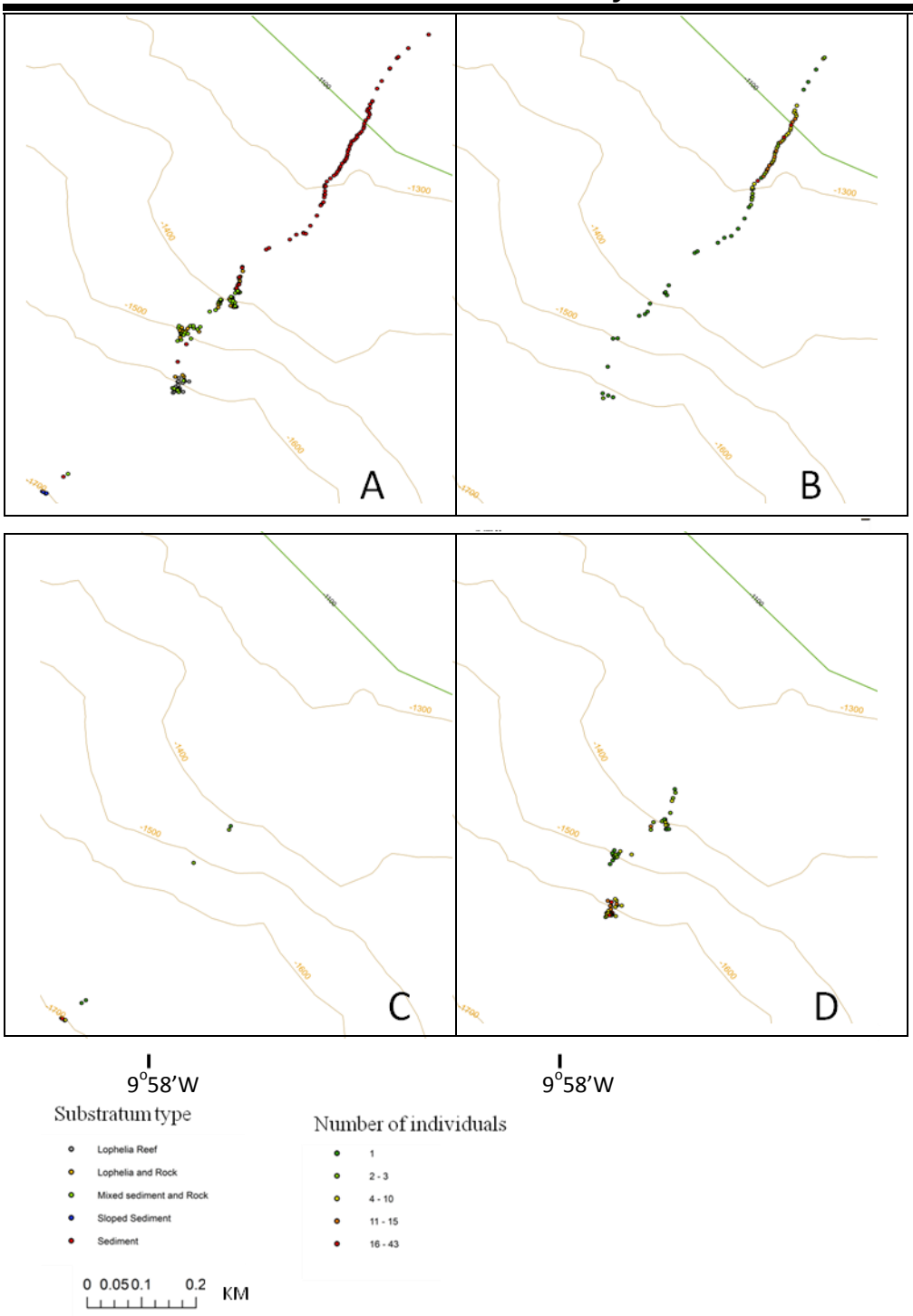

Figure 3.*16. Substratum type,* Acanella, Anthomastus *and* Lophelia *distribution within Isis Dive track 114. A= Substratum type, B-* Acanella *C=* Anthomastus *D=* Lophelia

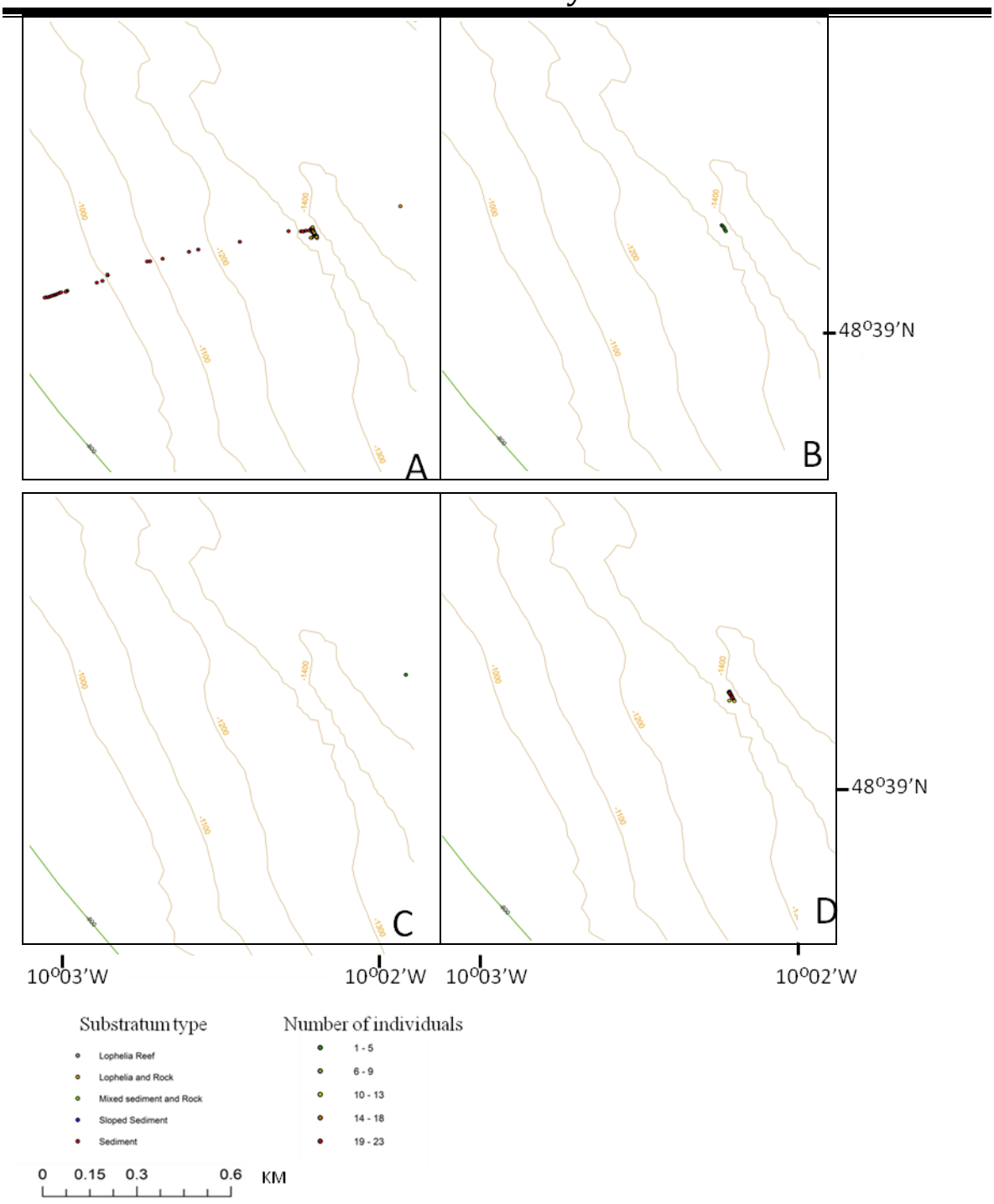

Figure 3.*17. Substratum type,* Acanella, Anthomastus *and* Lophelia *distribution within Isis Dive track 116. A= Substratum type, B-* Acanella *C=* Anthomastus *D=* Lophelia

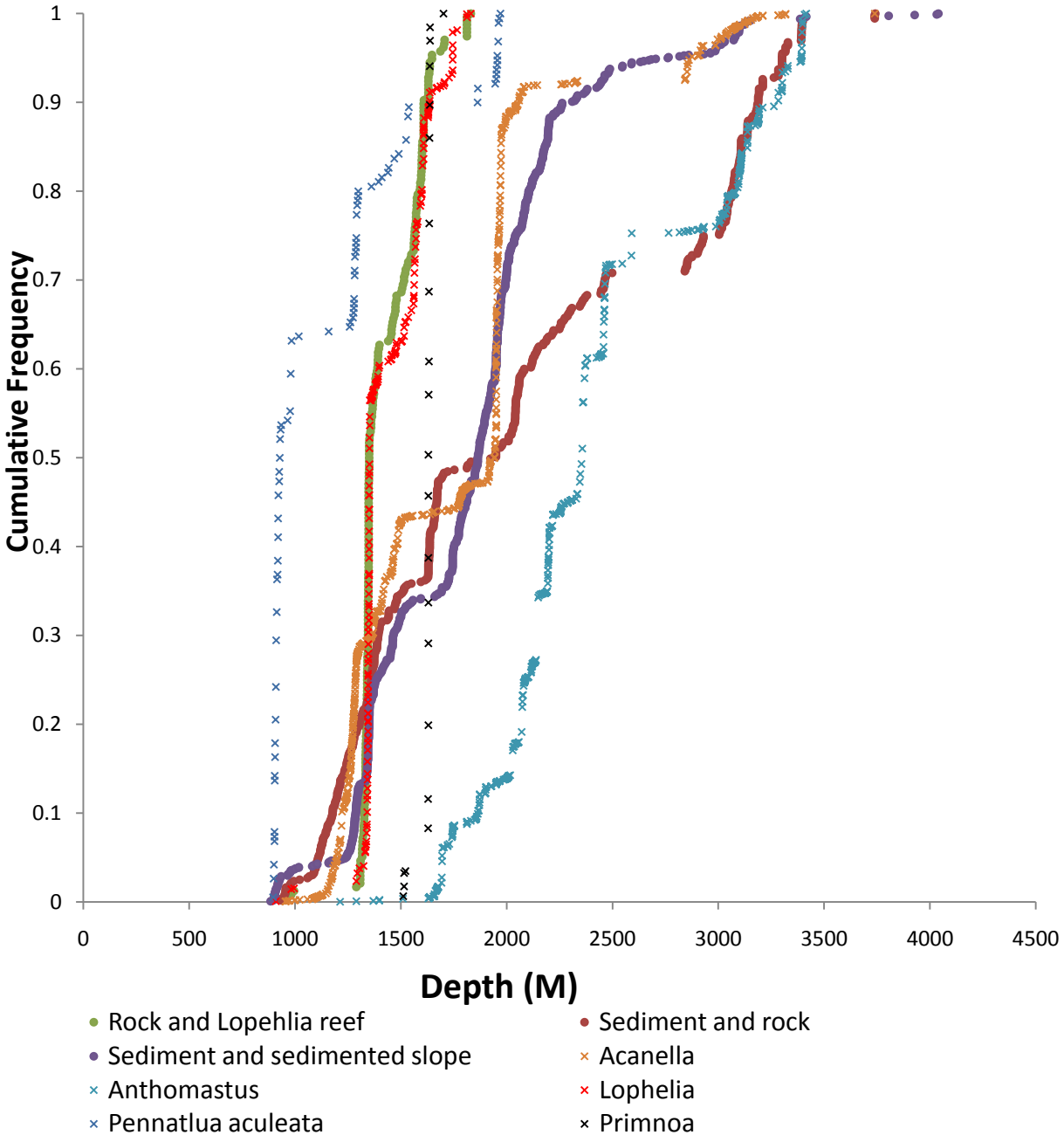

Figure 3.18 *Cumulative frequencies of the top five species which create dissimilarity between substrata types in Whittard Canyon.*

3.4 Discussion

3.4.1 Environmental setting

The Whittard Submarine Canyon lies on the border of the Irish Exclusive Economic Zone (EEZ), on the continental margin of the Bay of Biscay, which is often considered to be a deep-sea ecosystem hotspot along the European margin (Weaver *et al.*, 2004; Weaver *et al., 2*009; Van Rooij, 2010). The Whittard Canyon covers an area of over 10,000 km^2, reaching depths of over 4,000 m. The upper branches of the canyon have a steep sided v-shaped channel which changes to a u- shaped valley further down canyon. Gullies in the upper course turn to terraces and ridges further down the channel (Crowe, 2010). "*Lophelia reef"* substratum is found in the upper course of the canyon, but is absent as the canyon deepens. In a few patches dead *Lophelia* was observed with what looked like trawl marks though the centre of the patches, indicating previous trawling activity in the area. It is likely that this activity would have destroyed any *Lophelia* reef present within the region, resulting in a lower coral abundance than would have naturally been observed. Slow growth rates and sporadic breeding will lead to an elongated recovery period after such an event (Fossa *et al.*, 2002; Hall-Spencer *et al.*, 2002; Freiwald *et al.*, 2004; Mortensen *et al.*, 2008).

Sedimentation level increases further down the slopes, however, even at higher levels thin sediment layers are seen covering virtually all non-vertical surfaces. The high levels of sediment observed throughout this study are hardly surprising as canyons are known to be transport passageways of sediment from the slope to the deep sea (Rowe *et al., 1*982; Vetter and Dayton, 1998; Dunieveld *et al., 2*000).

3.4.2 Depth

Differences in water depth, and subsequently pressure, have often been suggested as responsible for changes in assemblage, species diversity, abundance and biomass in the deep-sea (Bianchellie *et al.*, 2010). However, the present study showed no significant differences between the assemblage compositions at different depths within the Whittard Canyon, in either 200 or 500 m depth bands. This is in agreement with Bianchellie *et al.* (2010), but contrasts others who found an increase in overall species diversity with depth (Jones *et al*., 2007; Pattenden, 2008). This difference could be attributed to the fact that this study focused on the overall assemblage composition and not individual species when investigating the effect of depth. When individual species were considered some patterns became apparent.

Lophelia was only found within the top 1,800 m. A finding which in congruent with the general understanding that Scleractinia have their highest density above 1,500 m (Squires, 1967; Rogers *et al., 2*007), as a result of the aragonite saturation horizon (ASH), the depth between water saturated and under-saturated with aragonite (Turley *et al., 2*007). This zones lies at a depth of about 2,000 m in the Northern Atlantic (Orr *et al.*, 2005; Guinotte *et al.*, 2006; Turley *et al., 2*007). Below this level *Lophelia* and other scleractinians would be subjected to aragonite dissolution and thus may be unable to create strong skeletons reducing survivorship with increasing depth. This will also have an effect on *Lophelia* reef associated species (Roberts *et al.*, 2006), as a result of reduced habitat or food.

Octocoral taxa such as *Anthomastus* are not dependent on aragonite to create their structure and thus can be found to greater depths. This was well illustrated in the present study where *Anthomastus* and other octocoral species were found in depths in excess of 3,500 m. However, some octocoral species appears to be depth limited, such as *Pennatula aculeata* which was found to only occur in the top 1,800 m examined. Nevertheless, this is more

likely a result of substratum availability rather than increased pressure as a function of depth. *Pennatula aculeata* requires sediment to be able to settle and root using its foot-like peduncle. As a rule sediment tends to become finer with increased depth, with a decreased organic carbon concentration (Tyler, 1995; Oliveira *et al.*, 2007). This change in sediment type may prevent the *Pennatula aculeata* from being able to root effectively meaning it is unable to grow successfully.

3.4.3 Assemblage structure on substratum types.

With the world's oceans having an estimated 660 canyon systems (De Leo *et al*., 2010) they are important ecosystems to understand. Very little work on canyon assemblage structures has been completed (Davies, 2008) with even less concentrating on the coral assemblage structure. Canyons are home to areas of steep exposed rock as well as areas of high sedimentation. Therefore it would be expected that they will be home to a variety of coral species, taking advantage of the varied substratum types (Carey *et al*., 1990; Mortensen and Buhl-Mortensen, 2005).

The most abundant family found upon sediment substratum within the Whittard Canyon was Isididae, a direct result of extensive *Acanella* patches. This was also demonstrated by the tracks of Dive 144 (Figure 3.16) where *Acanella* was seen to follow the availability of sediment. This finding is consistent with Mortensen *et al*. (2008) who found that *Acanella* dominated sediment areas within their study region along the Mid-Atlantic Ridge, despite being very different habitats. This would indicate that, like Pennatulacea, some species of the family Isididae have a root like system which allows them to grow successfully in sedimented areas (Gass and Willison, 2005**;** Woodby *et al*., 2009). It is this root like system which often causes Pennatulacea to be the most dominant feature within sedimented areas, though not in this study. Chrysogorgidae have also been found to colonise areas of sediment (Mortensen and Buhl-Mortensen, 2005; Woodby *et al*., 2009).

This was illustrated in the present study by an increase in the presence of *Radicipes* within sedimented areas in comparison to other substratum types. This is also consistent with the increase of Sprial corals along the AVR in the previous chapter (Chapter 2).

The most dominant family within the mixed sediment and rock was the Alcyoniidae comprised solely of *Anthomastus*, which requires a hard substratum for colonisation (Cordes *et al*., 2001). *Anthomastus* was found in all dives except one and shows a highly patchy distribution, with many individuals occurring on the side of rocks or on sedimented slope often forming areas of high density. *Anthomastus* that were observed on sediment slope could be a result of underlying rock which was difficult to visualise in the video footage (Watanabe *et al*., 2009).

Within the "*Lophelia* reef" and "*Lophelia* and rock" substratum types it was, unsurprisingly, *Lophelia* which dominated. It was also demonstrated that "*Lophelia* reef" and "*Lophelia* and rock" have the highest coral densities in comparison to the other substratum types, as a result of densely clustered *Lophelia* colonies. *Lophelia* habitats were also seen to separate from other substratum types in the MDS plot, indicating a difference in assemblage composition in comparison to the other substratum types within this study.

Unlike most other cold-water coral *Lophelia* is capable of creating reef-like structures (Turley *et al*., 2007). These structures lead to an increased habitat complexity and are home to many associated species including anemones and fish (Roberts *et al.*, 2006). Fish were also seen to increase within the vicinity of the reef in the present study (personal observation). Red gorgonians were only observed within the "*Lophelia* reefs" throughout this study, despite this the *Lophelia* substratum types were not found to have a high diversity of coral families (Table 3.3 and 3.4). This may indicate that although *Lophelia*

increases regional diversity because it forms a distinct community, at a local scale it can lead to a reduction in diversity by out-competing other coral species. At depth, where the *Lophelia* is unable to survive because of the ASH, a variety of other corals are able to fill the niche, resulting in a different assemblage than if *Lophelia* were present and a subsequently increased variety of coral families present.

Sediment slope did not have a significant increase in mean number of individuals over sediment. However, slope maps indicated that the highest abundance of corals per 100 m transect occurred where the slope was greatest (Figure 3.3). When individual species distribution was considered *Anthomastus* was shown to increase in areas with increased slope (Figure 3.13-14). *Lophelia* was generally observed on overhangs or on boulders in the sediment. This may be attributed to the fact that small-scale features, such as a boulders or rocks and slopes can create heterogenity on the seafloor surface which in turn can lead to an increase in water flow over the obstacle and subsequently food availability (see previous chapter for more in depth discussion) (Genin *et al*., 1986; Genin *et al*., 1989; Rogers, 1994; Dower and Mackas, 1996; Koslow, 2007). However, the difference in mean number of individuals observed per time period was not discernable. This may be ascribed to the occurrence of large patches of *Acanella* within the sediment throughout the study. It is also likely that most of the sediment slope areas are rock draped in sediment structures. Such structures are partial to periodic slump events which could wipe out the coral assemblage present and lead to a reduced density than would otherwise be observed (Okey, 1997).

Reduced effect of slope on the number of individuals observed per time period could also be an indication that food is not as limited within the Whittard Canyon as within other deep-sea areas. Slopes are expected to lead to an increase in the food concentration and availability within their vicinity as a result of increased water flow. However, canyons are

known to be conduits of sediment from the continental slopes into the deep-sea (De Stigter *et al., 2*007; Arzola *et al.,* 2008), with increased flow rates as a consequence of increased turbulence from meeting water masses and a higher intensity of internal waves (Quaresma *et al.,* 2007). These phenomena often lead to the creation of nepheloid layers and could lead to increased food availability within the canyon in comparison to other deep-sea habitats. This would be in agreement with Rowe (1971) who found that increased sediment transport within canyons leads to the provision of a food source in the deep- sea which otherwise would be absent. Should this be the case then the altered hydrodynamic regime within the canyon will cause the effect of slope upon the concentration of food material to become minimal.

3.4.4 Individual species occurrence

The three most abundant species observed throughout this study were *Anthomastus, Acanella* and *Lophelia*, accounting for almost 75 % of all observations, often occurring in high density patches. *Lophelia* are often found in high abundances as a result of their ability to create reef structures. Mortensen *et al*. (2008) found during a study of the Mid Atlantic Ridge (MAR) that *Anthomastus* were almost as abundant as *Lophelia* and were observed in 13 % of video sequences analysed, reaching a high density of almost 300 colonies within 100 m^2. *Acanella* was also found to be of high abundance in sedimented areas within this area of the MAR (Mortensen *et al*., 2008).

Distribution maps of *Acanella*, *Lophelia* and *Anthomastus* (Figure 3.14-3.17) illustrate that *Acanella* and *Lophelia* are mutually exclusive, as a result of substratum preferences. However, all three may be absent from areas where the substratum type present is optimal for colonisation. This is in agreement with Mortensen and Buhl-Mortensen (2004) who found areas of cobble and boulder devoid of gorgonians, despite being within the optimal

depth range. From this it can be concluded that factors other than substratum type play an important role in small-scale coral distribution patterns, within the canyon.

3.4.5 Food availability

Coral distribution within the canyon was observed to be patchy with large areas of *Anthomastus* and *Acanella* surrounded by areas with little or no coral occurrence. This cannot be attributed to either depth or substratum type. The deep-sea is known to be a food limited environment (Smith *et al*., 2009). Corals are passive suspension feeders and thus require a particle flux which is high enough to meet their metabolic rate, meaning not all areas are suitable for colonization (Thistle, 2003).

During the JC36 cruise the SAPs (stand-alone pump system) were used to measure the concentration of particles sinking to the sea floor within the canyon. Although POC (particulate organic carbon) is directly related to surface production the preliminary results from these demonstrated that some areas within the canyon are subject to higher organic input than others, concurring with Gage and Tyler (1991) that food availability within the deep-sea is patchy. This would impact on the food availability for corals, with material exported from the shelf to various branches within the canyon differing from one another (Masson, 2009). It is likely tha variability in food availability would be a more determinant factor in coral distribution than depth or substratum type. The majority of high density coral patches occur in the eastern branch of the canyon, indicating that there maybe a higher organic carbon input here than in the Western branch. This also relates back to the slope of the area as there is an increased slope in the Eastern branch in comparison to the Western branch, which in turn can lead to an increased food availability as previously discussed.

3.4.6 Coral assemblages within Whittard Canyon and along Axial volcanic ridge 45^{o}N on the Mid Atlantic Ridge

There is more than a three times increase in the number of coral colonies observed in the Whittard Canyon in comparison to the AVR, despite less video footage being analysed. The highest density per 100 m transect within the AVR is 59 individuals in comparison to 855 within the Whittard Canyon. However, it must be noted that the highest density of individuals within the Whittard Canyon occurred upon *"Lophelia reef"*, a substratum type which was not present upon the AVR, possibly as an effect of depth limitataions of the study, with *Lophelia* being unable to thrive below the ASH depth.

Eleven more tentative species were found within the Whittard Canyon than along the AVR, although not all of the species found on the AVR were found in the Whittard Canyon. For example there were no *Iridogorgia* or *Narella* found within the Whittard Canyon. Taxa in common between the two sites included the whip coral, *Umbellula*, *Paragorgia*, *Bathypathes* and *Anthomastus*. Species found within the Whittard and not along the AVR include *Acanella*, *Lophelia*, *Pennatula aculeata* and *Primnoa*. The absence of *Lophelia* in the AVR will be a direct result of the depth profile used; as previously discussed *Lophelia* can only occur above the aragonite saturation zone, which lies at 2,000 m in the Northern Atlantic (Turley *et al., 2*007). The study which took place in the AVR covered a depth range of 2,600-3,600 m, all deeper than the ASH, subsequently, no *Lophelia* were observed . Absence of *Acanella* and *Pennatula aculeata* are harder to explain. It may be that the sediment layer within the Whittard Canyon and the AVR are made up of different particle types and sizes which are not congruent with settlement of such corals. *Pennatula aculeata* was only found above 1,800 m within the Whittard a depth which was not investigated in the AVR and thus may have been absent in the AVR as a result of depth, or differences in sediment composition. The absence of *Narella* within the Whittard Canyon may also be a direct result of substraum type. In the AVR , *Narella* occured only on basalt pillows, a habitat type which was not observed in the Whittard Canyon. This difference between continental marine habitats (here Whittard Canyon) and

Oceanic marine habitats (the AVR) has also been observed by Hall-Spencer *et al.* (2007). They found seamounts were on average only 29% similar to the neighbouring continental slope, with some species only occurring in oceanic environments and others only occurring in oceanic habitats when comparing deep-sea coral distribution on seamounts, oceanic islands and continental slopes.

The dominant species change between the two areas, with the AVR dominant species mainly consisting of Whip coral and *Isididae* n. sp. 1 where as in the Whittard Canyon the dominant species are *Anthomastus*, *Acanella* and *Lophelia*. Again this may be a result of habitat type (as with *Lophelia*) or it could be that the food input with the two areas is different in both abundance and type.

Nutritional input from the surface waters will differ in different areas. The AVR is further from the continental shelf is believed to be free from continental processes such as fluvial action (Mitchell *et al.,* 2000). However, Whittard Canyon is close to the shelf, meaning it is prone to higher levels of nutrient input. Current regimes within the two areas also differ. The AVR is believed to be an enclosed system with periodic flushing events (Murton *et al.,* 1999) with water slowly homogenizing between flushing events (Saunders and Francis, 1985). Conversely Whittard Canyon is a much more active and open system, funnelling organic matter to depth via a variety of mechanisms including; tidal currents, internal waves and turbidity flows (Rowe *et al.,* 1982; Vetter and Dayton, 1998; Duinveld *et al.,* 2001; Quaresma *et al.,* 2007). This increase in activity and change in hydrodynamic regime in turn should lead to an increase in the food availability within the canyon in comparison to the AVR. This is illustrated by Figure 3.19 which shows the primary productivity of the Northern Atlantic and a zoomed in section incorporating the locations of both the AVR and the Whittard Canyon. The Whittard canyon lies on the border of the pink area (350-400 mol m^{-2} y^{-1}) indicating high levels of primary productivity where as the

AVR sits within the green area (150-250 mol m^{-2} y^{-1}) indicating reduced levels of primary productivity and subsequently reduced food input at depth. This may be partly attributed to higher nutrient input from the shelf into the Whittard Canyon, allowing a higher density of corals to be supported within the canyon system in comparison to the AVR. It is also likely that there will be a change in the nutritional value of the POC between the two areas.

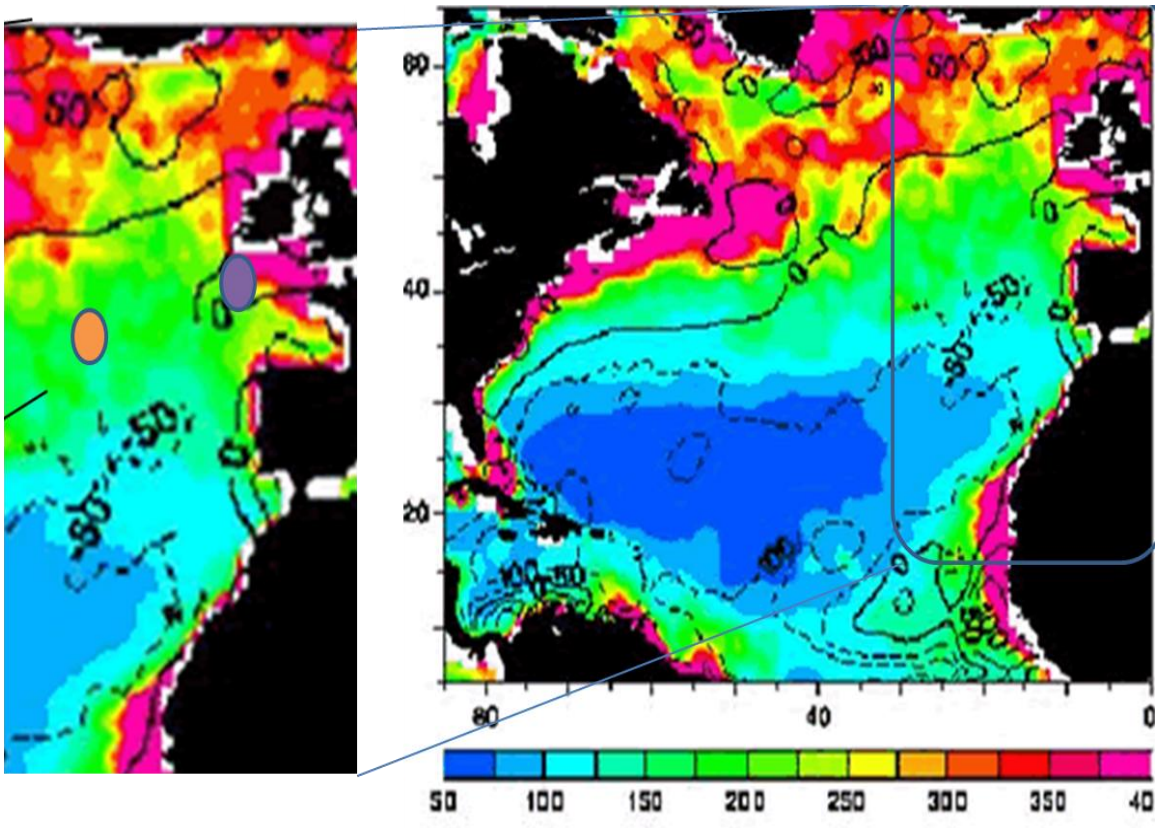

Figure 3. 19. Satellite based estimates of primary productivity (mol m^{-2} y^{-1}). Warmers colours indicate and area of increased productivity with blue indicating low productivity levels. The Whittard Canyon position roughly illustrated by the purple dot sits within the Pink area of productivity where as the AVR (Orange dot) sits within the green/ blue area, indicating reduced productivity upon the AVR. Images were modified from Sathyendranath *et al.* (1995).

The "*Amperima* event" famously demonstrated that a change in food input to the deep-sea can lead to a large change in the assemblage composition within that area (Billett *et al., 2*001, Billett *et al., 2*010). By looking at lipid content of the benthic assemblage it was

possible to conclude that certain organisms (mainly the holothurians *Amperima*) were able to take advantage of a relative change in the food composition, leading to selective feeding and competition resulting in a change in the assemblage composition (Billett *et al., 2*010). By looking at the gut contents of the holothurians it was possible to determine that different species have different biochemical requirements and thus will thrive under different conditions (Wigham *et al., 2*003). Although very little work has been undertaken on cold-water coral lipid content, Hamoutene *et al.* (2008) found that there were differences in lipid content between different species. Lipids are used as fat storage and thus can be used to trace at what kind of food and the amount of food they are eating. Gorgonians were found to have lower lipid content than soft corals, sea-pens and Antipatharia (Hamoutene *et al.,* 2008). It is also possible to use isotopic analysis to assess diet. Using $\delta^{13}C$ and $\delta^{15}N$ isotopic values Sherwood *et al.* (2008) found that *Ancathogorgia armata* fed at a higher tropic level than *Primnoa* sp. As deep-sea corals are azooxanthellate they depend entirely on external organic matter. Consequently the coral assemblages are indirectly fuelled by surface primary production as it sinks as particle fluxes (Duineveld *et al*., 2004). This would indicate that different coral species will thrive under different conditions and that the composition of the POC input to an area will have an impact on the coral assemblage. A difference in POC input may explain some assemblage changes between the two sites.

Slope was found to lead to an increase in the density of corals present within the AVR. However, this trend was not as clear cut within the Whittard Canyon. Again this may be a result of food input. The Whittard Canyon has naturally-enhanced particle concentrations and enhanced currents (Huvenne *et al.,* in prep) in comparison to the AVR. This may result in the enhanced flow created by water coming into contact with an obstacle (Genin *et al*., 1986; Genin *et al*., 1989) having less of an impact on food availability within Whittard Canyon in comparison to the slope effects on currents along the AVR.

3.4.5 Conclusions

This study has shown that substratum type has an effect on the Coral assemblages present within the Whittard Canyon. Coral densities were highest on *"Lophelia reef"* and "*Lophelia* and Rock", however the diversity of coral species was reduced here with *Lophelia* potentially out competing the other species. In this respect, although depth is not shown to have an effect on the assemblage structure per say, it does prevent *Lophelia* from dominating the entire canyon as a direct result of the ASH.

The distribution of corals within the Whittard Canyon was found to be patchy, with large aggregation of *Anthomastus* and *Acanella* occurring throughout the canyon, presumably as a result of food supply and quality as well as substratum type changing within different regions of the canyon. By comparing the results to the AVR of the MAR it is possible to conclude that although slopes do have an effect on the density of coral assemblages present at a local scale within a site, it is substratum type and food supply which are the most influential factors.

Chapter 4: The phylogenetic analysis of cold-water Octocorals

4.1 Introduction

Octocorals (Cnidaria: Anthozoa) are found in marine habitats ranging from the Arctic to the Antarctic and from intertidal to abyssal depths (Sánchez *et al*, 2003). Octocorals can grow individually or as coral gardens and are important structural components of some marine (McFadden *et al.,* 2010). Despite being the focus of numerous studies, the evolutionary history of octocorals remains poorly understood (Bayer, 1981). This limited understanding is partly a result of a near absent fossil record and a poor taxonomic resolution within octocorals. To improve our understanding of the evolution of octocorals there has been an increase in the use of molecular approaches to create phylogenetic trees in recent years, helping to understand the underlying evolutionary processes (France *et al.*, 1996; Bernston *et* al., 2001; Sánchez *et al.,* 2003, 2003a; McFadden *et al.,* 2004, 2006, 2010, 2011; Wirshing *et al.*, 2005; France, 2007). However, the phylogenetic relationships between the groups within the Octocorallia remain challenging, with taxonomic revisions occurring frequently, and much more remains to be resolved (McFadden *et al.,* 2006a, 2010).

The current taxonomic system in use was proposed by Bayer (1981) where he identified three Octocorallia orders: Pennatulacea (sea pens), Helioporacea (blue corals), and Alcyonacea (soft corals, gorgonians and stoloniferous forms) (see review by McFadden *et al.,* 2010). However, morphological identification has difficulties; very few deep-sea coral species have taxonomic descriptions published and many which are published lack informative illustrations, or any illustrations at all (Sánchez , 2007). Features which have traditionally been used to identify individuals include: growth form, axis composition, shape and arrangement of sclerites (McFadden *et al.,* 2010). However, it is not possible to create evolutionary trees from morphology alone, with high levels of intraspecific

variability and homoplasy hindering any attempts (Williams, 1992; Roberts *et al*., 2009) and until the advent of molecular techniques there was no attempt to create a comprehensive hypothesis for Alyconacea evolution (McFadden *et al.,* 2010).

The species- and population-level phylogenetic work upon octocorals severely lags behind most other invertebrate groups (McFadden *et al.,* 2010). Early phylogenetic work, which was based primarily on 18s and 28s rDNA markers supported a hypothesis of monophyly (one common ancestor) within the Octocorallia and the sister group Hexacorallia (McFadden *et al.,* 2010). *MSH1*, a unique protein coding a mitochondrial mismatch repair gene, believed to be a homologue of the *mut-s* gene in bacteria, was later discovered to be a synapomorphic character (a trait shared by two or more taxa and their most recent ancestor, but not the ancestor's ancestor) (McFadden *et al.,* 2010). To date, *MSH1* has been found in all octocoral families, where the mitochondrial DNA has been sequenced, but has not been found in any other metazoans (Culligan *et al.,* 2000). This, coupled with the fact that evolutionary rates in Octocorallia are relatively slow, often in the region of 50-100 times slower than the mitochondrial genomes from most other animals (Shearer *et al*., 2002; Hellberg, 2006; McFadden *et al.,* 2011), makes *MSH1* a suitable marker for determining phylogenetic relationships for octocorallia species. *MSH1* has been shown to have at least twice the variation of other protein-coding regions in the octocoral mitochondrial genome (France and Hoover, 2001; Wirshing *et al.,* 2005; Van der Ham, *et al*., 2009; McFadden *et al*., 2010) and has been predominantly used in Octocorallia phylogenetic research since its discovery.

ND2 (NADH dehydrogenase subunit 2) is also a mitochondrial protein-coding gene (McFadden *et al.,* 2004, 2010). NADH is a ubiquinone oxidoreductase complex, involved in the respiratory chain in both mitochondria and bacteria (Nakamaru-Ogiso *et al.,* 2010). Again the slow evolutionary rate of the mitochondrial genomes makes *ND2* a suitable marker for determining phylogenetic relations for Octocorallia species (Shearer *et al.,* 2002; McFadden *et al.,* 2011). Along with the *MSH1* gene the *ND2* gene, has been used in

phylogenetic reconstructions by McFadden *et al.* (2006), Wirshing *et al.* (2003) and Sánchez *et al.* (2003a).The use of mitochondrial DNA for phylogenetics also has advantages because, unlike the nuclear DNA, mitochondrial DNA is usually only passed on from the maternal parent to the offspring (Shearer *et al.,* 2002). The mitochondrial DNA recombine with copies of itself within the mitochondria, leading to a lower rate of recombination than nuclear DNA, which is inherited from both parents following recombination with each other (Dolan, 2008).

The first studies with sufficient taxa to allow relationships between Octocorallia families to be assessed were carried out by France *et al.* (1996) and Berntson *et al.* (2001). However, the most complete phylogenetic analysis to date was carried out by McFadden *et al.,* (2006) who constructed a phylogeny for Octocorallia using partial sequences for two mitochondrial protein-coding genes *ND2* and *MSH1* for 115 genera encompassing 46 families. Results indicated that there were two large distinct clades, one including Holaxonia, some Scleraxonia and Stolonifera, and the other including Pennatulacea, *Heliopora* and Calcaxonia, and one smaller unresolved clade that included families from Alcyoniidae and Coralliidae.

The phylogeny created by McFadden *et al.* (2006) supports the results of previous, less complete, phylogenies using 18S and 16S genetic markers carried out by France *et al.* (1996), Berntson *et al.* (2001) and Sánchez *et al.* (2003a) which all reported two or three distinct clades: one clade containing all of the sea-pens (Pennatulacea), Helioporacea and the sea fan sub-order Calcaxonia, another with the Alcyoniina and most of the Scleraxonia and Stolonifera. Although all studies differ slightly in the form of which these clades occur, there is a general agreement throughout. However, none of these correspond to the traditional ordinal divisions placed within the Octocorallia (McFadden *et al.,* 2006). As yet no analysis has included all genera within the Octocorallia and thus it is difficult to make a definitive statement regarding the hypothesis of monophyly of families.

It is suspected that most families do not represent monophyletic groups, for example the Acanthogorgidae have been shown to have two distinct lineages, but some exceptions do occur where monophyletic groups have been identified, including the Primnoidea and Isididae (McFadden *et al.,* 2006). However, ongoing studies are also beginning to imply a polyphyletic trend in many of these families (McFadden *et al.,* 2010). Previous studies have not had a high enough resolution to confidently determine familial level relationships, with the only relationship which is well supported occurring between the Pennatulacea and the calcaxonian family Ellisellidae (McFadden *et al.,* 2010). The low rate of evolution found within the mitochondrial DNA has hindered the study of phylogenetic relationships at species level (Shearer *et al.,* 2002; McFadden *et al.,* 2010).

Levels of variation among families of Octocorallia are within the range of 2.7-6.3 % in *16S* rDNA (France *et al.,* 1996, McFadden *et al.,* 2010), and less than 10% for *ND3*, *ND4L*, *ND2* and *ND6* (France and Hoover, 2001; McFadden *et al.,* 2004; McFadden *et al.,* 2010), with *MSH1* being found to have approximately twice this level of variation of other protein coding genes in the mitochondrial genome (France and Hoover, 2001; Van der Ham *et al*., 2009; McFadden *et al*. 2010). However, the level of differentiation within *MSH1* appears to vary within genera. The Keratoisidinae is easily distinguished from other families, as a result of an inversed gene order within the *MSH1* region (Brugler and France, 2008). However, there is very little divergence among the taxa within clades (France 2007, McFadden *et al.,* 2010). Even when combining *MSH1* with another gene such as *ND2* there is no improvement in the discrimination of congeneric morphospecies (Wirshing *et al*., 2005; McFadden *et al.,* 2010).

Further tests to identify a single gene which can be used for species-specific "barcoding", a process by which an unknown individual can be identified by comparing its genetic make-up to known species (McFadden *et al.,* 2011), have resulted in the conclusion that there is

currently no single gene or gene region which varies to a sufficient level to unmistakably distinguish between species (Van der Ham *et al.*, 2009; McFadden *et al.*, 2010, 2011), thus combined genes are required to ensure a higher level of reliability. It is the lack of a significant variation between inter- and intra-species differences which means that species barcoding is difficult. As a consequence of this, phylogenetic analyses are more likely to identify family differences than allow the identification of new species. However, intra-species differences rarely exceed 0.5% and thus it has been argued that anything above that should be regarded different species (McFadden *et al.*, 2011). It must also be noted that because of the general lack of understanding of taxonomic separation within the Octocorallia these molecular markers, however flawed, will help to create better taxonomic understanding by separating individuals into clades in which morphological characteristics can be compared (McFadden *et al.*, 2010).

4.1.1 Aims

The present study focuses on the creation of a phylogenetic tree from deep-sea octocorals primarily taken from the Northern Atlantic Ocean including from the Azores Islands, from the Mid-Atlantic ridge and with others taken from the North Sea and Antarctica. The aim of this chapter is to create a comprehensive phylogenetic tree of the order Octocorallia including new samples obtained from various sites within the Atlantic using both the *MSH1* and *ND2* genes. This will be achieved by addressing the following objectives:

1. Obtain octocoral samples and complete molecular analysis using the *MSH1* and *ND2* genes, to allow the creating on genetic alignments.
2. Obtain all published Octocorallia data for *MSH1* and *ND2* genes from NCBI and add this to the newly created data to produced one dataset.
3. Complete Phylogenetic analysis using MrBayes, PHYML and PAUP programmes to create full and comprehensive phylogenetic trees using the full data set and the individual genes separately.

4.2.Materials and methods

4.2.1 Sample procurement

A total of 118 ethanol-preserved octocoral specimens were used in this study. These were collected from a range of sources and depths (Table 4.1). The majority of the samples were collected using ROV *Isis* during R.R.S. *James Cook* cruise JC24 along the Mid- Atlantic Ridge (MAR) at 45^{o}N 27 ^{o}W as well as JC36 within the Whittard Canyon 48^{o} 15' N, 10^{o} 30'W, with others from R.V. *Celtic Explorer* cruise CE10014 within the Rockall Trough and Belgica Mound in the Northern Atlantic using ROV *Holland*. Two samples were obtained from the Bahamas and nine from the Antarctic, courtesy of Paul Tyler (University of Southampton, NOCS) and five from the MAR obtained from R.R.S. *James Cook* cruise JC48 courtesy of Claudia Alt (University of Southampton, NOCS), 8 from the Atlantic by Daniel Jones (University of Southampton, NOCS) and 31 from the Azores collected using Lula 500 submersible and as by catch of fisheries (Figure 4.1)

4.2.2 DNA extraction

DNA was extracted from the octocoral specimens using a DNeasy kit from Qiagen (West Sussex, UK) according to the manufacturer's recommendations. Briefly, the protocol involved using polyp tissue from the samples which was macerated, added to 180µl of ATL buffer and 20µl of proteinase K, and incubated overnight on a shaking table set at 800 rpm and 56^{o}C. 200 µl of buffer AL was added to the digest, followed by 200 µl of molecular grade 99% ethanol (Sigma-Aldrich, Dorset, UK). Samples were vortexed before being transferred into a DNeasy Mini Spin Column and centrifuged for 1 minute at 8,000 rpm. Once centrifuged the spin column was placed into a fresh collection tube and 500 µl of buffer AW1 added, this was then centrifuged at 8,000 rpm for 1 minute. Again the column was placed in a fresh collection tube and 200 µl of Buffer AW2 added and then

Table 4.1 Location and collection data for samples used within this study

Sample identifier	**Tentative identification**	**Area of collection**	**Latitude (N)**	**Longitude (W)**	**depth (M)**	**collection method**	**Collection date**	***ND2***	***MSH1***
5	*Narella*	Pico-Faial channel	38.290	28.370	**	submersible	28/11/08	N	Y
6	*Narella*	Pico-Faial channel	38.290	28.370	**	submersible	28/11/08	Y	Y
7	*Narella*	Pico-Faial channel	38.290	28.370	**	submersible	28/11/08	N	Y
8	*Narella*	Pico-Faial channel	38.290	28.370	**	submersible	28/11/08	N	Y
9	*Narella*	Pico-Faial channel	38.290	28.370	340	submersible	12/6/09	Y	N
10	*Narella*	Pico-Faial channel	38.290	28.370	340	submersible	12/6/09	Y	Y
11	*Viminella*	Pico-Faial channel	38.290	28.370	340	submersible	12/6/09	Y	N
12	*Viminella*	Pico-Faial channel	38.290	28.370	340	submersible	12/6/09	N	Y
13	*Viminella*	Pico-Faial channel	38.290	28.370	340	submersible	15/6/09	N	Y
14	*Acanthogorgia*	Pico-Faial channel	38.290	28.370	300	submersible	15/6/09	N	Y
15	*Viminella*	Pico-Faial channel	38.290	28.370	320	submersible	15/6/09	N	Y
An 1	*Lepidisis*	Antarctica	**	**	**	submersible	**	Y	Y
An 2	**	Antarctica	**	**	**	submersible	**	N	Y
An 3	**	Antarctica	**	**	**	submersible	**	N	N

An 4	*Corallium*	Antarctica	**	**	**	submersible	**	N	Y
An 5	*Corallium*	Antarctica	**	**	**	submersible	**	N	N
An 6	*Narella*	Antarctica	**	**	**	submersible	**	Y	Y
An 7	**	Antarctica	**	**	**	submersible	**	N	N
An 8	*Isidella*	Antarctica	**	**	**	submersible	**	Y	N
An 9	*Isidella*	Antarctica	**	**	**	submersible	**	Y	N
Az 1	*Acanthogorgia*	Faial, off Aeroporto Corvo, Fora do	38.518	**	457	bycatch	8/8/80	N	N
Az 10	*Acanthogorgia*	Aeroporto Terceira,	39.650	39.640	629	bycatch	22/6/07	N	N
Az 11	*Acanthogorgia*	Contendas	38.640	38.640	344	bycatch	6/5/07	Y	N
Az 12	*Acanthogorgia*	Graciosa	39.142	**	325	bycatch	5/6/07	Y	N
Az 13	*Acanthogorgia*	Condor de Terra	38.500	**	384	bycatch	15/4/07	N	Y
Az 14	*Acanthogorgia*	Princesa Alice	37.658	**	566	bycatch	13/10/06	Y	Y
Az 15	*Acanthogorgia*	Faial, NW Ponta	38.983	**	365	bycatch	15/3/82	N	Y
Az 16	*Acanthogorgia*	Condor de Terra	38.500	**	384	bycatch	15/4/07	N	N
Az 17	*Acanthogorgia*	Pico, Ponta da Ilha	38.407	38.370	347	bycatch	26/10/07	Y	Y

Az 18	*Acanthogorgia*	Pico, Ponta da Ilha	38.407	38.370	347	bycatch	26/10/07	Y	Y
Az 19	*Acanthogorgia*	Condor de Terra	38.500	**	384	bycatch	15/4/07	Y	N
Az 2	*Acanthogorgia*	Ponta E de Condor	38.510	**	329	bycatch	5/6/08	N	N
Az 20	*Acanthogorgia*	Azores	30.066	**	420	bycatch	20/11/07	Y	N
Az 3	*Acanthogorgia*	Azores	38.510	**	468	bycatch	11/4/07	N	N
Az 4	*Acanthogorgia*	Corvo, Fora do Aeroporto	39.650	39.640	629	bycatch	22/6/07	N	N
Az 5	*Acanthogorgia*	Voador, Açores	38.325	**	318	bycatch	12/3/07	N	N
Az 6	*Acanthogorgia*	Voador, Açores	38.325	**	318	bycatch	12/3/07	Y	Y
Az 7	*Acanthogorgia*	São Jorge, Aç	**	**	265	bycatch	1/3/07	Y	Y
Az 8	*Acanthogorgia*	Condor de Terra	38.500	**	291	bycatch	22/3/07	Y	N
Az 9	*Acanthogorgia*	Mateus	38.339	**	524	bycatch	30/10/06	Y	N
B 1	*Gyrophyllum*	Bahamas	**	**	**	ROV	15/5/08	Y	N
B 2	*Seapen*	Bahamas	**	**	**	ROV	20/5/08	Y	Y
Ce 23	*Acanella*	PSB, Rockall or Belgica	**	**	**	ROV	**	Y	Y
Ce 28	*Acanella*	PSB, Rockall or Belgica	**	**	**	ROV	**	N	N

Ce 32	*Acanella*	PSB, Rockall or Belgica	**	**	**	ROV	**	Y	Y
Ce 41	*Isidella*	PSB, Rockall or Belgica	**	**	**	ROV	**	Y	Y
Ch 139	*Isidella*	Whittard Canyon	48.369	10.037	3106	ROV	17/7/08	Y	Y
Ch 140	Keratoisidinae	Whittard Canyon	48.369	10.037	3078	ROV	17/7/08	Y	Y
Ch 141	*Chrysogorgia*	Whittard Canyon	48.369	10.037	3060	ROV	17/7/08	Y	Y
Ch 142	*Chrysogorgia*	Whittard Canyon	48.369	10.037	3060	ROV	17/7/08	Y	Y
Ch 143	*Chrysogorgia*	Whittard Canyon	48.369	10.037	3060	ROV	17/7/08	Y	Y
Ch 144	Keratoisidinae	Whittard Canyon	48.369	10.037	3060	ROV	17/7/08	Y	Y
Ch 158	*Chrysogorgia*	Whittard Canyon	48.369	10.037	2963	ROV	17/7/08	Y	Y
Ch 159	Keratoisidinae	Whittard Canyon	48.369	10.037	2864	ROV	17/7/08	Y	Y
Ch 168	*Acanella*	Whittard Canyon	48.369	10.037	2864	ROV	17/7/08	Y	Y
Ch 17	*Chrysogorgia*	Whittard Canyon	48.557	11.130	2489	ROV	28/6/09	Y	Y
Ch 182	*Paramuricea*	Whittard Canyon	48.602	9.960	1676	ROV	18/7/08	Y	Y
Ch 188	*Radicipes*	Whittard Canyon	48.602	9.960	1887	ROV	18/7/08	Y	Y
Ch 193	*Isidella*	Whittard Canyon	48.602	9.960	1359	ROV	18/7/08	Y	N
Ch 199	*Paramuricea*	Whittard Canyon	48.602	9.960	1339	ROV	18/7/08	N	Y

Ch 231	*Paramuricea*	Whittard Canyon	48.457	9.957	2117	ROV	20/7/08	N	N
Ch 232	*Distichoptilum gracile*	Whittard Canyon	48.457	9.957	2119	ROV	20/7/08	Y	Y
Ch 233	*Acanella*	Whittard Canyon	48.457	9.957	2021	ROV	20/7/08	Y	N
Ch 234	*Acanella*	Whittard Canyon	48.457	9.957	1997	ROV	20/7/08	N	Y
Ch 236	*Acanella*	Whittard Canyon	48.457	9.957	1997	ROV	20/7/08	Y	Y
Ch 29	*Radicipes*	Whittard Canyon	48.557	11.130	2477	ROV	28/6/09	Y	Y
Ch 35	Keratoisidinae	Whittard Canyon	48.737	11.165	2219	ROV	29/6/09	Y	N
Ch 42	Keratoisidinae	Whittard Canyon	48.737	11.165	2191	ROV	29/6/09	Y	Y
Ch 64	*Primnoa*	Whittard Canyon	48.869	11.130	1695	ROV	2/7/09	Y	Y
Ch 69	**	Whittard Canyon	48.869	11.130	1629	ROV	2/7/09	N	Y
Cl	*Seapen*	Mid-Atlantic ridge	49.139	27.757	**	trawl	27/6/10	N	Y
Cl 20	*Acanthogorgia*	Mid-Atlantic ridge	48.987	28.406	850	trawl	23/6/10	Y	Y
Cl 40	Keratoisidinae	Mid-Atlantic ridge	49.139	27.757	**	trawl	27/6/10	Y	Y
Cl18	*Acanthogorgia*	Mid-Atlantic ridge	48.987	28.406	850	trawl	23/6/10	Y	Y
Cl45	*Gyrophyllum sp.*	Mid-Atlantic ridge	49.109	27.926	2700	trawl	28/6/10	Y	Y
D 1	**	Rosebank North	61.141	3.672	1186	ROV	**	N	N

D 2	*Geresemia*	South Uist	61.267	2.997	1157	ROV	**	Y	Y
D 3	**	South Uist	61.267	2.997	1157	ROV	**	N	N
D 4	**	Tornado	60.562	4.456	1050	ROV	**	Y	Y
D 5	*Protoptilum*	Tornado	60.562	4.456	1050	ROV	**	Y	Y
D 6	**	Tornado	60.562	4.456	1050	ROV	**	Y	N
D 7	**	Nigeria	3.116	6.819	1366	ROV	**	Y	Y
D 8	*Protoptilum*	Nigeria	3.116	6.819	1366	ROV	**	N	Y
J c3	Keratoisidinae	Mid-Atlantic ridge	**	**		ROV		Y	N
Jc 4	*Isidella*	Mid-Atlantic ridge	**	**		ROV		Y	Y
Ma 11	*Narella*	Mid-Atlantic ridge	45.713	28.033	3151	ROV	5/6/08	Y	Y
Ma 12	*Radicipes*	Mid-Atlantic ridge	45.649	27.847	3063	ROV	5/6/08	Y	Y
Ma 13	*Lepidisis*	Mid-Atlantic ridge	45.853	28.002	3013	ROV	5/6/08	Y	Y
Ma 14	*Lepidisis*	Mid-Atlantic ridge	45.709	27.974	2998	ROV	5/6/08	Y	Y
Ma 15	**	Mid-Atlantic ridge	45.666	27.987	2940	ROV	5/6/08	N	N
Ma 16	*Radicipes*	Mid-Atlantic ridge	45.425	28.153	2881	ROV	5/6/08	Y	Y
Ma 17	*Radicipes*	Mid-Atlantic ridge	45.654	27.929	2878	ROV	15/6/11	Y	Y
Ma 18	New	Mid-Atlantic ridge	45.654	27.929	2878	ROV	15/6/11	Y	Y

Ma 19	*Isidella*	Mid-Atlantic ridge	46.592	27.818	3472	ROV	16/6/08	Y	Y
Ma 20	New	Mid-Atlantic ridge	45.777	27.864	3378	ROV	16/6/08	Y	Y
Ma 21	Keratoisidinae	Mid-Atlantic ridge	45.586	27.997	3179	ROV	17/6/08	Y	N
Ma 22	Keratoisidinae	Mid-Atlantic ridge	45.609	27.833	2947	ROV	19/6/08	Y	Y
Ma 23	*Narella*	Mid-Atlantic ridge	45.556	28.124	2867	ROV	19/6/08	N	N
Ma 24	*Radicipes*	Mid-Atlantic ridge	45.570	28.052	2863	ROV	19/6/08	Y	Y
Ma 25	*Radicipes*	Mid-Atlantic ridge	45.497	28.080	3083	ROV	19/6/08	Y	Y
Ma 26	Keratoisidinae	Mid-Atlantic ridge	45.682	28.012	2783	ROV	19/6/08	Y	Y
Ma 27	New	Mid-Atlantic ridge	45.549	27.959	2812	ROV	21/6/08	Y	Y
Ma 28	*Isidella*	Mid-Atlantic ridge	45.531	28.004	2749	ROV	21/6/08	Y	Y
Ma 29	*Isidella*	Mid-Atlantic ridge	45.546	28.071	2655	ROV	21/6/08	Y	Y
Ma 3	**	Mid-Atlantic ridge	45.589	28.101	2697	ROV	1/6/08	N	Y
Ma 30	Keratoisidinae	Mid-Atlantic ridge	45.563	27.967	2805	ROV	21/6/08	Y	Y
Ma 31	**	Mid-Atlantic ridge	45.399	27.874	2617	ROV	4/6/08	N	Y
Ma 32	*Lepidisis*	Mid-Atlantic ridge	45.597	27.811	3328	ROV	17/6/08	Y	Y
Ma 33	New	Mid-Atlantic ridge	45.490	27.854	2890	ROV	17/6/08	Y	Y
Ma 34	Keratoisidinae	Mid-Atlantic ridge	45.596	27.834	3020	ROV	17/6/08	Y	N

Ma 4	**	Mid-Atlantic ridge	45.612	28.023	2651	ROV	1/6/08	N	N
Ma 5	**	Mid-Atlantic ridge	45.667	27.800	3598	ROV	1/6/08	Y	Y
Ma 6	Keratoisidinae	Mid-Atlantic ridge	45.648	27.844	**	ROV	4/6/08	Y	N
Ma 9	Keratoisidinae	Mid-Atlantic ridge	45.641	28.020	2030	ROV	4/6/08	Y	Y
Ma10	Keratoisidinae	Mid-Atlantic ridge	45.783	27.847	3398	ROV	5/6/08	Y	Y

**= data unavailable/unrecorded at collection

Y indicates successful amplicfiction of the gene, N indicates unsuccessful amplification.

Figure 4.1. New sampling sites used for this study. Numbers represent the number of samples obtained from the given area

centrifuged for 3 minutes at 14,000 rpm. Following this step the spin column was placed into a 2 ml micro centrifuge tube and 200 µl of elution buffer AE was pipetted directly onto the DNeasy membrane, this was left for 1 minute at room temperature and finally centrifuged at 8,000 rpm for 1 minute, the eluted DNA was stored at -20 ^{o}C prior to further analysis.

4.2.3 Polymerase chain reaction (PCR)

Polymerase chain reaction (PCR) was carried out using Illustra PuRe-Taq ready-to-go PCR beads (GE Healthcare, Bucks, UK); which contain 200 µM of each dNTP, 10 mM Tris-HCL (pH 9 at room temperature), 50 mM KCl, 1.5mM $MgCl_2$ and 2.5 units of PuReTaq DNA polymerase. These beads are temperature-stable until hydrated with 25µl PCR mix. The PCR mixture consisted of DNA template in solution with AE buffer obtained from the DNeasy kit, nuclease-free water and 10 pmol of both forward and reverse primer (Table 4.2). Multiple primers were used in the study as a result of unsuccessful amplification of degraded DNA using published primers in both *ND2* and *MSH1* genes. Also because of the gene inversion within Keratoisidinae sub-family of Isididae separate *MSH1* primers were required for these samples.

PCR reactions were performed using a Bio-Rad (Herts, UK) MyCycler^{TM} thermocycler following the below temperature profile – with each primer pair amplifying successfully at 52 ^{o}C, despite slight changes in fragment length.

1 Initial denaturation;	15 minutes at 95 ^{o}C
35-40 amplification cycles	1 minute at 94 ^{o}C
	1 minute at 52 ^{o}C
	2 minutes at 72 ^{o}C
1 Final extension;	15 minutes at 72 ^{o}C

Table 4.2 Primers used in study

Primer name	Gene targeted	Primer sequence 5'-3'	Source
16S647F	*ND2*	ACACAGCTCGGTTTCTATCTACCA	McFadden *et al*., 2004
*ND2*1418R	*ND2*	ACATCGGGAGCCCACATA	McFadden *et al*., 2004
ND2 new f	*ND2*	CTATGTTGKACACAGGCTA	This study
ND2 new reverse	*ND2*	GATAGTGCCCCYAACACGAAG	This study
CO3bam5657F	*MSH1*	GCTGCTAGTTGGTATTGGCAT-	France pers comm
Mutchry3458r	*MSH1*	TGAAGYAAAAGCCACTCC-	France pers comm
ND42599F	*MSH1*	GCCATTATGGTTAACTATTAC	France and Hoover, 2002
Msh3458r	*MSH1*	TSGAGCAAAAGCCACTCC	Sánchez *et al*., 2003a
chrkm*MSH1*F	*MSH1*	CCYATTGAACAARTTGCCTC-	This study
chrkm*MSH1*R	*MSH1*	GGCYRAAAATAGAGYAATWCC	This study
new reverse	*MSH1*	AGAATAAAYCYGRGATACTGC	This study

The amplified products were separated by size using electrophoresis on a 1% agarose gel buffered in TAE (Tris-acetate-EDTA) and stained with 1.5 µl per 10 ml of agarose resulting in a concentration of $1\mu g\ ml^{-1}$ of ethidum bromide. 3 µl of PCR product along with 2 µl loading dye was added to each well. A 100 base pair ladder (Qiagen West Sussex, UK) was used to estimate the size of the amplified DNA product. The gels were run for 30 minutes at 72 volts. Results were visualised using a UV transilluminator determining the

size of the amplified region, and if the size is correct for the amplicon expected. All reactions were run with a negative control for contamination detection.

For some samples amplification was not possible with the standard primers and thus new internal primers were designed for both genes, resulting in multiple primers being used per gene as mentioned previously. This was suspected to be a result of degraded DNA.

4.2.4 Primer design

Some samples were unable to be amplified using existing primers. The reason for this was thought to be degraded DNA samples as the majority that could not be amplified were old specimens. It was therefore decided to create intermediate primers, in the hope that by targeting a smaller amplicon it would be possible to get positive results which could then be combined to produce the entire sequence for the targeted gene. This was achieved using the following technique.

Acanthogorgia sequences already obtained during this study as well as 12 partial *ND4* and *MSH1* Octocorallia sequences downloaded from the NCBI database (Table 4.3) were aligned using Mega V4. ND4 fragments were included in the alignment where possible as this was where the forward primers were found to lie for the MSH1 gene. *Acanthogorgia* was used because it was primarily the *Acanthogorgia* samples obtained from the Azores (Az samples) which were successfully amplified using the existing primers.

Each of the original forward and reverse primers were run against the alignment to search for the priming site. The reverse primer had to be reverse complemented before this could occur successfully. Once priming locations were identified, it was then possible to locate a region within the sequence which would be suitable for internal primer placement.

The longest sequence containing both *ND4* and *MSH1*, where the original primers spanned, was chosen to be the target against which primers would be designed. This sequence was then uploaded into Primer Premier Version 5 (available from http://www.premierbiosoft.com/primerdesign/) to assist with primer design. The new internal forward primer was designed to work with the existing reverse primer and the new internal reverse was designed to work with the existing forward. To ensure the primers designed would be as successful as possible the following rules of design were taken into consideration:

- Melting temperature should fall between 50 and 60 °C
- 40-60% of Oligonucleotides should be either the G nucleotide or the C nucleotide.
- Annealing temperature difference between both primers should not differ >5°C.
- Self-complementary hairpins and dimers should be minimal and avoided where possible
- False priming (where the primer sits on the wrong area within the genetic sequence) and cross dimers (primers self annealing or annealing to one another resulting in a template capable of being extended by the polymerase) should also be avoided where possible
- Ideally primers should start and end with 1-2 G or C nucleotides, as this allows for a stronger bond to the targeted sequence.

Table 4.3 Published sequences used in the alignment for MSH1 primer design.

NCBI Accession number	Species	Original authors
AY268461	*Acanthogorgia* sp.	LePard, 2003
GU563306	*Acanthogorgia* sp. 1	McFadden,*et al.*, 2011
GU563307	*Acanthogorgia* sp. 2	McFadden *et al.*, 2011
GU563308	*Calcigorgia* sp.	McFadden *et al.*, 2011
GU563309	*Calcigorgia beringi*	McFadden *et al.*, 2011
GU563300	*Acanthogorgia* cf. *armata*	McFadden *et al.*, 2011
GU563305	*Paramuricea* sp.	McFadden *et al.*, 2011
GU563303	*Swiftia pallida*	McFadden *et al.*, 2011
GU563304	*Placogorgia* sp.	McFadden *et al.*, 2011
GU563302	*Swiftia* sp.	McFadden *et al.*, 2011
GU563301	*Alaskagorgia aleutiana*	McFadden *et al.*, 2011
GQ868348	*Chrysogorgia* sp.	McFadden *et al.*, 2011
GQ868343	*Radicipes* sp.	McFadden *et al.*, 2011

This was achieved by locating an area within the target sequence which would allow roughly 500 bp to be sequenced when used in conjunction with the existing reverse primer. The primer sequence was subsequently moved along the DNA fragment until the above properties could be fulfilled as best as possible. This was repeated with the reverse primer resulting primer sequences can be found in table 4.2. An example alignment is shown in Figure 4.2 against which primer chkmsh1F was designed.

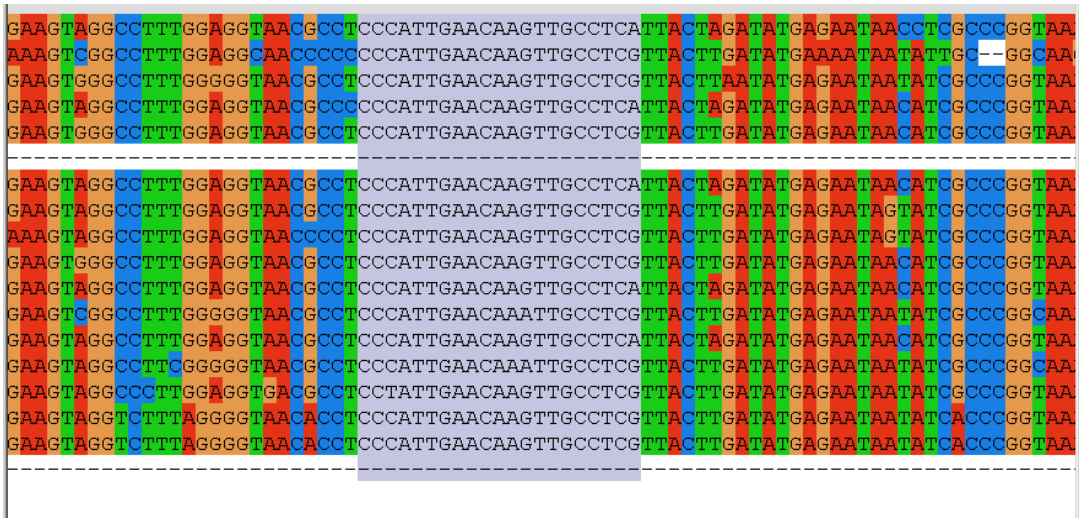

Figure 4.2 Primer Chrkmsh1f alignment and placement beginning at nucleotide position 305. When paired with Msh3458r a product of 581 bases was predicted.

A satisfactory position was achieved for the forward primer beginning at location 305, with a predicted product size of 581 bases. The reverse was located at position 604, with the resulting product estimated to be 564 bases long. A second reverse was designed to ensure allow further success to be achieved this began at location 508 and resulted in a project roughly 468 bases.

To allow PCR condition to be optimised a gradient PCR was run using temperature range 48-58^{o}C for the annealing temperature for the primer using DNA sample Ma16- *Radicipes*, from which positive results were previously obtained, and a negative control. Results indicated that the new reverse paired with the existing forward (new reverse with Nd42599F) and the new forward paired with the existing reverse (Msh3458r with chrkmsh1f) with 52 ^{o}C producing the best results and thus the new primer combinations were used for problematic DNA samples.

The above process was repeated for the creation of intermediate *ND2* primers. However, there were only two *ND2* sequences for *Acanthogorgia* available from NCBI (Genbank Accession numbers **DQ297437** and **DQ297436**). These sequences were not long enough to allow alignment with the original forward and reverse primers and so a whole genome was searched for, for which no results were returned. A Holaxonia genome of was found for the species *Pseudopterogorgia bipinnata* (**DQ640646**). This genome was aligned with the existing *Acanthogoria* sequences as well as those *ND2* sequences from successfully amplified *Acanthogorgia* samples (Az7, Az8, Az9, Az14 Az17, Az18), and also the original primers. From this alignment new primers were designed against the longest *Acanthogorgia* sequences (Az14) with additions from the *Pseudopterogorgia bipinnata* sequence to ensure the sequences had sufficient length to incorporate the primers using the same technique as for *MSH1,* with the following primers meeting the criteria most successfully. The forward primer begins at position 339 resulting in a product around 454 bp, with the reverse primer beginning at 613 with a resulting product of around 613 bp. Again 52 % yield positive PCR results using MA16- *Radicipes*.

4.2.5 PCR cleanup of amplified fragments.

Prior to sequencing, residual primers and dNTPs, salts and polymerase were separated from the PCR product using the Qiagen QIAquick PCR-Purification kit according to the manufacturer's recommendations. Briefly, 110 µl of Buffer PB was added to the PCR product, mixed via pipetting and added to a spin column and before centrifugation for 1 minute at 8,000 rpm. The spin column was transferred to a new collection tube and 750 µl of buffer PE was added and centrifuged for 1 min at 8,000 rpm. The spin column was centrifuged for a further minute to dry the column before being transferred to a new collection tube. 30 µl of buffer EB (10 mM Tris-CL, pH 8.5) was added to elute the DNA, this was left to stand for 1 minute before centrifuging for 1 minute at 8000 rpm. When degraded DNA samples were suspected the elution step used deionised water in the place of EB buffer as this has been reported to improve downstream sequencing results (Dr C.

Gubili, University of Southampton, NOCS, pers. comm.). The concentration of the extracted DNA fragments was measured at 260nm using a NanoDrop ND1000 spectrophotometre and the extracts were diluted using ultrapure water to a concentration of 10 ng/µl before being sequenced externally by SourceBioscience (University of Oxford) using an Applied Biosystems ABI 3730 XL 96-capillary sequencer.

Sequences obtained were aligned with the forward sequence of the same sample to create a consensus sequence using computer package Geneious (Drummond *et al.*, 2011). Consensus sequences were corrected manually and any ambiguities in base calling were resolved using chromatograms. Consensus sequences could not be made where the returned sequences contained too many ambiguities or were shown to have a poor quality. A BLASTn search was performed in Genbank (http://www.ncbi.nlm.nih.gov/) for each consensus sequence, to allow a putative sequence identification to be made. A variety of octocoral families were identified throughout this search thus it was decided to include all families and genera throughout, to allow the creation of the most informative phylogenetic trees possible.

4.2.6 Phylogenetic analysis

A general search for both Octocorallia *ND2* and Octocorallia *MSH1* in NCBI (National Center for Biotechnology Information) allowed all available sequences to be downloaded. Where there were multiple identical sequences for the same species, only two were included. Those which showed heterogeneity within the same species were kept for further analysis. This resulted in a total of five data sets which could be assembled for analysis- 1) All *MSH1* published sequences plus samples from this study (626 sequences) 2) All *ND2* published sequences plus samples from this study (287 Sequences) 3) *MSH1* sequences obtained for samples which also have *ND2* available obtained from, Sánchez *et al.* (2003), Wirshing *et al.* (2005), McFadden *et al.* (2006) and this study (208 samples) 4) *ND2* sequences obtained for samples which also have *MSH1* available obtained Sánchez *et al.*

(2003), Wirshing *et al*. (2005), McFadden *et al.* (2006) and this study (208 samples) 5) combined data set of both *MSH1* and *ND2* genes from McFadden *et al.,* 2006, Wirshing *et al*, 2005, Sánchez *et al.,* 2003 and this study (208 samples Appendix 3). By creating these five data sets it was possible to allow the most complete data sets to be produced as well as allow a direct comparison between species which had sequences available for both genes.

Each data set was aligned using ClustalX 2.1 (Larkin *et al*., 2007), the resulting alignments were subsequently corrected by eye in Mega_4 (Tamura *et al*., 2007) using both the nucleic acids and the translated amino acids to ensure accuracy of alignments. To ensure alignments were consistent with those previously published they were compared with data sets obtained from McFadden (Mudd University Institute, pers. comm.) which were used in McFadden *et al.,* (2006). This ensured that the phylogenetic predictions generated from this analysis were directly and unambiguously comparable with those in the literature. Sequences were trimmed to allow the inclusion of as many samples as possible within subsequent analysis. This resulted in an alignment length of 423 base pairs for *ND2* and 709 base pairs for *MSH1*. Any samples shorter than this were removed from alignments. Sequences used in each analysis can be found in Electronic Appendix 3.

Each of the five data sets was subject to phylogenetic analysis. Following the selection of the most appropriate model of sequence evolution using Akaike Information Criterion in Mrmodeltest 2.3 (Nylander, 2004) (Table 4.4) Bayesian phylogenetic analysis was conducted using MrBayes 3.1.2 (Huelsenbeck and Ronquist, 2001), each data set was run using four chains with two parallel runs set at a temperature of 0.01 until the average standard deviation between the split frequencies was less than 0.01. Unfortunately this was not possible for data set1 as it took 15,000,000 generations to reach a spilt frequency of below 0.01, this amount of data caused computational issues when producing the consensus tree, therefore the analysis was only run for 2,000,000 generations to allow a rough tree to be produced. Maximum parsimony models were run using PAUP* 4.0b (Swofford, 2002) with 100 bootstrap replicates. PhyML 3.0 (Guindon & Gascuel, 2003)

maximum-likelihood analysis was performed under 500 replicates once the model of best fit was determined using Modeltest 3.7 (Posada & Crandall, 1998) (Table 4.4). Unfortunately, because of computational limitations Phyml 3.0 was not conducted on data set 1)- all *MSH1* available and thus will not be included in the results. Maximum-Parsimony was run using Bioportal, a web based portal for phylogenetic analysis supported by the University of Oslo (Kumar *et al.,* 2009). Bayesian analysis was conducted in the same manner as all other data sets. Finally to examine intra and inter-specific variation within the genes *MSH1* and *ND2* pairwise genetic distances (uncorrected P) were calculated on PAUP* 4.0b for data sets 3 and 4. The three different analyses were conducted to allow a comparison between techniques and to strengthen the reliability of the results.

Resulting trees were visualized using Treeview 1.6.6 (Page, 2001). Because Octocorallia are the only known metazoans to contain the *MSH1* gene (Culligan *et al.,* 2000; McFadden *et al.,* 2006) it was not possible to root trees with a non-Octocorallian outgroup. McFadden *et al.* (2006) found that both *Erythropodium* and *Briareum* were often placed at the base of trees and could be used for rooting; it was therefore decided to use *Briareum* sp. as the out-group within this study. Once rooted, each topology within a data set was compared and a consensus tree created based on the Maximum likelihood topology with Bayesian and Maximum likelihood statistics included.

Table 4.4 Models selected for phylogenetic analysis.

	AIC model selected	Phyml Model used	Proportion of invariable sites	Gamma distribution
All *MSH*1	GTR= I + G	not possible	0.27	1.2
All *ND*2	GTR= I + G	GTR	0.22	1.2
*MSH*1 from both	GTR= I + G	GTR	0.25	1.1
*ND*2 from both	GTR= I + G	GTR	0.23	1.09
Both *MSH*1 and *ND2* together	GTR= I + G	GTR	0.2	0.99

AIC= Akaike Information Criterion selected by Mrmodeltest 2.3 (Nylander, 2004) and Phyml model used was selected using Modeltest 3.7 (Posada & Crandall, 1998) with the proportion of invariable sites and Gamma distribution inputted to achieve the best possible phylogenetic representation. GTR = General Time-Reversible models with GTR I+G indicating invariable sites and Gamma distribution are taken into consideration during computation.

4.4 Results

4.4.1 – All MSH1

MSH1 samples were obtained from NCBI (National Center for Biotechnology Information) resulting in a total of 626 sequences (Appendix 3 Table ap3.1). Alignments consisted of 709 base pairs including indels with fragments ranging from 159 to 191 amino acids in length. 572 characters were parsimony-informative. Computational limitations meant that it was not possible to complete Phyml prediction as this required too much processing memory, even for a multi-processor machine held at the University of Oslo, Bayesian analysis was unable to be completed due to an error in the final processing as a result in the files being too large because of the 15,000,000 generations required to reach a p of <0.01. This prevented the consensus trees from being created for this data set. An analysis of the data set using only 2,000,000 generations was possible to complete but is not entirely reliable with p= 0.046 (Electronic Appendix 3a Figure 4.1) as a result only the maximum parsimony (MP) tree will be presented (Electronic Appendix 3a Figure 4.2.)

For MP tree topology a monophyletic origin of all octocorals used within his study. The majority of the specimens included in this analyses group into one large clade (Clade A) (Figure 4.3, Electronic Appendix 3a Figure 4.2). This clade contained species belonging to both the sub-orders Holaxonia and Alcyoniina. Samples obtained in this study which were found in Clade A were *Acanthogorgia* from which the majority of the Azorean samples were shown to group together in one sub-clade. Others included sample Ma33 which represents a new species and is grouped with Alcyoniina, as well as samples of *Gersemia a*nd *Paramuricea* identified in this study both via nucleotide blasting and taxonomic techniques were possible. All other samples were shown to occur away from Clade A. There is a clear definition between genera with individuals from *Sinularia, Sarophyton, Plexaura,* and *Alcyonium* clearly separated into subclades- indicating a monophyletic evolutionary pattern in each genus.

The majority of the samples obtained in study were not included in Clade A. From the PAUP output it is difficult to distinguish further clades from sub-clades and thus these groupings will be referred to as branches. There is a distinct grouping among *Chrysogorgia* species, all occurring from one branch. The Isididae occurred on branches with no other families, however they were spread over four distinct branches, indicating a that this genus is polyphyletic (Figure 4.4). One of these branches is comprised mainly of specimens obtained in study, including three new species (Ma10, Ma18, Ma27) as well as two known samples which have recently been assigned to the new genus *Jasonisis* (pers comm. Scott France, Louisiana University , Les Watling, Hawaii University). One branch also contains all samples of the *Acanella* genus, the third branch is not as well defined with a mixture of genera occurring throughout. Unresolved species are placed at the bottom of the tree. Pennatulacea all group together from one branch with another distinct grouping of *Corallium* and *Paragorgia* and some Alcyoniina (Figure 4.5)

The rough Bayesian (Electronic Appendix 3a Figure 4.1) tree alludes to the presence of multiple clades within this data group. Clade A corresponds to Clade A in the MP tree. There are also indications that Chrysogorgiidae species group together. Isididae species are also seen to group together- however there are many small branches within the main group. There is also a consistent grouping of Pennatulacea all occuirng together from one branch with another distinct grouping of *Corallium* and *Paragorgia* and some Alcyoniina. However this tree topology cannot be fully relied upon as previously stated.

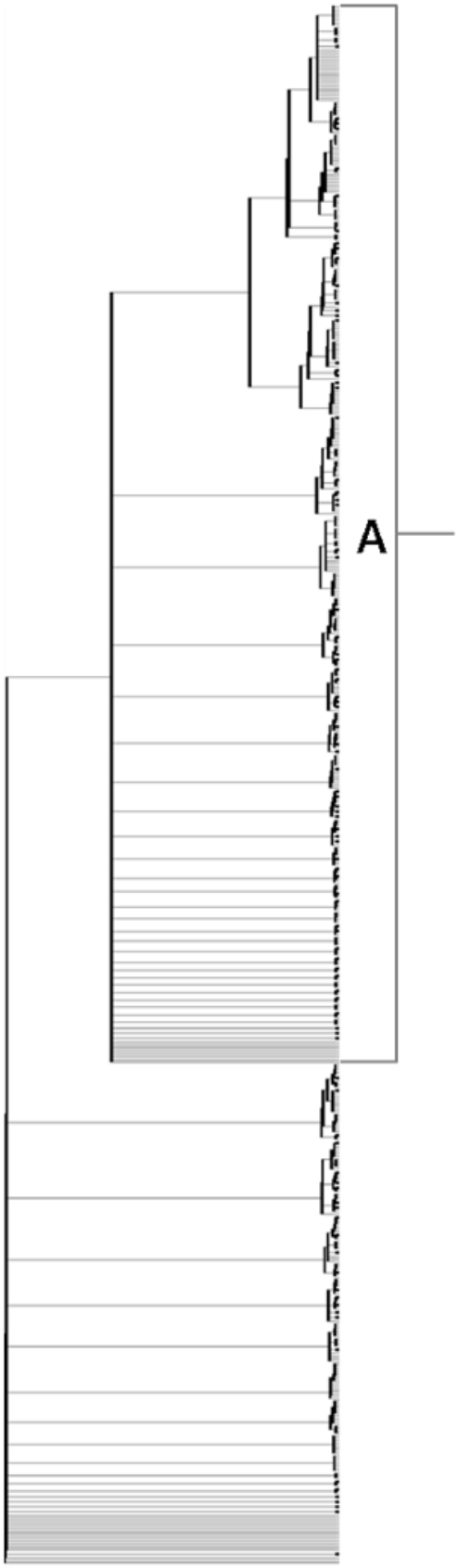

Figure 4.3 Entire MSH1 tree topology for Octocorallia using maximum-parsimony. It is possible to see one large clade A, and many other branches. See electronic appendix 3a figure 4.2 for more detailed image including species names.

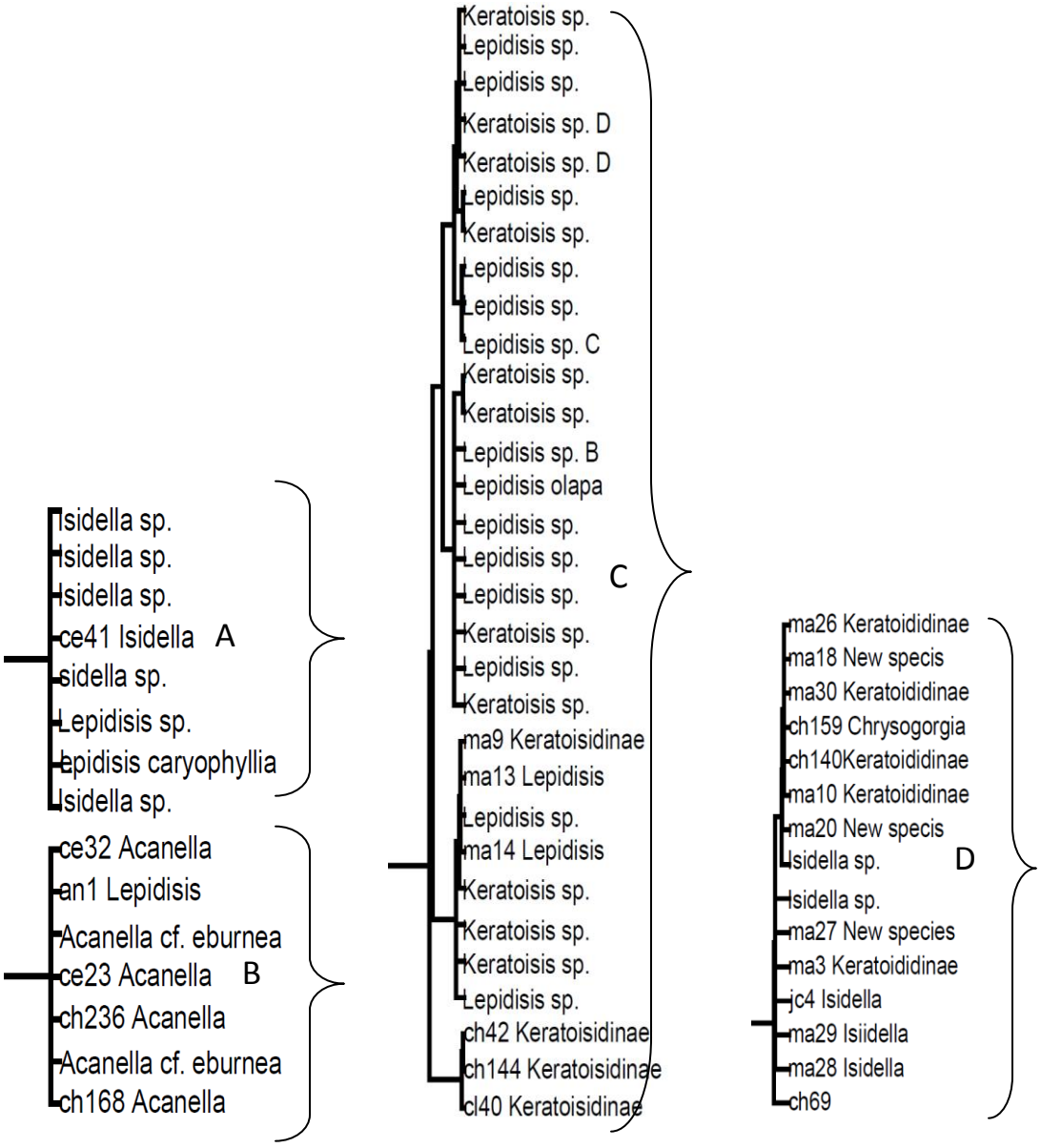

Figure 4.4 Enlarged Isididae maximum parsimony branch topography for all MSH1 illustrating the presence of four distinct Isididae branches (A-D) within the topology. Also see electronic appendix 3a figure 4.2 for further detail.

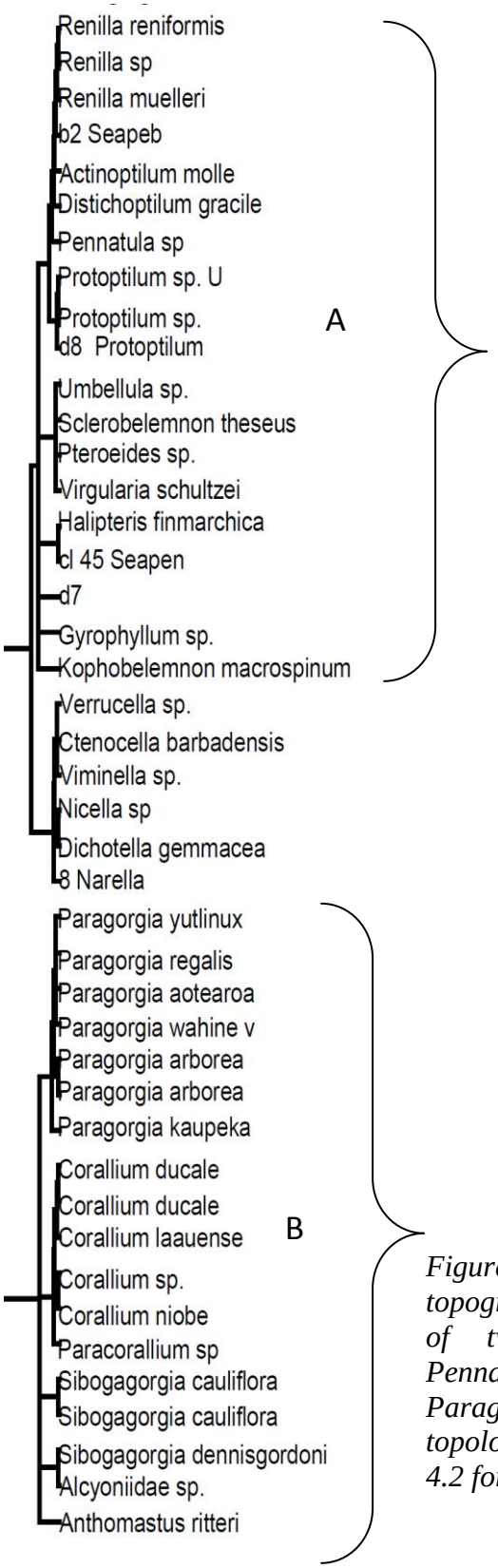

Figure 4.5 Maximum parsimony branch topography for all MSH1 illustrating the presence of two distinct branches which support Pennatulacea species (A) and Corallium and Paragorgia species (B) respectively within the tree topology. Also see electronic appendix 3a figure 4.2 for further detail.

4.4.2- All *ND2*.

ND2 sequences were obtained from the NCBI and this study resulting in a total of 287 sequences (Appendix 3 Table ap3.2). Alignments consisted of 423 base pairs including indels. Of these 154 (36.41%) sites were without polymorphism and 366 were parsimony-informative. Alignments ranged from 134 to 138 amino acids in length. Support for the tree nodes is higher for Bayesian values than Maximum-Likelihood (ML) (Figures 4.6-4.8, Electronic appendix 3a figure 4.3-4.5 for further detail).The maximum-likelihood tree was used for visualization.

Bayesian MP and ML analyses all produced similar topographies with very few discrepancies (Electronic appendix 3a figure 4.3-4,5). Maximum parsimony was found to the most divergent of the three topologies with a large number of "single" species occurring at the base of Clade A (Electronic appendix 3a figure 4.5), with Bayesian and ML having very similar topographies with just a few branch switches. Slight differences occur within placements on the individual tree topologies but species present upon individual branches remained consistent. The majority of branches which were well supported by Bayesian analysis (> 90 %) also had good support from maximum-likelihood (> 70 %) with Bayesian values being consistently higher (Figures 4.6-4.8).

A monophyletic origin to all Octocorals was observed. Three distinct and well supported clades (A-C) can be seen from the analysis with a small out-cropping of two *Erthropodium caribaeorium* samples occurring separate from all other samples at D (Figure 4.6). Clade A (Figure 4.7) contains all *Acanthogorgia sp* identified from this study, except Az19 which falls into clade B, with the main clade grouped with *Acanthogorgia angustiflora* and *Villogorgia.* Most Azorean samples of *Acanthogorgia* group together in one sub-clade; however, those taken from further north along the MAR group in with *Paramuricea* sample, strongly indicating that Acanthogordidae are a polyphyletic group. Sample Ma33 which represents a new species and is grouped with Alcyoniina, as well as samples of

*Gersemia a*nd *Paramuricea* identified throughout this study are also present within this clade. Other members of Clade A include species belonging to both the sub-orders Holaxonia and Alcyoniina. *Muricea* and *Eunicea* species are shown to group into subclades.

Clade B contained the remainder of the new samples collected throughout this study (Figure 4.8). Three sub-clades within clade B are composed entirely of samples obtained in this study representing the Isididae and Chrysogorgiidae families. The new species (described in chapter 5) Ma18, Ma20 and Ma27 are all present within the well supported Isididae sub-clades. Isididae species appear to be polyphyletic in origin; some *Acanella* species are strongly grouped with Pennatulacea, away from the main sub-clades. Isididae genera are spread throughout the clades rather than grouped together indicting poor resolution at the genus level. *Radicipes* spp. are all clustered in a well supported sub-clade, indicating an apparent single origin; other Chrysogorgiidae species are also well grouped within well supported branches, indicating good resolution at genus level within the Chrysogorgiidae. However Ch17-*Chrysogorgian* sp. is present within a sub-clade otherwise composed of Isididae species. Sequences belonging to the order Pennatulacea also occur within a well supported sub-clade in Clade B as well as some Calcaxonia species (Figure 4.8).

The third and smallest of the well defined clades –Clade C (Figue 4.8) does not contain any samples from the present study and is comprised of samples published in the NCBI database comprising of: *Corallium* sp, *Paragorgia* sp a single *Sibogagorgia* sp and some Alcyoniina. Again this clade is well supported by both Bayesian and ML bootstrap values.

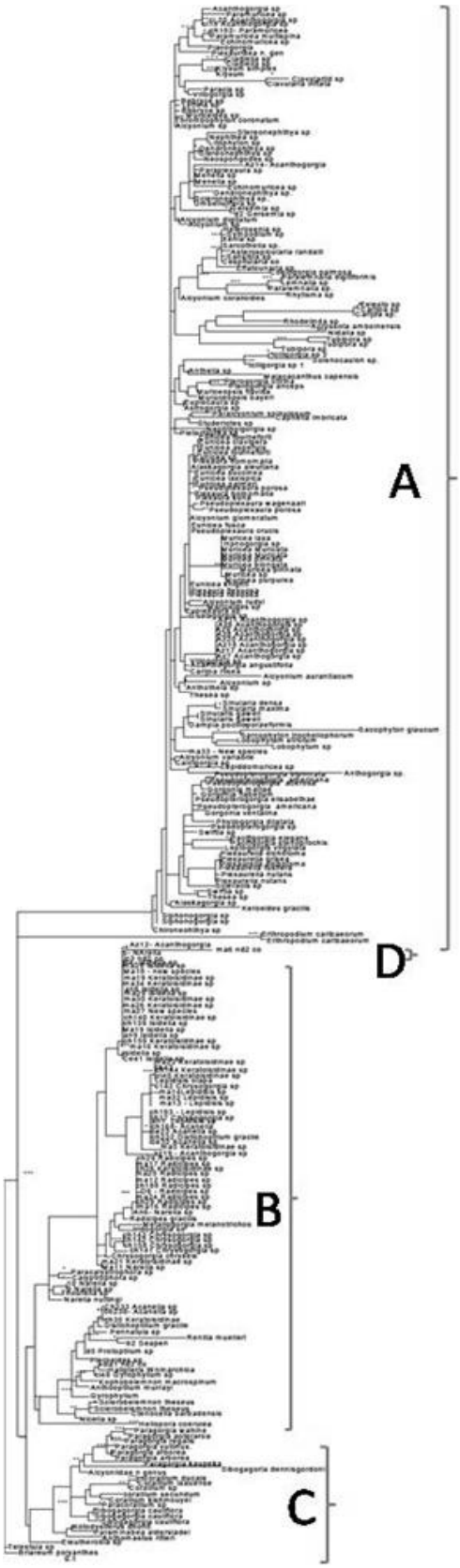

Figure 4.6 Entire ND2 tree topology for Octocorallia. It is possible to see three large clades A,B and C each containing subclades. There is also a small outcropping of Erythododium species (D). *Tree rooted by* Briareum *species. Also contained in electronic appendix 3a figure 4.3 for further detail.*

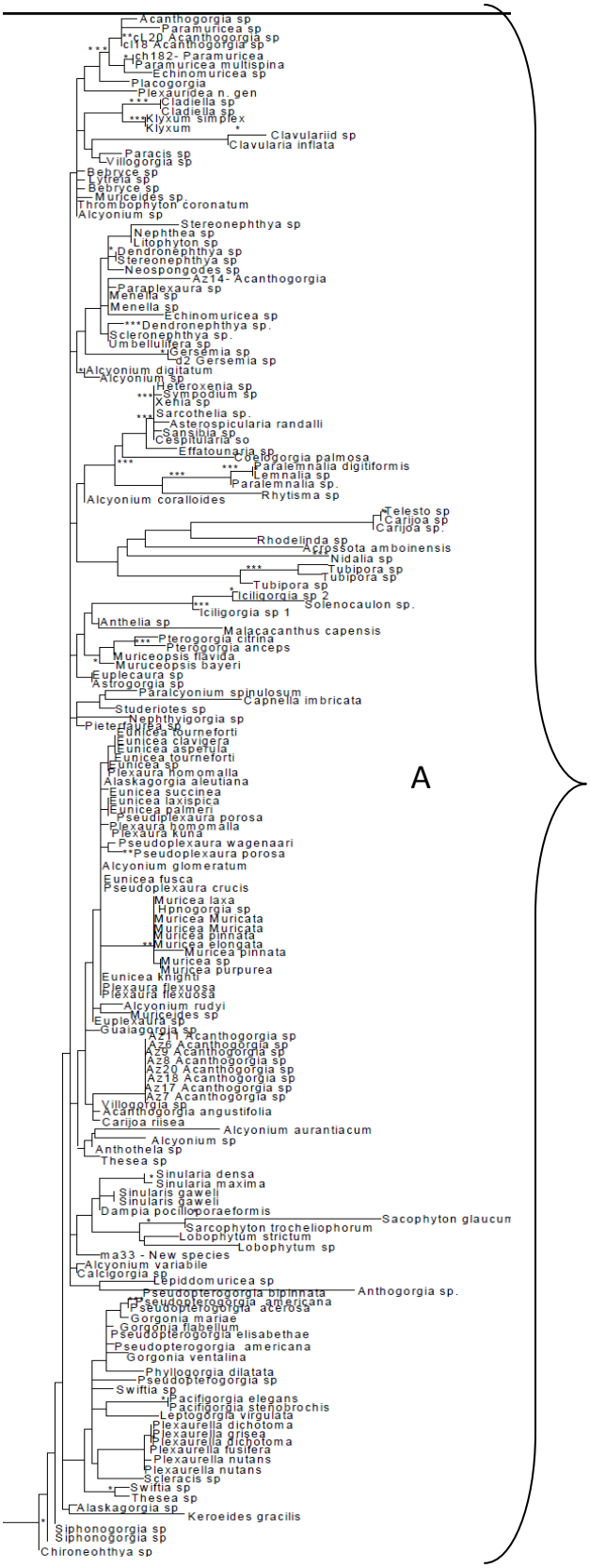

Figure 4.7. *Entire ND2 tree topology for Octocorallia enlarged for clade A *=>70% maximum-likelihood support **= >90 % Bayesian support at the nodes ***= >70% maximum-likelihood support and >90 % Bayesian support at the nodes. Tree rooted by* Briareum *species. Also contained in electronic appendix 3a figure 4.3 for further detail*

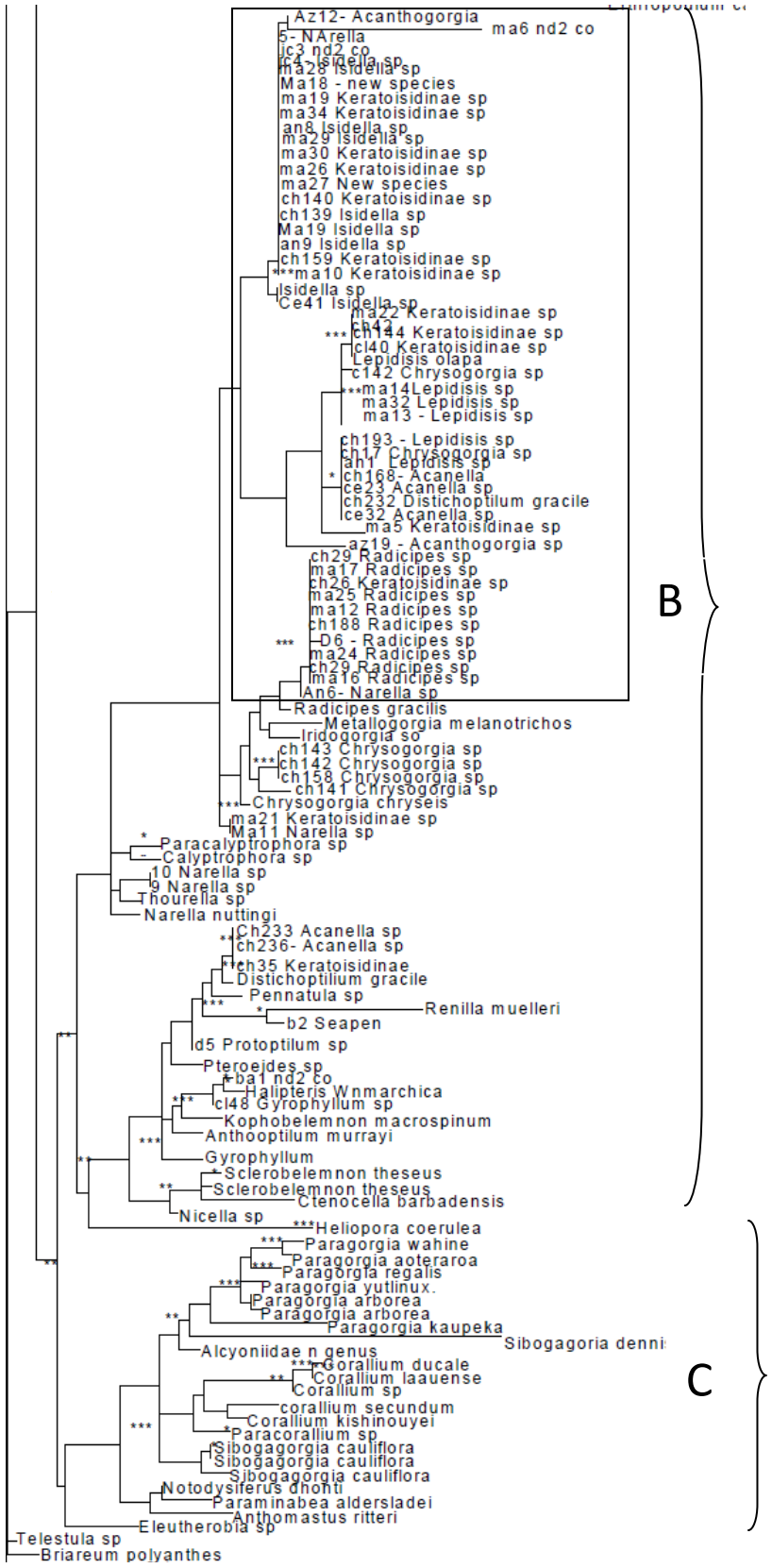

*Figure 4.8. Entire ND2 tree topology for Octocorallia enlarged for clade B and C *=>70% maximum-likelihood support **= >90 % Bayesian support at the nodes ***= >70% maximum-likelihood support and >90 % Bayesian support at the nodes the box represent sub-clades composed of samples obtained throughout this study. Tree rooted by* Briareum *species. Also contained in electronic appendix 3a figure 4.3 for further detail.*

4.4.3- *MSH1* from samples containing both *MSHI* and *ND2*

A total of 208 sequences were obtained from Sánchez *et al.* (2003), Wirshing *et al*. (2005), McFadden *et al.* (2006) and this study (Appendix 3 table ap3.3). Alignments contained a total of 709 base pairs including indels with fragments ranging from 159 to 191 amino acids in length. Of these bases pairs 266 (37.52%) sites were invariant with 452 sites being parsimony informative. The majority of the length variation can be attributed to large indels present within Keratoisidinae species.

Bayesian, maximum parsimony and maximum-likelihood analyses all produced similar topographies (electronic appendix 3a Figure 4.6-4.8). However, of the three topographies maximum parsimony is the most divergent with a large number of "single" species occurring at the base of clade A (Electronic appendix 3 Figure 4.9). There were slight differences within the branch placements upon the tree between all topographies but species present upon individual branches remained constant. The Maximum- likelihood topography obtained from Phyml was used for visualization within this study (Figure 4.9-4.11). The majority of branches which were well supported by Bayesian analysis (> 90 %) also had good support from maximum parsimony (> 70 %) (Figure 4.9-4.11).

Two distinct clades (A and B) were observed from the analyses as well as one smaller clade (C) (Figure 4.9). Clade A is well supported by both ML and Bayesian bootstrap values (Figure 4.10) and contains all bar one (Az17) samples belonging to the sub-order Holaxonia as well as some soft corals from Alcyoniina. This Clade also contains all new *Acanthogorgia* specimens except one (Az17) which could be a result of incorrect sequencing or contamination within the sample. However, these samples do not all occur on the same sub-clade indicating a polyphyletic origin. Ma33, representing a new Genus (which was branched alone), is also within this clade grouped in a sub-clade containing Alcyoniina soft corals, despite having what appears to be a hard skeleton (see Chapter 5 for further discussion of this specimen). Specimens from the genus *Plexaurella* are closely

grouped within the tree, as are *Muricea* samples, whose position is well supported. Holaxonia and Alcyoniina do not mix amongst sub-clade but are distributed throughout the entirety of Clade A.

Clade B, which was well supported by Bayesian values but less so by maximum-likelihood probabilities (Figure 4.11), contained all representatives of the sub-order Calcaxonia (one Holaxonia was also present Az17, but as previously stated it is suspected this is an error in sequencing rather than a genuine result and thus will not be considered) and all from the order Pennatulacea. The majority of new sequences obtained from this study were also included in this clade including three out of the four new species (described in Chapter 5) which grouped within well supported Isididae sub-clades. Although there is strong support and indication for monophyly within the Isididae the resolution of genera is poor with mixing occurring between genera, resulting in a poor quality signal for genus separation. It is also clear that the majority of samples obtained for this study fall within the Isididae order, with an entire sub-clade (Figure 4.11) containing 11 individuals being composed of new samples. This includes a sample believed to be of the newly described genus *Jasonisis* (Alderslade, pers com), and two other new species. All Chrysogorgiidae samples are also found in clade B, with both *Radicipes* and *Chrysogorgia* samples being strongly clustered. These positions are well supported by Bayesian and ML bootstraps. All Pennatulacea are found within one well-supported sub-clade including two samples obtained in this study, supporting the idea of a monophyletic order Pennatulacea.

A third very small clade (C) containing only four samples obtained from NCBI database (Alcyoniidae n gen, *Anthomastus ritteri, Corallium ducale* and *Eleutherobia* sp) was also present. These samples represent the family Alcyoniidae and a precious coral *Corallium.* No samples from the present study were observed within this clade. This clade was not shown to be well supported by Bayesian and ML bootstrap values.

Figure 4.9. *MSH1 from samples containing both MSHI and ND2 tree topology for Octocorallia *=>70% maximum-likelihood support **= >90 % Bayesian support at the nodes ***= >70% maximum-likelihood support and >90 % Bayesian support at the nodes. Tree rooted by* Briareum *species. Also contained in electronic appendix 3a Figure 4.6 for further detail.*

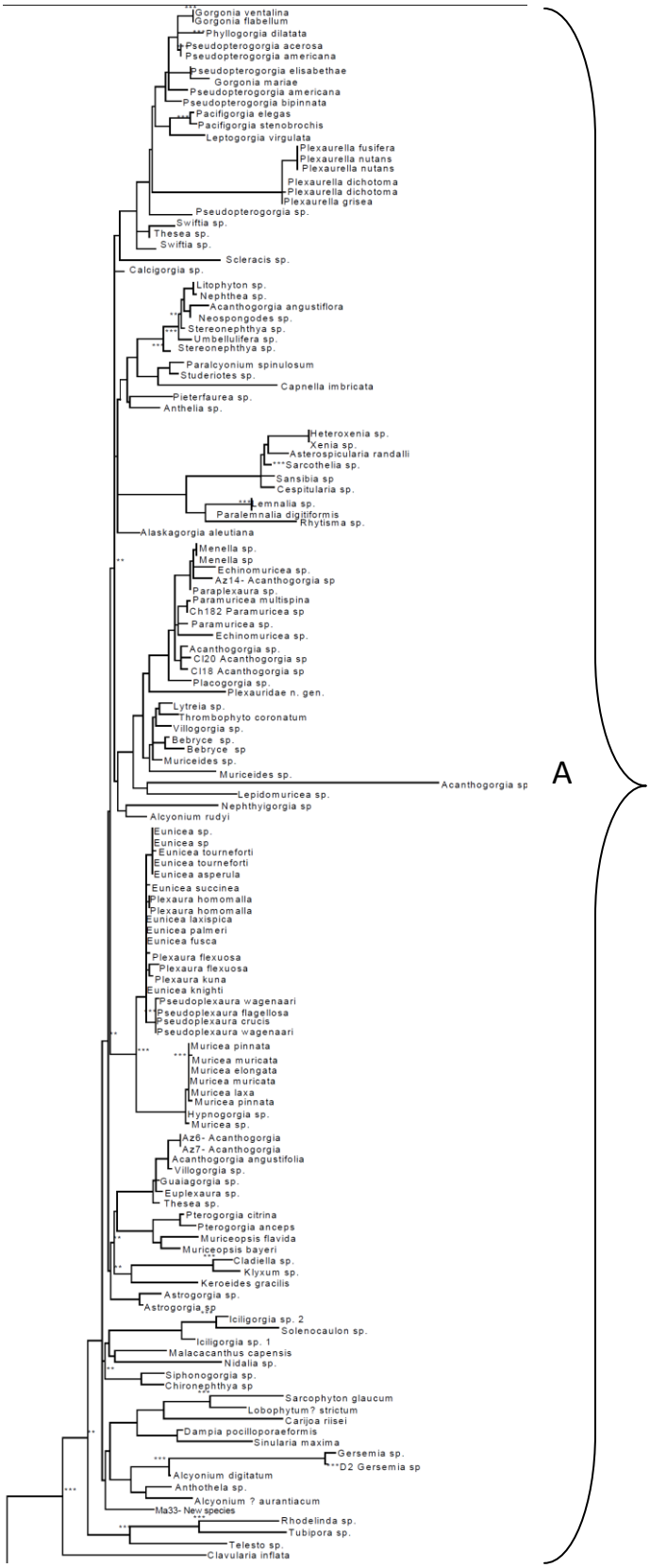

Figure 4.10. *ND2 from samples containing both MSHI and ND2 tree topology for Octocorallia enlarged for Clade A. *=>70% maximum-likelihood support **= >90 % Bayesian support at the nodes ***= >70% maximum-likelihood support and >90 % Bayesian support at the nodes. Tree rooted by* Briareum *species. Also contained in electronic appendix 3a Figure 4.6 for further detail.*

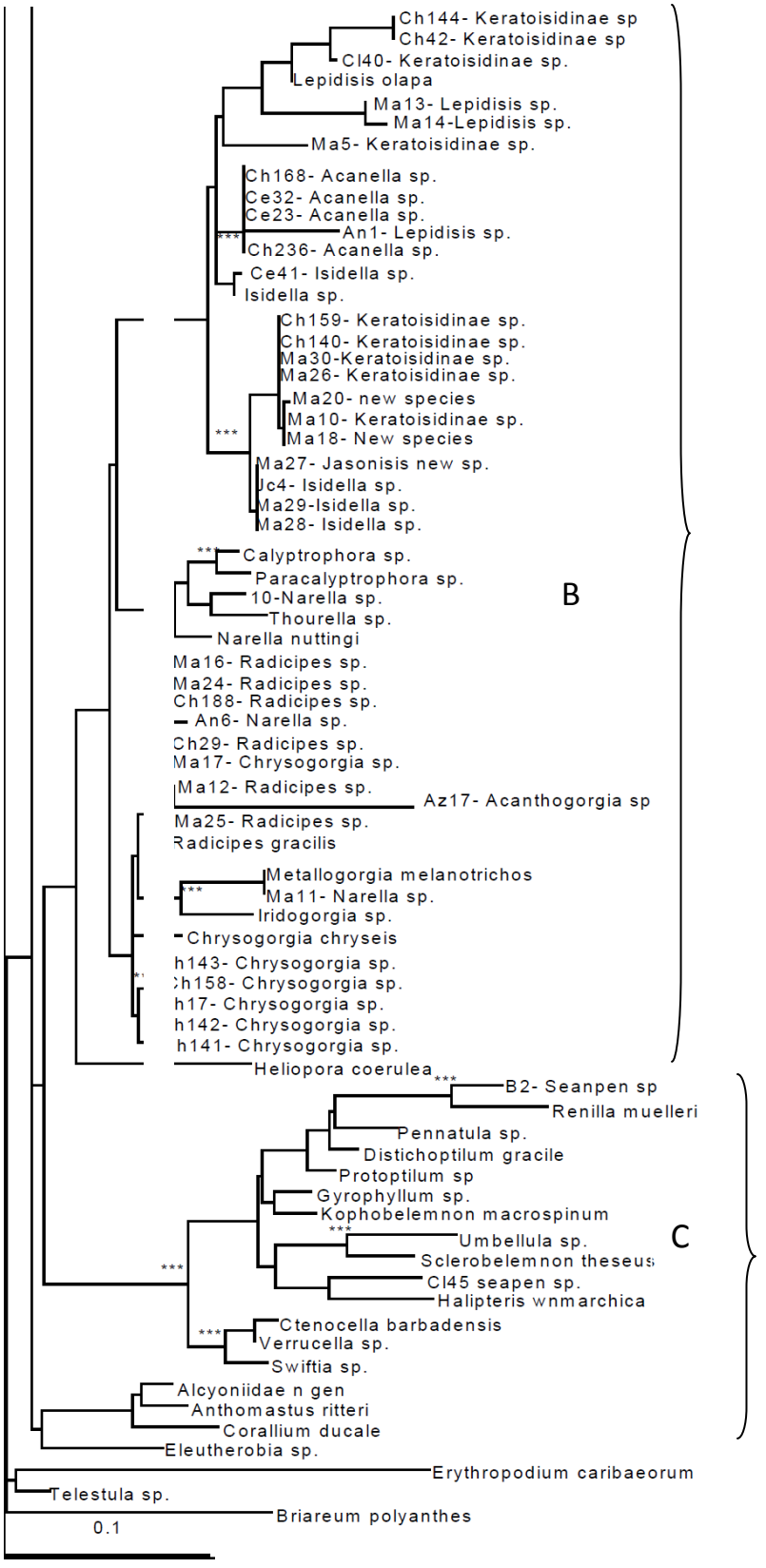

Figure 4.11. *ND2 from samples containing both MSHI and ND2 tree topology for Octocorallia enlarged for clade B and C. *=>70% maximum-likelihood support **= >90 % Bayesian support at the nodes ***= >70% maximum-likelihood support and >90 % Bayesian support at the nodes. Tree rooted by* Briareum *species Also contained in electronic appendix 3a Figure 4.6 for further detail.*

4.4.4 -*ND2* from samples containing both *MSHI* and *ND2*

ND2 sequences were obtained from Sánchez *et al.* (2003), Wirshing, *et al.* (2005), McFadden *et al*. (2006) and this study resulting in a total of 208 sequences (Appendix 3 table ap3.3). Alignments consisted of 423 base pairs including indels. Of these 181 (42.79%) sites were without polymorphism and 195 were parsimony-informative. Alignments ranged from 134 to 138 amino acids in length. Support for the tree nodes is higher for Bayesian values than maximum-likelihood (Figure 4.12-4.14). The ML tree was used for visualization.

Tree topography is similar for all three analyses, Bayesian, maximum parsimony and maximum-likelihood. The main differences occur within the maximum-parsimony tree where an extra small clade can be observed (Electronic Appendix 3a figure 4.9-4.11). Branch topography varies between trees but there is a general consistency in samples branched together. Again the maximum parsimony tree shows slight differences with the presence of many "single" species occurring at the base of Clade A (Electronic Appendix 3a figure 4.11). Both maximum-likelihood and Bayesian trees contain "single" species but these are spread throughout the clades rather than placed at the base (Electronic Appendix figures 4.9 and 4.10).

Tree topology indicated a monophyletic origin within the Octocorallia. Within this two large well supported clades (A and B) and a third, less well supported smaller clade can be seen (Figure 4.12). Clade A (Figure 4.13) is well supported by both Bayesian and ML values and contains very few of the samples obtained during this study. All *Acanthogorgia* samples can be found within this clade along with some soft corals including *Gersemia* spp. and *Paramuricea* spp. (Figure 4.13). *Acanthogorgia* species do not cluster together indicating they have a polyphyletic origin, however the braches on which these species

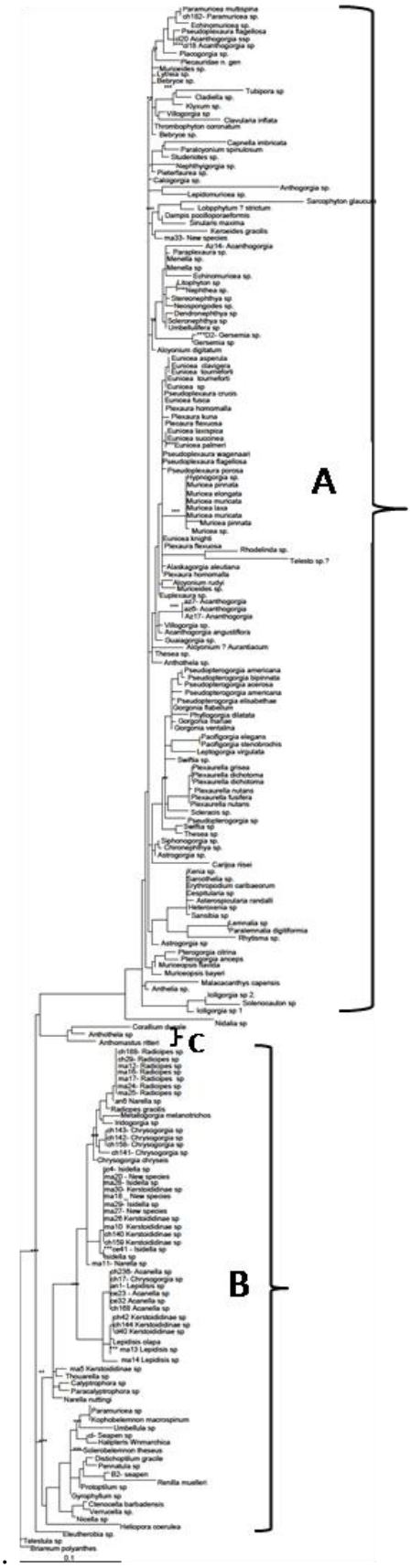

Figure 4.12. *ND2 from samples containing both MSHI and ND2 tree topology for Octocorallia *=>70% maximum-likelihood support **= >90 % Bayesian support at the nodes ***= >70% maximum-likelihood support and >90 % Bayesian support at the nodes. Tree rooted by* Briareum *species. Also contained in electronic appendix 3a Figure 4.9 for further detail*

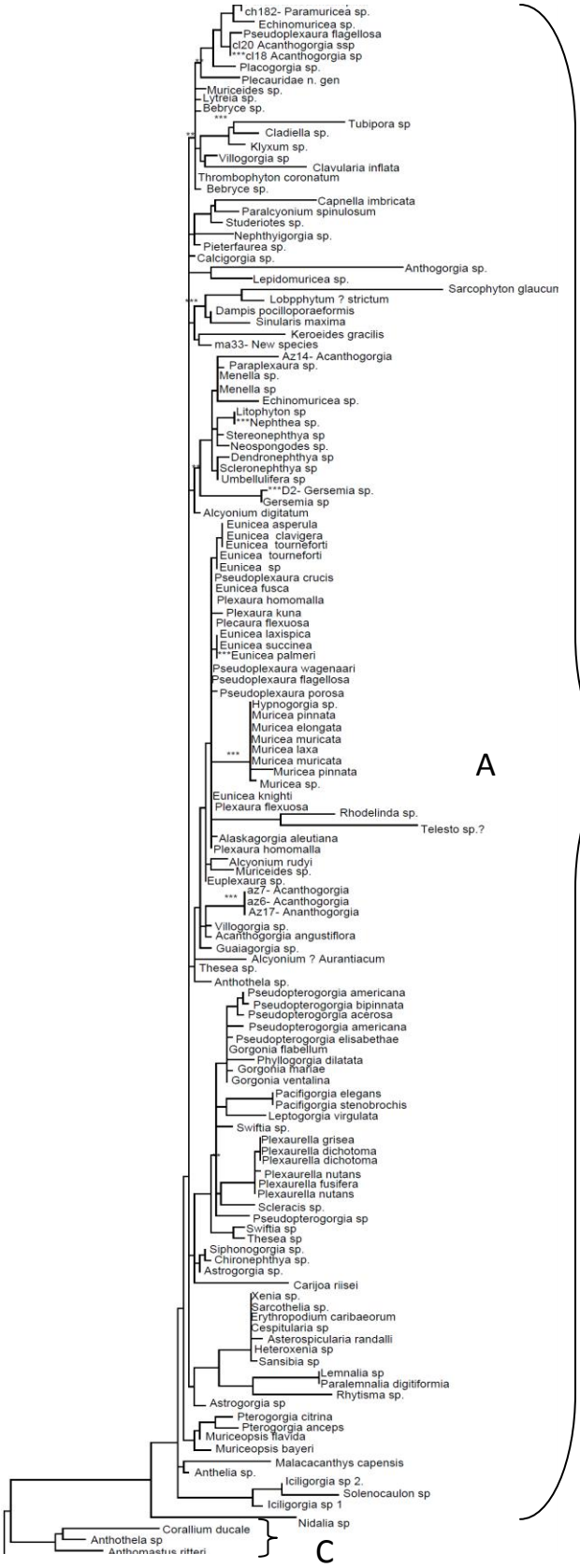

Figure 4.13 *ND2 from samples containing both MSHI and ND2 tree topology for Octocorallia enlraged for clade A and C. *=>70% maximum-likelihood support **= >90 % Bayesian support at the nodes ***= >70% maximum-likelihood support and >90 % Bayesian support at the nodes. Tree rooted by* Briareum *species. Also contained in electronic appendix 3a Figure 4.9 for further detail.*

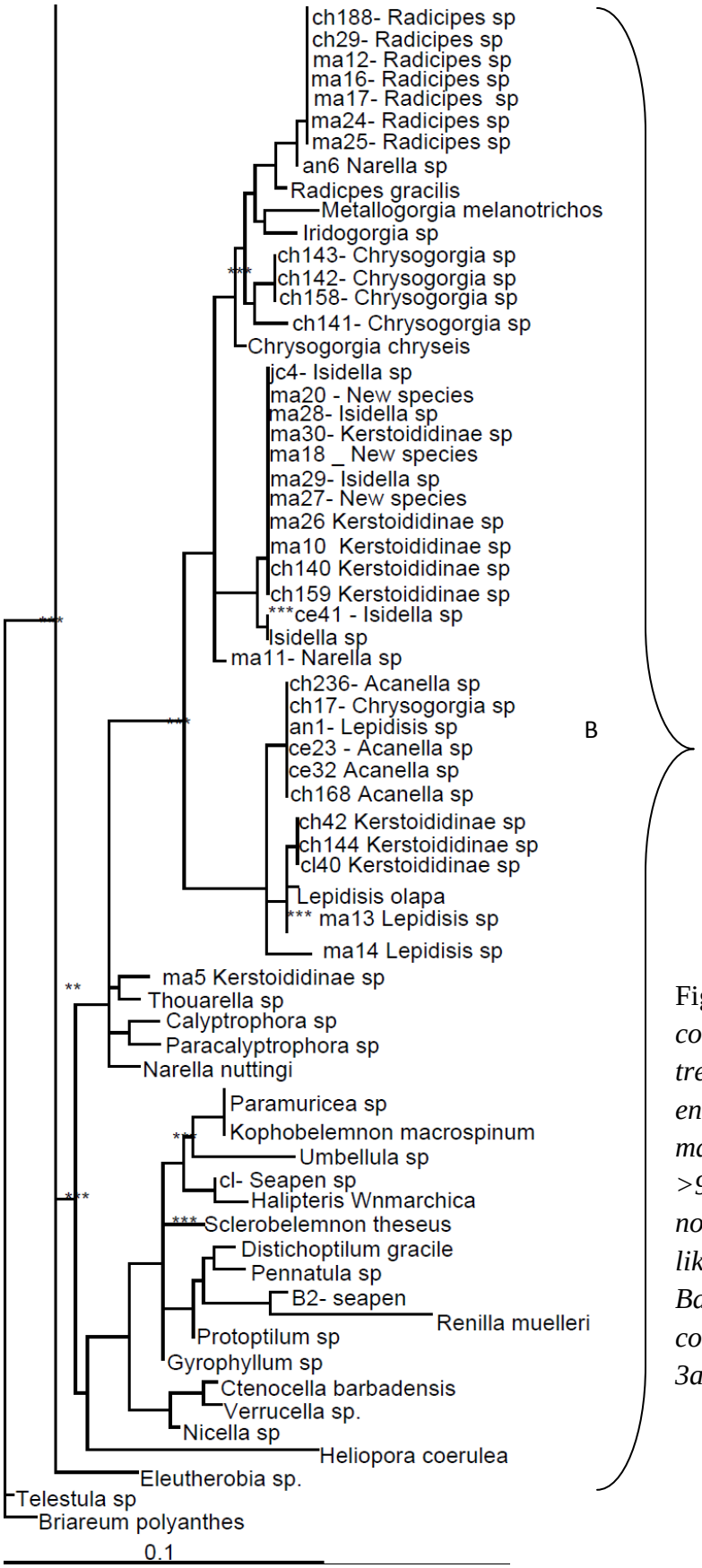

Figure 4.14. *ND2 from samples containing both MSHI and ND2 tree topology for Octocorallia enlarged for clade B. *=>70% maximum-likelihood support **= >90 % Bayesian support at the nodes ***= >70% maximum-likelihood support and >90 % Bayesian support at the nodes . Also contained in electronic appendix 3a Figure 4.9 for further detail*

occur are well supported by Bayesian and ML values. This clade also contains all samples from the sub-order Holaxonia as well as some soft corals from Alcyoniina. Samples Ma33, representing a new species (described in chapter 5), was branched with *Keroeides gracilis* closely placed near a branch containing Alcyoniina species. *Eunicea* species are closely branches together as are *Plexaurella* species.

A second well supported clade- Clade B, (Figure 4.14) contains all representatives of the sub-order Calcaxonia and the order Pennatulacea. The majority of new sequences obtained within this study occur within this clade. Isididae species (including three new species described within Chapter 5) fall into three well supported sub-clades, two of which contain only sequences from this study. Of these three sub-clades two occur as a monophyly with the third sub-clade appearing to have a separate evolutionary origin which is closely related to the Chrysogorgiidae, indicating an overall polyphyletic origin of Isididae. Sample Ch17, *Chrysogorgia* sp., was placed within the Isididae species. Chrysogorgiidae species are also all closely grouped together within the clade, with a small well supported sub-clade of Chrysogorgia species. Sequences belonging to the order Pennatulacea fall within a single sub-clade indicating a monophylogenetic origin (Figure 4.14). A very small sub-clade containing three species belonging to the Calcaxonia occurs at the base of the well supported Pennatulacea sub-clade.

Clade C (Figure 4.13) which is not well supported by Bayesian or ML bootstraps contains a single species of *Corallium* is along with *Anthomastus ritteri* and *Anthothela sp*. No sequences generated in the current work were included within this clade.

4.4.5- Combined *MSH1* and *ND2*

A total of 208 sequences were obtained from Sánchez *et al.* (2003), Wirshing, *et al.* (2005), McFadden *et al*. (2006) and this study (Appendix 3 table ap3.3). Alignments

contained a total of 709 base pairs including indels with fragments ranging from 159 to 191 amino acids in length from *MSH1* and 423 bases pairs including indels with fragments ranging from 134 to 138 amino acids in length for *ND2*. This resulted in an alignment of 1,132 base pairs. Of these nucleotide alignments 447 (39.49%) sites were invariant and 647 sites were parsimony informative. The majority of length variation between samples can be attributed to large indels present within Keratoisidinae species within the *MSH1* gene.

Tree topography is similar for all analyses (Bayesian, maximum parsimony and maximum-likelihood) (Electronic Appendix 3a Figures 4.12-4.14). Support for nodes is highest for Bayesian values than ML. As the Bayesian and ML trees were sufficiently similar the ML tree was used for visualization (Electronic Appendix 3a Figures 4.12-4.13). The majority of variance in topography occurred within the maximum-parsimony tree where clades are not as well defined and the presence of many "single" species at the base of Clade A (Electronic Appendix 3a Figure 4.14).

Four well supported clades can be visualized (A-D) (Figure 4.15). A monophyletic origin of all Octcorallia species was observed. Clade A (Figure 4.16) is the largest of the clades and contains all samples belonging to the sub-order Holaxonia as well as some Alcyoniina. Very few of the new sequences generated in this work occur within this clade with only the *Acanthogorgia* sample, Ma33 representing a new genus, and a *Gesemia* sp. being present. *Acanthogorgia* spp. do not appear to be well grouped within the tree. Branches within this clade are well resolved but positions do move between the individual tree topologies (Electronic Appendix 3a Figures 4.12-4.14). Ma33 is grouped with samples belonging to the family Alcyoniinae. *Muricea* sp. are very well grouped occurring on a single branch. *Plexaurella* and *Eunicea* are also well grouped within the tree, with the *Eunicea* branch being well supported. Holaxonia and Alcyoniina do not mix amongst the sub-clade but are distributed throughout Clade A.

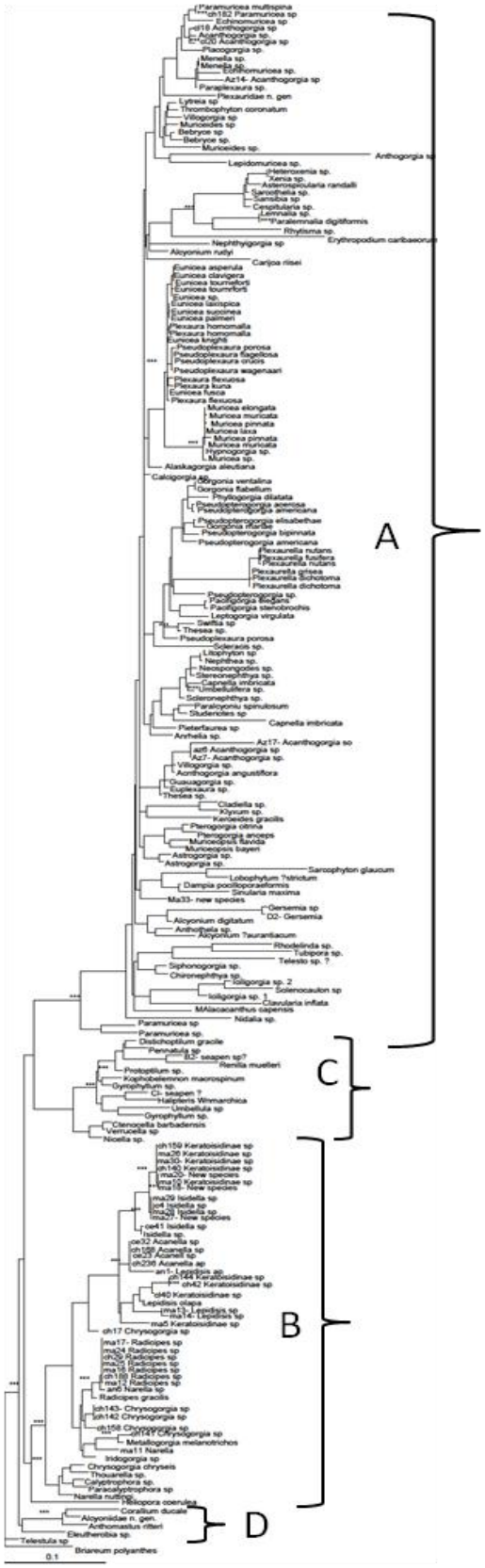

Figure 4.15 *MSH1-ND2 tree topology for Octocorallia. It is possible to see four distinct clades as indicated by the letters A-D. *=>70% maximum-likelihood support **= >90 % Bayesian support at the nodes ***= >70% maximum-likelihood support and >90 % Bayesian support at the nodes. Tree rooted by* Briareum *species. Also contained in electronic appendix 3a figure 4.12 for further detail.*

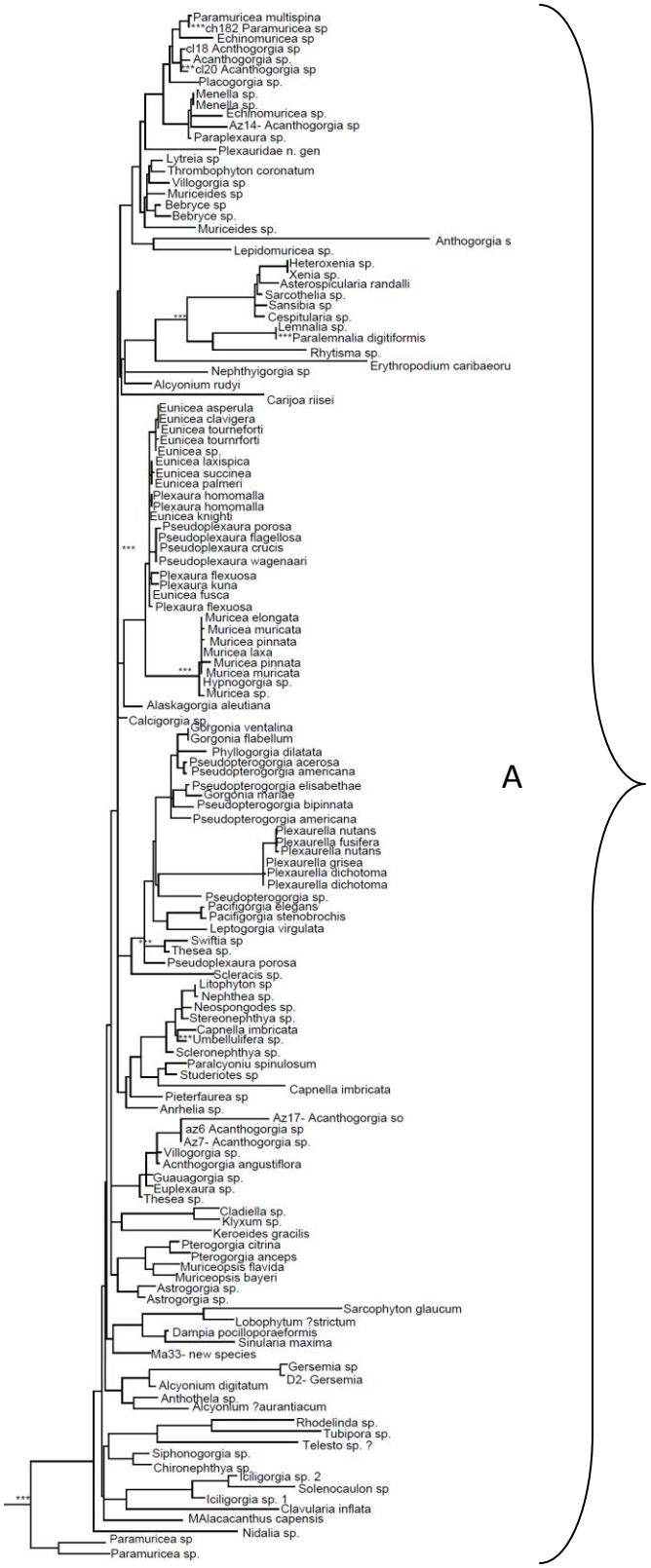

Figure 4.16 *MSH1-ND2 tree topology for Octocorallia enlarged for clade A. *=>70% maximum-likelihood support **= >90 % Bayesian support at the nodes ***= >70% maximum-likelihood support and >90 % Bayesian support at the nodes. Briareum was used as an outgroup for rooting. Also contained in electronic appendix 3a figure 4.12 for further details*

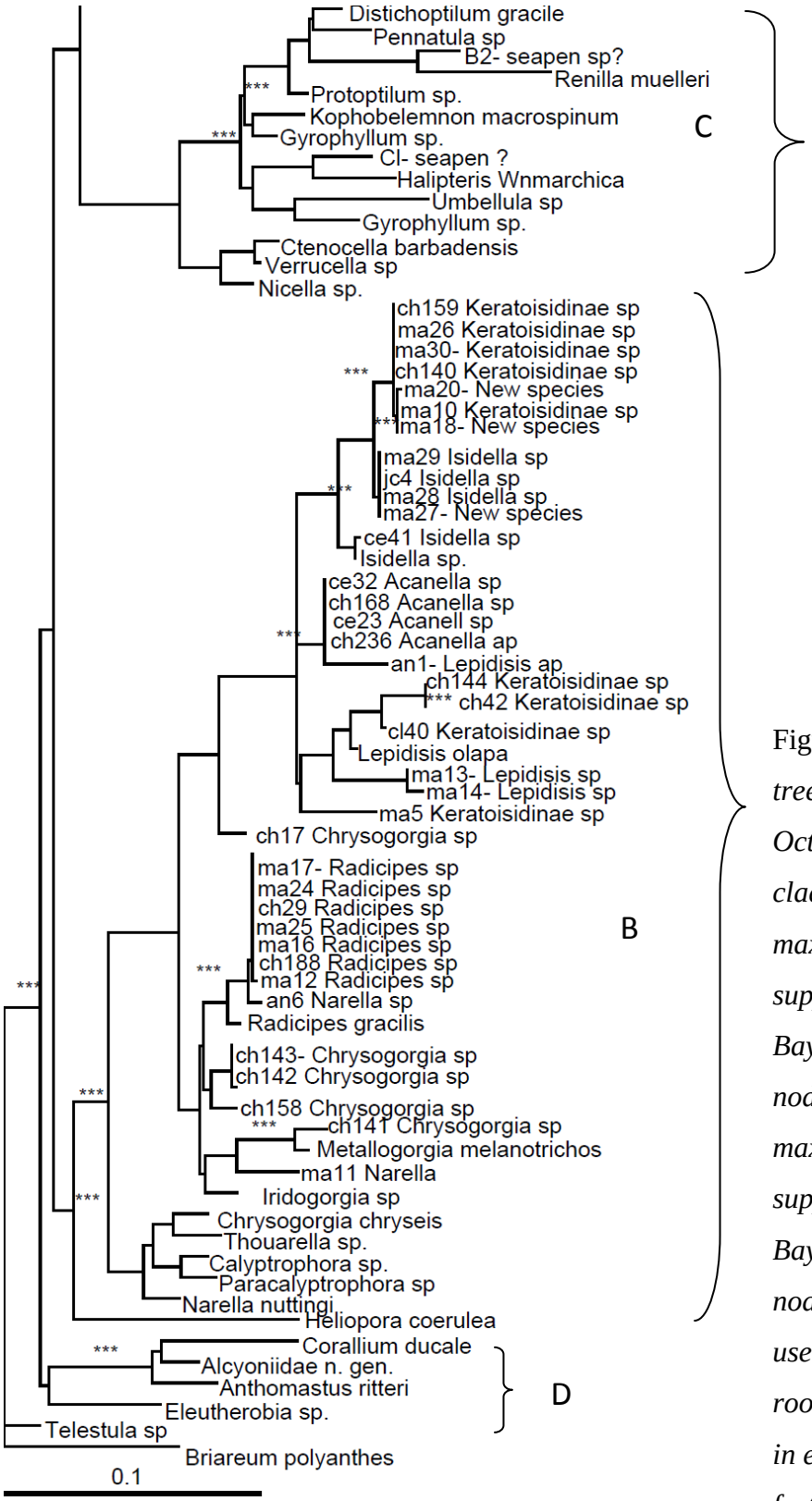

Figure 4.17 *MSH1-ND2 tree topology for Octocorallia enlarged for clade B-D. *=>70% maximum-likelihood support **= >90 % Bayesian support at the nodes ***= >70% maximum-likelihood support and >90 % Bayesian support at the nodes. Briareum was used as an outgroup for rooting. Also contained in electronic appendix for further detail.*

Clade B is well supported by both Bayesian and ML values (Figure 4.17). This clade is made up almost entirely of sequences obtained in this study belonging to the families Isididae and Chrysogorgiidae. Five well supported sub-clades within this group are made up of new sequences including those of the 3 new species MA27, Ma18 and Ma20 (described within chapter 5 of this thesis). Species of the Isididae appear to be monophyletic; however, there is not a good separation between genera with sub-clades containing more than one genus, indicating taxonomic and molecular discrepancies. *Radicipes* spp. are well grouped together within one well supported sub-clade.

Clade C, which is not well supported by Bayesian and ML bootstraps, contains species from the Order Pennatulacea including two obtained from this study as well as some Calcaxonia. Although the clade is not well supported the three of the four branches are well supported. This clade is positioned between clades A and B in both Bayesian and ML trees. However, within the MP tree this clade occurs at the base of clade B (Electronic Appendix 3a Figure 4.14). Despite this, all samples within the clade remain consistent throughout all topographies.

The fourth and final clade (D) is very small and only consists of 4 samples belonging to the Alcyoniina and a single *Corallium* species (Figure 4.17). This clade contains two branches one, containing only a single species which is not well supported and the second containing the remaining species which is well supported by Bayesian and ML bootstraps. This clade occurs at the base of the tree in all topographies and is well supported by Bayesian values. The clade contains no sequences generated in this study.

4.4.6 Genetic Distances.

Uncorrected- p values, which correspond to percentages, were calculated for samples used in data sets 3 and 4. For both *MSH1 and ND2* genes samples of the same species have less

than 1 % divergences in genetic distance (Figure 4.18). When considering species from the same genus 57 % of individuals for *ND2* and 50 % for *MSH1* have a divergence of less than 1 %. *ND2* is shown to have a higher divergence within the same genus than *MSH1* with 5 % of individuals having a genetic divergence of up to 12 % (p value of 0.12) in comparison to no individuals of *MSH1* having a divergence of over 8 %. However, when individuals from different genera are considered *MSH1* has a higher divergence than *ND2*. 2.5 % of individuals have less than 1 % divergence in the *ND2* gene, in comparison to only 0.7 % of *MSH1*. The maximum divergence observed in *ND2* for this data set is 16.4 % in comparison to 26.8 % in the *MSH1* gene. Within *ND2* 1-4 % divergence is the most common with 34 % of individual pairs, where as in *MSH1* the most common divergence is 13-16 % with 38 % of pairings occurring within this category.

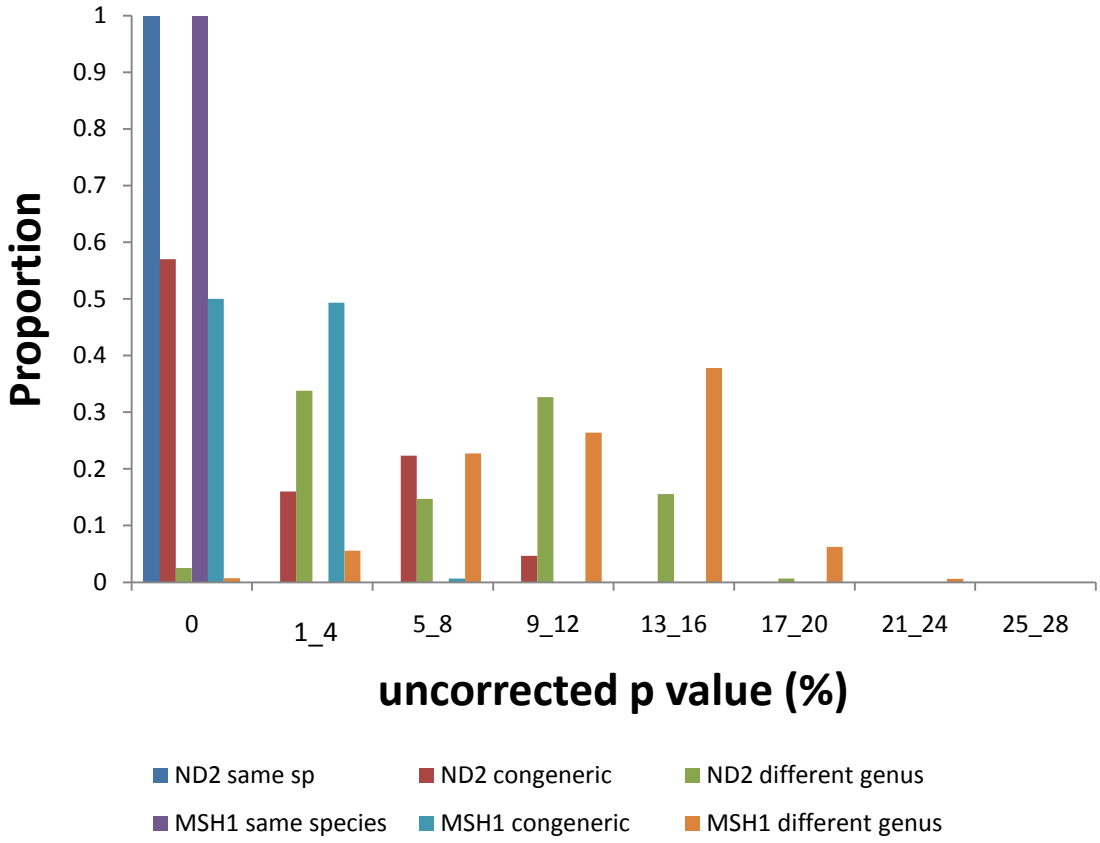

Figure 4.18 Genetic distances beween Octocoral individuals for both MSH1 *and* ND2 *genes. Genetic distances are calaucted as uncorrected p values from* PAUP.

4.5. Discussion

Phylogenetic analysis of Octocorallia species has begun fairly recently. Previously genes such as 18s and 28s rDNA markers were used to estimate phylogeny. However, the discovery that that evolutionary rates in Octocorallia are relatively slow, often in the region of 50-100 times slower than the mitochondrial genomes from most other animals (Shearer *et al*., 2002; Hellberg, 2006; McFadden *et al.*, 2011) has lead to the increased use of mitochondrial gene markers such as *ND2* and *MSH1* in recent studies, such as those by Sánchez *et al.* (2003), Wirshing *et al.* (2005) and McFadden *et al.*, (2006). The present study focuses on the creation of a phylogenetic tree using deep-sea octocorals primarily collected from the Northern Atlantic Ocean including from the Azores Islands, the Mid-Atlantic ridge and with others taken from the North Sea and Antarctica, along with samples from NCBI to create the most comprehensive phylogenetic trees within the Octocorallia to date.

Three different phylogenetic topographies were used throughout the study, maximum-likelihood, Bayesian and maximum parsimony. Maximum parsimony (MP) is a non-parametric test using a character-based method to estimate tree topology. Maximum-likelihood (ML) is similar to parsimony. However, it is a parametric test which uses a specific model of evolution, selected by Modeltest. As a result of these differences in approach it is suspected that ML produces more accurate trees than MP (DeBry and Abele, 1995). Bayesian topologies also use a statistical likelihood function using models of evolution selected by Mrmodeltest software, however, topologies are estimated using Bayes' theorem, relating the probability that the tree is correct with the model of evolution, producing many trees. By using all three of these estimations of topology it was possible to compare the output and results were robust.

Five data sets for *ND2* and *MSH1* genes were analysed. These consisted of - 1) All *MSH1* sequences available plus samples from this study (626 sequences) 2) All *ND2* sequences

available plus samples from this study (287 Sequences) 3) *MSH1* sequences obtained for samples which also have *ND2* available obtained from Wirshing et al. (2005), Sánchez et al. (2003), McFadden et al. (2006), and this study (208 samples) 4) *ND2* sequences obtained for samples which also have MSH1 available obtained from McFadden *et al.*. (2006), Wirshing *et al*. (2005), Sánchez *et al.* (2003) and this study (208 samples) 5) combined data set of both *MSH1* and *ND2* genes from McFadden *et al.*, 2006, Wirshing *et al*, 2005, Sánchez *et al.*, 2003 and this study (208 samples Appendix 3). These samples included a range of species including representatives from Alcyoniina and Isididae.

The reason for the use of these five data sets was not only to allow the most comprehensive phylogenetic analyses for Octocorallia to date to be achieved (via the use of data sets 1 and 2), but also to allow more in-depth differences between topologies dependent upon the gene used to be identified. It would also allow the determination of whether using more than one gene can lead to a higher resolution tree topology. This was achieved using data sets 3-5 which use the same individuals throughout analyses with the individual *MSH1* gene (data set 3) the individual *ND2* gene and the combination of these genes together (data set 5).

It is known that the Isididae sub-family Keratoisidinae has undergone a gene inversion within the *MSH1* region, expected to have occurred in one event. This results in these species being unable to be amplified by the standard Octocoral *MSH1* primers and must be amplified with Keratoisidinae specific primers (Brugler and France, 2008). This inversion leads to difficulties in aligning samples from a range of Octocoral species, resulting in the inclusion of a large number of indels within the alignment. This difficulty maybe a reason as to why there are very few studies which have dealt with both Isididae and non-Isididae species using the *MSH1* gene, with a tendency to deal with the Isididae separately from other octocoral families. This inversion and the occurrence of a number of indels within the Keratoisidinae indicates a monophyletic origin within this sub-family.

The *ND*2 gene within the Octocorals did not show this variation between the Isididae and non-Isididae species and was fairly well conserved across species. This meant there were few indels with the number of amino acids used within the study only varying by four. This results in a variance of 12 base pairs in a fragment 423 length which represents a maximum of 2.8 % length variance. This is in comparison to the *MSH*1 which varies in length from 159-191 amino acids which equates to a variance of 96 base pairs. It must also be noted that every sequence from the *MSH*1 gene contains indels, thus has a higher variance between species gene than *ND*2. This increase in variance would indicate that *MSH1* is a more informative gene for barcoding than *ND2*. By combining these genes it is expected that a higher resolution phylogenetic model can be achieved.

4.5.1 Tree topology comparisons

In all data sets tree topologies between different analyses were similar although the MP tree created by PAUP had the most divergent topology (Electronic Appendix). Clade B for all data sets was generally well conserved between analyses although branch placement varied; samples grouped within branches are well conserved between analyses. Within all data sets Clade A contains many "single" species. The MP analysis visualizes these "single" species to occur at the base of the clade rather than being distributed throughout clade as they are in the ML and Bayesian trees. This indicates that the MP analysis is not as rigorous as the ML and Bayesian trees, leading to the construction of a "simpler" topography, thus both Bayesian and ML models use more stringent criteria and thus are expected to create a more realistic phylogenetic tree. This means that both Bayesian and ML models are theoretically more robust than MP analysis, this is supported by the tree topologies produced within this study. As it was only the maximum parsimony tree which was able to be completed for data set 1) All *MSH1* sequences available plus samples from this study (626 sequences) it is difficult to allow a complete comparison to the other data groups as this was the most divergent topology type.

Tree topologies between the different data sets are relatively well conserved despite this, there are a few differences between the different genes. The tree topology created from the combined gene is expected to produce the most realistic phylogenetic representation, as a result of increased genetic information.

4.5.2 Comparison of the concatenated dataset versus individual genes

The main difference between the tree topologies produced between the joint genes and the individual genes is that both *MSH1* and *ND2* trees produce three distinct clades whilst the joint *MSH1-ND2* tree produces four clades. This extra clade contains the Pennatulacea. Although all tree topologies group the Pennatulacea samples together within the individual *MSH1* and *ND2* trees they are incorporated in the large clade B and do not produce a distinct clade. However, all topologies agree on the occurrence of a monophyletic origin within the order Pennatulacea. This is also in agreement with McFadden *et al.* (2006) who found the Pennatulacea grouped within a clade with Calcaxonia and Alcyoniina, distinct from the Holaxonia. It is likely this slight difference in topology is a result of increased resolution within the joint tree because of an increased number of base pairs and amino acids which can be compared. However, McFadden *et al.* (2006) do not agree on the presence of a fourth clade when genes are joined and also consider these to be incorporated within the large clade A.

Clades demonstrated within this study were largely congruent with those produced by McFadden *et al.*,(2006) who found that there were two main clades of Octocorals; clade 1 (Holaxonia-Alcyoninna) and clade 2 (Calcaxonia-Pennatulacea), this is also in agreement with Sánchez *et al.* (2003a) who using 16 s and 18s markers found two distinct clades one containing Calcaxonia and Scleraxonia and the other Alcyoniina, Holaxonia and again Scleraxonia . McFadden *et al's* (2006) clade 1 also closely corresponds to Berntson *et al's.* (2001) clade C using the 16S and 18S genes, these were both the equivalent of the Clade A found within this study. McFadden's clade 2 (Calcaxonia-Pennatulacea) corresponded

with Clade B within this study for the separate trees. However, within the joint gene tree this clade became separated into two smaller clades with the Pennatulacea in one and Calcaxonia in another. This difference could be a result of increased sample numbers within this study with a minimum of 208 sequences in comparison to the 115 used by McFadden *et al.* (2006). It may also be the result of the increased number of Isididae species present within this study, which as previously stated have an inverted gene order with the *MSH1* region. This discrepancy could go some way towards the explanation of the separation of the Pennatulacea away from the other clades when increased resolution is achieved.

McFadden *et al.* (2006), also found a third small clade (*Anthomastus*-*Corallium*) which closely corresponds to Clade 3 within this study. This clade was enlarged in data set 2 (all ND2 species) as a result of the inclusion of an increased number of *Corallium* species within the study. It was also noted that Paragorgidae species were also included in this clade in data set 2 and on the same branch as *Corallium* in data set 1. As no species of Paragorgidae were included in Sánchez et *al.* (2003), Wirshing *et al.*(2005) or McFadden *et al.* (2006), it is not possible to conclude if this would be in agreement with their studies. However, this is in agreement with Herrera *et al.* (2010) who found that there was strong support for a monophyly of Coralliidae species and *Paragorgia* species.

Data set 2 also illustrated the presence of a very small fourth clade which was only comprised of two specimens of *Erythropodium caribaeorum* between Clades A and B (Figure 4.2). McFadden *et al.* (2006), also found that *Erythropodium caribaeorum* species separated from other octocoral species and had mentioned their use as an out-group along with *Briareum polyanthes*. As these species did not group together within the present analysis it was not possible to use both as an out-group and thus the decision was made to use *Briareum polyanthes* by itself. The separation of *Erythropodium caribaeorum* within data set 2 would indicate that this would make a successful out-group for *ND2*. However,

no such separation was seen in *MSH1* datasets indicating *Erythropodium caribaeorum* is not a useful out-group for this gene.

Within the clades found in the present study the sub-clades do not tend to represent family separations based on morphological segregations. This is in agreement with Wirshing *et al*. (2005) who found that although all phylogenetic reconstructions produced similar topologies, none of them agreed with familial arrangements hypothesized by Bayer (1981). Some sub-clades are more highly resolved than others; for example *Muricea* species and *Eunicea* species were found to group well within Clade A, again agreeing with Wirshing *et al.* (2005) and the Chrysogorgiidae, especially *Radicipes* species, grouped well within Clade B of all treatments within this study. *Acanthogorgia* species were found to be polyphyletic occurring in more than one sub-clade within Clade A. This is in agreement with McFadden *et al.* (2006) who showed two distinct lineages of Chrysogorgiidae.

The close phylogenetic relationship of the *Eunicea* spp. and *Plexaura* spp. illustrated by the tree topologies has been attributed to their restricted geographic distribution within the Western Atlantic (Sánchez *et al*., 2003). It is also likely that as a result of their placement in the trees and to similarities in sclerite structure, branching and calyx as described by Wirshing *et al*. (2005) that *Pseudoplexaura* and *Plexaura* are closely related. Perhaps they should be reclassified as Gorgoniidae family and not the Plexauridae where they are currently classified. This misclassification has been supported by mineralisation and chemotaxonomic analyses (as discussed by Wirshing *et al*., 2005).

Isididae species are also very well grouped within all phylogenetic reconstructions produced. However, at genus level resolution become less defined with no sub-clade containing only one genus; this is in agreement with France (2007) who found not only different genera occurring throughout sub-clades but also different branching type, indicating again that morphological separations do not agree with molecular ones.

The *ND2* topologies indicate the presence of a polyphyletic origin of the Isididae species. It is difficult to say whether data set one indicates polyphyletic or monophyletic origin as a result of a reduced resolution; however, it is clear that the Isididae occur within three branches in the tree topology. Both joint gene trees and the *MSH1*-only tree indicate monophyletic origin. This may be a result of the inverted gene order in *MSH1* within the Keratoisidinae indicating which would cause the family to group together as a result of a single evolutionary event. However, this rearrangement is not present in the *ND*2 gene and thus any differences between Keratoisidinae and other samples will contribute towards a polyphyletic origin within the Isididae as small changes will not be overpowered by large indel created within the *MSH1* as a result of gene rearrangement. This would be in agreement with Duenas and Sánchez, (2009) who belived that the high levels of lability within the Isididae indicate that they have evolved independently multiple times. McFadden *et al.* (2010) also noted that there has been increased evidence of polyphyletic origins in Isididae from unpublished data.

Watling *et al,* (in prep) noted that within the phylogeny created by McFadden *et al.* (2006) there were ten deep-sea species from the families Chrysogorgiidae, Isididae and Primnoidae which all grouped together in a single clade, with three sub-clades corresponding to the individual families. This is also shown within this study with the presence of sub-clades containing only deep-sea species of Chrysogorgiidae and Isididae obtained from this study within Clade B, which would suggest evolution from a single ancestor (Figure 4.19). When shallow-water species of the same families are included in the analysis the Chrysogorgiidae and Isididae become polyphyletic (Watling *et al.,* in prep; France Louisiana University pers. comm.). This would suggest that deep-sea corals have under gone *in-situ* radiation (Watling *et al.,* in prep). From this it can only be concluded that further work and increased publishing of existing data is required to allow a comprehensive view of evolutionary histories between species.

4.5.3 Genetic Distances.

Within this study it was found that *ND2* had a higher scope of variation within the same genus, yet a smaller variation between genera than that found with *MSH1*. Previous findings stated that the variance of *ND2* between families was below 10 % (France and Hoover, 2001; McFadden *et al.,* 2004; McFadden *et al.,* 2010); however, herein it was found that the same genus could vary up to 12 % with inter-generic variations reaching levels of 16 %. This could again be attributed to the increased number of specimens used within this study as well as the inclusion of new species that have not yet been assigned a genus and appear to have a high level of genetic divergence from previously known species, especially Ma33.

MSH1 was found to have higher inter-generic variation with distances reaching up to 26 %. This is in agreement with previous studies who found that *MSH1* had approximately twice the level of variation than other protein-coding regions in Octocorallia (France and Hoover, 2001; Van der Ham *et al*., 2009; McFadden *et al*. 2010). This could be a direct cause of the gene inversion within Isididae species. Both genes were found to have levels of variation of less than 1% within samples of the same species with most occurring at levels of less than 0.5 %. This would be in accordance with McFadden *et al.* (2011) who stated that any pairs with a variance of above 0.5 % should be considered different species.

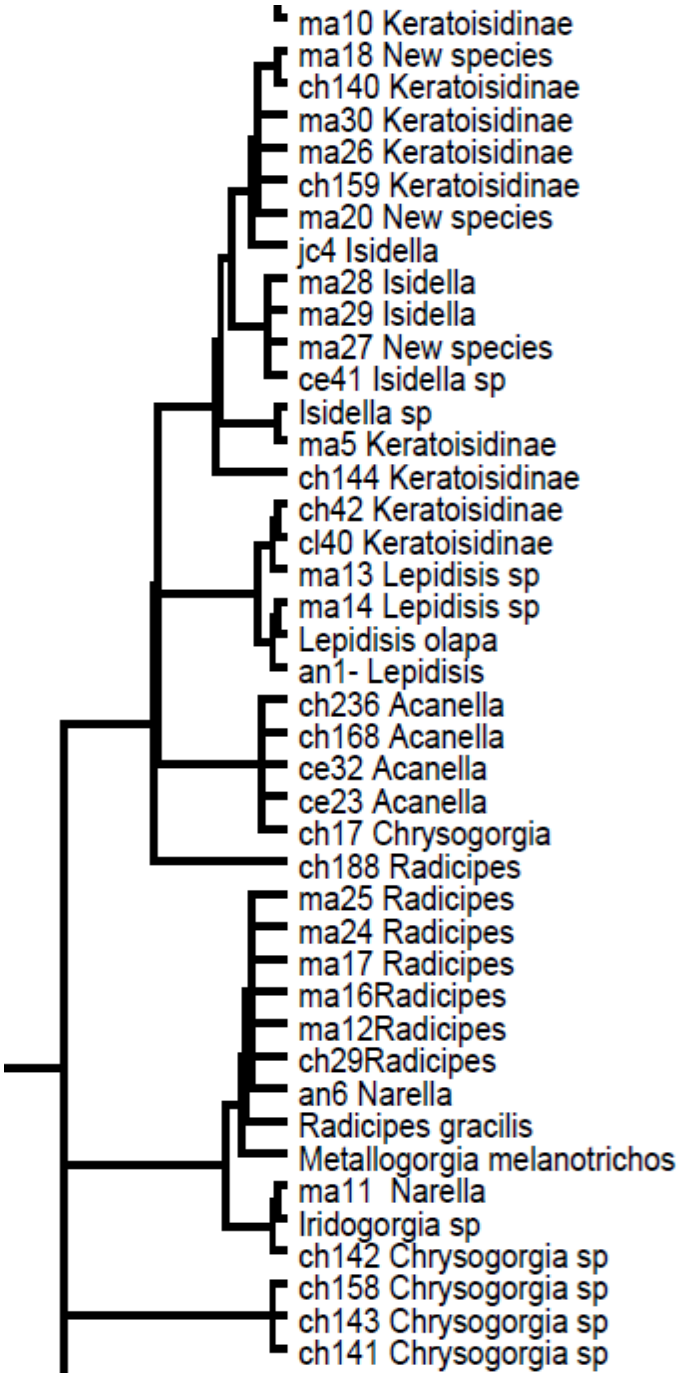

Figure 4.19 *MSH1tree topology for Octocorallia enlarged for clades containing only deep-sea Isididae or Chrysogogiidae species.*

It is clear from this study and previous studies that although *MSH1* is the most divergent marker used on Ocotcorallia to date, it is still not possible to use this as a barcoding gene. A successful barcoding gene should be able to distinguish clearly between species of the same genus and with low divergence rates within genera. However, *MSH1* does have a higher resolution for the separation of genera than other genetic markers available, with *ND2, ND3, ND4L, ND6* and *16S* all having lower levels of variation (France and Hoover, 2001; McFadden *et al.,* 2004; McFadden *et al.,* 2010). The results of this study support the idea that no single genetic marker is able to unequivocally identify a single species thus far (Van der Ham *et al.,* 2009; McFadden *et al.,* 2010, 2011).

By the inclusion of a joined *MSH1-ND2* gene tree this study demonstrated that the use of multiple genes on the same specimen increased tree resolution and allowed a new clade to be designated. This indicated that the use of multiple gene analysis will increase the likelihood of a correct genetic identification of a given sample. However, it must also be noted that it is quite common for genetic and taxonomic identification to disagree with one another and thus it is important that more joint work is completed to allow a more comprehensive picture of the phylogenetic and taxonomic relationships to be attained.

4.5.4 Conclusion

This study has demonstrated the Octocorallia are monophyletic, however many families within the Octcorallia are polyphyletic. It was also found that that the molecular taxonomic relationships do not agree with traditional morphological taxonomic separations. Tree topologies of the different phylogenetic analyses were found to be fairly consistent within a data set with MP being the most divergent. The inclusion of an increased number of samples and a joint gene topology leads to the creation of a fourth clade, indicating that for a more comprehensive understanding of the taxonomic relationships at genus and species level a study incorporating multiple representatives of all families and genera within the order, utilising multiple genes is required.

Chapter 5: New deep-sea coral species from the Mid-Atlantic Ridge 45°N

5.1 Introduction

Despite its size and diversity of animal communities, the deep sea still remains one of the least studied environments on Earth. Thus, as with many other deep-sea taxa very little is known regarding the taxonomy of the deep-sea corals. This is mainly a result of the paucity of sampling resulting in even the most common of deep-sea coral species being poorly studied (Gage and Tyler, 1991; Etnoyer, 2008).

The word taxonomy, arises from the Greek for arrangement and method, and is the classification of organisms using morphological and more lately, molecular traits to group and identify them. Taxonomy has been used since the 1730s when Linnaeus developed the system of binomial nomenclature for species naming using the genus and the specific epithet (Rose, 2009). Following this system each individual is placed within a Kingdom, Phylum, Class, Order, Family, Genus and finally Species. Corals lie within the Kingdom: Animalia, Phylum: Cnidaria, Class: Anthozoa which is itself divided into four main sub-classes: Zoantharia, Hexacorallia, Octocorallia, and Ceriantipatharia. Within these orders there are multiple families and thousands of species. Among all higher taxonomic groups of cnidarians, the Octocorallia are arguably the least understood, with current taxonomies considered unstable both at family and genus level (McFadden *et al*., 2006, 2010).

Overall understanding of taxonomic and phylogenetic relationships within the octocorals has been hampered in the past by poor fossil record, widespread plasticity, paucity of morphological characteristics and a widespread intraspecific variation such as growth forms (McFadden *et al.*, 2006). Past literature of coral taxonomy has often neglected to include an adequate number of detailed illustrations or has provided none

at all, and type specimens are often badly preserved and poorly curated which can often lead to confusion (Sanchez, 2007). The main reason for the lack of fossil record is that octocorals are not easily preserved because "once dead their skeletons do not persist very long on the seafloor" (Roberts *et al*., 2009). Those individuals that do persist long enough to create a fossil are still incredibly difficult to identify effectively. This is because the features used to identify corals cannot be applied to fossilised specimens (Giammon and Stanton, 1980).

Originally the Octocorallia was divided into seven orders: the Helioporacea, Pennatulacea, Alcyonacea, Gorgonacea, Stolonifera, Telestacea and Protoalcyonaria as defined by Hickson (1930). Primarily these orders were defined by growth form, however, upon review Bayer (1981) realised that although Helioporacea and Pennatulacea had distinguishable morphological characteristics the remaining orders graded into one another and thus this was not plausible as a distinct morphological separation of taxa. Bayer therefore revised the groupings leaving Helioporacea and Pennatulacea as they were and placing the remaining orders into a single order known as Alcyonacea, which now encompasses all soft corals, gorgonians and stoloniferous corals (McFadden *et al.*, 2006, 2010).

Within the Alcyonacea there are ~30 families, the Helioporacea includes 2 families and Pennatulacea 14 families (see Chapter 1 for a full list of families contained in Octocorallia). The order Helioporacea is unique among octocorals in that the species contained within it produce a solid-crystalline aragonite skeletal matrix rather than producing a skeleton created of scleroproteinaceous gorgonin and/or calcite (Daly *et al.*, 2007; McFadden *et al.,* 2010). The order Pennatulacea contains the seapens which also have a distinct morphology, including the presence of a peduncle, allowing them to anchor in soft sediment (Woodby *et al.*,2009: McFadden *et al.,* 2010). All other octocorals are placed within the Alcyonacea which presently lacks any defining synapomorphies (McFadden *et al.,* 2010).

Attempts have been made to separate Alcyonacea into sub-orders but thus far these have all concentrated on taxonomic methods and not phylogenetic representation often resulting in phylogenetic topologies which disagree with genus placement (Daly *et al.*, 2007; McFadden *et al.*, 2010). The features used within these attempts have mainly focused on axial morphology. Individuals which do not contain a skeletal axis have been placed into sub-orders Alcyoniina, Stolonifera and Protoalcyonaria. Those with a solid axis are placed into sub-order Calcaxonia, those with a hollow axis are placed into sub-order Holaxonia and those with an axis composed mainly of calcium carbonate sclerites which may be fused or unfused into sub-order Scleraxonia (McFadden *et al.*, 2010).

An understanding of coral diversity has mainly relied on morphological characteristics to divulge relationships between species (Dueñas and Sánchez , 2009**)**. Sclerite morphology is the most effective way to differentiate between octocoral species (Janes and Mei Wah, 2005). Sclerites (Figure 5. 1) are small, internal, calcium carbonate skeletal structures which are found within octocorals, and have the dual purpose of support and structural defence against predators (West, 1998).

Sclerites occur in a variety of shapes dependent on the species and the area of the polyps from which they are extracted. It is the arrangement and shape and size of these sclerites which are often used to identify a species. However, West (1997, 1998) has shown that the same species of coral can have varying lengths and density of sclerites within different individuals and thus shape must be considered as a more important identifying factor. To allow an accurate identification to be made sclerites from a variety of locations on the individual must be taken and examined which can be very labour intensive (Janes and Mei Wah, 2005).

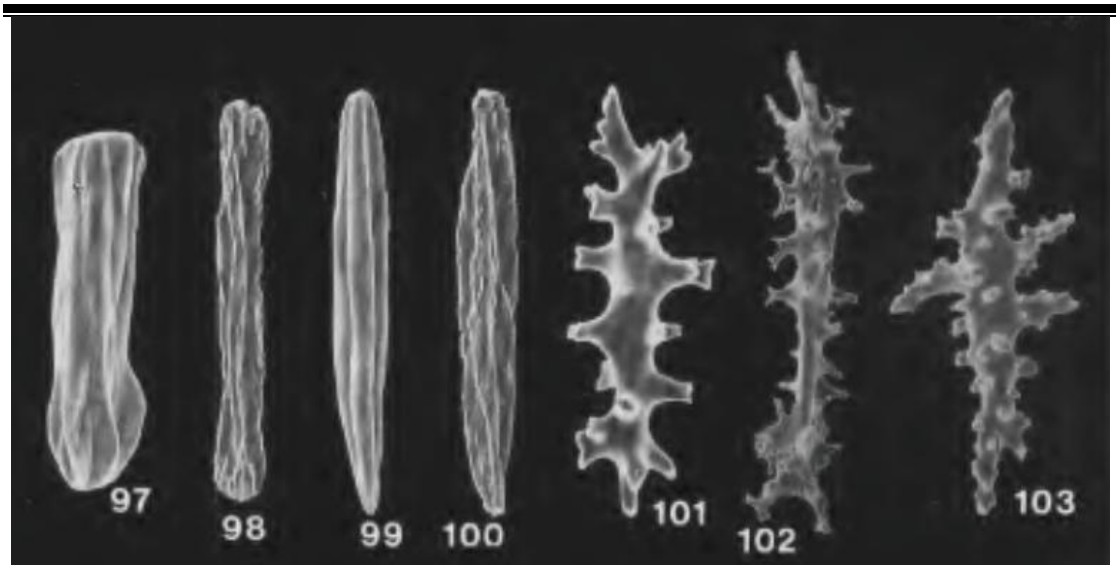

Figure 5.1. A variety of different sclerite shapes found within corals 97= three-Flanged rod, 98= three-flanged rod with serrated edged, 99= three-flanged spindle, 100= three-flanged spindle with serrated edges, 101 = spiny spindle, 102= Anastomosing branched spindles, 103= Branched spindle. Modified from Bayer et al, 1983 a scale bar was not provided

Other features may also be used in coral taxonomy to identify an individual (Sánchez , 2007). These include polyp armatures, axial skeletons and colony morphology (Janes and Mei Wah, 2005, Sánchez, 2007). However, these traits have a high level of homoplasy, with many having no usable landmarks (Sánchez and Lasker, 2003). The surface detail and overall shape of the sclerites is the most important diagnostic feature for identifying species (Janes and Mei Wah, 2005, Sánchez, 2007). Identification can be further complicated by the fact that there is often a high degree of variation in features such as polyp and sclerite morphology, making identification from keys and pictures difficult to achieve accurately (McFadden *et al.,* 2006, Aguilar and Sánchez, 2007). Additionaly one coral species can occur in several growth forms and colours (West *et al.*, 1993), making octocoral taxonomy possibly one of the most challenging in the invertebrates.

The difficulties are well illustrated by Cairns and Baco (2007) where five new species of the octocoral genus *Narella* are described. They found that species distinguishing features such as polyp spine development cannot only vary between individuals and species but can also be dependent upon the polyp position within the colony, making even microscopic identification difficult, especially when the samples do not comprise of the whole colony (Cairns and Baco, 2007). West (1997) found that the sclerites present within the gorgonian species *Briareum asbestinum* differ in length within and among populations, with both biotic (level of predation) and abiotic (current speed and depth) factors having an effect on these.

The morphology of a species has also been shown to change dependent upon the depth at which it is found. In the shallow water species *Briareum asbestinum* depth has been shown to affect the length and width of the colony; those in shallow water having a stouter and shorter appearance than those which occur at depth (West *et al.,* 1993). Should this hold true for deep-sea corals it would be expected that morphology of deep-sea coral colonies will be long and slender. Shallow water colonies were also found to have a higher number of polyps and shorter sclerites (West, 1993), again implying that deep-sea corals will have few polyps and long sclerites. It is also possible that an increase in current leads to a reduction in the sclerite length (to prevent breaking), as seen in shallow water species (West, 1993). This would lead to a change in the sclerite structure dependent upon exposure to currents, meaning those individuals on slopes would have smaller sclerites than those on the flat.

Genetic analysis is a useful tool in grounding taxonomic traits for species identification. By creating taxonomic trees it is possible to determine if a trait is found solely within one species, or family, and thus can be used for identification. Should a trait occur throughout the tree then this would not be a useful character for determining the species (France, 2007). By using taxonomy and genetic sequence data together a more congruent identification can occur and the appreciation of morphological characters would improve (Dueñas and Sánchez , 2009). This is important as over time there has

been a reduction in scientific expertise in alpha taxonomy and more interest in molecular techniques.

5.1.2 Isididae species

The octocoral family Isididae, commonly known as bamboo corals are sendentary, non-tropical octocorals (Tracey *et al.,* 2007) which have a wide distribution throughout the world's oceans (Bayer, 1956; Watling *et al.,* in prep), occurring in both deep and shallow-water habitats. They are currently divided into four subfamilies: Isidinae, Keratoisidinae, Mopseinae and Circinisidinae (Alderslade, 1998; Watling *et al.,* in prep).

It is believed deep-sea or cold-water Isididae occur mainly on elevated, hard rocky substrata in high water flow areas (Copley *et al.,* 1996; Mortensen *et al.,* 2008; Orejas *et al.,* 2009; Morris *et al.,* In prep). Isididae corals are long-lived species, within peak abundance occurring between 200-1,500 m depth (Dueñas and Sánchez , 2009). They have a recognisable appearance with the presence of dark-coloured gorgonin proteinaceous nodes and light calcitic internodes on their skeletons (France, 2007; Etnoyer, 2008; Duenas and Sánchez , 2009), which can often be visualised using modern filming and photographic techniques used in deep-sea exploration (France, 2007). The calcitic component of the skeleton provides the support for the colony allowing it to grow in areas of high current and the gorgonin provides flexibility (Tracey *et al.,* 2007). It had previously been suggested that this family was polyphyletic with the evolution of proteinaceous nodes alternating with calcareous internodes occurring four separate times creating the four families (Watling *et al.,* in prep). Covering the skeleton there is a layer of coenenchyme which contains sclerites and bears polyps (Tracey *et al.,* 2007).

It is not possible to identify accurately individual corals to the species level purely from visual records, as species may have more than one growth form or colour, meaning one

species can be mistaken for more than one or vice verse. For accurate identification samples for taxonomic and/or genetic work are required.

The taxonomic descriptions which have previously occurred on Isididae have predominantly been carried out by Bayer and Alderslade. The six characteristics which have previously been used to identify and classify bamboo corals are listed below (Bayer and Stefani, 1987: France, 2007)

1. Polyp retractability
2. Colony branching
3. Axial skeleton structure
4. Sclerite morphology
5. Sclerite arrangement
6. Polyp operculum

However, many of these traits have been found to show character lability (France, 2007; Dueñas and Sánchez , 2009). Within the subfamily Keratoisidinae there is a variety of branching and shape forms, with *Keratoisis* containing both branched and unbranched forms, *Lepidisis* including some branched specimens and unbranched specimens, *Isidella* having few branches which occur from the nodes and *Acanella* having a bush-like appearance with multiple branches from the node. However, France (2007) has shown via the use of phylogentic analysis, that branching structure (branched, unbranched) is not a synapomorphic character (a character which is shared by two or more taxa illustrating a closer relationship) but is distributed throughout the taxonomic tree and thus should not be used to distinguish between genera *Keratoisis* and *Lepidisis*. The high levels of lability within the Isididae, which are believed to have evolved independently multiple times, as identified though phylogenetic analysis, (Dueñas and Sánchez , 2009), would indicate that the current taxonomic system is inaccurate and requires revision.

5.1.3 Aims of chapter

Recent work along the Mid-Atlantic Ridge at 45°N and within the Whittard Canyon using the ROV *Isis* has allowed the serendipitous collection of coral fragments, some of which were identified to be isidids. Taxonomic work was carried out for the identification of the isidids. This lead to the discovery of four new species. The aim of this chapter is to identify and describe new cold-water coral species found along the AVR at 45°N upon the MAR. This will be achieved by addressing the following objectives:

1- Obtain Octocoral taxonomic samples and identify those which are new to science.
2- Process and describe the new species using a new characteristic system implemented by Les Watling (Hawaii) and Scott France (Louisiana), obtaining SEM pictures to successfully illustrate findings.
3- Compare new species to known species descriptions to identify any similarities between them.
4- Use genetic data, namely the MSH1 gene, to create a phylogenetic tree and assess where the new species are situated in comparison to known Isidids, to support species descriptions.

5.2.Materials and methods

5.2.1 Specimen collection

Samples were obtained from between 2,600 and 3,600 m depth using the ROV (remotely operated vehicle) *Isis* during a RRS *James Cook* cruise in June/July 2008 (JC24) to the AVR of the Mid-Atlantic Ridge at approx 45° 30' N. *Isis* was fitted with 6 cameras, used for both piloting and scientific purposes. *Isis* was also fitted with two Kraft manipulator arms equipped with a claw able to break coral samples from the sample colony identified using the on board cameras. Colonies identified for collection were placed into a single biobox on the starboard side of the ROV. To ensure correct identification of samples at the surface frame grabs were taken of the sample colony before collection and of the sample as it was placed into the biobox, these were printed

off before samples surfaced. Once at the surface samples were identified using the frame grabs, they were directly fixed in ethanol and labelled with a unique sample id as well as depth and location of collection.

5.2.2 Polyp Dissection

Taxonomic samples were placed into a petri dish and covered in 95% ethanol. These were then examined and measured using the Olympus SZX 16 dissecting microscope, and photographs of individual polyps taken using the Olympus u-TVi, X-2 Japan, 3.3 mega pixel camera and the computer software Rincon. Polyps were dissected using forceps, removing the tentacles and pharynx of the individual and placing them into separate microscope dishes, the polyp body and coenenchyme tissue being placed in a further two dishes. 100% Sodium Hypochlorite was added to each dish and left for 5 minutes (or until bubbles stopped being produced) to release the sclerites. Sclerites were rinsed with a pipette a minimum of five times in deionised water until all traces of bleach were removed. Polyp body sclerites were then placed onto a glass slide and examined under the Olympus BX51 compound microscope. Individual sclerites were photographed and measured using the Olympus u-TVi, X-2 Japan, 3.3 mega pixel camera and Rincon software; this was repeated thirty times for each polyp section. Measurement calibrations were carried out using a calibration slide for the 100, 200 and 400 times lenses individually to ensure an accurate measurement could be obtained (Table 5. 1).

Table 5. 1 Calibration levels for Rincon measurements

Lens magnification strength	**No of pixels per µm**	**Calibration name**
100	2.89	Spatial 4
200	5.79	Spatial 3
400	11.6	Spatial 2

5.2.3 SEM

Scanning electron microscope (SEM) stubs were created using Luster A1 pi mount 12.7 mm diametre stubs. The stubs were divided into four sections via the placement of eyelashes (Figure 5. 1). Once sclerites are dissected and fully rinsed in deionised water a small paint brush is used to select individual sclerites which were transferred and mounted onto the stub using carbon-coated double sided tape. Each of the four sections contains sclerites from a separate body location, polyp location on the top, coenenchyme to the left, pharynx in the centre and tentacles to the right (Figure 5. 2). Each stub was labelled on the outside of the SEM stub container.

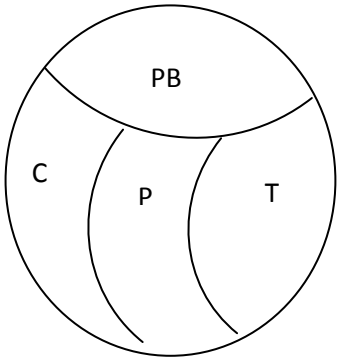

Figure 5. 2. Scanning electric microscope stub layout. PB= polyp body, C= coenenchyme, P= Pharynx, T= Tentacle. Curved lines illustrate the placement of eyelashes.

A single polyp from each sample was removed, and placed into 95 % ethanol overnight. These polyps were then dehydrated by placing them in a sealed bath of 100 % ethanol for ten minutes, this was repeated three times in fresh ethanol, after which the polyps were and dried using the Samdri Critical Point Dryer. Following drying the polyps were also mounted onto SEM stubs using double-sided carbon tape. All stubs were then coated in gold-palladium, using the Hummer 6.2 Sputter Coater for use in the SEM.

Images were obtained of sclerites and polyps using a Hitachi S-800 SEM and its associated digital capture board. At least 6 representatives of every sclerite type were captured ensuring a good representation of all shapes and sizes of sclerite. Files were

labelled with image number, area of sclerite origin, and level of magnification. Following capture sclerite images are saved and isolated from their background using Adobe photoshop. Otherwise the images were unaltered in accordance with current scientific image processing guidelines.

5.2.4 Species descriptions

Species descriptions were based on characters compiled by Les Watling and Scott France (Table 5. 2). For each of the 40 characters the individuals are scored, using SEM pictures and the specimen as reference. From these scores it is possible to generate a comprehensive description of the individual (see appendix 4 table app 4.1 for individual scores).

5.2.5 Genetic analysis

A total of 60 new octocoral *msh1* sequences were obtained using the methods described in Chapter 4, including those of the 4 species described herein. These along with 36 specimens from Isididae, 4 *Acanthogorgia* and 1 *Leptogorgia* (used as an out-group) obtained from NCBI (Table 5. 3) were aligned using Clustal x and adjusted by eye. Following selection of the Akaike Information Criteria (AIC) Model GTR +G analysis using MrModeltest 2.3 (Nylander, 2004) Bayesian phylogenetic analysis was conducted using MrBayes (3.1.2) (Huelsenbeck & Ronquist, 2001). Maximum-likelihood analysis was also performed using PhyML 3.0 (Guindon & Gascuel, 2003) under 500 bootstrap replications, using the TVM+G model of evolution (AIC) as chosen by Modeltest 3.7 (Posada & Crandall, 1998) with a gamma distribution of 0.62. Maximum parsimony under 100 bootstaps was performed using PAUP* 4.0b (Swofford, 2002). PAUP* 4.0b was also used to calculate pairwise genetic distances (uncorrected *p*) to allow the examination of variation between species.

Table 5. 2. Keratoisidinae character list used to generate descriptions.

1)Polyp shape expanded: **0**, tall, height > 2 times width; **1**, short, height < 2 times width

2)Polyp shape contracted: **0**, polyp columnar **1**, polyp "volcano"; **2**, polyp bent midway

3)Inter-tentacular needles when contracted: **0**, needles parallel to polyp axis; **1**, needles tented over mouth ("volcano"); **2**, needles flared outward

4)Polyp width at tentacle origin: **0**, about as wide as at mid-polyp; **1**, much narrower than at mid-polyp; **2**, wider than at mid-polyp

5)Tentacle position when contracted: **0**, folded over toward center of polyp; **1**, pulled down with oral disk; **2**, not curled, tips touching

6)top of polyp needle sclerites: **0**, 8 individual protruding sclerites; **1**, needle sclerites in groups; **2**, no needles

7)arrangement of sclerites on **basal** part of polyp body: **0**, longitudinal; **1**, oblique; **2**, horizontal; **3**, random

8)arrangement of sclerites on **distal** part of polyp body: **0**, longitudinal; **1**, oblique; **2**, horizontal; **3**, random

9)arrangement of sclerites on **adaxial vs abaxial** polyp body: **0**, similar; **1**, different

10)polyp body sclerites, arrangement: **0**, loose in tissue; **1**, imbricated over whole body

11)polyp body sclerites: **0**, sparse; **1**, dense

12)basal polyp body needles **0**, present; **1**, absent

13)basal polyp body rods: **0**, present; **1**, absent

14)basal polyp body flat rods (L:W>4): **0**, present; **1**, absent

15)basal polyp body scales(L:W 3 or less): **0**, present; **1**, absent

16)distal polyp body needles **0**, present; **1**, absent

17)distal polyp body rods: **0**, present: **1**, absent

18)distal polyp body flat rods: **0**, present; **1**, absent

19)distal polyp body scales: **0**, present; **1**, absent

20)polyp body rods, curvature: **0**, straight; **1**, curved at ends

21)polyp body needles ornamentation: **0**, smooth, **1**, fine tubercles; 2, long grooves

22)tentacle rods: **0**, present; **1**, absent

23)tentacle rods or flat rods, arrangement on non-pinnule side: **0**, longitudinal along tentacle; **1**, horizontal

24)tentacle pinnule flat rods: **0**, present; **1**, absent

25)tentacle scales: **0**, present; **1**, absent (but is distinction between flat rod and scale arbitrary/subjective?)

26)polyp or tentacle rods, ornamentation: **0**, smooth: **1**, with fine tubercles; **2**, long grooves

27)polyp or tentacle rods, ends: **0**, smoothly rounded; **1**, with knobs or ridges

28)pharyngeal sclerites, type: **0**, small toothed rods; **1**, flat rods, no teeth; **2**, absent

29)Granular sclerites ("couscous"): **0**, present; **1**, absent

30)axis, hollow core, diametre relative to entire axis diametre: **0**, about 10-35%; **1**, about 50% or more; **2**, not present

31)axis, polyp density: **0**: low, with obvious space between polyps (eg. ≈1 polyp diametre); **1**, high, polyps crowded

32)axis, sclerite arrangement: **0**, along axis; **1**, across axis or random: 2, absent

33)axis sclerites needles **0**, present; **1**, absent

34)axis sclerites flat rods: **0**, present; **1** absent

35)axis sclerites rods: **0**, present; **1**, absent

36)axis sclerites scales: **0**, present; **1**, absent

37)axis ornamentation: **0**, smooth; **1**, with longitudinal grooves

38)axis branching pattern: **0**, not branched; **1**, branched; **2**, distal fork

39)axis branching pattern: **0**, at the node; **1**, basally at the internode; **2**, midway or further along the internode

40)over-all colony form

To allow the identification of a species it is scored on each of the above characteristics which can then allow a comprehensive description to be create.

5.3. Results

Four new species of bamboo corals were collected and are described below:

5.3.1 Sample Ma27

Family: Isididae

Subfamily: Keratoisidinae

Genus: *Jasonisis*

Species: n. Sp. 1Ma27

Material examined: Holotype. North Atlantic, Mid-Atlantic Ridge, 45°28.774 N, 27°53.084 W, depth 2,812 m, ROV *Isis* Dive 93, sample JC24-93-52, June 2008. 4cm long section of 95% ethanol preserved specimen, as well as dried skeletal sections (Figure 5.3).

Diagnosis:

The adult colony is a large branched bush, attached to a rock substraum by a solid white rounded holdfast (Figure 5. 4). The *in-situ* adult colony is branched from the node in a planar fashion with polyps occurring in two alternating rows along the flanks of the branch. When preserved the polyps, are conical or volcano in shape when contracted. Polyps do not appear to retract fully. Polyps are tall, about 4 times as tall as wide. Polyp tissue on the living colony is pink in colour with the branches maintaining a white colouration. Sclerites consist of long rods and short flat rods in the polyp body, small flat rods in the tentacle, bow-tie rods in the coenenchyme and short tooth rods in the pharyngeal regions.

Table 5. 3.Collection data for samples used in this study.

Tentative ID	Sample id	*msh1* Accession number	Collection location	Depth (M)	Reference
Acanella cf. eburnea		**GQ245878**	Corner seamount	855	Thoma *et al.*,2009
Acanella cf. eburnea		**GQ245879**	Corner seamount	1,217	Thoma *et al.*,2009
Acanthogorgia cf. armata		**GU563300**	Rehoboth Seamount	1,827	McFadden *et al*., 2011
Acanthogorgia sp		**GU563306**	Aleutian Ridge	1,692	McFadden *et al*., 2011
Acanthogorgia angustiflora		**DQ297418**	Bear Seamount	unknown	McFadden *et al*., 2006
Acanthogorgia sp.		**AY268461**	Bishop Seamount, Hawaii	unknown	McFadden *et al*., 2006
Isidella sp.		**EF060015**	Manning seamount	1,550	France , 2007
Isidella sp.		**EF060016**	Caloosahatchee seamount	1,642	France , 2007
Isidella sp.		**EF060018**	Kelvin seamount	2.593	France , 2007
Isidella sp.		**EU293798**	unknown	unknown	Brugler and France, 2008
Isidella sp.		**GU933631**	Kelvin seamount	2,593	McFadden *et al*., 2011
Keratoisis sp.		**EF060023**	Manning seamount	1,826	France , 2007
Keratoisis sp.		**EF060025**	Manning seamount	1,469	France , 2007
Keratoisis sp.		**EF060027**	Aleutian Ridge	2,031	France , 2007
Keratoisis sp.		**EF060037**	Manning seamount	1,735	France , 2007

Keratoisis sp.	**EF060044**	Hawaiian Islands	507	France , 2007
Keratoisis sp.	**EF060045**	Retriever seamout	1,982	France , 2007
Keratoisis sp.	**EF060046**	Kelvin seamount	2,130	France , 2007
Keratoisis sp. D	**GU933629**	Bear Seamount	1,478	McFadden *et al*., 2011
Keratoisis sp. D	**GU933630**	Manning seamount	1,496	McFadden *et al*., 2011
Lepidisis caryophyllia	**EF060017**	Gilbert Canyon	2,152	France , 2007
Lepidisis sp.	**EF060019**	Hawaiian Islands	1,067	France , 2007
Lepidisis sp.	**EF060030**	Balanus seamount	1,815	France , 2007
Lepidisis sp.	**EF060041**	Kelvin seamount	2,252	France , 2007
Lepidisis sp.	**EF060042**	Kelvin seamount	1,990	France , 2007
Lepidisis sp.	**EF060043**	Bear seamount	2,000	France , 2007
Lepidisis sp.	**EF060047**	Kelvin seamount	1,857	France , 2007
Lepidisis sp.	**EU100103**	unknown	unknown	France , 2007
Lepidisis sp. B	**GU933632**	Retriever seamout	2,012	McFadden *et al*., 2011
Leptogorgia alba	**AY268452**	unknown	unknown	LePard 2003
Isidella sp.	**EF060021**	Pensacola seamount	1,500	France , 2007
Isidella sp.	**EF060022**	Kelvin seamount	2,554	France , 2007
Keratoisis sp.	**EF060028**	Aleutian Ridge	2,031	France , 2007
Lepidisis olapa	**DQ297426**	Cross Seamount	unknown	McFadden et al., 2006
Lepidisis sp.	**EF060024**	Corner seamount	2,137	France , 2007
Lepidisis sp.	**EF060026**	unknown	unknown	France , 2007
Lepidisis sp.	**EF060038**	Picket Seamount	2,060	France , 2007

Lepidisis sp.		**EF060039**	Picket Seamount	1,946	France , 2007
Lepidisis sp. C		**GU933633**	Nashville seamount	2,103	McFadden et al., 2006
Acanella	Ce32	**to be submitted**	PSB, Rockall or Belgica	unknown	This study
Acanella	Ch168	**to be submitted**	Whittard Canyon	2.864	This study
Acanella	Ce23	**to be submitted**	PSB, Rockall or Belgica	unknown	This study
Acanella	Ch236	**to be submitted**	Whittard Canyon	1,997	This study
Acanthogorgia	Az13	**to be submitted**	Condor de Terra	384	This study
Acanthogorgia	Az17	**to be submitted**	Pico, Ponta da Ilha	347	This study
Acanthogorgia	Az6	**to be submitted**	Voador, Açores	318	This study
Acanthogorgia	Cl20	**to be submitted**	Mid-Atlantic Ridge	850	This study
Acanthogorgia	Cl18	**to be submitted**	Mid-Atlantic Ridge	850	This study
Acanthogorgia	Az14	**to be submitted**	Princesa Alice	566	This study
Acanthogorgia	Az15	**to be submitted**	Faial, NW Ponta dos Cedros	365	This study
Acanthogorgia	Az4	**to be submitted**	Corvo, Fora do Aeroporto	629	This study
Acanthogorgia	Az5	**to be submitted**	Voador, Açores	318	This study
Acanthogorgia	Az7	**to be submitted**	4,5 milhas da costa; NW de São Jorge, Açorzes	265	This study
Chrysogorgia	Ch143	**to be submitted**	Whittard Canyon	3,060	This study
Chrysogorgia	Ch17	**to be submitted**	Whittard Canyon	2,489	This study
Chrysogorgia	Ch158	**to be submitted**	Whittard Canyon	2.963	This study
Gersemia	d2	**to be submitted**	South Uist	1,157	This study
Isidella	Ma 28	**to be submitted**	Mid-Atlantic Ridge	2,749	This study
Isidella	Ma 29	**to be submitted**	Mid-Atlantic Ridge	2,655	This study
Isidella	Ce41	**to be submitted**	PSB, Rockall or Belgica	unknown	This study

Isidella	jc4	**to be submitted**	unknown	unknown	This study
Isidella	Ma 3	**to be submitted**	Mid-Atlantic Ridge	2,697	This study
Keratoisidinae	Cl40	**to be submitted**	Mid-Atlantic Ridge	unknown	This study
Keratoisidinae	Ma 26	**to be submitted**	Mid-Atlantic Ridge	2,783	This study
Keratoisidinae	Ma 30	**to be submitted**	Mid-Atlantic Ridge	2,805	This study
Keratoisidinae	Ch140	**to be submitted**	Whittard Canyon	3.078	This study
Keratoisidinae	Ch42	**to be submitted**	Whittard Canyon	2,191	This study
Keratoisidinae	Ma5	**to be submitted**	Mid-Atlantic Ridge	3598	This study
Keratoisidinae	Ch144	**to be submitted**	Whittard Canyon	3,060	This study
Keratoisidinae	Ch159	**to be submitted**	Whittard Canyon	2,864	This study
Keratoisidinae	Ma10	**to be submitted**	Mid-Atlantic Ridge	3,398	This study
Lepidisis	An1	**to be submitted**	Antarctica	unknown	This study
Lepidisis	Ma 13	**to be submitted**	Mid-Atlantic Ridge	3,013	This study
Lepidisis	Ma9	**to be submitted**	Mid-Atlantic Ridge	2,030	This study
Lepidisis	Ma 14	**to be submitted**	Mid-Atlantic Ridge	2,998	This study
Narella	Ma 11	**to be submitted**	Mid-Atlantic Ridge	3,151	This study
Narella	5	**to be submitted**	pico-faial channel	unknown	This study
Narella	6	**to be submitted**	pico-faial channel	unknown	This study
Narella	7	**to be submitted**	pico-faial channel	unknown	This study
Narella	8	**to be submitted**	pico-faial channel	unknown	This study
Narella	An6	**to be submitted**	Antarctica	unknown	This study
New	Ma 18	**to be submitted**	Mid-Atlantic Ridge	2,878	This study
New	Ma 20	**to be submitted**	Mid-Atlantic Ridge	3,378	This study
New	Ma 33	**to be submitted**	Mid-Atlantic Ridge	2,890	This study
New	Ma 27	**to be submitted**	Mid-Atlantic Ridge	2,812	This study

Paramuricea	Ch182	**to be submitted**	Whittard Canyon	1,676	This study
Paramuricea	Ch199	**to be submitted**	Whittard Canyon	1,339	This study
Primnoa	Ch64	**to be submitted**	Whittard Canyon	1,695	This study
Radicipes	Ch29	**to be submitted**	Whittard Canyon	2,477	This study
Radicipes	Ma 12	**to be submitted**	Mid-Atlantic Ridge	3,063	This study
Radicipes	Ma 16	**to be submitted**	Mid-Atlantic Ridge	2,881	This study
Radicipes	Ma 17	**to be submitted**	Mid-Atlantic Ridge	2,878	This study
Radicipes	Ma 25	**to be submitted**	Mid-Atlantic Ridge	3,083	This study
Radicipes	Ch188	**to be submitted**	Whittard Canyon	1,887	This study
Radicipes	Ma 24	**to be submitted**	Mid-Atlantic Ridge	2,863	This study
Distichoptilium gracile	d8	**to be submitted**	Nigeria	1,366	This study
Seapen	d7	**to be submitted**	Nigeria	1,366	This study
Seapen	b2	**to be submitted**	Bahamas	unknown	This study
Unknown	An2	**to be submitted**	Antarctica	unknown	This study
Unknown	Ch69	**to be submitted**	Whittard Canyon	1,629	This study
Unknown	Cl45	**to be submitted**	Mid-Atlantic Ridge	2,700	This study
Unknown	d4	**to be submitted**	Tornado	1,050	This study

Description: (from video frame grab, one small section of holotype and skeletal matter).

Colony form in the adult is a large planar fan arising from a short single stem attached to a large rounded holdfast (Figure 5. 4). Coenenchyme tissue is white, with the larger branches looking almost bone-like. The coenenchyme produces a thick layer over the axial skeleton. Polyps are absent on the lower stem of the specimen, but are present over the rest of the colony, arrayed in two alternating rows along the branches. Branching occurs at the node with one or two branches originating at each branch point. Branches mostly point upwards at acute angles from the origin. The nodes are very short, often only 1-2 mm in length. Internodes at the base of the colony and on main stems are also moderately short, about 1-2cm in length. On the sampled branch, internodes were 8 mm in length.

Polyps are pink when alive, turning a mottled brown in alcohol. The polyps are tall, approximately 8 mm high and 3 mm wide, have a circular base and occur with more than one polyp width between them. When contracted the tentacles fold towards the centre of the polyp but do not become fully retracted to the oral disk, rather the tentacles fold in the manner of curled fingers (Figure 5. 5c and d). When the tentacles are fully extended they appear fleshy and extend away from the mouth.

The polyp body contains a dense population of sclerites. These sclerites occur in two forms; long flat rods and short flat rods, some of which are constricted midway along the long side to create an almost bow tie appearance (Figure 5. 6). Large flat rods are in the range of 225-430 µm in length with the shorter flat rods being 120-170 µm. Striations occur longitudinally along some of the rods, with the edges often being fluted. There are also some small tubercles present on the longer flat rods. Crossed flat rods occur occasionally (Figure 5. 6). The sclerites are arranged horizontally in the basal polyp section and longitudinally in the distal section, all tightly packed together. The arrangement of sclerites on the adaxial and abaxial surfaces is similar. No intertentacular needles are present.

Tentacle sclerites are more or less longitudinally arranged and densely packed. They consist only of small flat rods (60-200 µm) (Figure 5. 7). These are ornamented with longitudinal striations and some show fluted edges.

Pharyngeal sclerites were sparse and consisted of small toothed rods which have longitudinal striations (Figure 5. 8). These sclerites are generally longer than wide, with a length of 50-102 µm. The teeth are bluntly rounded.

The coenenchyme has a good supply of small "bow-tie" flat rods (Figure 5. 9) with longitudinal striations. There are some misshapen sclerites which resemble those in the pharyngeal region. These sclerites run along the axis, ranging in length from 90-233 µm.

The central axis of the sampled branch contains a hollow core which is less than 50% of the axis diametre. From the skeletal matter that originates from the base of the colony the large thick stems contain a hollow core of less than 10 % of the diametre of the sample (Figure 5. 3). The outer surface of the skeleton has longitudinal striations. The nodes are dark in colour and slightly knicked into the skeleton.

Remarks: This specimen has been placed into the genus *Jasonisis* recently described by Alderslade based on a specimen collected from the Tasman Sea (Alderslade and McFadden, 2011). This placement is based both on genetic data (see below) and morphological features. Sclerite structure shown is consistent with the genus holotype with the presence of rods which have ornamentation in the form of striations which Alderslade and McFadden (2011) referred to as "mound-like protuberances that are elongate" and the

rounded edge. They share this unique sclerite form as well as the thick coenenchyme. Meaning this specimen can be confidently placed within the new Genus *Jasonisis*.

Figure 5.3. Sample Ma27 used for description collected from 45°N on the Mid-Atlantic Ridge. A)Sample specimen preserved in ethanol illustrating polyp placement and shape B) Sample core, with hollow centre illustrated by the arrow taking up less than 10 % of the diametre.

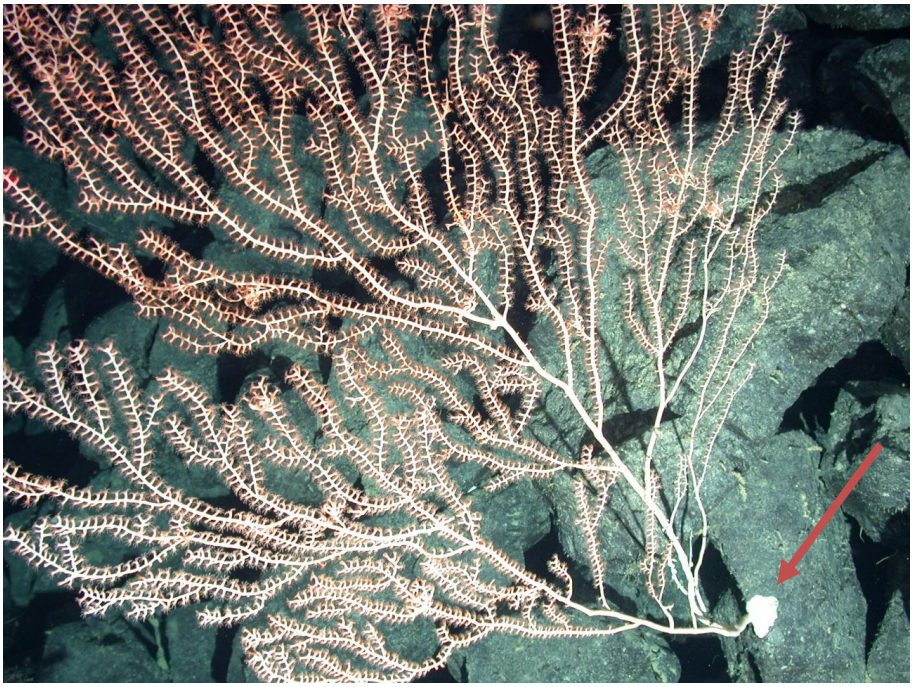

Figure 5.4. Living Ma27 colony photographed at 2,812m depth from 45°N on the Mid-Atlantic Ridge. Image clearly shows the presence of a large white solid holdfast, illustrated by the arrow attaching the colony to the rock scarp, the planar shape of the specimen and the abundance and size of polyps.

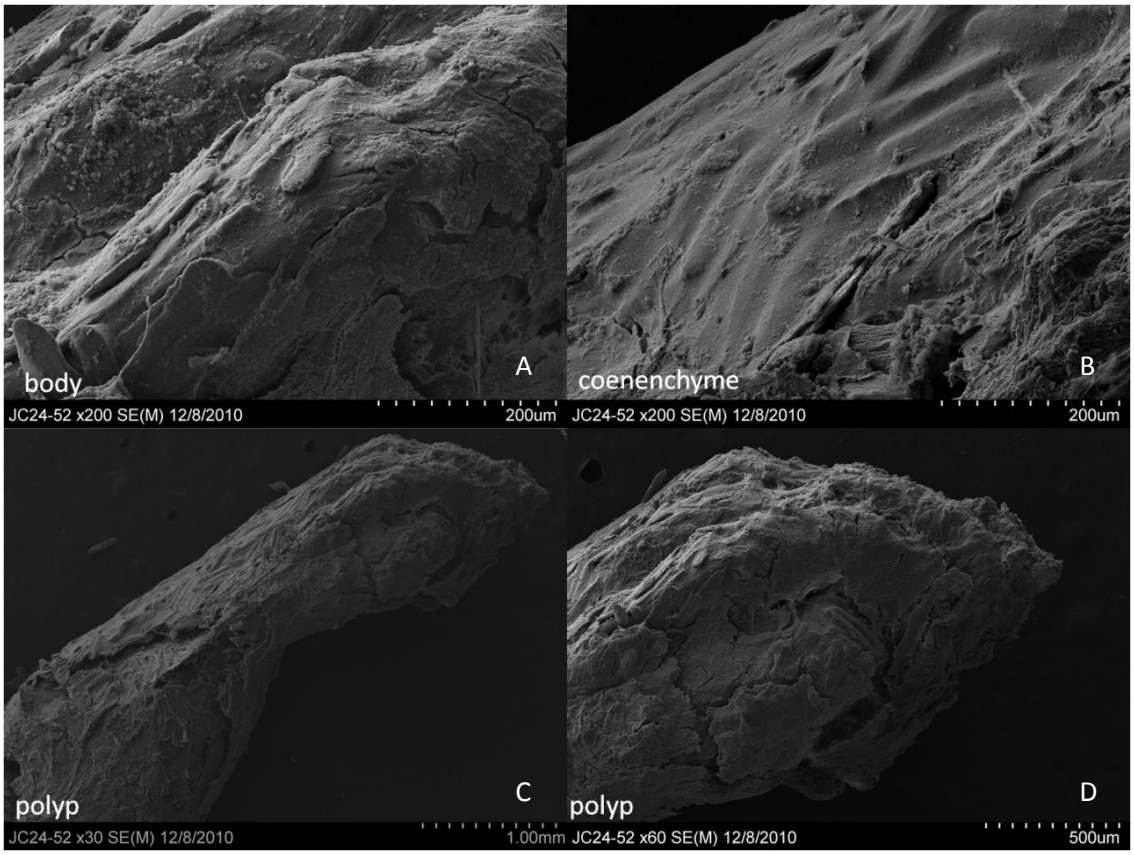

Figure 5. 5. SEM images of sample Ma27 from 45°N on the Mid-Atlantic Ridge. SEM pictures show A) the close up of polyp body, B) close up of the sclerite arrangement in the coenenchyme C) Full polyp D) close up of the fist like shape of tentacle as they contract. Numbers associated with bar scales represent the entire length of the scale bar, with numbers below each image representing magnification values.

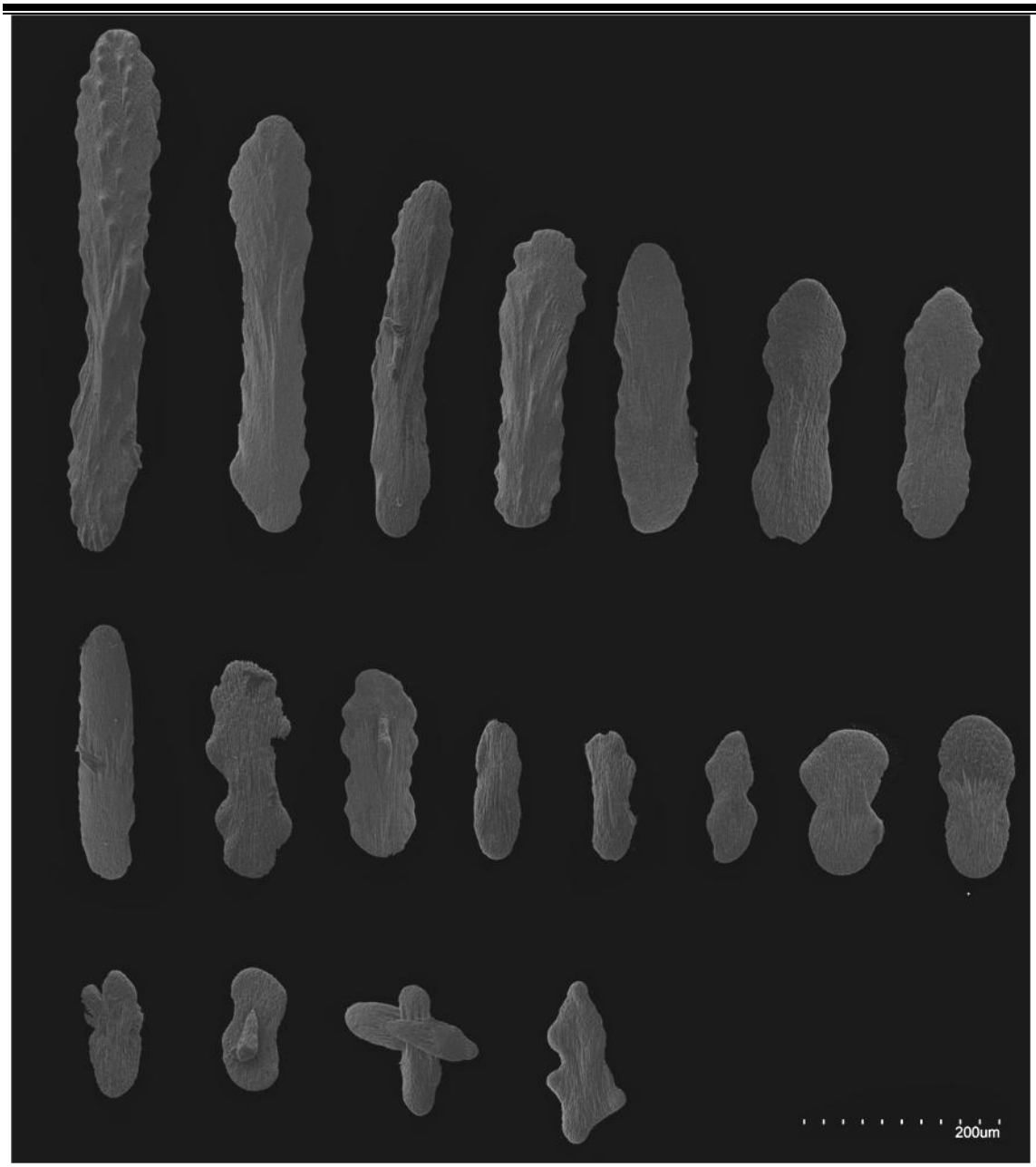

Figure 5. 6. SEM pictures of sclerites found in the polyp body of Ma27 collected from 45^{o}N on the Mid-Atlantic Ridge. Illustrates the presence of ornamented rods (top) and bow tie sclerites (middle) as well as some deformed sclerites (bottom) within the specimen. Scale bar = 200 µm

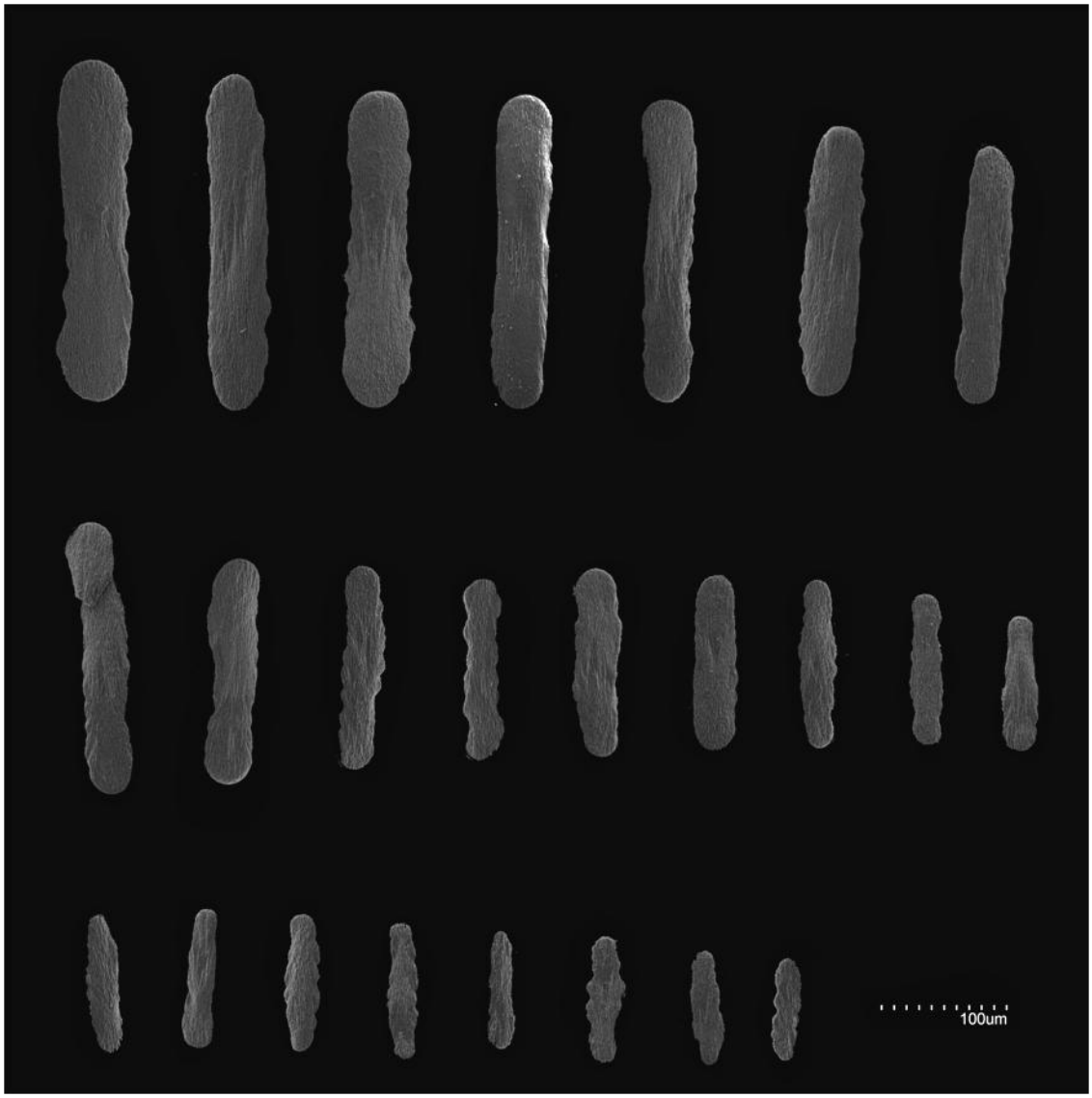

Figure 5. 7. SEM pictures of sclerites found in the polyp tentacles of Ma27 collected from 45°N on the Mid-Atlantic Ridge. Illustrates the presence of ornamented rods within the specimen. Scale bar = 100 µm

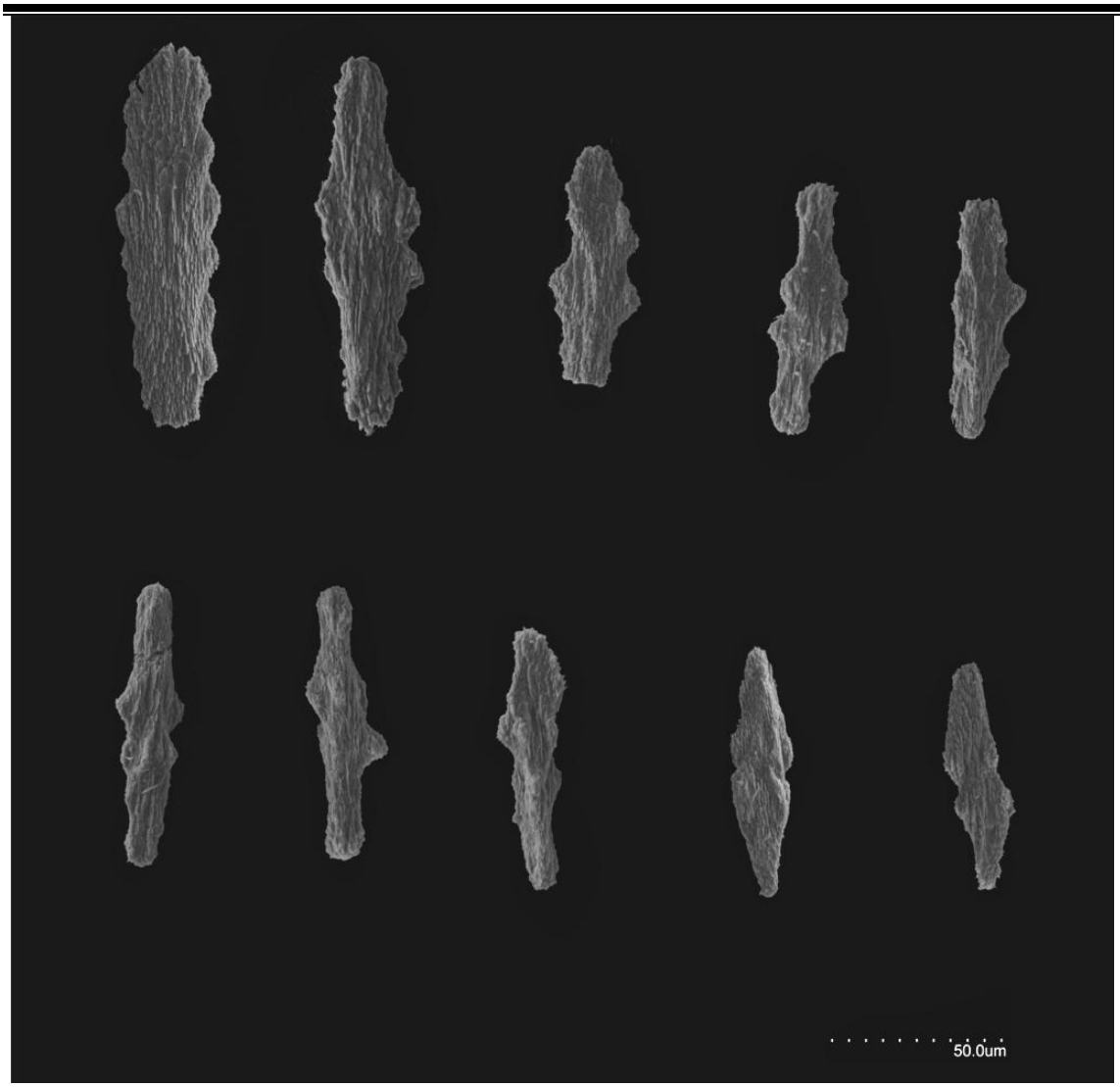

Figure 5. 8. SEM pictures of sclerites found in the polyp pharynx of Ma27 collected from 45°N on the Mid-Atlantic Ridge.SEM photograph iIllustrates the presence of small toothed rods within the pharynx of the individual.

Scale bar = 50 µm

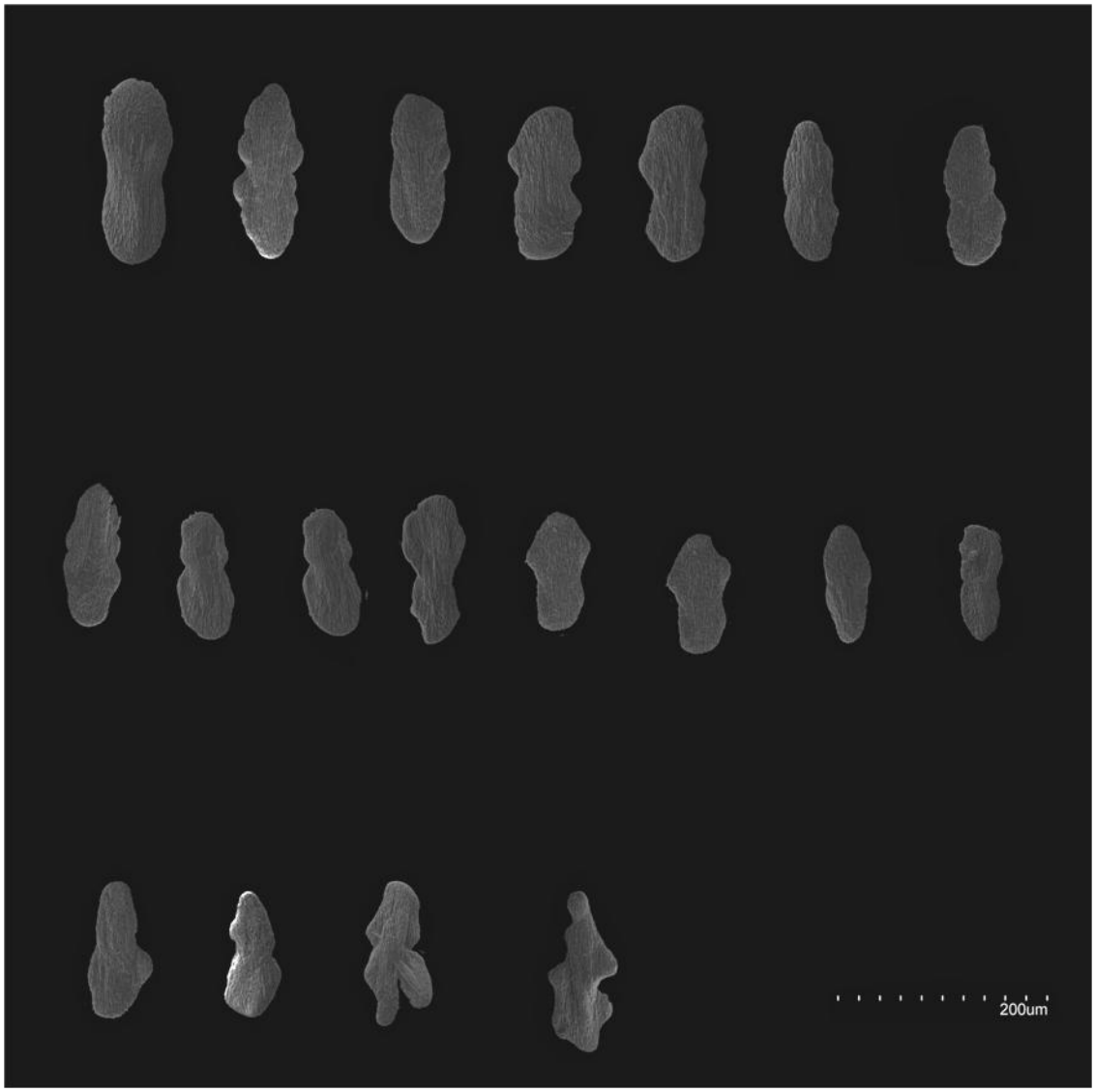

Figure 5.9. SEM pictures of sclerites found in the coenenchyme of Ma27 collected from 45°N on the Mid-Atlantic Ridge. SEM photograph illustrates presence of small bow-toe flat rods within the coenenchyme- characteristic of the new genus Jasonisis. *Scale bar = 200 µm*

5.3.2 Sample Ma18

Family: Isididae

Subfamily: Keratoisidinae

Genus: A /*Jasonisis*

Species: n. Sp. 2. Ma18

Material examined: Holotype. North Atlantic Mid-Atlantic Ridge, 45°35.697 N 27°48.229 W, depth 3,378 m sampled during ROV *Isis* Dive 89, sample Jc24-89-44 June 2008. 8 cm long section of 95% ethanol preserved specimen (Figure 5. 10 A).

Diagnosis:

The adult colony consists of a central stem with two branches (the origin of which are unclear from the photographs), attached to a rock by a circular holdfast (Figure 5. 11). Polyps cover the entire length of the stem, with the exception of a few centimetres at the base, and are found encompassing the entire stem. Tentacles do not enter the oral disk during contraction but simply touch tips above it (Figure 5. 12 C, D). The living colony shows pink polyps with fleshy tentacles when fully extended. The individual also produced a thick mucosal discharge and was seen to produce a blue bioluminescent hue when brought to the surface. Sclerites found within the specimen were rod shaped with a variety of sizes observed throughout the different regions.

Description: (from video frame grab and one small section from the holotype).

The colony, as seen *in-situ*, consists of a central stem with two branches (the origin of which cannot be determined so it is not known whether this species branches at the nodes or internodes), attached to a rock by a solid holdfast (Figure 5. 11). The coenenchyme is pink, thick and fleshy in life, but leaches all colour when preserved. Polyps are not present at the base of the colony and it is suspected they do not occur until after the first node (this

cannot be confirmed as the base of the colony was not collected). Nodes are dark and easily visible though the coenenchyme from the collected specimen. The two branches present on the *in-situ* specimen these are seen oriented upwards with acute angle to the point of origin (Figure 5. 11).

When alive the pink polyps occur all around the branches with no obvious distribution pattern. Polyps are mainly volcano shaped with a few buds and occur at a low density with more than one polyp width between them. Polyps are short with a mean length of 7.2 mm and mean width of 4.5 mm. Tentacles do not curl into the oral disk during contraction but simply touch tips above it (Figure 5. 12). The in situ image (Figure 5. 11) shows that the tentacles are long and fan out when extended.

The polyp body contains a dense population of sclerites. Sclerites occur in two main forms: long rods and short rods with the occassional deformed sclerite (Figure 5. 13). The long rods range from 300-550 µm in length with the shorter rods measuring 95-200 µm. The polyp body sclerite arrangement changes from horizontal to random moving from the basal to the distal region. Sclerite arrangement is consistent on both the adaxial and abaxial polyp regions. The long rods have an extremely smooth appearance with only occasional tubercles near the tapered edge. The short rods contain longitudinal grooves, with some tapering more at one end than the other (Figure 5. 13). No obvious curvature is seen along these rods.

Tentacle sclerites also consist of long and short rods, with the larger rods occurring along the outer edge of the tentacle and the short rods populating the centre. The long rods, measuring 120-335 µm in length, are smooth with very few longitudinal grooves, with some containing tubercles near the tapered end. The short rods (75-100 µm in length) have a more rugged appearance with more prominent longitudinal grooves, often having fluted

edges and again some tapering at one end more than the other (Figure 5. 14). Intertentacular needle sclerites were absent.

The coenenchyme contains a high density of sclerites, that are also rod shaped, ranging from 90-140 µm in length (Figure 5. 15). Sclerites lie longitudinally along the colony branch.

The pharynx contains sparsely-spaced, small, slightly toothed to scalloped or fluted flat rods (approx 65-114 µm in length) which are always longer than they are wide (Figure 5. 16).

The central axis of the branch sampled appears thick but contains a central hollow core comprising more than 50% of the axis diametre. The outer surface of the axis has longitudinal striations running along its length, with very dark nodes measuring 2 mm occurring. The length of internodes cannot be determined form the samples but appears to be at least 5 cm.

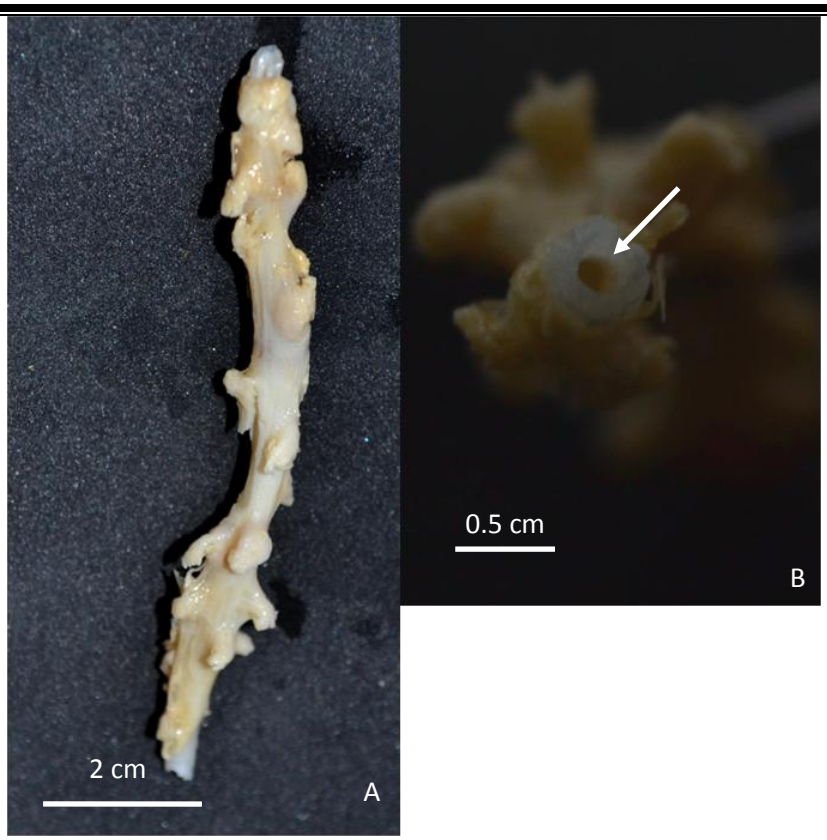

Figure 5. 10. Sample Ma18 used for description collected from 45°N on the Mid-Atlantic Ridge. A) Sample specimen preserved in ethanol illustrating polyp placement and shape B) Sample core, with hollow centre, indicated by the arrow, taking up more than 50 % of the diametre.

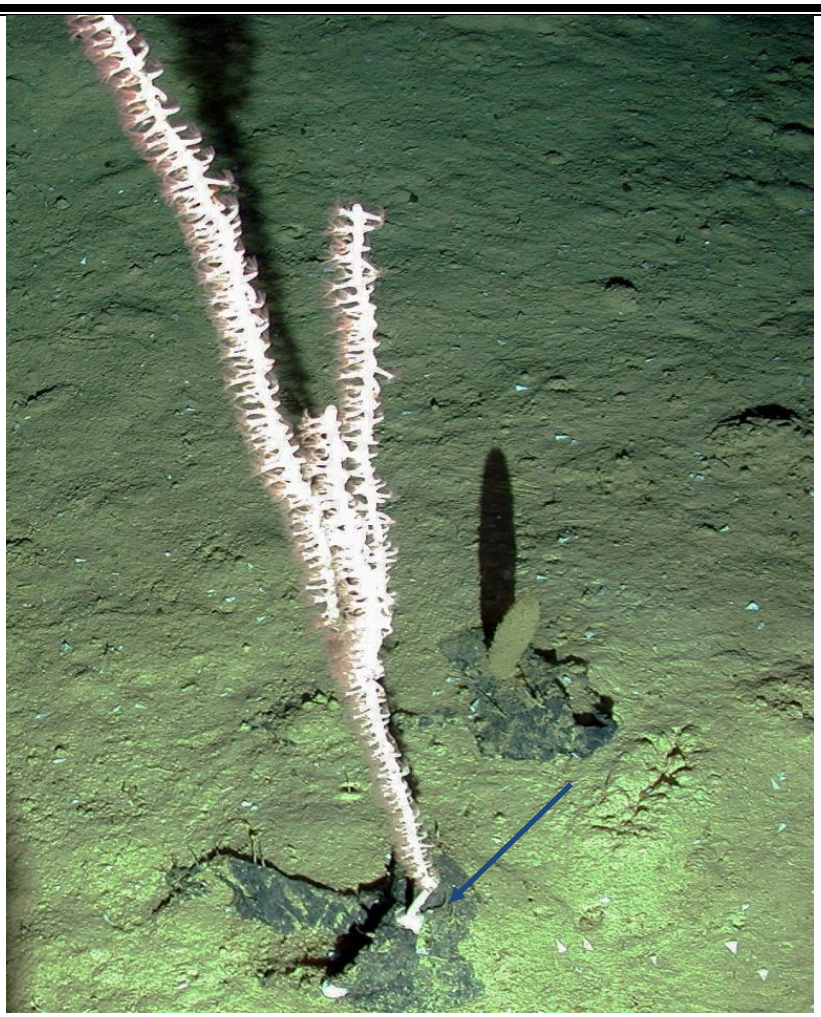

Figure 5. 11. In situ picture of Ma18 taken at 3,378 m at 45°N on the Mid-Atlantic Ridge. Image clearly illustrates the present of a white solid holdfast, illustrated by the arrow, attaching the specimen to a small rock in the sediment. One central stem and 2 branches whose origin cannot be determined are seen, with polyps appearing large and fully extended.

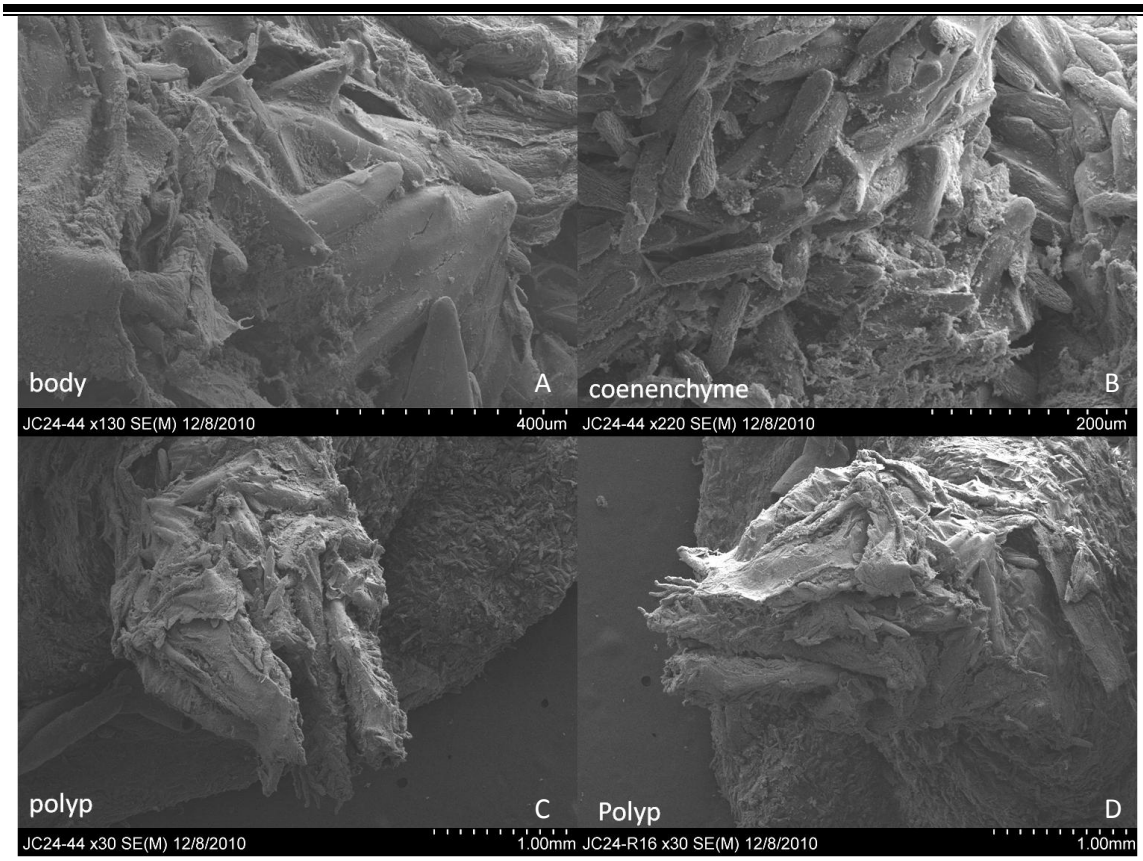

Figure 5. 12. SEM images of sample Ma18 from 45°N on the Mid-Atlantic Ridge. Sem pictures show A) close up of polyp body B) close up of the sclerite arrangement in the coenenchyme along the axis, without flesh removal C) Full polyp D) Close-up of tentacle touching above the mouth to create an almost volcanic appearance when contracted. Numbers associated with bar scales represent the entire length of the scale bar, with numbers below each image representing magnification values.

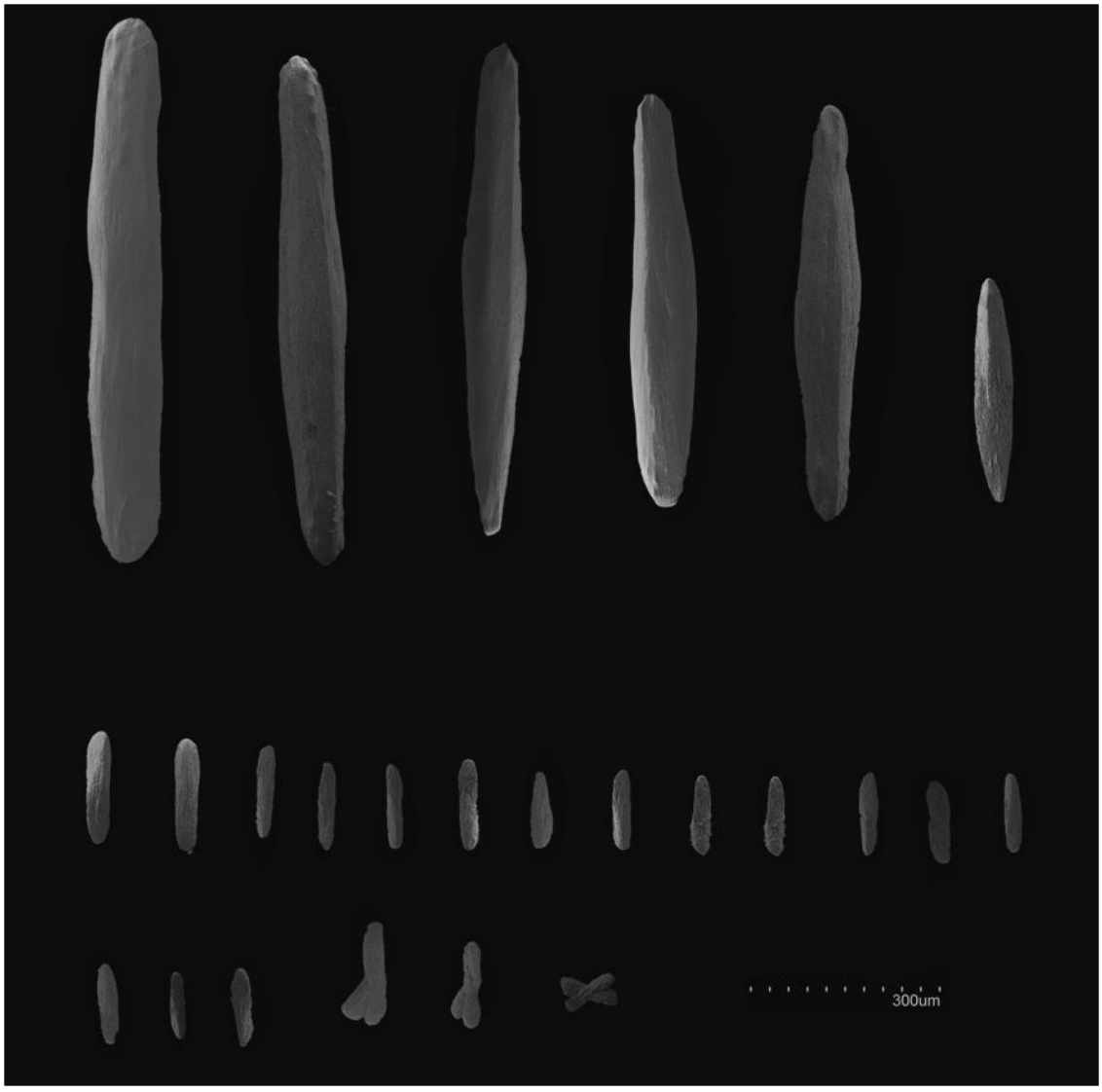

Figure 5. 13 SEM pictures of sclerites found in the polyp body of Ma18 from 45°N on the Mid-Atlantic Ridge. Illustrates presence of long smooth rods with occasional ornamentation (top) short rods (middle and bottom) and deformed sclerites (Bottom). Scale bar = 300 µm

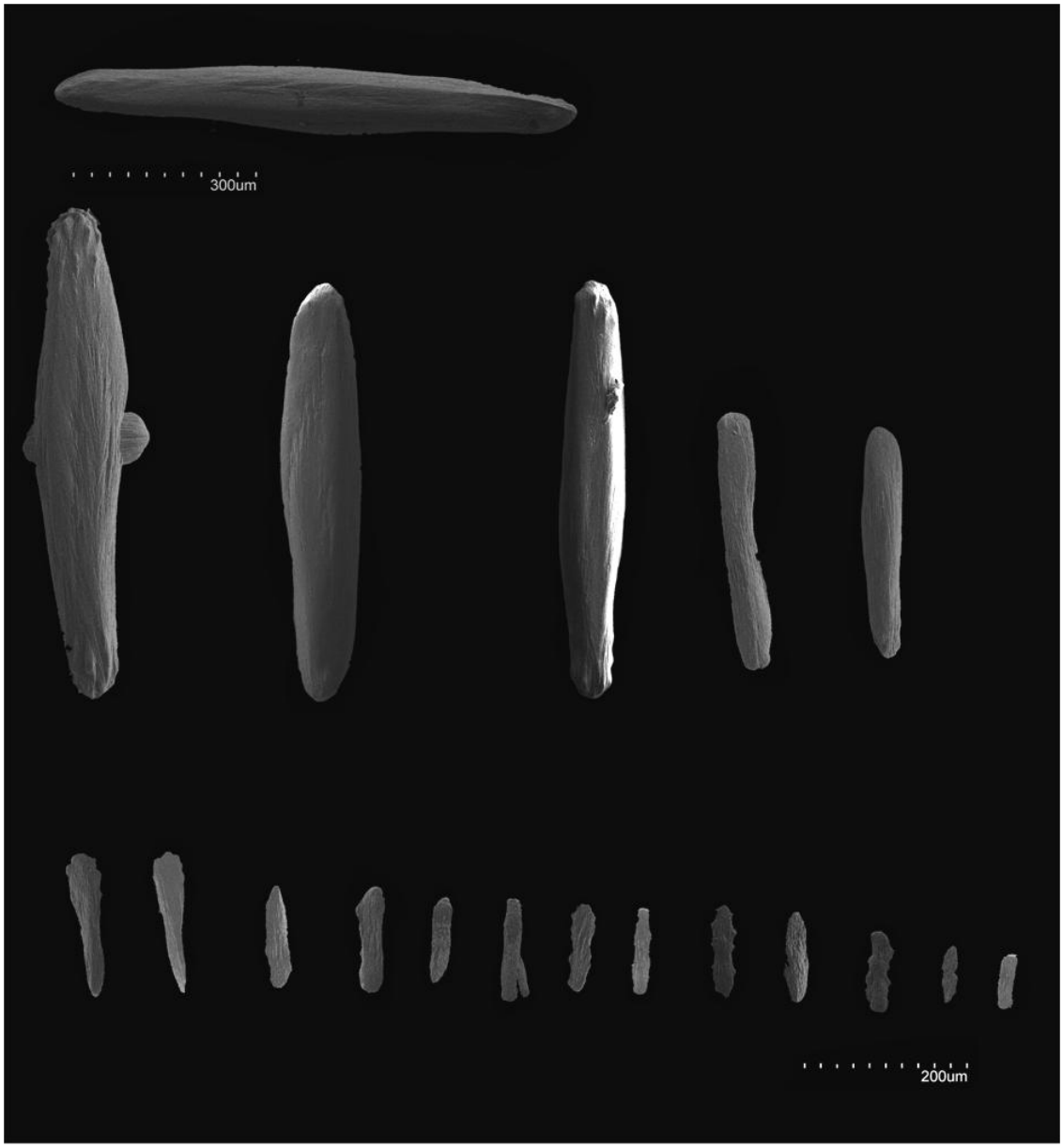

Figure 5. 14 SEM pictures of sclerites found in the polyp tentacles of Ma18 from 45^{o}N on the Mid-Atlantic Ridge. Illustrates presence of long smooth rods with occasional ornamentation (top) short rods (middle) Scale bar = 300 µm and 200 µm respectivly.

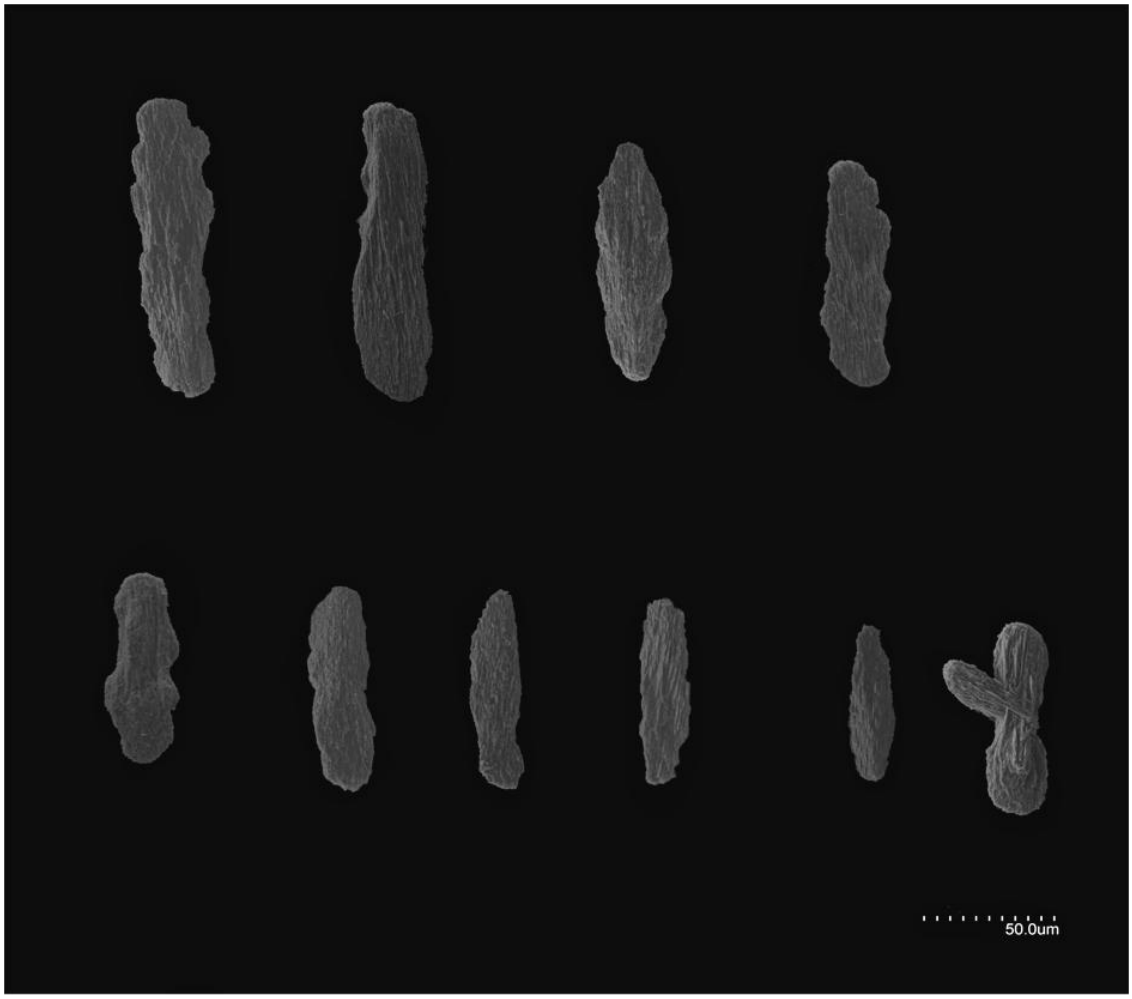

Figure 5. 15 SEM pictures of sclerites found in the pharynx of Ma18 from 45°N on the Mid-Atlantic Ridge. Illustrates presence of toothed rods within the pharynx. Scale = 50 µm.

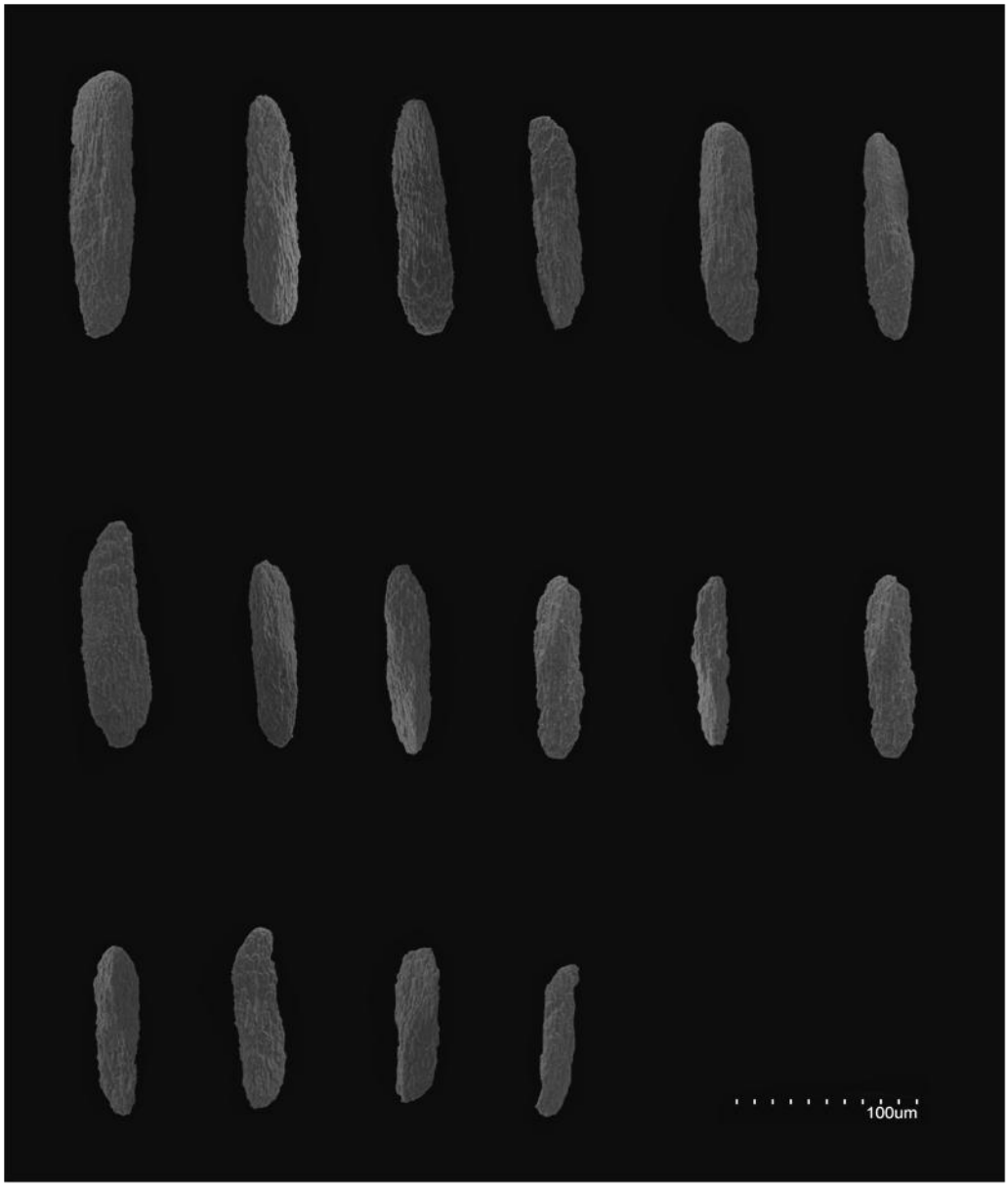

Figure 5. 16. SEM pictures of sclerites found in the coenenchyme of Ma18 from 45°N on the Mid-Atlantic Ridge.This SEM photograph illustrates the presence of small rod shaped sclerites present with the coenenchyme of the individual. Scale bar = 100 µm

5.3.3 Sample Ma20

Family Isididae

Subfamily Keratoisidinae

Genus- expected new genus A

Species- n. Sp. 3 Ma20

Material examined: Holotype. North Atlantic Mid-Atlantic Ridge, 45°24.916 N 27°54.103 W, depth 2,878 m during an *ROV Isis* dive 88, sample JC24-88-38 June 2008. 4 cm long section of 95% ethanol preserved specimen (Figure 5. 17).

Diagnosis:

The adult colony is an unbranched whip attached to a rocky substratum by a solid circular holdfast (Figure 5. 18). The coenenchyme is thick and white whilst the polyp tentacles and oral disk are pink. Polyps occur around the entire stem and along the length of the individual except for approximately the first ten centimetres from the holdfast (determined from the in situ picture) Polyps are wider than they are tall, giving a bud-like appearance. During contraction the tentacles fully fold into the oral disk. The *in-situ* colony picture shows the polyps extended and the pink tentacles outstretched. Sclerites are rod-like in shape with a variety of long and short rods occurring throughout the specimen.

Description :(video frame grab and small section of holotype)

The *in-situ* colony is an unbranched whip, attached to a rock scarp face by a sturdy circular holdfast (Figure 5. 18). The coenenchyme is thick and white in colour and the tentacles and oral cavity are pink. During contraction tentacles fully retract and pack tightly into the oral cavity (Figure 5. 19). When preserved the polyp and coenenchyme tissue becomes

very tough due to the high density of imbricated sclerites covering the individual. No branches were observed.

Individual polyps are short, with an average height of 4 mm and an average width of 7.5 mm creating a bud-like shape. Polyps are densely packed all around the branch with less than a polyp's width between them. Polyp body sclerites consist of long rods (200-990 µm) with the occasional split rod creating a crossed appearance (Figure 5. 20). The rods often have a slight reduction in width half way along the length. Longitudinal grooves and tip tubercles are often present. Fluting also occurs at the tapered end of some sclerites. Sclerites are arranged horizontally on both the basal and distal regions of the polyps, with adaxial and abaxial arrangement remaining consistent.

Tentacle sclerites consist of both large and small flat rods, ranging in size from 80 µm to 570 µm (Figure 5. 21). Sclerite striations are present with some sclerites showing fluting along the distal edges. Some sclerites also have tubercles present at the distal edges, with others being more tapered at one end than the other. Large rods are distributed around the edge of the tentacles whilst the smaller ones populate the centre. There were no intertentacular needle sclerites observed.

The coenenchyme is densely packed with rod-shaped sclerites running parallel to the branch. The sclerites vary in length from 105-405 µm. These rods have an obvious three dimensional structure with some possessing ridges, longitudinal striations, and often fluted ends (Figure 5. 22), with a slight bend in the body. The coenenchyme also contains "split" sclerites which range in shape including a "dragon-fly" shape (Figure 5. 22).

Pharyngeal sclerites are flat rods with fluted rather than toothed margins (Figure 5. 23). These are always longer than they are wide with a length ranging from 60 – 150 µm. Lateral teeth are bluntly rounded and vary in occurrence from dense to rare. "Split" sclerites occur.

The central axis is straw-like, with very thin outer wall and a hollow core occupying more than 50 % of the relative diametre. The outer surface of the axis appears smooth, with a dark nodes present measuring 0.5 mm in length. It is not possible to measure internodes from this small sample.

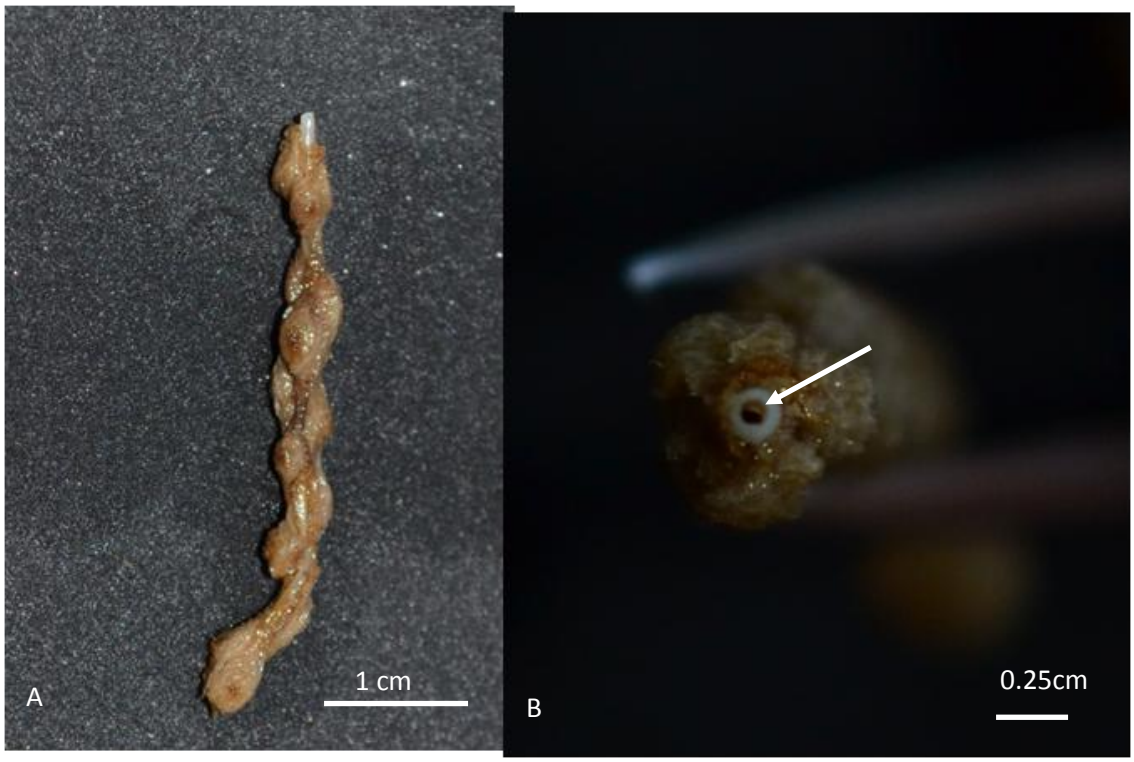

Figure 5. 17. Sample Ma20 used for description collected from 45°N on the Mid-Atlantic Ridge. A) Sample specimen preserved in ethanol illustrating polyp placement and shape B) Sample core, with hollow, highlighted by the arrow centre taking up more than 50 % of the diametre creating a straw like appearance.

Figure 5. 18. In situ image of Ma20 taken at 2,878 m at 45°N on the Mid-Atlantic Ridge. The picture illustrates the sample was a whip-like individual attached to a rock by an unknown holdfast. Polyps can be seen to be abundant and tightly packed over surface the specimen as highlighted by the arrow.

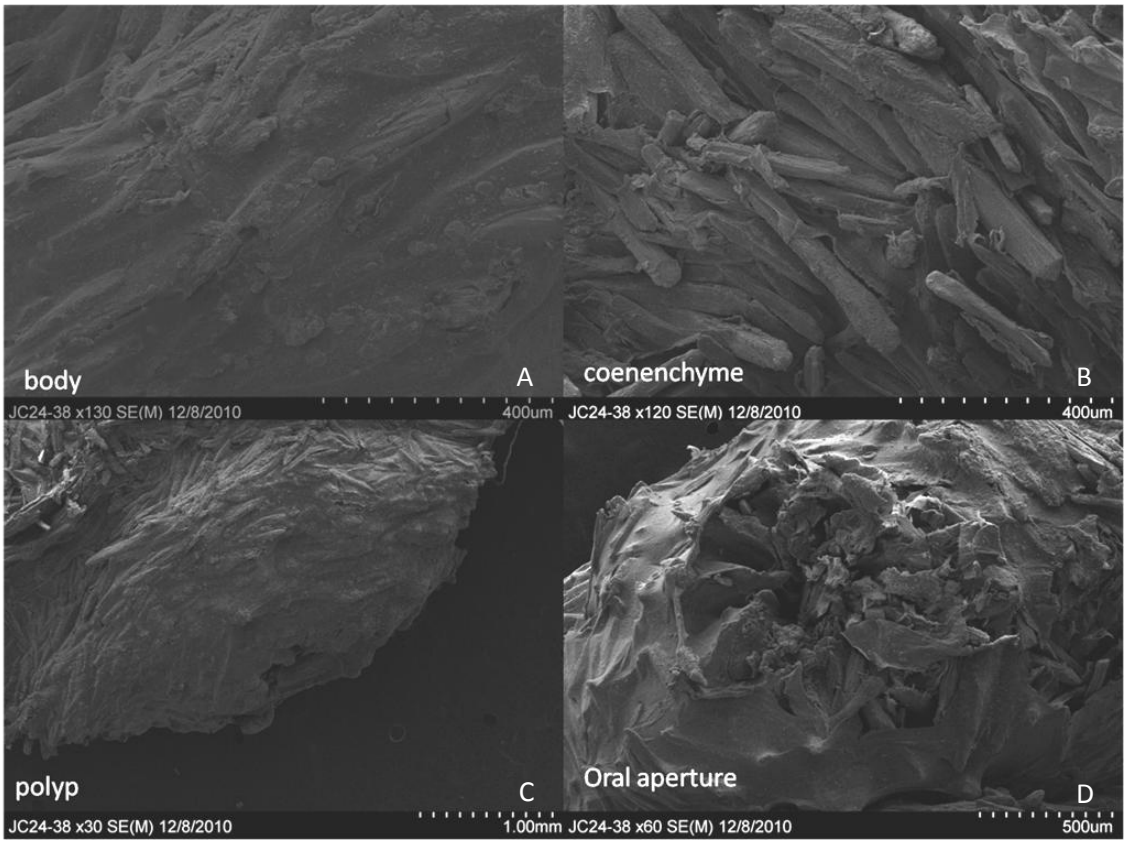

Figure 5. 19. SEM images of sample Ma20 from 45°N on the Mid-Atlantic Ridge. SEM pictures show A) close up of polyp body, B) close up of the sclerite arrangement in the coenenchyme along the axis, without flesh removal C) Full polyp D) Close of tentacle becoming fully retracted into the oral aperture. Numbers associated with bar scales represent the entire length of the scale bar, with numbers below each image representing magnification values.

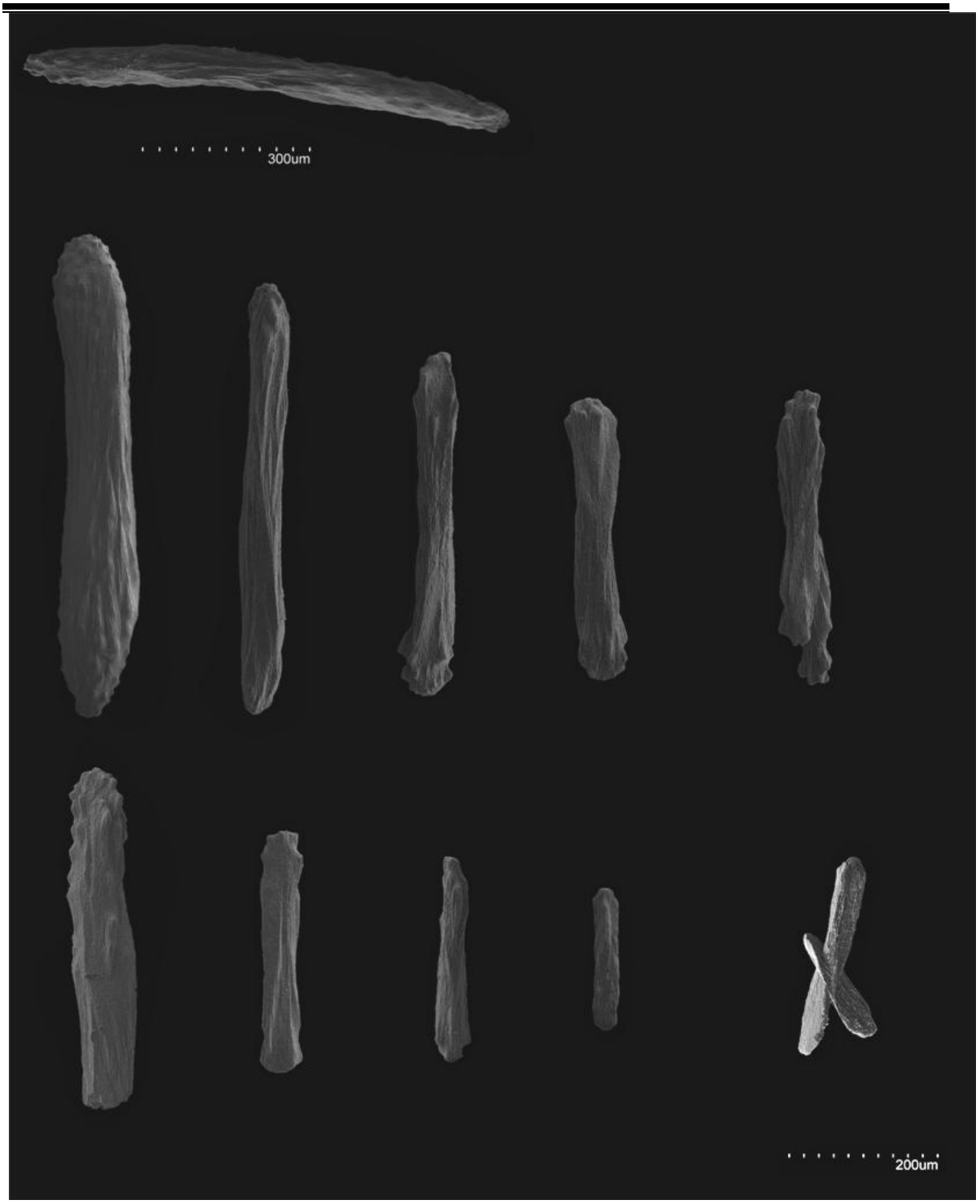

Figure 5. 20. SEM images of sclerites from polyp body from sample Ma20 from 45°N on the Mid-Atlantic Ridge. Illustrates the presence of large (top) and small (bottom) rods with the presence of tubercles and fluting. Scale bar = 300 µm and 200 µm respectively.

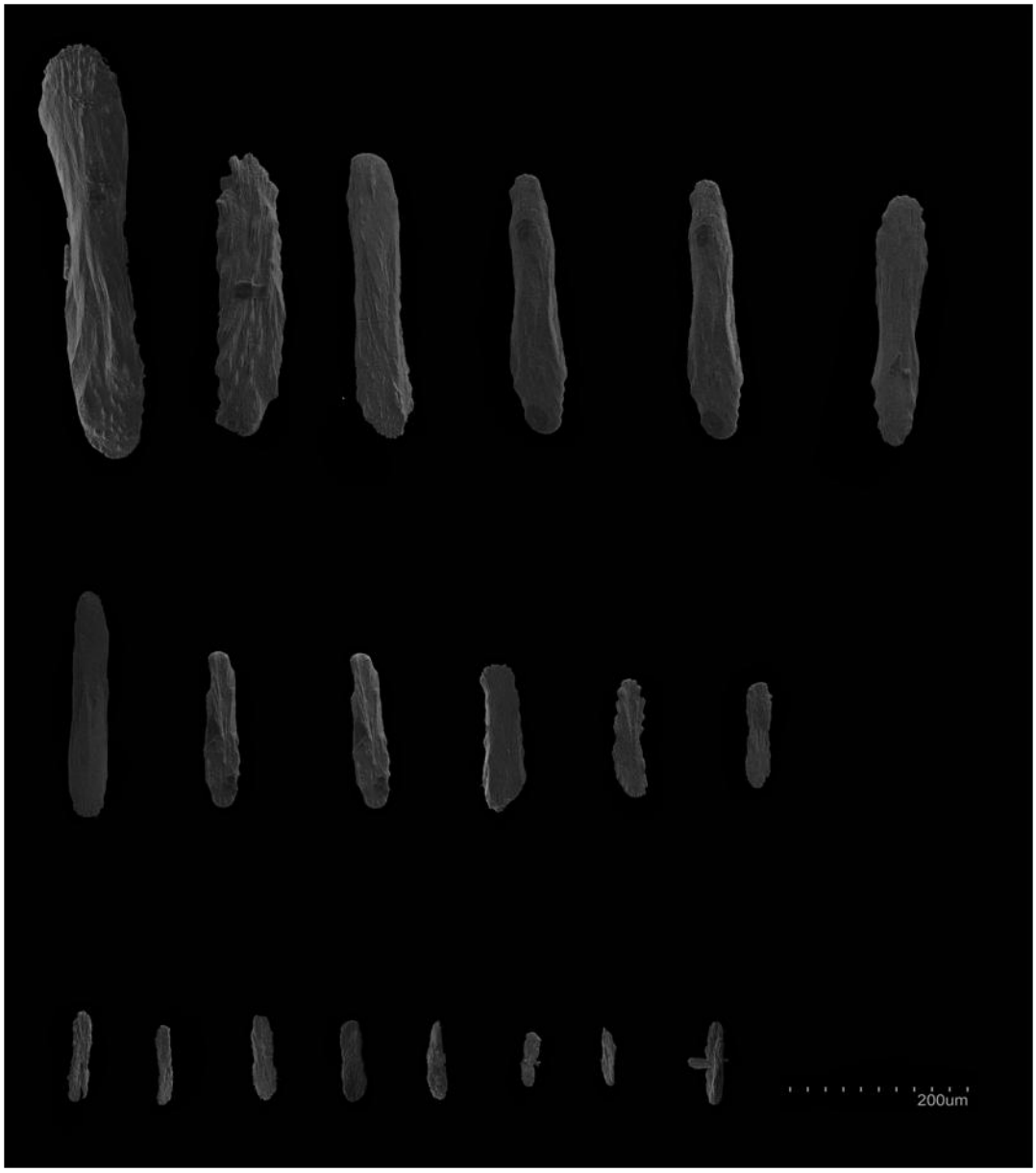

Figure 5. 21. SEM images Sclerites from of polyp tentacles from sample Ma20 from 45°N on the Mid-Atlantic Ridge. Illustrates the presence of large (top) and small (bottom) rods with the presence of tubercles and fluting. Scale bar = 200 µm

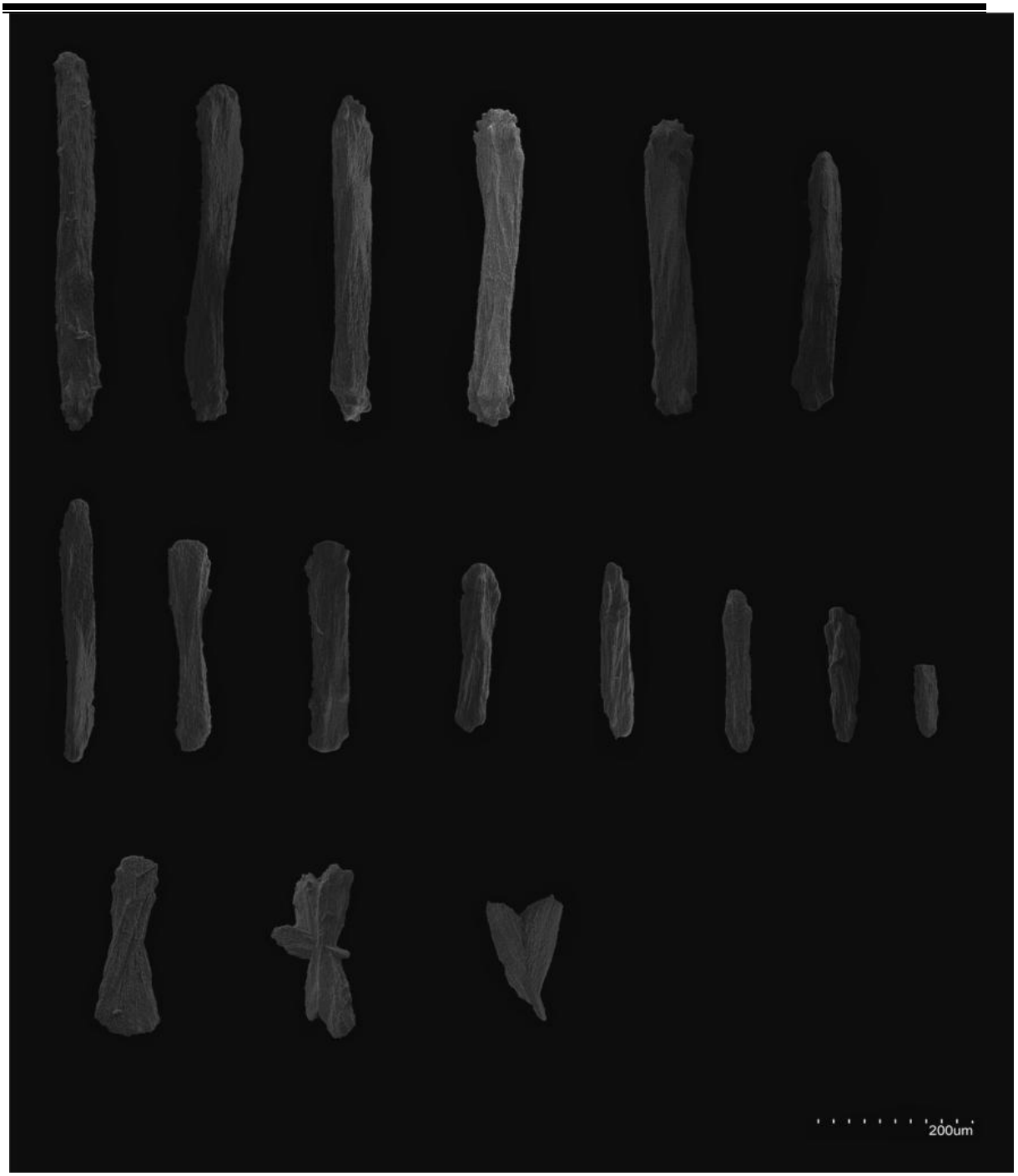

Figure 5.22. SEM images of sclerites from the coenenchyme from sample Ma20 from 45°N on the Mid-Atlantic Ridge. Image iIllustrates the presence of large (top) and small (middle) rods with the presence of tubercles and fluting. There are often also split sclerites present in a variety of shapes (Bottom). Scale bar = 200 µm

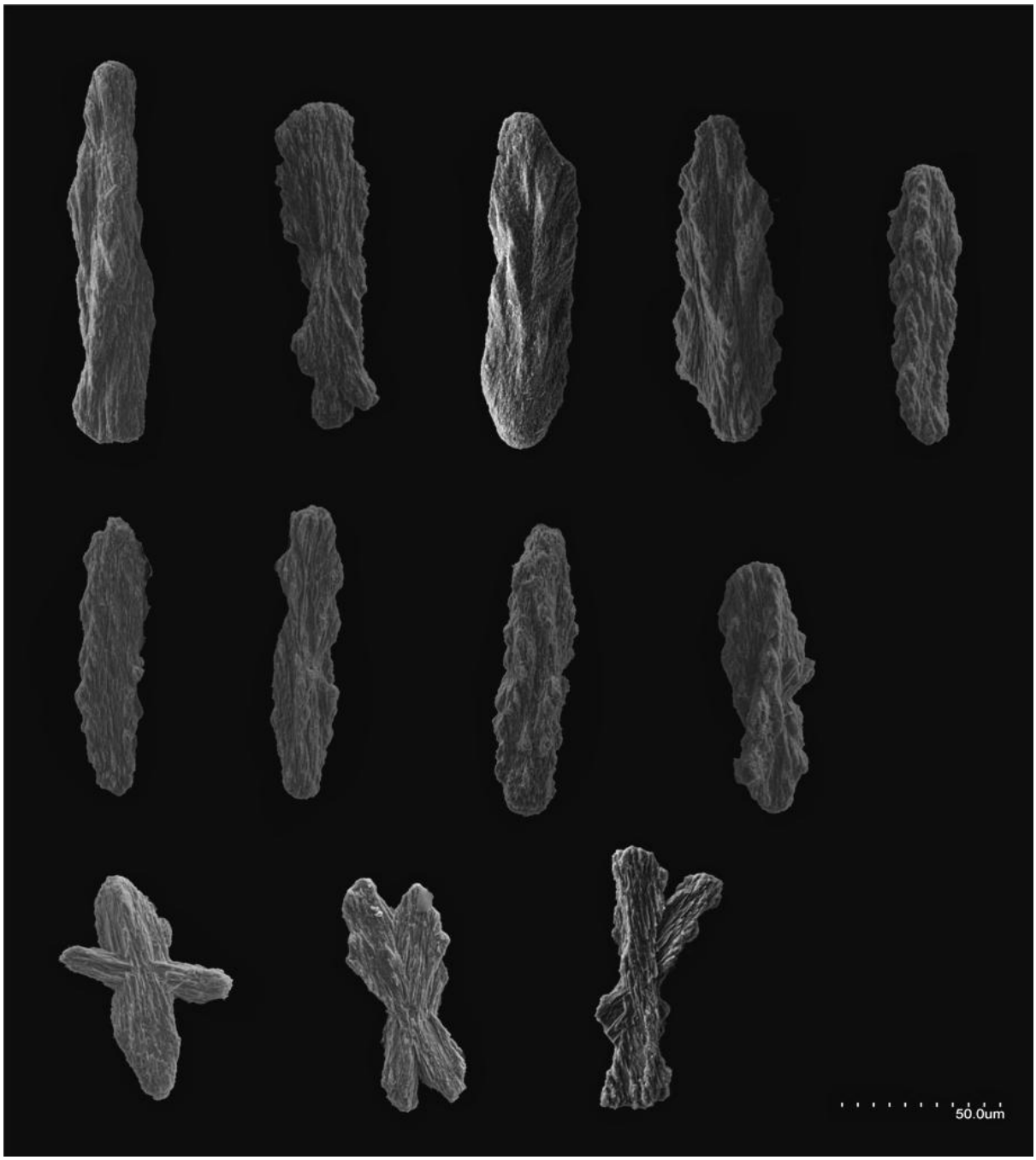

Figure 5.23. SEM images of sclerites from the polyp pharynx from sample Ma20 from 45°N on the Mid-Atlantic Ridge. This illustrates the presence of fluted flat rods and the appearance of deformed sclerites within the pharynx of sample Ma20. Scale bar = 50 µm

5.3.4 Sample Ma33

Family: Unknown

Subfamily: Unknown

Genus: B Gen. Nov

Species: N. sp. 4 Ma33

Material examined: Holotype. North Atlantic, Mid-Atlantic Ridge, 45°29.025 N 27°51.253 W, depth 2,890 m, collected during ROV *Isis* Dive 79, sample JC24-79-16 May 2008. Entire colony measuring approximately 10 cm in length and preserved in 95% ethanol (Figure 5. 24).

Diagnosis:

There is no good *in-situ* image of this specimen, as it was collected retrospectively from a rock sample, attached by a solid holdfast (Figure 5. 24). The coenenchyme is cream in colour. Polyps are very sparse along the axis and are taller than they are wide. When contracted tentacles do not fully retract into the oral aperture but touch tips above it to produce a volcano shape in the polyps (Figure 5. 25 D). Rock particles were found attached to some polyp tips. Sclerites have a variety of forms with the body containing rods, tapered bow-ties, clubs and diamonds, tentacles contain tapered bow-ties, diamonds and rods, coenenchyme mainly tapered bow-ties and rods and the pharyngeal region containing sectioned rods, which are flattened in the middle causing almost a twist.

Description: (holotype section)

The holotype consisted of a single stranded individual, with a cream-coloured coenenchyme (Figure 5. 24). It has a whip-like appearance and a very fine skeleton. Nodes are rare but are dark and can be clearly seen though the tissue. Polyps are present in two parallel rows along the individual. The polyps are sparse with more than a single polyp width between them.

Polyps are cream in colour in life and turn brown in ethanol. They are short with an average height of 4 mm and width of 2.7 mm creating a volcano shape. Some polyps had small pieces of rock attached to the tentacles. When contracted the tentacles do not enter the oral aperture but lean towards one another with tips touching above it. In some cases the polyps becomes nipped creating almost a waist-like appearance before the tentacle origin.

Polyp body sclerites are densely packed and imbricated with a random distribution along the basal and distal region. Adaxial and abaxial regions have a similar arrangement. Sclerites occur in a variety of shapes including, rods, tapered bow-ties, diamonds and "Neanderthal clubs" (Figure 5. 26). The "Neanderthal clubs" often have sharp tubercles along the "handle", some extending to the club end. Tubercles also occur on some tapered bow-ties and the larger rods; none were observed on the short rods. The length of sclerites varies from 115-430 µm, with the tapered bow-ties often being the largest.

Tentacle sclerites consist of: tapered bow-ties, diamonds, rods and crosses (which could be split rods) (Figure 5. 27). They vary in length from 60-200 µm, all have longitudinal striations, with tapered bow-ties also showing some tubercles. Sclerites are arranged vertically along the tentacles with the larger sclerites lining the outside edges.

The coenenchyme contains a high density of longitudinally-arranged sclerites varying in length from 120-300 µm. The sclerites consist of tapered bow-ties, rods and the occasional diamond shape (Figure 5. 28). Some tapered bow-ties have tubercles. Rods can be either flat or contain twists.

Pharyngeal sclerites are very sparse and with a length of 50-110 µm. They are not the "typical bamboo" sclerite of toothed rods but are instead rods with one end often flatter than the other (Figure 5. 29). All are longer than they are wide.

The axis has a hollow core which takes up approximately 10 % of the total diametre. Very few nodes measuring 1 mm in length occur but they are dark and can be seen through the coenenchyme. The length of internodes is at least 5 cm. The outer surface of the axis has longitudinal striations.

Figure 5. 24. Sample Ma33 used for description collected from 45°N on the Mid-Atlantic Ridge. A)Sample specimen preserved in ethanol illustrating polyp placement and shape B)Sample core, with hollow centre taking up around 10 % of the diametre, highlighted by the arrow C) In-situ picture of Ma18 taken at 2,890 m at 45°N on the Mid-Atlantic Ridge. Illustrates the sample was a whip like individual attached to a rock by a solid holdfast highlighted by the arrow.

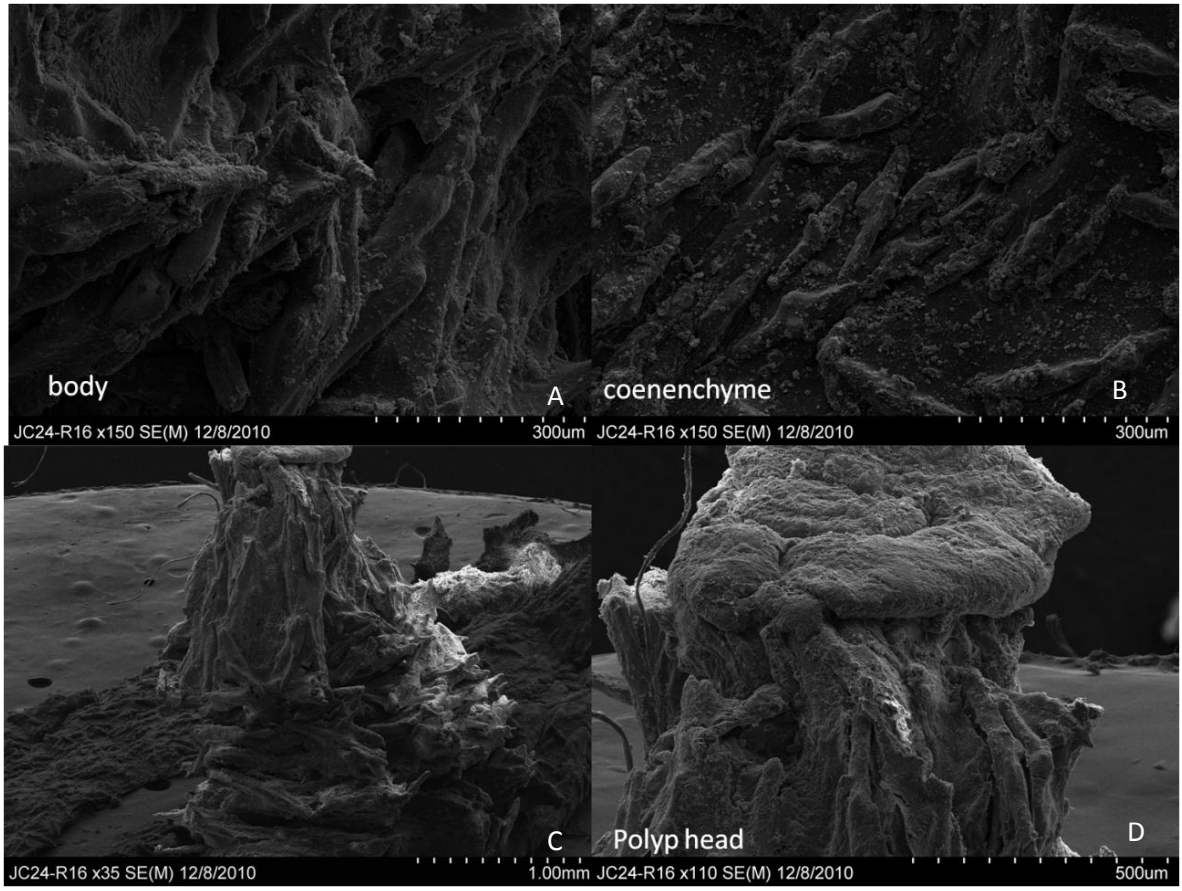

Figure 5. 25. SEM images of sample Ma20 from 45°N on the Mid-Atlantic Ridge. SEM pictures show: A) A close up of polyp body B) Close up of the sclerite arrangement in the coenenchyme along the axis, without flesh removal C) Full polyp D) Close up of the tentacle with their rock "hat". Numbers associated with bar scales represent the entire length of the scale bar, with numbers below each image representing magnification values.

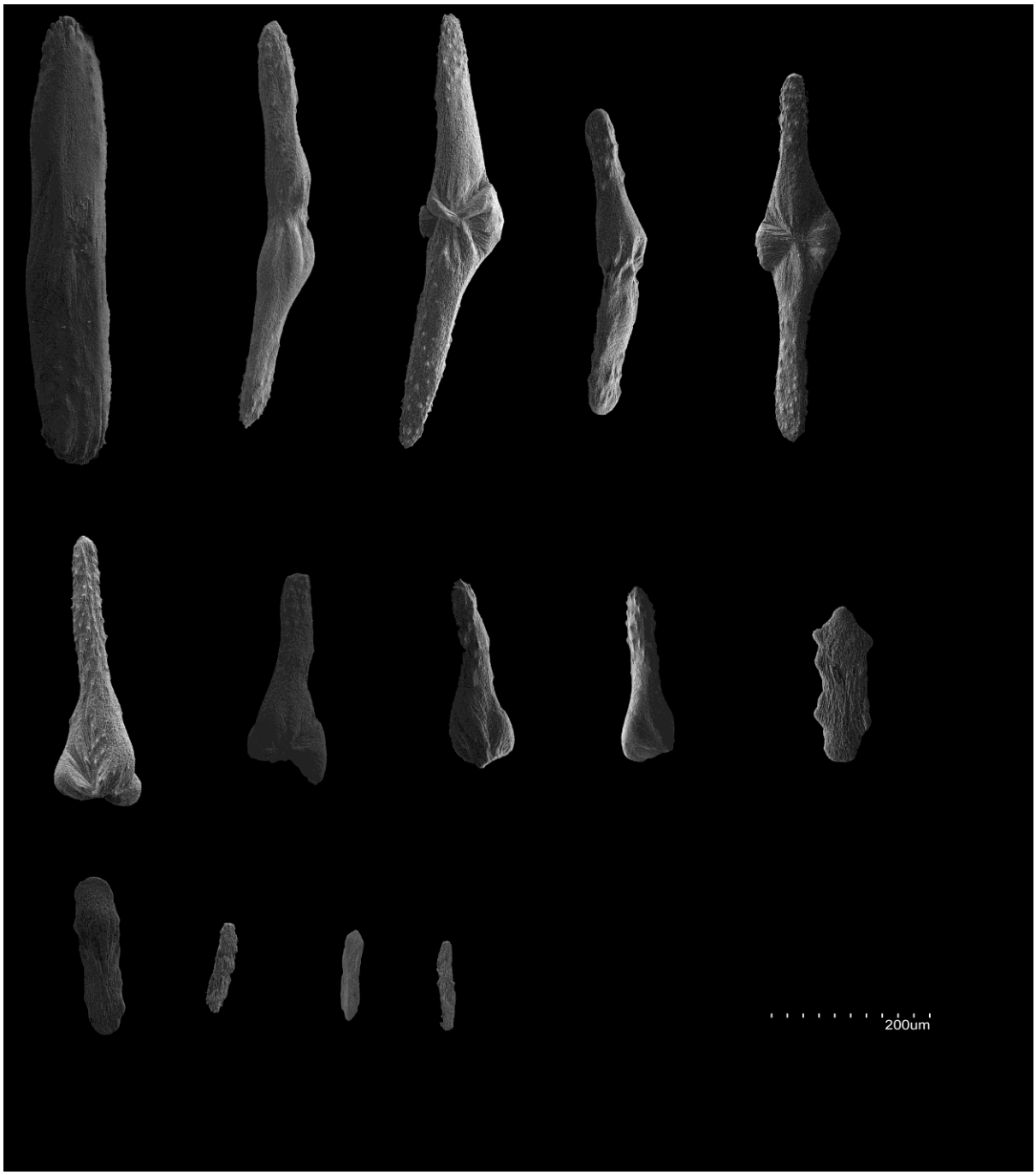

Figure 5. 26. SEM images of sclerites of the polyp body of sample Ma33 from 45°N on the Mid-Atlantic Ridge. Illustrates the presence of rods (top left and bottom) tapered- bowties (top middle) diamonds (top right) and Neanderthal clubs (Middle). Scale bar = 200 µm.

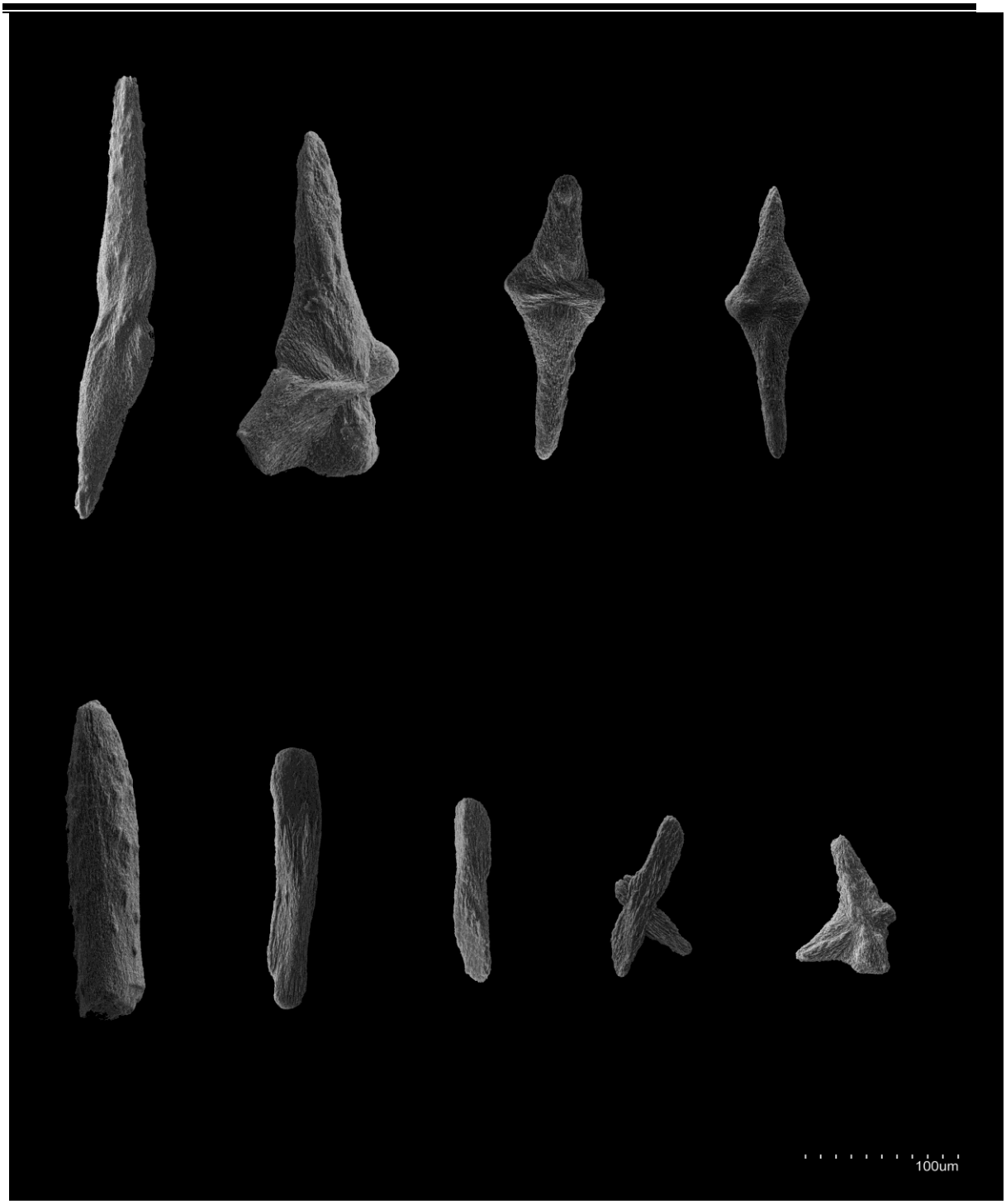

Figure 5. 27. SEM images the polyp tentacles of sample Ma33 from 45°N on the Mid-Atlantic Ridge. Illustrates the presence tapered- bowties (top left) diamonds (top right) and rods (Bottom left) and split sclerites (bottom right) Scale bar = 100 µm.

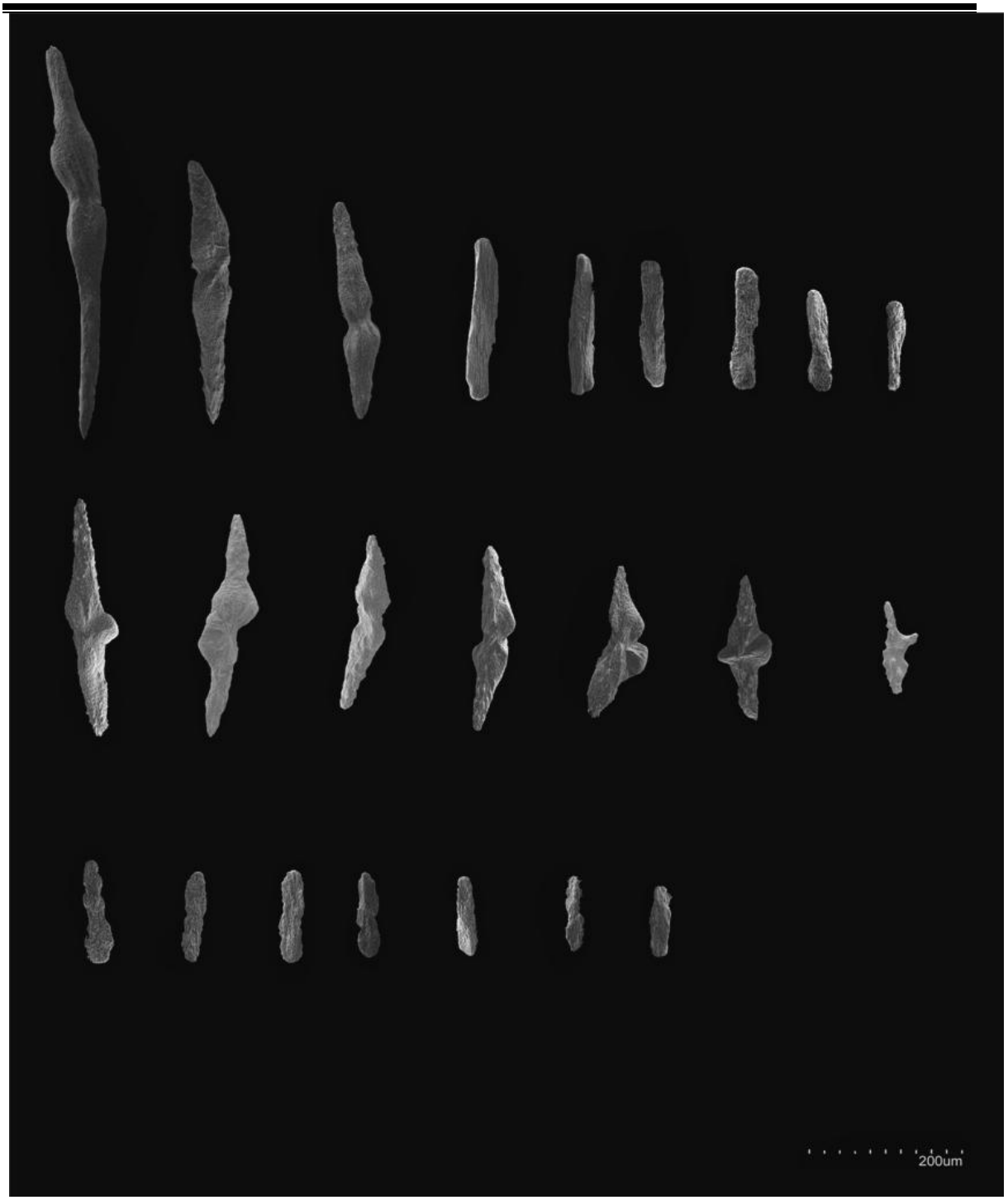

Figure 5.28. SEM images of the coenenchyme of sample Ma33 from 45°N on the Mid-Atlantic Ridge. Illustrates the presence tapered- bowties rods and diamonds. *Scale bar = 200 µm.*

Figure 5. 29. SEM images of sclerites from the pharynx of sample Ma33 from 45^{o}N on the Mid-Atlantic Ridge. Illustrates the presence of tapered rods within the pharynx . Scale bar = 200 µm.

5.3.5 Molecular analysis

In total, 60 specimens including the 4 new species (Ma18, Ma20, Ma33, Ma33) were successfully amplified and sequenced for the *msh1* mitrochondrial gene. To ensure the inclusion of as many samples as possible in the study the sequences were trimmed to 709 bp in length including indels. These were aligned with 36 specimens from the Isididae along with four *Acanthogorgia* and one *Leptogorgia* (which was used as an out-group for

rooting the tree) and phylogenetic analysis carried out. *Acanthogorgia* was included in this analysis because Ma33 was not amplified using CO3bam5657F (Brugler & France, 2008) paired with mut3458R (Sánchez *et al*., 2003) primers, which the remaining three were indicating this specimen did not belong to the Isididae sub-family Keratoisidinae. Previous discussions with Scott France indicated that within his trees Ma33 grouped near *Acanthogorgia*, therefore representatives were included in the tree.

Bayesian, maximum parsimony and Maximum likelihood trees all showed similar topographies (Electronic appendix 4.a figures 5.1-5.3). One large clade (A) including all Isididae species, a further smaller clade (B) containing the *Acanthogorgia* species and AZ samples (bar AZ17) as well as Cl20- *Acanthogorgia* sp., Cl18 *Acanthogorgia* sp., Ch182 *Paramuricea* sp. and Ch199 *Paramuricea* sp., with a further branch containing only Ma33 and D2- *Gersemia* sp. These clades are well supported by Bayesian posterior probabilities (Figure 5.30). The large clade contains 7 sub-clades with *Keratoisis* and *Lepidisis* being present throughout sub-clades indicating genus distinctions are poorly defined. One sub-clade is made up primarily of novel species contained throughout this study (Figure 5.30).

Of the four new species three were positioned within clade A, with only MA33 not appearing within this clade. MA33 was assigned to a branch along with D2 *Gersemia* sp only. This branch fell outside the Isididae clade. Both Ma18 and Ma20 were assigned the sub-clade containing only novel sequences from this study. Ma27 appeared within the sub-clade along with EF060022 *Isidella* (from the Atlantic) and EF060021 *Isidella* (from the Pacific). Through personal communication with France and Alderslade it is understood that EF060022 *Isidella* has recently been assigned to the new genus *Jasonisis.*

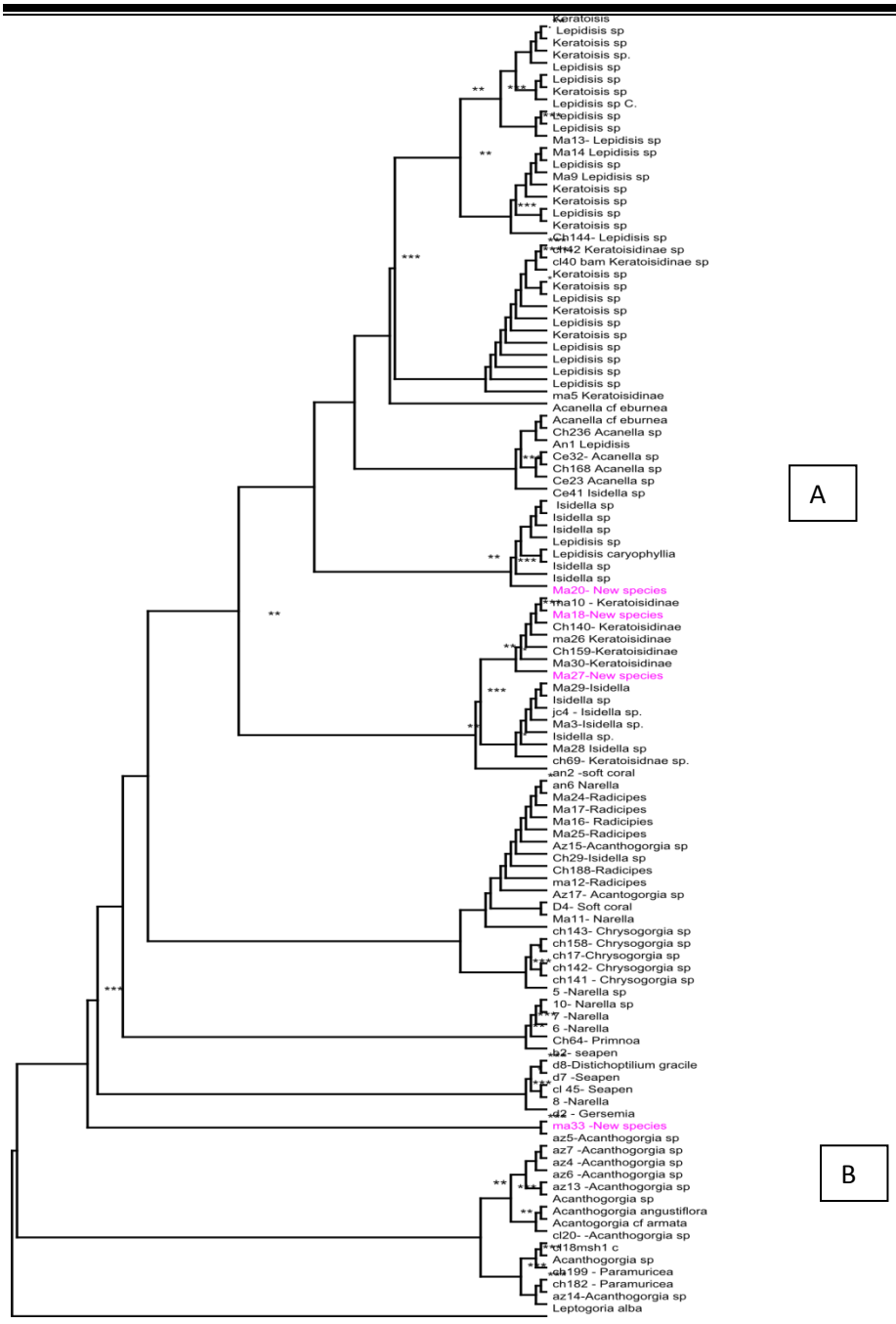

Figure 5. 30. Phylogeny of Octocorallia inferred from msh1 region sequences. The tree is rooted with Leptogorgia alba ** above branches indicate support for each node based Bayesian/ML inference ** = >90 % baysien support *** = >90 % baysien and >70% maximum-likelihood support. New species highlighted in pink. Rooted with* Leptogorgia sp. *Electronic appendix 4.a figures 5.1-5.3 show further detail*

When pairwise genetic distances (uncorrected p) are calculated it becomes clear that there is a higher level of genetic variance between genera than within them (Figure 5. 31). From this figure it is shown that 17 % of species within the same genus had 0% variance within the *msh1* gene region in comparison to 9 % from different genera. The majority of congeneric species have less than 6 % variance between them with the higher percentages in this case generally being attributable to *Acanthogorgia* sp. which had up to 13.5 % variance between individuals. Between-genus variance peaked at 20.9 % between a soft coral and a bamboo (samples D2 and Cl45). The most common distances were between 4.1-6 % and 12.1-14 % together accounting for around 39 % of species combinations. Sample Ma33 had a minimum genetic distance of 6.3 % and a maximum of 13.9 % within this study indicating this species is genetically distant from the other species used in this study.

5.4. Discussion

The discovery of high species diversity within the deep-sea in the past century has lead to the increase in focused research to discover the species present within our seas. An example of such a project is the Census of Marine Life. From this project, and others like it, it has become clear there are many organisms within the deep-sea which are yet to be discovered and described. From the RRS *James Cook* cruise JC24 in 2008, which was primarily a geology cruise, four new species of octocoral were recovered from depths between 2,600 and 3,600m along the Mid-Atlantic Ridge. Unfortunately it is the case that the material preserved from these individuals was primarily preserved for genetic investigation and thus the specimens are not ideal for taxonomic work. However, even from these small imperfect specimens it was clear new species had been found and thus should be described.

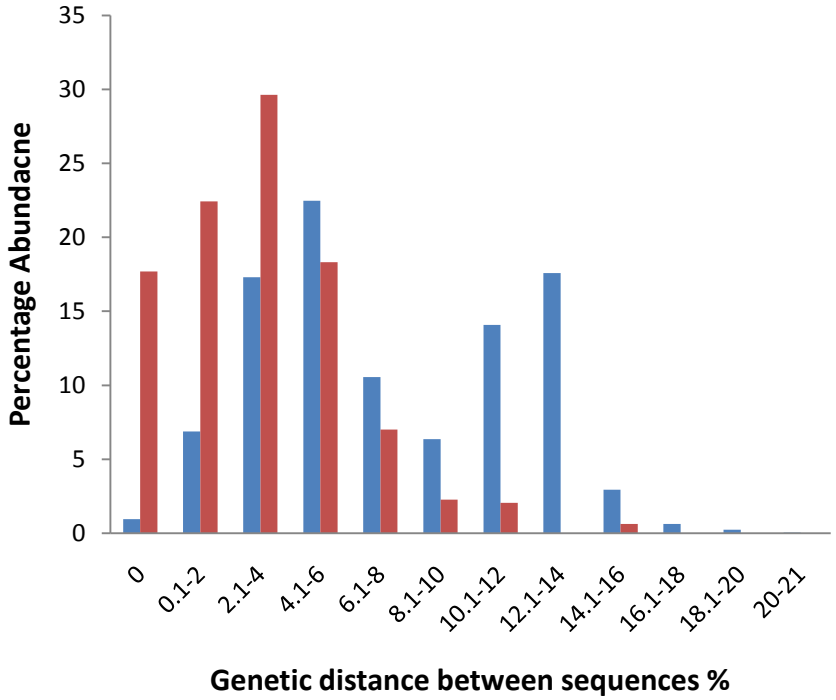

Figure 5. 31. Genetic distances between different sequences in both congeneric samples and sample from different genus.Pairwise genetic distances (uncorrected p) calculated using PAUP 4.0b (Swofford, 2002) to allow the examination of variation between species in the same genus (red) and of different genus (blue) to be compared.*

Three of these new species (Ma27, Ma18, Ma20) have been assigned to the sub-family Keratoisidinae based both on morphological and molecular data. The fourth species (Ma33) is more problematic. It is clear from the genetic data that this individual is not within the Isididae sub-family Keratoisidinae. Members of this sub-family have a unique mitochondrial gene order so they require different primers to allow the amplification of the *msh1* region (Brugler and France, 2008). Ma33 was not amplified using the primers CO3bam5657F (Brugler & France, 2008) paired with mut3458R (Sánchez *et al*., 2003) but was successful using the primer pair ND4L2475F-Mut3270R, which is known to span the *nad4L-Msh1* junction found in the non-Keratoisidinae octocoral mitochondrial genome (Brugler and France, 2008). Also when visualised upon a taxonomic tree Ma33 is grouped

away from all other Isididae. When considering the larger taxonomic tree produced from combining *MSH1* and *ND2* genes (electronic appendix 3a Figures 4.12-4.14) Ma33 occurs in close vicinity to Alcyoniinae within a clade containing Holoaxoina and Alcyoniina, away from Isididae species, strenghthing the suggestion that Ma33 does not belong in the Isididae.

When examining morphology Ma33 has hints of Isididae origin, including the presence of nodes and internodes on the skeleton, and a hollow core. However, the sclerite structures observed from this specimen have not been recorded elsewhere. It was suggested by France (pers. Comm.) that the specimen could fit within the genus *Isidoides*, within the Chrysogorgiidae. However, comparison of sclerites with images provided by Espirit Heestand from Louisiana University (Figure 5. 32 and 5.33) of Isidoides has allowed the rejection of this hypothesis, as it was obvious that the sclerites were not of the same structural form.

Personal communication with two of the world's top octocoral taxonomists Les Watling, from Hawaii University and Phil Alderslade from CSIRO, Australia, has confirmed that neither has seen sclerites of this form previously. Alderslade noted that if the "Twinning" in the longer sclerites was regarded as abnormal then it could pass for a species in the *Keratoisis-Lepidisis* complex, however the abundance of "twinned" sclerites and the genetic placement with a soft coral and away from all Isididae would mitigate against this.

One theory which could account for the presence of an Isididae-like skeleton along with the placement of the individual with soft-corals could be that this could be a case of one coral species overgrowing another. This has been observed many times in shallow water where species competing for space will overgrow one another (Chornesky, 1989). Watling has also observed a species within the genus *Clavularia* belonging to the Stolonifera order

overgrowing old Isididae skeletons (pers. comm.). However, as yet it has not been possible to prove or disprove this theory. The main issues preventing this are the lack of material and the want to preserve said material in good condition to allow for cataloguing as a holotype at a later date.

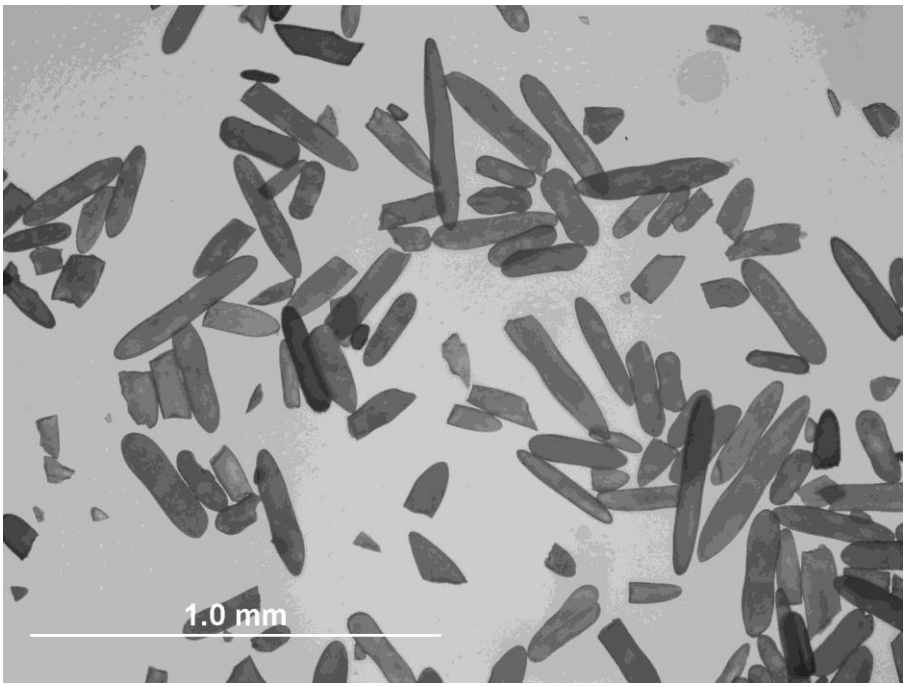

Figure 5. 32 Isidoides Body wall sclerites. Supplied by Espirit Heestand from Louisiana University

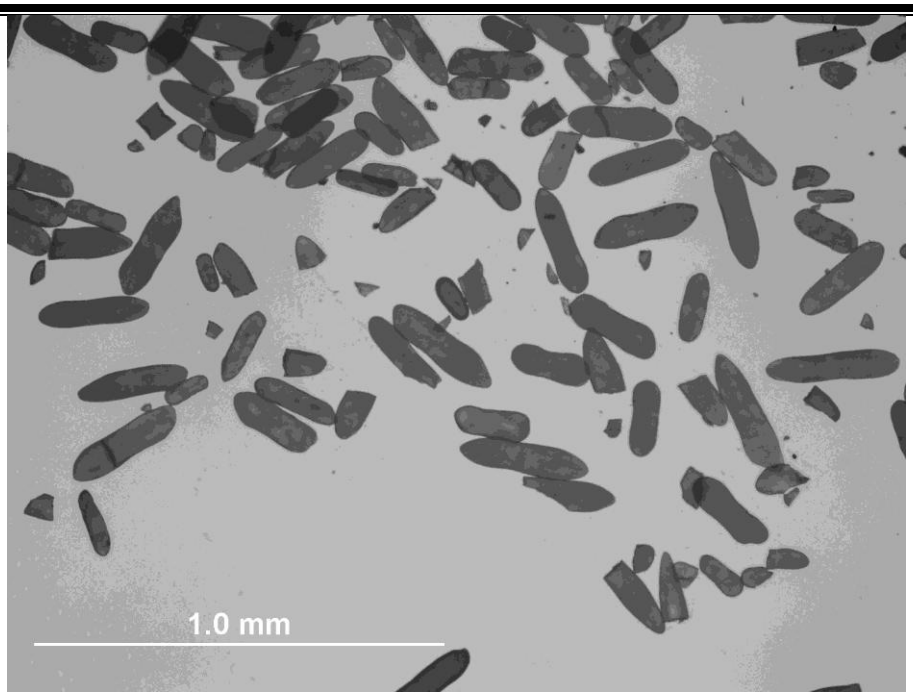

Figure 5. 33 Isidoides branch sclerites. Supplied by Espirit Heestand from Louisiana University.

It could also be possible that this species is an "almost bamboo" such as the scleraxonian coral *Parisis* which looks like it has nodes but these are not built in the same way as Isididae (Janes and Mei Wah, 2005). However, this would not account for the placement of the species in phylogenetic tree. The overall conclusion regarding this small specimen is that is a previously unknown species which thus far cannot be assigned to a genus or family from either morphological or molecular data.

The placement of Ma27 within the new genus *Jasonisis* described by Alderslade and McFadden (2011) is strengthened by the molecular data placing this specimen in a sub-clade along with EF060022 *Isidella* sp. from the Atlantic which has recently be assigned to this genus (Pers. Comm. with Les Watling and Scott France). The Ma27 species was sampled at a depth of 2,812 m and EF060022 *Isidella* sp. was sampled at 2,554 from the

Kelvin seamount. This could suggest that this new genus is endemic to the deep-sea and the limited scope of deep-sea exploration would explain why it has not been previously described.

It may also be possible to place Ma18 within the genus *Jasonisis*. Ma18 contains the sclerite structure described by Alderslade and McFadden (2011) being "predominantly flattened and scale-like, elongate to oval, commonly with more or less rounded ends and pronounced lobed margin" with the occurrence of more smooth rods within the polyps body than were present within the type specimen *Jasonisis thresheri*. However, the overall sclerite shape along with the presence of a hollow axis and a thick coenenchyme, as well as the successful amplification using CO3bam5657F (Brugler & France, 2008) paired with mut3458R (Sánchez *et al*., 2003) primers would suggest a possible placement within this genus.

Ma20 does not conform to the genus *Jasonisis* and does not fit into any other described genus. The presence of retractibility and shape of the polyps and long striated rods within the colony indicate this could represent a new genus. However, the placement of this specimen into the same clade as Ma18 away from Ma27 both in this chapter and in phylogenetic trees produced from *MSH1* and *ND2* genes as well as a combined data set (Electronic appendix 3a 4.1-4.14) would indicate that Ma18 and Ma20 are sister taxa and are more closely related genetically to one another than to Ma27 despite the morphological findings. It is also clear from these findings that although the gene inversion within the Keratoisidinae indicates a monophyly within the Isididae they are not well resolved at a genus level and it is likely that taxonomic revisions are required within this group, to take into accout their taxonomic placments. Although, it is not suggested that genetic distance is a absolute in determining species or genus status generally the closer they are in distance the shorter time period since they diverged from one another (McFadden *et al.*, 2011).

McFadden *et al.* (2011) have shown that *msh1* shows little divergence among congeneric species in octocorals and thus is limited as a species-specific barcode. However within this study it was found that although 69 % of congeneric species comparisons showed less than 6.1 % distance, some from *Acanthogorgia* had more than 12 % genetic distance. This would support the fact that *MSH1* alone is not suitable for genetic barcoding. With such a high level of genetic distance these *Acanthogorgia* would clearly have been placed in different genus. It could, however, be that there was slight contamination within the samples which cause such anomalies or that like many other corals these individuals should not have been placed in the same genus to begin with. These results would suggest that *MSH1* bar-coding would be more successful in some genera than others. It is obvious that one must consider both morphological and molecular data before any conclusions regarding a species placement can be made.

Traditionally the characteristics used for morphological identification of species of Isididae include, colony branching, polyp retractability, skeletal structure, sclerite morphology, sclerite arrangement and polyp operculum structure (Bayer and Stefani, 1987: France, 2007). It has since been found that branching is not an effective method of determination and cannot be used as a distinguishing feature between *Lepidisis* and *Keratoisis* (France, 2007). It is now thought that the most important features to allow an accurate description of species of Isididae, and most likely all octocoral species, is the presence, type and arrangement of sclerites (Watling and France, 2011). This is enhanced by the fact that the type specimen for the new genus *Jasonisis* on the surface looks very much like other Isididae species from photos or video. This could be a reason why this genus had been undescribed despite it being found in three different locations thus far.

By implementing the new Keratoisidinae character list of Watling and France (Pers. Comm) it is possible to know exactly which features must be considered for an accurate specimen description as well as ensuring any new descriptions are consistent, despite a

general lack of up to date taxonomic keys for the group. This will prevent problems such as the genus *Keratoisis* being used as a convenient group to place any species with branching from the internode, despite differing polyp morphologies (Watling *et al.*, in prep). *Keratoisis* is a genus very much in need of revision. A revision could also be used as a tool to assess previous descriptions to ensure one species has not been described by two separate people under different names, or the same person mistakenly believing two specimens are two separate species as a result of a plastic feature such as branching patterns. Improving molecular techniques will also allow a greater understanding of evolutionary history between individuals and allow species determining features to be identified.

5.5.Conclusion

The research cruise JC24 led to the serendipitous discovery of four new deep-sea coral species, of which there are in the family Isididae. Molecular and taxonomic analysis has shown these samples represent a recently described genus by Alderslade and McFadden (2011) *Jasonisis* as well as at least one other new genus if not two new genera.

It is important that for accurate taxonomic descriptions and phylogenetic placements to be achieved both morphological and molecular data are integrated. It is also important that there is the implementation of the standard description criteria between different labs, such as the character list used within this study. It is also clear from literature and molecular data that many of the species previously described need to be revisited and a general overhaul of coral taxonomy is required.

Chapter 6: Summary and future work.

The aim of this study was to address several questions regarding the Distribution, Ecology and Phylogenetics of cold-water corals observed within the Northern Atlantic. These are listed below with a summary of results concerning each topic.

6.1 Determine if depth, substratum, or slope have an effect on cold-water coral assemblages along the AVR at 45°N and within the Whittard Canyon.

6.1.1 Depth

Neither study showed an effect of depth on the coral assemblages present within the study areas and thus it was not considered an important variable. Despite this when looking at individual species it was clear some depth effect was present. A clear example of this was within the Whittard canyon where *Lophelia* was only observed within the top 2,000 m of the water column, this was attributed to the ASH. This indicated that although the overall assemblage structure does not change significantly with depth there are changes in distribution which occur within an individual species.

6.1.2 Substratum

It was found both along the AVR and within the Whittard Canyon that cold-water coral assemblages changed with a change in substratum type. There was an increase in coral abundance found upon hard substratum in comparison to soft sedimented substratum, with *Lophelia* ecosystems (only found within the Whittard Canyon) found to have the highest abundance of corals present.

Coral assemblages occurring on sediment substratum differed from those on hard rock by the increase in Pennatulacea, increases in *Acanella* and some Chrysogorgiidae species (such as Spiral coral and *Radicipes*). There were also observations of coral species which have previously only been observed on hard substratum within the sediment substratum. This was attributed to the possibility of small rocks occurring under the surface which cannot be visualised in the videos. Coral assemblages occurring on rock were found to have a greater number of species and families present upon them in both study areas, indicating that corals generally require a hard bottom to colonise. Mixed rock and sediment ecosystems were found to be more influenced by the presence of rock than sediment, with a large variety of families being present. *Lophelia* ecosystems, which were only found within the Whittard canyon as a result of depth profiles covered, were found to have the highest abundance of individuals but a low diversity of species or families. It was suspected hat this was caused by *Lophelia* out competing other coral species and thus reducing diversity. However no substratum type was fully utilised by the corals, indicating further factors had an effect.

6.1.3 Slope

Slope was found to lead to an increase in the number of individuals observed within the AVR, but was not found to have a significant effect on the assemblages within the Whittard Canyon. The increase in the number of individuals observed on rock slopes in comparison to flat rock along the AVR was attributed to an increase in food, as a result of a change in the hydrographic regime created by the slope. The reduced effect of slope within the Whittard Canyon was thought to be as a result of a generally complex hydrographic regime which results in a higher food input to the canyon system, thus reducing the effect of slope over non-sloped areas.

6.2 Compare cold-water coral assemblages along the AVR at 45°N and within the Whittard Canyon.

A greater than a three times increase in the number of coral colonies observed occurred in the Whittard Canyon with a maximum of 855 individuals per 100 m transectin comparison to the AVR with a maximum of 59 individuals. This was inspite of less video footage being analysed. The largest increase was observed within the *"Lophelia reef"*, a substratum type which was not present upon the AVR.

Eleven more tentative species were found within the Whittard Canyon than along the AVR. However, the 20 species found in the AVR were not all common to the Whittard Canyon, with an absence of *Iridogorgia* or *Narella* within the Whittard Canyon. Species found within the Whittard Canyon and not along the AVR included *Acanella*, *Lophelia*, *Pennatula aculeata* and *Primnoa*. These differences were attributed to a change in substratum type and a different depth profile between the two sites.

The dominant species were also found to change between the two areas, with the AVR dominant species mainly consisting of Whip coral and *Isididae* n. sp. 1 in comparison to *Anthomastus*, *Acanella* and *Lophelia* in the Whittard Canyon. This was also attributed to predicted changes in the POC input to the respective areas, with the Whittard Canyon hypothesised to have a higher level of primary production input, as a result of its proximity to the continental shelf as well as its complex hydrographic regime. It was also hypothesised that there could be a change in the composition of the POC input, which may favour different species within the different areas.

6.3 Create a comprehensive phylogenetic tree of the order Octocorallia including new samples obtained from various sites within the Atlantic using both the MSH1 and ND2 genes.

Phylogenetic trees were created for *ND2* and *MSH1* genes as well as a joint tree. Each data set (bar all *MSH*1 samples available) was subjected to three phylogentic analyses Bayesian phylogenetic analysis was conducted using MrBayes 3.1.2 (Huelsenbeck and Ronquist, 2001). Maximum parsimony models were run using PAUP* 4.0b (Swofford, 2002) with 100 bootstrap replicates. PhyML 3.0 (Guindon & Gascuel, 2003) maximum-likelihood analysis was performed under 500 replicates. It was clear from all data sets that the tree topologies created by these three methods were fairly consistent, with maximum-parsimony being the most divergent. However, these topologies did not agree with the taxonomic divisions placed by Bayer (1981)

Individual gene topologies create three well-supported clades, Clade A containing *Acanthogorgia* sp and members of the Alcyoniina as well as previously sequenced Holoaxoina and Alcyoniina. Clade B containing the remainder of species obtained throughout this study (including members of the Isididae and Chrysogorgiidae families) as well as previously sequenced Calcaxonia and Pennatulacea species. This clade contained a sub-clade composed entirely of species obtained throughout this study. A third and very small clade, Clade C, contained representatives of Alcyoniina.and *Corallium*, as well as *Paragorgia* species when considering all *ND2* sequences available. These results are in fairly good agreement with previously published results.

When the joined *ND2* and *MSH1* trees were considered four clades were visualised. The fourth clade was composed of Pennatulacea species, which had been removed from Clade

B. This was not in agreement with previous studies and was attributed to the increase in samples used as well as the increased resolution obtained from the use of two genes.

In agreement to previous studies genetic distances were seen to be larger between genera using *MSH1* in comparison to *ND2*. Despite this the resolution is not high enough to allow the accurate identification of species solely from one gene.

6.4 Identify and describe new cold-water coral species found along the AVR at 45°N upon the MAR.

Four new species of deep-sea octocorals were identified and described using a new character table established by Les Watling (Hawaii University) and Scott France (Louisiana University). From this it was possible to allow the placement of Ma27 into the newly described genus *Jasonisis* from Alderslade (pers comm.) Ma20 could also be tentatively be placed within this genus with Ma18 and Ma33 representing new species with the possibility of new genera.

Phylogenetic data strengthens the placement of Ma27 in *Jasonisis* as a result of its placement in the tree along with a species recently assigned to this genus by Watling and France (pers. comm.). Ma 18 and Ma20 were found to be sister taxa occurring within the Keratoisidinae sub-clades within the tree. Ma33 was somewhat more difficult to assign.

Morphologically Ma33 shares skeletal features with the Isididae, yet the sclerite structure has not been encountered previously and molecular data places the specimen in non-Isididae clades, most commonly related to Alcyoniina species. It is therefore unclear where

the taxonomic placement of this species should be set and more work is required before this can be accurately placed. This illustrates clearly that it is important to attain both morphological descriptions and molecular data from a species to allow accurate identification and taxonomic placement to be achieved. Taxonomic revisions of many species are required to allow for this.

6.5 Future work

It is evident from the present study that there is still much to be done on the distribution, ecology and phylogenetics of cold-water corals observed within the Northern Atlantic. To allow a more coherent understanding it is important that focussed studies occur incorporating: video transects, photographic stills, substratum sampling and focused octocoral sampling for both taxonomic and molecular work. The collection of these data along with collaborative works with different institutes to ensure the consistent methods and data interpretations would allow for a higher resolution study of Octcorallia within the Northern Atlantic.

It was clear both from this study and current literature that there is a discrepancy between phylogenetic placement and taxonomic placement of a variety of different octocoral species. To address this it would be beneficial to revisit old species descriptions. It would also be beneficial to identify common features present within the taxonomic clades to ensure descriptions are based on useful features and not plastic features.

References :

Aguilar, C., Sánchez, J.A. 2007. Phylogenetic hypotheses of gorgoniid octocorals according to burrow type Lebensspuren on the Cape Verde Abyssal Plain. Internationale Revue der gesamten Hydrobiologie, Berlin **80**:153-170.

Alderslade, P. 1998. Revisionary systematics in the gorgonian family Isididae, with descriptions of numerous new taxa (Coelenterata: Octocorallia*).* Records of the Western Australian Museum, Supplement No. 55: 359 pp

Alderslade,P. McFadden, C.S. 2007 Pinnule-less polyps: validation of the soft coral genus *Acrossota* and a new genus and new species of Indo-Pacific Clavulariidae (Coelenterata: Octocorallia). *Zootaxa* **1400:** 27-44.

Alderslade, P., McFadden,C.S. 2011. A new genus and species of the family Isididae from a CMAR Biodiversity study, and a discussion on the subfamilial placement of some nominal isidid genera (Coelenterata: Octocorallia). *Zootaxa*, Submitted.

Alvarez-Perez , *G*., Busquets, P., De Mol, B., Sandoval, N.G., Canals, M., Casamor, J.L.,2005. Deep-water coral occurrences in the Strait of Gibraltar. In; Freiwald, A. Roberts. J.M. (Ed.), Cold-Water Corals and Ecosystems. Springer Berlin Heidelberg, New York, pp 207-221

Arzola R.G., Wynn, R. B., Lastras, G., Masson, D. G. ,Weaver. P. P. E. 2008. Sedimentary features and processes in the Nazare and Setubal submarine canyons, west Iberian margin. *Marine Geology* **250**:64-88.

Auster, P.J. 2005 Are deep-water corals important habitats for fishes? . In; Freiwald, A. Roberts. J.M. (Ed.), Cold-Water Corals and Ecosystems. Springer Berlin Heidelberg, New York, pp 747-760.

Babcock, R. 1990. Reproduction and development of the blue coral *Heliopora coerulea* (Alcyonaria: Coenothecalia). *Marine Biology*, **104**: 475-481.

Bayer, F.M. 1956. Octocorallia. Treatise on Inveribrate Paleonotology, Part F. Coelenterata. University of Kansas Press, Lawrence, Kanasa. pp 166-231.

Bayer, F.M. 1981. Key to the genera of Octocorallia exclusive of Pennatulacea (Coelenterata: Anthozoa), with diagnoses of new taxa. P*roceedings of the Biological Society of Washington* **94:** 902-947.

Bayer, F.M., Grasshoff, M, Verseveldt, J. 1983. Illustrated trilingual glossary of morphological and anatomical terms applied to Octocorallia. Leiden. The Netherlands.

Bayer, F.M., Stefani, J., 1987. New and previously known taxa of isidid octocorals (Coelenterata: Gorgonacea), partly from Antarctic waters. *Proceedings of the Biological Society of Washington* **100:** 937-991.

Berntson, E.A., Bayer, F.M,, McArthur, A.G., France, S.C. 2001. Phylogenetic relationships within the Octocorallia (Cnidaria: Anthozoa) based on nuclear 18 s rRNA sequences. *Marine Biology* **138:** 235-246.

Bett, B. J., Rice, A.L, Thurston, M.H. 1995. A quantitative photographic survey of "spoke-burrow" type Lebensspuren on the Cape Verde Abyssal Plain. Internationale Revue der gesamten Hydrobiologie, Berlin **80**:153-170.

Bianchelli, A., Zeppilli, G.D., Danovaro, R., 2010. Metazoan meiofauna in deep-sea open slopes: A large-scale comparison with focus on the rare taxa. *Deep-sea research, 1* **57:** 420-433.

Bilewitch,J.P., Coates,K.A., Currie,D.C. Trapido-Rosenthal,H.G 2010. Molecular and morphological variation supports monotypy of the octocoral *Briareum Blainville* 1830 (Octocorallia: Alcyonacea) in the Western Atlantic. *Proceedings of the Biological Society of Washington*, **123:** 93-112.

Billett, D.M., Lampitt, A.L., Rice, A.L., Mantoura, R.F.C., 1983. Seasonal sedimentation of phytoplankton to the deep sea benthos. *Nature* **302**: 520–522.

Billett, D. S. M., Bett, B. J., Rice, A. L., Thurston, M. L., Galéron, J., Sibuet, M., Wolff, G. A. 2001. Long-term change in the megabenthos of the Porcupine Abyssal Plain (NE Atlantic). *Progress In Oceanography* **20**:325-348.

Billett, D. S. M., Bett, B. J., Reid, W. D. K., Boorman, B., Priede I. G., 2010. Long-term change in the abyssal NE Atlantic: The 'Amperima Event' revisited. *Deep Sea Research Part II* **57**:1406-1417.

Boehlert, G. W., Mundy B.C. 1993. Ichthyplankton assemblages at seamount and oceanic islands. *Bulletin of Marine Science* **53**:336-361.

Brugler MR, France, S.C. 2008. The Mitochondrial Genome of a Deep-Sea Bamboo Coral (Cnidaria, Anthozoa, Octocorallia, Isididae); Genome structure and putative origins of replication are not conserved among Octocorals. *Journal of Molecular Evolution* **67:** 125-136.

Bryan, T.L., Metaxas, A., 2006. Distribution of deep-water corals along the North American continental margins; Relationships with environmental factors. *Deep-Sea Research Part I* **53:** 1865-1879.

Buhl-Mortensen, L., Mortensen, P.B., 2005. Distribution and diversity of species associated with deep-sea gorgonian corals off Atlantic Canada. In; Freiwald, A., Roberts. J.M. (Ed.), Cold-Water Corals and Ecosystems. Springer Berlin Heidelberg, New York, pp. 849-879.

Burgess, S.N., Babcock, R.C. 2005. Reproductive ecology of three reef-forming, deep-sea corals in the New Zealand region. . In; Freiwald, A., Roberts. J.M. (Ed.), Cold-Water Corals and Ecosystems. Springer Berlin Heidelberg, New York, pp701-713

Cacchione, D. A., Rowe, G. T., Malahoff, A. 1978. Chapter 4: Submersible investigation of outer Hudson Submarine Canyon. *in* D. J. Stanley, G. Kelling, (ed). Sedimentation in submarine canyons, fans and trenches. Dowden, Hutchinson and Ross, Stroudsberg, Pennsylvania.

Cairns, S.D., Bayer, F.M. 2005. A review of the genus *Primnoa* (Octocorallia: Gorgonacea:Primnoidae), with the description of two new species. *Bulletin of Marine Science*.**77:** 225-256

Cairns, S.D., 2007. Deep-water corals; an overview with special reference to diversity and distribution of deep-water Scleractinian corals. *Bulletin of Marine Science* **81:** 311-322.

Cairns, S. D., Baco A. 2007. Review and five new Alaskan species of deep-water octocoral *Narella* (Octocorllia:Primnoidae). *Systematics and Biodiversity* **5:** 391-407,

Cairns, S.D. 2009. Influence of Frederick (Ted) M. Bayer on deep-water octocoral research. *Marine Ecology Progress Series*. **397:** 7-10.

Canals, M., Puig, P., de Madron, X. D., Heussner, S., Palanques, A., Fabres J. 2006. Flushing submarine Canyons. *Nature* **444**:354-357

Carey Jr, A. G., Stein, D. L., Rona, P. L. 1990. Benthos of the Gorda Ridge axial valley (NE Pacific Ocean): Taxonomic composition and trends in distribution. *Progress In Oceanography* **24**:47-57.

Chave, E. H., Jones, A. T. 1991. Deep-water megafauna of the Kohala and Haleakala slopes, Alenuihaha Channel, Hawaii. *Deep Sea Research Part A.* **38**:781-803.

Cheung, M., Cooper, A., Duran, C., Field, M., Heled, J., Kearse, M., Markowitz, S., Moir, R., Stones-Havas, S., Sturrock, S., Thierer, T., Wilson, A. 2011. Geneious v5.4, Available from http://www.geneious.com/

Chornesky, E.A.1989. Repeated reversal during spatial competition between corals. *Ecology* **70:** 843-855.

Clark, M. R., Tittensor, D., Rogers, A.D., Brewin, P., Schlacher, T., Rowden, A., Stocks, K., Consalvey. M., 2006. Seamounts, Deep-Sea Corals and Fisheries: Vulnerability of Deep-Sea Corals to Fishing on Seamounts Beyond Areas of National Jurisdiction UNEP-WCMC, Cambridge, UK:80pp.

Clark, M.R., Rowden, A.A., Schlacher, T., Williams, A., Consalvey, M., Stocks, K.I., Rogers, A.D., O'Hara, T.D., White, M., Shank, T.M., Hall-Spencer, J.M., 2010. The ecology of seamounts: structure, function, and human impacts. *Annual Review of Marine Science* **2**: 253-278.

Clarke, K. R., Warwick, R.M., 1994. Changes in Marine Communities: An approach to statistical analysis and interpretation. Plymouth Marine Laboratory, UK.

Coma, R., Gili, J-M., Zabala, M., Riera. T., 1994. Feeding and prey capture cycles in the aposymbiotic gorgonian *Paramuricea clavata*. *Marine Ecology Progress Series* **115**:257-270.

Copley, J.T.P., Tyler, P.A., Sheader, M., Murton, B., German, C. 1996. Megafauna from sublittoral to abyssal depths along the Mid-Atlantic Ridge south of Iceland. *Oceanologica Acta* **19**: 549-559

Copley, J.T.P., Jorgensen, P.B.K., Sohnt, R.A. 2007 Assessment of decadal-scale ecological change at a deep Mid-Atlantic hydrothermal vent and reproductive time-series in the shrimp *Rimicaris exoculata.* Journal of the marine biological association of the United Kingdom **87:**859-867 DOI: 10.1017/S0025315407056512

Cordes, E. E., Nybakken, J. W., VanDykhuizen, G. 2001. Reproduction and growth of *Anthomastus ritteri* (Octocorallia:Alcyonacea) from Monterey Bay, California, USA. *Marine Biology* **138**:491-501.

Crowe, B. M. 2010. An Interpretation of the Morphology and Recent Sedimentary Processes of Whittard Submarine Canyon, Bay of Biscay, North-Eastern Approaches. BSc Earth Science ER4001 Honours Dissertation. University of Southampton.

Culligan, K.M., Meyer-Gauen, G., Lyons-Weiler, J., Hays, J.B. 2000. Evolutionary origin, diversification and specialization of eukaryotic MutS homolog mismatch repair proteins. *Nucleic Acids Research*: **28:** 463–471.

Cunningham, M. J., Hodgson, S., Masson, D. G., Parson, L. M. 2005. An evaluation of along- and down-slope sediment transport processes between Goban Spur and Brenot Spur on the Celtic Margin of the Bay of Biscay. *Sedimentary Geology* **179**:99-116.

Daly, M., Brugler, M.R., Cartwright, P., Collins, A.G., Dawson, M.N., Fautin, D.G., France, S.C., McFadden, C.S., Opresko, D.M., Rodriguez, E., Romano, S.L., Stake. J.L., 2007. The phylum Cnidaria: A review of phylogenetic patterns and diversity 300 years after Linnaeus. *Zootaxa*. **1668:** 127-182.

Dana, J.D. 1863. Manual of geology: treating the principles of the science with special reference to American geological history, for the use of colleagues, academics and schools of science Vol. T. Bliss co., Philadelphia.

Davies, J., Guinan, J., Howell, K., Stewart, H., Verling, E. 2008. MESH South West Approaches Canyons Survey (MESH Cruise 01-07-01) Final Report. MESH Partnership, 2008.

De Leo, F. C., Smith, C. R., Rowden, A. A., Bowden, D. A., Clark, M. R., 2010. Submarine canyon: hotspots of benthic biomass and productivity in the deep sea. *Proceeding of the Royal Society B* **277**:2783-2792.

De Stigter, H. C., Boer, W., De Jesus Mendes, P. A., Jesus, C. C., Thomsen, L., van den Bergh, G. D., van Weering, T. C. E. 2007. Recent sediment transport and deposition in the Nazare Canyon, Portuguese continental margin. *Marine Geology*. **246**:144-164.

DeBry, R.W., Abele, L.G. 1995. The relationship between parsimony and maximum-likelihood analyses: Tree scores and confidence estimates for three real data sets. *Molecular Biology and Evolution* **12:** 291-297

Deuser, W. G., Ross, E.H. 1980. Seasonal change in the flux of organic carbon to the deep Sargasso Sea. *Nature.* **283**:364-365.

Deuser, W. G. 1986. Seasonal and inter-annual variations in deep-water particle fluxes in the Sargasso Sea and their relation to surface hydrography. *Deep-sea Research I.* **33**:225-246.

Dolan, E. 2008. Phylogenetics, Systematics and Biogeography of Deep-Sea Pennatulacea (Anthozoa:Octocorallia): Evidence from Molecules and Morphology. University of Southampton, School of Ocean and Earth Science, Southampton, U.K., Doctoral Thesis.

Dower, J. F., Mackas, D.L. 1996. "Seamount effects" in the zooplankton community near Cobb Seamount. *Deep-sea Research 1* **43**:837-858

Drake, D. E., Gorsline, D. S. 1973. Distribution and transport of suspended particulate matter in Hueneme, Redondo, Newport and La Jolla Submarine Canyons, California. *Geological Society of America Bulletin* **84**:3949-3969.

Dueñas LF, Sánchez JA. 2009. Character lability in deep-sea bamboo corals (Octocorallia, Isididae, Keratoisidinae). Marine Ecology Progress Series **397:** 11-23.

Duineveld, G., Lavaleye, M., Berghuis, E. de Wilde P. 2001. Activity and composition of the benthic fauna in the Whittard Canyon and the adjacent continental slope (NE Atlantic). *Oceanologica Acta* **24:** 69-83

Duineveld, G.C.A., Lavaleye, M.S.S., Berghuis, E.M. 2004. Particle flux and food supply to a seamount cold-water coral community (Galicia Bank, NW Spain). *Marine Ecology Progress Series* **277:**13-23.

Eastman, J. T., Barry, J.P. 2002. Underwater video observation of the Antarctic toothfish *Dissostichus mawson*i (Perciformes: Nototheniidae) in the Ross Sea. *Antarctica Polar Biology* **25**:391-395.

Etnoyer, P.J., 2008. A new species of *Isidella* bamboo coral (Octocorallia: Alcyonacea: Isididae) from northeast Pacific seamounts. *Proceedings of the Biological Society of Washington* **121:** 541-553.

Ewing, M., Worzel J.L. 1967. Early development of ocean-bottom photography at Woods Hole Oceanographic Institution and Lamont Geological Observatory. Page 310 *in* Hersey. J.B, (ed) Deep-Sea Photography. The John Hopkins Press, Baltimore.

Fautin, D.G., Guinotte, J.M.,James, C.O. 2009. Comparative depth distribution of corallimorpharians and scleractinians (Cnidaria: Anthozoa). *Marine Ecology Progress Series* **397**: 63-70.

Feussner, K.D. McLenachan,T.A. 2008 Survey of the genus *Sarcophyton* in Fijian waters from 2001-2005. Unpublished

Fossa, J. H., Mortensen, P.B., Furevik, D.M. 2002. The deep-water coral *Lophelia pertusa* in Norwegian waters: distribution and fishery impacts. *Hydrobiologia* **471**:1-12

France, S.C., Hoover, L.L. 2002. DNA sequences of the mitochondrial COI gene have low levels of divergence among deep-sea octocorals (Cnidaria: Anthozoa). *Hydrobiologia* **471:** 149-155.

France, S.C., Rosel, P.E., Agenbroad, J.E., Mullineaux, L.S., Kocher, T.D. 1996. DNA sequence variation of mitochondrial large-subunit rRNA provides support for a two-subclass organization of the Anthozoa (Cnidaria) *Molecular Marine Biology and Biotechnology* **5**:15–28.

France, S.C. 2007. Genetic analysis of bamboo corals (Cnidaria: Octocorallia: Isididae): Does lack of colony branching distinguish *Lepidisis* from *Keratoisis*? *Bulletin of Marine Science* **81**: 323-333.

Frederiksen, R.A., Jensen, A., Westerberg, H., 1992. The distribution of the scleractinian coral *Lophelia pertusa* around the Faeroe Islands and the relation to internal tidal mixing. *Sarsia* **77:** 157-171.

Freiwald, A., 2002. Reef-forming cold-water corals. In: Wefer, G., Billett, D., Hebbeln, D., Jorgensen, B., Schluter, M., Van Weering, T.C.E. (Eds.), Ocean Margin Systems. Springer, Heidelberg, pp. 365-385.

Freiwald, A., Fossa, J.H., Grehan, A., Koslow, T., Roberts, J.M. 2004. Cold-water coral reefs. Out of sight-no longer out of mind. UNEP-WCMC,

Gage J.D., Tyler, P.A. 1991. Deep-sea Biology: A Natural History of Organisms at the Deep-sea Floor. Cambridge University Press.

Gage, J. 2003. Food inputs, utilisation, carbon flow and energetics. In: Ecosystems of the World: Ecosystems of the Deep Ocean. P.A. Tyler, (ed). Amsterdam: Elsevier. Gebruk, pp. 313–426.

Garcia, R., van Oevelen, D., Soetaert, K., Thomsen, L., De Stigter, H. C., Epping, E. 2008. Deposition rates, mixing intensity and organic content in two contrasting submarine canyons. *Progress In Oceanography* **76**:192-215.

Gass, S.E., Willison, M.J.H. 2005. An assessment of the distribution of deep-sea corals in Atlantic Canada by using both scientific and local forms of knowledge. . In; Freiwald, A, Roberts, J.M. (Ed.) Cold-Water Corals and Ecosystems. Springer Berlin Heidelberg, New York, pp 223-245.

Gebruk, A.V., Budaeva, N.E., King, N.J. 2010. Bathyal benthic fauna of the Mid-Atlantic Ridge between the Azores and the Reykjanes Ridge. *Journal of Marine Biological Association of the United Kingdom* **90:** 1-14.

Genin, A., Dayton, P.K., Lonsdale, P.F., Spiess, F.N. 1986. Corals on seamount peaks provide evidence of current acceleration over deep-sea topography. *Nature* **322**:59-61.

Genin, A., Nobel, M., Lonsdalke, P.F. 1989. Tidal currents and anticyclonic motions on two North Pacific seamounts. *Deep-sea Research 1* **36**:1803-1815.

Giammona, C.P., Stanton JR, R.J. 1980. Octocorals from the middle eocene stone city formation, Texas. *Journal of Paleontology* **54:** 71-80.

Grehan, A., Unnithan, V., Wheeler, A., Monteys, X., Beck, T.,Wilson, M., Guinan, J., Foubert, A., Klages, M., Theide, J. 2004. Evidence of major fisheries impact on cold-water corals in the deep waters off the Porcupine Bank, west coast of Ireland: are interim management measures required? ICES CM 2004/AA:07 International Council for the Exploration of the Sea, Copenhagen.

Guindon, S., Gascuel, O., 2003 A simple, fast, and accurate algorithm to estimate large phylogenies by maximum likelihood. *Systematic Biology* **52:** 696–704.

Guinotte, J.M., Orr, J., Cairns, S., Freiwald, A., Morgan, L.E., George, R.Y. 2006. Will human-induced changes in seawater chemistry alter the distribution of deep-sea scleractinian corals? *Frontiers in Ecology* **4:** 141-146.

Haedrich, R.L., Rowe, G.T., Polloni, P.T., 1975. Zonation and faunal composition of epibenthic populations on the continental slope south of New England, *Journal of Marine Research*, **33:** 191-212.

Hall-Spencer, J., Allain, V. Fossa, J.H. 2002. Trawling damage to Northeast Atlantic ancient coral reefs. *Proceedings of the Royal Society of London* **269:** 507-511.

Hall-Spencer, J., Rogers, A., Davies, J., Foggo, A. 2007. Deep-sea coral distribution on seamounts, oceanic islands, and continental slopes in the Northeast Atlantic. In Conservation and adaptive management of seamount and deep-sea coral ecosystems George, R.Y., Cairns, S.D. (eds), Rosenstiel School of Marine and Atmospheric Science, University of Miami p 135-146.

Hamoutene, D., Puestow, T., Miller-Banoub, J., Wareham, V. 2008. Main lipid classes in some species of deep-sea corals in the Newfoundland and Labrador region (Northwest Atlantic Ocean). *Coral reefs* **27**:237-246.

Heger, A., Ieno, E.N., King, N.J., Morris, K.J., Bagley, P.M., Priede, I.G., 2008. Deep-sea pelagic bioluminescence over the Mid-Atlantic Ridge. *Deep-sea Research II* **55**:126-136.

Hellberg, M.E. 2006. No variation and low synonymous substitution rates in coral mtDNA despite high nuclear variation. *MBC Evolutionary Biology* **6:** doi 10.1186/1471-2148-1186-1124.

Herrera, S., Baco, A., Sánchez, J. A. 2010. Molecular systematics of the bubblegum coral genera (Paragorgiidae, Octocorallia) and description of a new deep-sea species. *Molecular Phylogenetics and Evolution* **55**:123-135.

Hersey, J. B. 1967. Deep-Sea Photography. Johns Hopkins Press, Balitmore.

Hickson, S.J. 1930. On the classification of the Alcyonaria. *Proceedings of the Zoological Society of London* **100**:229–52.

Hotchkiss, F. S., Wunsch, C. 1982. Internal waves in Hudson Canyon with possible geological implications. *Deep-sea Research* **29**:415-442.

Huelsenbeck, J.P., Ronquist, F. 2001. MRBAYES: Bayesian inference of phylogenetic trees. *Bioinformatics* **17:** 754-755.

Huvenne, V.A.I., Tyler, P.A., Masson, D.G., Fisher, E., Hauton, C., Huhnerbach, V., LeBas, T.P., Wolff, G.A., 2011. Innovative mapping reveals cold-water coral refuge in submarine canyon. In preparation.

Jaimeson, A. Hadal environments of the world- in prep

Janes, M. P., Mei Wah, L. 2005. Octocoral Taxonomy workshop Laboratory Manual. Results of the International Workshop on the Taxonomy of Octocorals March 20-26, 2005. University of Kerala, India. :35p.

Johnson, N.A., Campbell, J.W., Moore, T.S., Rex, M.A., Etter, R.J., McClain, C.R., Dowell, M.D. 2007. The relationship between the standing stock of deep-sea macrobenthos and surface production in the western North Atlantic. *Deep-sea Research I* **54**: 1350-1360.

Jones, D.O.B., Bett, B.J., Tyler, P.A., 2007. Depth-related changes to density, diversity and structure of benthic megafaunal assemblages in the Fimbul ice-shelf region, Weddell Sea, Antarctica. *Polar Biology* **30:** 1579-1592.

Koslow, T. 2007. Seamounts and deepwater coral reefs. *in* T. Koslow, (ed) The silent deep. The discovery, ecology and conservation of the deep-seas. The university of Chicago press., Chicago. pp 114-133

Kumar, S., Skjæveland, A., Orr, R.J.S, Enger, P., Ruden, T., Mevik, B., Burki, F., Botnen A., Shalchian-Tabrizi, K. 2009 AIR: A batch-oriented web program package for construction of supermatrices ready for phylogenomic analyses. *BMC Bioinformatics*, 10:357

Lampitt, A.L., Antia, A.N., 1997. Particle flux in Deep-seas: regional characteristics and temporal variability. *Deep-sea Research I* **44**: 1377-1403.

Larkin, M.A., Blackshields, G., Brown, N.P., Chenna, R., McGettigan, P.A., McWilliam, H., Valentin, F., Wallace, I.M., Wilm, A., Lopez, R., Thompson, J.D., Gibson, T.J., Higgins, D.G., 2007. *Clustal W and Clustal X version 2.0. Bioinformatics **23:** 2947-2948.*

Larsson, A.I., Purser, A. 2011. Sedimentation on the cold-water coral *Lophelia pertusa;* Cleaning efficiency from natural sediments and drill cuttings. *Marine Pollution Bulletin***, 62:** 1150-1168.

Lastras, G., M. Canals, R. Urgeles, D. Amblas, M. Inanov, L. Droz, B. Dennielou, J. Fabres, T. Schoolmeester, A. Akhemtzhanov, D. Orange, and A. Garcia-Garcia. 2007. A walk down the Cap the Creus canyon, Northwestern Mediterranean Sea: Recent processes inferred from morphology and sediment bedforms. *Marine Geology*, 246, 176-192.

Lasker, H.R., Brazeau, D.A., Calderon, J., Coffroth, M.A., Coma, R., Kim, K. 1996. *In-situ* rates of fertilization among broadcast spawning gorgonian corals. *Biological Bulletin* **190**: 45-55.

Le Goff-Vitry, M. C., Pybus, O.G., Rogers, A.D. 2004. Genetic structure of the deep-sea coral *Lophelia pertusa* in the northeast Atlantic revealed by mircosatellites and internal transcribed spacer sequences. *Molecular Ecology* **13**:537-549.

Ledwell, J.R., Montgomery, E.T., Polzin, K.L., Laurent, R.W., Schmitt, R.W., Toole, J.M. 2000. Evidence for enhanced mixing over rough topography in the abyssal ocean. *Nature* **403**, 179-182.

Lepard, A. 2003. Analysis of variation in the mitochondrial encoded *msh1* in the genus *Leptogorgia* (Cnidaria:Octocorallia) and implications for population and systematic studies. M.Sc thesis, University of Charleston, South Carolina. 99 p.

Levin, L. A., Etter, R.J., Rex M.A., Gooday, A.J., Smith, C.R., Pineda, J., Stuart, C.T., Hessler, R.R., Pawson, D. 2001. Environmental influences on regional deep-sea species diversity. *Annual Review of Ecology Systems.* **32**:51-93.

Lindner, A., Cairns, S.D, Cunningham, C.W. 2008. From offshore to onshore: Multiple Origins of Shallow-water Corals from deep-sea ancestors. *Plos one* **3**:e2429 doi:2410.1371/journal.pone.0002429.

Chapter 6: References

Masson DE. 2009. RRS James Cook Cruise 36, 19 Jul-28 Jul 2009. The Geobiology of Whittard Submarine Canyon. Southampton, UK: National Oceanography Centre, Southampton, 53pp (National Oceanography Centre Southampton Cruise Report, No 41).

Matthias, T., Godfrey, J.S. 2003. Chapter 15: Hydrology of Atlantic Ocean Regional Oceanography: an Introduction. Daya Publishing House, Delhi, pp 254-270

McCave, I. N., Hollister, C.D. 1985. Sedimentation under deep-sea current systems: Pre-Hebble ideas. *Marine Geology* **66**:13-24.

McFadden, C.S. 2004 Molecular Systematics of the Octocorallian Order Alcyonacea Unpublished

McFadden, C.S., Tullis, I.D., Hutchinson, M.B., Winner, K., Sohm, J.A. 2004. Variation in Coding (NADH Dehydrogenase Subunits 2, 3 and 6) and Noncoding Intergenic Spacer Regions of the Mitochondrial Genome in Octocorallia (Cnidaria: Anthozoa). *Marine Biotechnology* **6:** 516-526

McFadden, C.S., Frances, S.C., Sánchez, J.A., Alderslade, P. 2006. A molecular phylogenetic analysis of the Octocorallia (Cnidaria:Anthozoa) based on mitochondrial protein-coding sequence. *Molecular Phylogentics and Evolution* **41:** 513-527.

McFadden, C.S., Alderslade, P., van Ofwegen, L.P., Johnsen, H., Rumevichientong, A., 2006a. Phylogenetic relationships within the tropical soft coral genera *Sarcophyton* and *Lobophytum* (Anthozoa, Octocorallia). *Invertebrate Biology* **125:** 288-305

McFadden,C.S., Van Ofwegen, L.P., Beckman, E.J., Benayahu, Y. Alderslade, P. 2009. Molecular systematics of the speciose Indo-Pacific soft coral genus, *Sinularia* (Anthozoa: Octocorallia) *Invertebrate Biology* **128:** 303-323

McFadden, C.S., Sánchez, J.A., France, S.C. 2010. Molecular Phylogenetic Insights into Evolution of Octocorallia: a Review. *Integrative and Comparative Biology* doi:10.1093/jcb/icq056: 1-22.

McFadden, C.S., Benayahu, Y., Pante, E., Thoma, J.N., Nevarez, P.A., France, S.C. 2011. Limitations of mitochondrial gene barcoding in Octocorallia. *Molecular Ecology Resources* **11:** 19-31.

Menzies, R.J., George, R.Y., Rowe, G.T. 1973. Abyssal environment and ecology of the world's oceans. John Wiley and Sons, New York.

Mienis, F., De Stingter, H., C, White, M., Duineveld, G.C.A., De Hass, H., van Weering, T.C.E., 2007. Hydrodynamic controls on cold-water coral growth and carbonate-mound development at the SW and SE Rockall Trough margin, NE Atlantic Ocean. *Deep-sea Research I* **54**: 1655-1674.

Mills, C.1983, Problems of deep-sea biology: an historical perspective. In Rowes, G.T (ed) Deep-sea biology. The sea, volume 8, John Wiley and Sons, New York p 1-79

Mitchell, N.C., Tivey, M.A., Gente, P., 2000. Seafloor slopes at mid-ocean ridges from submersible observations and implications for interoperating geology for seafloor topography. *Earth and Planetary Science letters,* **183:** 543-555.

Morgan, L.E., Etnoyer, P., Scholz, A.J., Mertens, M., Powell, M., 2005. Conservation and management implications of deep-sea coral and fishing effort distributions in the Northeast Pacific Ocean. In; Freiwald, A., Roberts. J.M. (Ed.), Cold-water Corals and Ecosystems. Springer-Verlag Berlin Heidelberg pp. 1171-1187.

Morganstern, N.R., 1967. Submarine slumping and initiation of Turbidity currents. In Richards, A.F. (ed) Marine Geo-techniques, University of Illinois press. Pp 189-220.

Morris, K.J., Tyler, P.A., Murton, B., Rogers, A.D., In prep. Coral distribution along the Mid-Atlantic Ridge at 45ºN. *Deep Sea Research I.*

Mortensen, P. B., Buhl-Mortensen, L. 2004. Distribution of deep-water gorgonian corals in relation to benthic habitat features in the Northeast Channel (Atlantic Canada). *Marine Biology* **144**:1223-1238.

Mortensen, P. B., Buhl-Mortensen., L. 2005. Deep-water corals and their habitats in The Gully, a submarine canyon off Atlantic Canada. *In* Freiwald, A., Roberts. J.M., (ed). Cold-Water Corals and Ecosystems Springer-Verlag Berlin Heidelberg New York. P 247-277

Mortensen, P. B., Buhl-Mortensen, L., Gebruk, A.V. Krylova, E.M. 2008. Occurrence of deep-water corals on the Mid-Atlantic Ridge based on MAR-ECO data. *Deep-sea Research II* **55**:142-152.

Mullineaux, L. S., Mills. S.W, 1996. A test of the larval retention hypothesis in seamount-generated flows. *Deep-sea Research 1* **44**:745-770.

Murton, B. J., Redbourn, L. J., German, C. R., Baker, E. T. 1999. Sources and fluxes of hydrothermal heat, chemicals and biology within a segment of the Mid-Atlantic Ridge. *Earth and Planetary Science Letters* **171:**::301-317.

Nakamaru-Ogiso, E., Han, H., Matsuno-Yagi, A., Keinan, E., Sinha, S.C., Yagi, T., Ohsishi, T. 2010. The *ND2*subunit labelled by a photoaffinity analogue of asimicin, a potent complex 1 inhibitor. *FEBS Letters*, **584** 883-888

Nylander, J., 2004. MrModeltest, version 2.3. Available from the author, website: http://www.ebc.uu.se/systzoo/staff/nylander.html.

Okey, T. A. 1997. Sediment flushing observations, earthquake slumping, and benthic community changes in Monterey Canyon head. *Continental Shelf Research* **17**:877-897.

Oliveira, A., Santos, A. I., Rodrigues, A., Vitorino, J. 2007. Sedimentary particle distribution and dynamics on the Nazare canyon system and adjacent shelf (Portugal). *Marine Geology* **246**:105-122.

Oliveria , A., Vitorino, J., Rodriques, A., Jouanneau, J.M., Dias, J.A, Weber, O., 2002. Nepheloid layer dynamics on the Nazare canyon System and adjacent shelf (Portugal). *Progress in Oceanography*, **52:**195-213

Orejas, S., Lopez-Gonsalez, P.J., Gili, J.M., Teixido, N., Gutt, J., Arntz, W.E. 2002. Distribution and reproduction ecology of the Antarctic octocoral *Ainigmaptilon antarcticus* in the Weddell sea. *Marine Ecology Progress Series* ***231:*** *101-114.*

Orejas, C. Gili, J.M., Lopez-Gonzalez, P.J., Hasemann, C., Arntz, W.E. 2007. Reproduction patterns of four Antarctic octocorals in the Weddell Sea: an inter-specific, shape and latitudinal comparison. *Marine Biology* **150:** 551-563.

Orejas, C. G. A., Lo Iacano, C., Puig, P., Gili, J., Dale, M.R.T. 2009. Cold-water corals in the Cap de Creus canyon, northwestern Mediterranean: spatial distribution, density and anthropogenic impact. *Marine Ecology Progress Series* **397:** 37-51.

Orejas, C., Ferrier-pages, C., Reynaud, S., Beraud, E., Tsounis, G., Allemand, D., Gili, J.M. 2011. Long-term growth rates of four Mediterranean cold-water coral species maintained in aquaria. *Marine Ecology Progress Series* **429:** 57-65.

Orr, J.C., Fabry, V.J., Aumont, O., Bopp, L., Doney, S.C., Feely, R.A., Gnanadesikan, A., Gruber, N., Ishida, A., Joos, F., Key, R.M., Lindsay, K., Maier-Reimer, E., Matear, R., Monfray, P., Mouchet, A., Najjar, R.G., Plattner, G.-K., Rodgers, K.B., Sabine, C.L., Sarmiento, J.L., Schlitzer, R., Slater, R.D., Totterdell, I.J., Weirig, M.-F., Yamanaka, Y., Yool, A., 2005. Anthropogenic ocean acidification over the twenty-first century and its impact on calcifying organisms. *Nature* **437:** 681-686.

Page, R.D.M. 2001 Tree view programme available from Http://taxonomy.zoology.gla.ac.uk/rod/rod.html

Parrin, A.P., Netherton, S.E., Bross, L.S., McFadden, C.S. Blackstone,N.W. 2009. Symbiotic algae and the gastrovascular system of a stoloniferan octocoral: A laboratory model for the study of coral bleaching. Unpublished

Parson, L. M., Murton ,B.J., Searle, R.C., Booth, D., Evans, J., Field, P., Keeton, J., Laughton, A., McAllister, E., Millard, N., Redbourne, L., Rouse, I., Shor, A., Smith, D., Spencer, S.,

Summerhayes, C., Walker, C. 1993. En echelon volcanic ridges at the Reykjanes Ridge: a life cycle of volcanism and tectonics. *Earth and Planetary Science Letters* **117**:73-87.

Pattenden, A. D.C. 2008. The influence of submarine canyons on the structure and dynamics of megafaunal communities. University of Southampton, School of Ocean and Earth Science, Southampton, U.K., Doctoral Thesis.

Pitcher, T.J., Morato, T., Hart, P.J.B., Clark, M.R. Haggan, N., Santos, R.S. Seamounts: Ecology, Fisheries and Conservation. Blackwell publishing

Posada, D., Crandall, K.A. 1998 Modeltest: testing the model of DNA substitution. *Bioinformatics* **14:** 817–818.

Powers, D. 1970. A numerical taxonomic study of Hawaiian Reef corals. *Pacific Science,* **24:** 180-186.

Prada,C., Schizas, N.V., Yoshioka, P.M. 2008. Phenotypic plasticity or speciation? A case from a clonal marine organism *BMC Evolutionary Biology***. 8:** 47

Quaresma, L. S., Vitorino, J., Oliveira, A., da Silva, J. 2007. Evidence of sediment resuspension in nonlinear internal waves on the western Portuguese mid-shelf. *Marine Geology*, **246**:123-143.

Ramirez-Llodra, E., Tyler, P.A., Baker, M.A., Bergstad, O.A., Clark, M.R., Escobar, E., Levin, L.A., Menot, L., Rowden, A.A., Smith, C.R., Van Dover., C.L. 2001. Man and the last great wilderness: Human impact on the Deep Sea. *Plos one.* **6:** e22588. doi:10.1371/journal.pone.0022588

Reid, G. S., Hamilton, D. 1990. A Reconnaissance Survey of the Whittard Sea Fan, Southwestern Approaches, British Isles. *Marine Geology* **92**:69-86.

Ribes, M., Coma, R., Gili, J-M. 1999. Heterogeneous feeding in benthic suspension feeders: The natural diet and grazing rate of the temperate gorgonian *Paramuricea clavata* (Cnidaria:Octocorallia) over a year cycle. *Marine Ecology Progress Series* **183**:125-137.

Rice, A. L., Aldred, R.G., Darlington, E., Wild, R.A. 1982. The Quantitative Estimation of the Deep-Sea Megabenthos; a new approach to an old problem. *Oceanologica Acta* **5**:63-72.

Rice, A.L., Tyler, P.A., Paterson, G.J.L. 1992. The pennatulid *Kophobelemnon stelliferum* (Cnidaria: Octocorallia) in the Porcupine Seabight (North-east Atlantic Ocean). *Journal of the Marine Biological Association of the United Kingdom* **72:**417-434.

Ridente, D., Foglini, F., Minisini, D., Trincardi, F., Verdicchio, G. 2007. Shelf-edge erosion, sediment failure and inception of Bari Canyon on the southwestern Adriatic Margin (Central Mediterranean). *Marine Geology* **246**:193-207.

Risk, M. J., Heikoop, J.M, ,Snow, M.G., Beukens, R. 2002. Lifespans and growth patterns of two deep-sea corals: *Primnoa resedaeformis* and *Desmophyllum cristagalli*. *Hydrobiologia* **471**:125-131.

Roberts, C.M. 2002. Deep impact: the rising toll of fishing in the deep sea. *Trends in Ecology and Evolution* **17:** 242-245

Roberts, J., Wheeler, A.J., Freiwald, A. 2006. Reefs of the deep: the biology and geology of cold-water coral ecosystems. *Science* **312**:543-547.

Roberts, J.M., Wheeler. A.J., Freiwald A., Cairns, S. 2009. Cold-Water Corals: The biology and Geology of deep-sea coral Habitats. Cambridge University Press, Cambridge.

Rogers, A. D. 1994. The Biology of Seamounts. *Advances in Marine Biology* **30**:305-350.

Rogers, A.D. 1999. The biology of *Lophelia pertusa* (Linnaeus 1758) and other deep-water reef-forming corals and impacts from human activities. *International Review of Hydrobiology* **84:** 315-406

Rogers, A. D. 2004. The Biology, Ecology and Vulnerability of Deep-Water Coral Reefs. Report for the World Conservation Union for the 7th Convention of Parties, Convention for Biodiversity, Kuala Lumpur, February 8th – 19th. http://www.iucn.org/themes/marine/pubs/pubs.htm.

Rogers, A.D., Baco, A.R., Clark, A.M., Shank, T.M., Griffiths, H., Hart, T., and Hall-Spencer, J.M., 2007. Corals on Seamounts. In: Pitcher, T.J., Morato, T., Hart, P.J.B., Clark, M.R., Haggan, N., Santos, R.S. (Eds.), Seamounts: Ecology, Fisheries and Conservation. Blackwell, Oxford UK, pp. 141-169

Rose A. 2009. Coral taxonomy. www.Coralscience.org.

Rowe, G. T. 1971. The exploration of Submarine Canyons and their Benthic Faunal Assemblages. *Proceedings of the Royal Society of Edinburgh (B*) **17**:159-169.

Rowe, G. T., Keller, G., Edgerton, H., Staresinic, N., MacIlvaine, J. 1974. Time-lapse photography of the biological reworking of sediments in Hudson submarine canyon. *Journal of Sedimentary Petrology* **44**:549-552.

Rowe, G.T., Polloni, P.T., Haedrich, R.L., 1982. The deep-sea macrobenthos on the continental margin of the Northwest Atlantic Ocean. *Deep-Sea Research*, **29:** 257-278

Samadi, S., Bottan, L., Macpherson, E., De Forges, B.R., Boisselier, M. 2006. Seamount endemism questioned by the geographic distribution and population genetic structure if marine invertebrates. *Marine Biology* **149**:1463-1475.

Sánchez, J.A., Lasker, H.R. 2003. Patterns of Morphologic Integration in Branching Colonies of Marine Modular Organisms: supra-module organization in Gorgonian Corals. *Proceedings of the Royal Society of London B.* **270:** 2039-2044. (DOI: 10.1098/rspb.2003.2471)

Sánchez , J.A., Lasker, H.R., Taylor, D.J. 2003a. Phylogenetic analyses among Octocorals (Cnidaria): mitochondrial and nuclear DNA sequences (Isu-rRNA, 16S and ssu-rRNA,

18s) support two convergent clades of branching gorgonians. *Molecular Phylogentics and Evolution* **29:** 31-42.

Sánchez, J.A., McFadden, C.S., France, S.C., Lasker, H.R. 2003b. Molecular phylogentic analyses of shallow-water Caribbean octocorals ITS2 and their predicted RNA secondary structures. *Molecular Phylogentics and Evolution Molecular Phylogenetics & Evolution*. **29:** 31-42

Sánchez, J.A., Cairns, S.D. 2004. An unusual new gorgonian coral (Anthozoa: Octocorallia) from the Aleutian Islands, Alaska, *Zoologische Mededelingen*, **78:** 1-16.

Sánchez, J.A. 2007. A new genus of Atlantic octocorals (Octocorallia: Gorgoniidae): Systematics of gorgoniids with asymmetric scelerites. *Journal of Natural History* **41:** 493-509.

Sathyendranath, S., Longhurst, A., Caverhill, C.A., Platt, T 1995, Regionally and seasonally differentiated primary production in the North Atlantic. *Deep-Sea Research* **42:**1773-1802

Saunders, P. M., Francis, T. J. G. 1985. The search for hydrothermal sources on the Mid-Atlantic Ridge. *Progress In Oceanography* **14**:527-536.

Schlacher, T.A., Schlacher-Hoenlinger, M.A., Williams, A., Althaus, F., Hooper, J.N.A. 2007. Richness and distribution of sponge megabenthos in continental margin canyons off South-Eastern Australia. *Marine Ecology Progress Series*. **340:** 73-88

Schroeder, W.W., Brooke, S.D., Olson, J.B., Phaneuf, B., McDonough III, J.J., Etnoyer, P. 2005. Occurance of deep-water *Lophelia pertusa* and *Madrepora oculata* in the Gulf of Mexico. . In; Freiwald, A., Roberts. J.M. (Ed.), Cold-Water Corals and Ecosystems. Springer Berlin Heidelberg, New York. pp 297-307.

Searle, R.C., Murton, B.J., Achenbach, K., LeBas, T., Tivey, M., Yeo, I., Cormier, M.H., Carlut, J., Ferreira, P., Mallows C., Morris, K., Schroth, N., van Calsteren, P., Waters, C. 2010.

Structure and development of an axial volcanic ridge: Mid-Atlantic Ridge, 45°N. *Earth and Planetary Science Letters*. **299**, 228-24

Sebens, K. P. 1984. Water flow and coral colony size: Interhabitat comparisons of the octocoral *Alcyonium siderium*. *Proceedings National Academy of Science USA* **81**: 5473-5477

Sebens, K. P., Helmuth, B., Carrington, E., Agius, B. 2003. Effects of water flow on growth and energetics of the scleractinian coral *Agaricia tenuifolia* in Belize. *Coral reefs* **22**:35-47.

Shearer, T.L., Van Oppen, M.J.H., Romano, S.L., Rheide, G.W. 2002. Slow mitochondrial DNA sequence evolution in the Anthozoa (Cnidaria). *Molecular Ecology* **11:** 2475-2487.

Shepard, F. P., Curray, J. R., Inman, D. L., Murray, E. A., Winterer, E. L., Dill, R. F. 1964. Submarine Geology by Diving Saucer. *Science* **145**:1042-1046.

Shepard, F. P. 1975. Tidal components of currents in submarine canyons. *Journal of Geology* **84**:343-350.

Sherwood, O.A., Jamieson, R.E., Edinger, E.N., Wareham, V.E. 2008. Stable C and N isotopic composition of cold-water corals from the Newfoundland and Labrador continental slope: Examination of trophic, depth and spatial effects. *Deep-sea research*, **55:** 1392-1402

Sherwood, O.A., Edinger, E.N. 2009. Ages and growth rates of some deep-sea gorgonian and antipatharian corals of Newfoundland and Labrador. *Canadian journal of fisheries and Aquatic science*, **66:** 142-152.

Shester, G., Ayers, J. 2005. A cost effective approach to protecting deep-sea coral and fishing effort distributions in the Northeast Pacific Ocean. . In; Freiwald, A., Roberts. J.M. (Ed.), Cold-Water Corals and Ecosystems. Springer Berlin Heidelberg, New York, pp 1151-1169.

Simpson, A. 2009. Reproduction in Octocorals (Subclass Octocorallia): A Review of Published Literature. Version 16 July 2009. In Deep-Sea Corals Portal, http://www.ucs.louisiana.edu/~scf4101/Bambooweb/.

Smith, D. K., Cann J.R. 1992. The role of seamount volcanism in crustal construction at the Mid-Atlantic Ridge (24°-30°N). *Journal of Geophysical Research*. **97**:1645-1658.

Smith, D.K., Cann, J.R. 1993. Building the crust at the Mid-Atlantic Ridge. *Nature*, **365**: 707-715

Smith, D.K., Cann, J.R., 1999. Constructing the upper crust of the Mid-Atlantic Ridge: a reinterpretation based on Puna Ridge, Kilauea Volcano. *Journal of Geophysical Research B* **104:** 379-399.

Smith, P. J., McVeagh, S.M., Mingoia, J.T., France, S.C. 2004. Mitochondrial DNA sequence variation in deep-sea bamboo corals (Keratoisidinae) species in the southwest and northwest Pacific Ocean. *Marine Biology* **144**:253-261.

Smith, K.L., Ruhl, H.A., Bett, B.J., Billett, D.S.M., Lampitt, R.S., Kaufmann, R.S., 2009. Climate, carbon cycling and deep-ocean ecosystems. Proceedings of the National Academy of Science **106:** 19211-19218.

Squires, D.F., 1967. The evolution of the deep-sea coral family Micrabaciidae. *Studies in Tropical Oceanography* **5**: 502-510

Stefanescu, C., Morales-Nin, B., Massuti, E. 1994. Fish assemblages on the slope in the Catalan sea (Western Mediterranean): Influence of a Submarine Canyon. *Journal of the Marine Biological Association United Kingdom.* **74:** 499-512.

Sun, Z., Hamel, J.F., Edinger, E., Mercier, A. 2010. Reproductive biology of the deep-sea octocoral *Drifa glomerata* in the Northwest Atlantic. *Marine Biology*, **157:** 863-873.

Svoboda, A. 1985. Diver-operated cameras and their marine-biological uses.*in* J. D. George, Lythgoe, G.I, Lythgoe, J.N, (ed) Underwater Photography and Television for Scientists. Clarendon Press, Oxford.

Swofford, D.L., 2002. *PAUP*. Phylogenetic Analysis Using Parsimony*, Version 4. Sinauer Associates.

Tamura, K., Dudley, J., Nei, M., Kumar, S., 2007. MEGA4: Molecular Evolutionary Genetics Analysis (MEGA) software version 4.0. *Molecular Biology and Evolution* **24:** 1596-1599.

Taviani, M., Freiwald, A., Zibrowius, H., 2005. Deep coral growth in the Mediterranean Sea: an overview. . In; Freiwald, A., Roberts. J.M. (Ed.), Cold-Water Corals and Ecosystems. Springer Berlin Heidelberg, New York, pp 137-156.

Thistle, D. 2003. The deep-sea floor: an overview. P. A. Tyler, (ed). Ecosystems of the world Vol 28. Ecosystems of the deep oceans Elsevier, Amsterdam. pp 5-37

Thoma, J.N., Pante, E., Brugler, M.R, France, S.C., 2009. Deep-sea octocorals and antipatharians show no evidence of seamount-scale endemism in the NW Atlantic. *Marine Ecology Progress Series*, **397:** 25-35.

Thomson, C.W, Murray, J., 1889. Report of the Scientific results of the Voyage of H.M.S. *Challenger*, during the years 1873-1879. Zoology volume XXXI. Description of genera and Species, Alcyonaria. Printed for her majesty stationary Office, London.

Thresher, R.E. 2009. Environmental and compositional correlates of growth rate in deep-water bamboo corals (Gorgonacea; Isididae). Marine Ecology Progress Series, **397:** 187-196.

Thurnherr, A.M., Richards,A.F., German,C.R. Lane-Serff G.F., Speer K.G. 2002. Flow and mixing in the Rift Valley of the Mid-Atlantic Ridge. *Journal of Physical Oceanography.*, **32,** 1763–1778,

Tittensor, D.P., Baco, A.R., Hall-Spencer, J.M., Orr, J.C., Rogers, A.D., 2010. Seamounts as refugia from ocean acidification for cold-water stony corals. *Marine Ecology* **31** (Suppl.1), 212-225.

Toucanne, S., Zaragosi, S., Bourillet, J. F., Naughton, F., Cremer, M., Eynaud, F., Dennielou B. 2008. Activity of the turbidite levees of the Celtic-Armorican margin (Bay of Biscay) during the last 30,000 years: Imprints of the last European deglaciation and Heinrich events. *Marine Geology* **247**:84-103.

Tracey, D.M., Neil, H., Marriott, P., Andrews, A.H., Cailliet, G.M., Sánchez, J.A. 2007. Age and growth of two genera of deep-sea bamboo corals (family Isididae) in New Zealand waters. *Bulletin* of Marine Science, **8:** 393-408.

Trincardi, F., Foglini, F., Verdicchio, G., Asioli, A., Correggiari, A., Minisini, D., Piva, A., Remia, A., Ridente, D., Taviani, M. 2007. The impact of cascading currents on the Bari Canyon Sysyem SW-Adriatic Margin (Central Mediterranean). *Marine Geology* **246**:208-230.

Tunnicliffe, V., Juniper, K.S., Sibuet, M. 2003 Reducing environments of the deep-sea floor. In: *Ecosystems of the World*, Volume 28, *Ecosystems of the Deep Oceans* P.A. Tyler (ed), London: Elsevier. pp 81–110.

Turley, C. M., Roberts , J. M., Guinotte, J.M. 2007. Corals in deep-water: will the unseen hand of ocean acidification destroy cold-water ecosystems? *Coral reefs* **26**:445-448.

Tyler, P.A., Zibrowius, H., 1992. Submersible observations of the invertebrate fauna on the continental slope southwest of Ireland (NE Atlantic Ocean). *Oceanologica Acta* **15:** 211-226

Tyler, P. A. 1995. Conditions for the existence of life at the deep-sea floor: an update. *Oceanography and Marine biology; An annual Review* **33**:221-244.

Tyler, P.A., Bronsdon, S.K., Young, C.M, Rice, A.L. 1995. Ecology and gametogenic biology of the genus *Umbellula* (Pennatulacea) in the North Atlantic Ocean. *Internationale Revue der gesamten Hydrobiologie und Hydrographie*. **80:**187-199

Tyler, P.A., 2003. Introduction. In; Tyler, P.A. (Ed.), Ecosystems of the world, Vol 28, Ecosystems of the deep Oceans. Elsevier, Amsterdam, pp. 1-3.

Tyler, P., Amaro, T., Arzola, R., Cunha, M.R., de Stigter, H., Gooday, A., Huvenne, V., Ingels, J, Kiriakoulakis, K. Lastras, G., Masson, D., Oliveira, A., Pattenden, A., Vanreusel, A., Van Weering, T., Vitorino, J., Witte, U., Wolff, G. 2009. Europe's grand canyon: Nazaré submarine canyon. *Oceanography* **22:**46–57, http://dx.doi.org/10.5670/oceanog.2009.05.

Van de Ham, J.L., Brugler, M.R., France, S. C. 2009. Exploring the utility of an indel-rich, mitochondrial intergenic region as a molecular barcode for bamboo corals (Octocorallia: Isididae). *Marine Genomics* **2:** 183-192.

Van Dover, C.L. 2000. The Ecology of deep-sea hydrothermal vents. Princeton University Press, Princeton, New Jersey.

Van Rooij, D., De Mol, L., Ingels, J., Versteeg, W., Rüggeberg, A., Jauniaux, V., TSS party. 2010. Cruise Report Belgica 10/17b, Belgica BiSCOSYSTEMS II, Leg 2, Whittard Canyon. Ghent University, Belgium, Ghent

Vargas, S., Eitel, M., Breedy, O., Schierwater, B. 2010. Molecules match morphology: mitochondrial DNA supports Bayer's Lytreia-Bebryce-Heterogorgia (Alcyonacea: Octocorallia) clade hypothesis. *Invertebrate Systematics*. **24:** 23-31

Vetter, E. W., Dayton, P. K. 1998. Macrofaunal communities within and adjacent to a detritus-rich submarine canyon system. *Deep-sea Research II* **45**:25-54.

Vetter, E. W., Dayton. P. K. 1999. Organic enrichment by macrophyte detritus, and abundance patterns of megafaunal populations in submarine canyons. *Marine Ecology Progress Series* **186**:137-148.

Vetter, E. W., Smith, C. R., De Leo F. C., 2010. Hawaiian hotspots: enhanced megafaunal abundance and diversity in submarine canyons on the oceanic islands of Hawaii. *Marine Ecology* **31**:183-199.

Wall, D., Tregenza, N., De Stinger, H., 2010. Exploring the feasibility of static acoustic monitoring for deep diving Whales. http://www.iwdg.ie/downloads/ecs08poster.pdf

Waller, R.G., Tyler, P.A. 2005. The reproductive biology of two deep-water, reef-building scleractinians from the NE Atlantic Ocean. *Coral Reefs.* **24**: 514-522.

Waller, R.G. 2005. Deep-water Scleractinia (Cnidaria:Anthozoa): current knowledge of reproductive processes. *In*; Freiwald, A., Roberts. J.M. (Ed.), Cold-Water Corals and Ecosystems. Springer Berlin Heidelberg, New York, pp 691-700

Watanabe, S., Metaxas, A., Sameoto, J., Lawton, P., 2009. Patterns in abundance and size of two deep-water gorgonian octocorals, in relation to depth and substrate features off Nova Scotia. *Deep-sea Research* 1 **56**: 2235-2248.

Watling, L., Norse, E.A., 1998**.** Disturbance of the Seabed by Mobile Fishing Gear: A Comparison to Forest Clearcutting. *Conservation Biology* **12:** 1180-1197.

Watling, L., Auster, P.J. 2005. Distribution of deep-water Alcyonacea off the Northeast Coast of the United States. *In* Freiwald, A., Roberts. J.M. (Ed.), Cold-Water Corals and Ecosystems. Springer Berlin Heidelberg, New York, pp 279-296.

Watling, L. 2007. New species of deep-sea Chrysogorgiidae (Octocorallia) from seamounts in the western North Atlantic. *Journal of the Marine Biological Association of the United Kingdom* **87:** 393-407

Watling, L., France, S., 2011. A new genus and species of bamboo coral (Octocorallia:Isididae:Keratoisidinae) from the New England Seamounts. *Bulletin of the Yale Peabody Museum*. In press.

Watling, L., France, S.C., Pante, E., Simpson, A. In prep. Biology of deep-water Octocorals. Advances in *Marine Biology* **60**.

Weaver, P. P. E., Boetius, A., Danovaro, R., Freiwald, A., Gunn, V., Heussner, S., Morato, T., Schewe, I., van den Hove, S. 2009. The Future of Integrated Deep-Sea Research in Europe The HERMIONE Project. *Oceanography* **22:** 178-191.

Weaver, P. P. E ., Billett, D. S. M., Boetius, A., Danovaro, R., Freiwald, A., Sibuet, M. 2004. Hotspot Ecosystem Research on the Margins of European Seas. *Oceanology* **17**:132-144

West, J. M., Harvell, C. D., Walls, A.M. 1993. Morphological plasticity in a gorgonian coral (Briareum asbestinum) over a depth cline. *Marine Ecology Progress Series* **94**:61-69.

West, J. M. 1997. Plasticity in the Sclerites of a Gorgonoan Coral: Tests of Water Motion, Light level and damage Cues. *Biology Bulletin* **192**:279-289.

West, J. M. 1998. The dual role of sclerites in a gorgonian coral: Conflicting functions for support and defence. *Evolutionary Ecology* **12**:803-821.

White, M., Mohn, C. 2004. Seamounts: a review of physical processes and their influence on the seamount ecosystem. Dept Earth and Ocean sciences, NUI Galway.

White, M., Mohn, C., De Stingter, H., C, Mottram, G. 2005. Deep-water coral development as a function of hydrodynamics and surface productivity around the submarine banks of the Rockall Trough, NE Atlantic. In; Freiwald, A., Roberts. J.M. (Ed.) Cold-Water Corals and Ecosystems. Springer Berlin Heidelberg, New York.pp 503-514.

White, M., Bashmachnikov, I., Aristegui, J., Martins, A. 2007. Physical processes and seamount productivity. *In* Pitcher, J. T. Morato, T., Hart, P.J.B., Clark, M.R. Haggan, N., Santos, R.S., (Ed) Seamounts: Ecology, Fisheries Conservation. Blackwell publishing. pp 65-84

Wigham, B.D., Hudson, I.R., Billett, D.S.M., Wolff, G.A.2003. Is long-term change in the abyssal Northeast Atlantic driven by qualitative changes in export flux? Evidence from the selective feeding in deep-sea holothurians. *Progress In Oceanography* **59**:409-411.

Williams, G.C. 1992. The Alcyonacea of southern Africa. Stoloniferous octocorals and soft corals (Coelenterata, Anthozoa). *Annals of the South African Museum* **100:** 249-358

Williams, G.C., Alderslade, P. 1999. Revisionary systematic of the Western Pacific soft coral Genus *Minabea* (Octocorallia;Alcyoniidae), with descriptions of a related new genus and species from the Indo-Pacific. *Proceeding of the California Academy of sciences* **51**: 337-364.

Willig, M. R., Kaufman, D. M., Stevens. R. D. 2003. Latitudinal Gradients of Biodiversity: Pattern, Process, Scale, and Synthesis. *Annual Review Ecology, Evolutionary, Systems*. **34**:273-309.

Wirshing, H.H., Messing, C.G., Douady, C.J., Reed, J., Stanhope, M.J., Shivji, M.S. 2005. Molecular evidence for multiple lineages in the gorgonian family Plexauridae (Anthozoa:Octocorallia). *Marine Biology* **147:** 497-508.

Woodby, D., Carlile, D., Hulbert, L. 2009. Predictive modelling of coral distribution in the Central Aleutian Islands, USA. *Marine Ecology Progress Series* **397**:227-240

Yeo, I., Searle, R.C., Achenbach, K.L., Le Bas, T.P., Murton, B. J. 2011. Eruptive hummocks: Building blocks of the upper ocean crust. *Geology* .In press

Young, C.M., 2009. Communities on Deep-Sea Hard Bottoms. *In:* Wahl, M. (Ed.), Marine hard bottomed communities, Ecological studies 206. Springer-Verlag, Berlin.

Zaragosi, S., Bourillet, J.F., Eynaud, F., Toucanne, S., Denhard, B., Van Toer, A., Lanfumey, V. 2006. The impact of the last European deglaciation on the deep-sea turbidite systems of the Celtic-Armorican margin (Bay of Biscay). *Geo-Marine Letters* **6:** 317-32